Tropospheric Circulation and Jet Streams

By
E. Reiter

Department of Atmospheric Science
Colorado State University
Fort Collins, Colorado

Colorado State University

Department of Atmospheric Science

Paper No. 153

Chapter 4

Tropospheric Circulation and Jet Streams

E. REITER

Global wind systems

Physical causes of large-scale tropospheric circulations

It is evident from the equation of motion:

$$\dot{V} = -\alpha\nabla p - 2\Omega \times V - \nabla\Phi + \alpha F \tag{1}$$

that large-scale, quasi-permanent atmospheric circulation systems can be maintained against frictional forces only if an external energy source continuously provides the necessary pressure gradients. We easily recognize the sun's radiation as such a source of energy which, through its absorption by the ground, produces a temperature gradient and, therefore, a density gradient between equator and pole.

If nothing other than these density gradients—and the resulting pressure gradients—were acting on the atmosphere, we would expect the development of a simple trade wind or Hadley cell; air flowing poleward aloft, out of a warm high-pressure belt with a compensating return flow towards the equator at low levels. Rising air motions would prevail at low latitudes, sinking motions over the polar regions. If this circulation were to reach a steady state, balance between pressure gradients and frictional forces would be required. Such a circulation system does not prevail in the earth's atmosphere, however, due to the rotation of the system. The outstanding characteristics of the real tropospheric circulation, as we observe them under mean conditions, may be listed as follows:

(*1*) The Hadley cell does not extend from the equator to the pole, but is confined to low and subtropical latitudes (see Fig.1).

(*2*) An indirect circulation cell (sinking warm air, rising cool air) is observed in middle

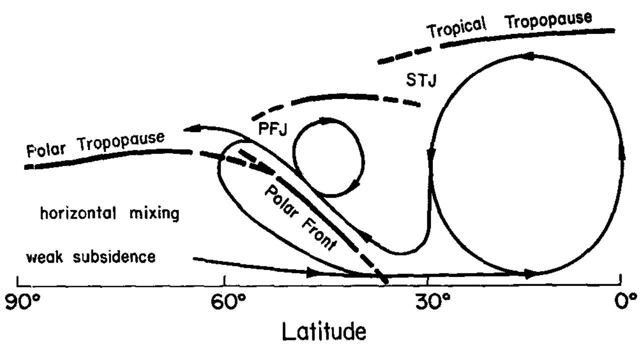

Fig. 1. Schematic representation of the mean meridional circulation in the Northern Hemisphere during winter. Heavy lines = tropopauses and polar front. PFJ = polar front jet stream and STJ = subtropical jet stream. (After PALMÉN, 1954.)

latitudes, giving rise to a 3-cell structure of the tropospheric circulation (PALMÉN, 1954). (3) Horizontal temperature gradients are concentrated in narrow "frontal zones". Winds in the upper troposphere follow nearly geostrophic conditions:

$$0 = -\alpha\nabla p - 2\boldsymbol{\Omega} \times \boldsymbol{V} \tag{2}$$

in the steady state atmosphere. Consequently, upper tropospheric wind systems will also be concentrated into narrow high-speed bands, i.e., in the "jet streams."

For a study of the principal laws governing these characteristics, the earth's atmosphere with all its complexities provides a rather poor laboratory, because: (*a*) the deflecting Coriolis force, governing the geostrophic wind relationship, is a function of latitude on a rotating globe; (*b*) the heat sources and sinks are not uniformly distributed around the globe, due to the different heat capacities of continents and oceans, and to the release of latent heat in precipitation processes; (*c*) orographic effects significantly disturb the atmospheric flow; (*d*) hemispheric and seasonal differences have to be taken into account; and, (*e*) heat sources and sinks in the ozonosphere and ionosphere may have a significant influence on tropospheric motions.

In addition to these difficulties, research on the general circulation suffers another great disadvantage; the atmosphere provides a laboratory which does not allow the *repetition* of experiments. The mean state of the atmospheric motion is made up of a large number of individual weather situations, none of them completely alike. Thus, instead of controlling and varying an experiment, the meteorologist has to resort to a statistical treatment of the large number of cases provided by actual weather sequences in the atmosphere.

A way to overcome most of these frustrating difficulties was found by resorting to "geophysical model experiments" on the one hand and to "theoretical modeling" with the aid of electronic computers on the other (e.g., RIEHL and FULTZ, 1957, 1958; FULTZ, 1960; ADEM, 1962; SMAGORINSKY, 1963). The atmosphere may in first approximation be represented by an incompressible fluid, e.g., by water. This simplification allows us to use actual temperatures instead of potential temperatures. In order to find out whether or not a latitude-dependent Coriolis parameter plays an important role in shaping the general circulation (as for instance suggested by ROSSBY's (1945) wave equation), a flat "dish pan" may be substituted for a spherical earth.

An infinite variety of experiments may be performed with such models. In order to establish their significance in explaining circulation processes in the actual atmosphere, certain modeling criteria will have to be fulfilled, so that results obtained in the model may be related to actual conditions (ROSSBY, 1926; FULTZ, 1951; see also REITER, 1961a, 1963a).

The conclusions one may draw from such modeling experiments as to the physical causes of the observed tropospheric circulation are discussed in the following paragraphs.

(*1*) The driving agents of the general circulation are the pressure gradients built up by differential heating between equator and pole. To keep the circulation at a steady state, heat has to be transported from source to sink regions by a mean meridional circulation and/or by horizontal "eddies" of the size of planetary and cyclone waves.

(*2*) In a rotating system the contact of the circulating fluid with the ground provides sources and sinks of angular momentum. Under steady state conditions, sources and sinks will have to balance each other in magnitude.

(3) Atmospheric motions maintaining the heat transport between equator and pole also carry out the required angular momentum transport from sources to sinks. If air masses were to maintain their absolute momentum, any meridional displacement of air (or of water in a "dish pan") would result in zonal wind components relative to the earth. Westerlies would result from a poleward displacement of fluid, easterlies from an equatorward displacement.
If the absolute angular momentum:

$$\boldsymbol{G}_{\mathrm{a}} = \boldsymbol{r}_{\mathrm{a}} \cdot \left(\frac{\mathrm{d}\boldsymbol{r}}{\mathrm{d}t}\right) = r_{\mathrm{a}}^2 \boldsymbol{\Omega} \tag{3}$$

is conserved by a fluid parcel moving from latitude ϕ_1 to latitude ϕ_2 we derive the equation:

$$(\Omega+\omega_1)R^2\cos^2\phi_1 = (\Omega+\omega_2)R^2\cos^2\phi_2 \tag{4}$$

where $\omega = \dfrac{\mathrm{d}\lambda}{\mathrm{d}t}$ is the zonal angular momentum of a parcel of air *relative* to the earth, λ is the geographic longitude. Substitution of the expression for the zonal wind:

$$\mathrm{u} = \omega R \cos\phi \tag{5}$$

into eq.4 yields:

$$\mathrm{u}_1 \cos\phi_1 - \mathrm{u}_2 \cos\phi_1 + \mathrm{u}_2 \cos\phi_1 - \mathrm{u}_2 \cos\phi_2 = -\Omega R(\cos^2\phi_1 - \cos^2\phi_2) \tag{6}$$

For an infinitesimally small meridional displacement we may replace differences by differentials. With the transformation from a polar into a Cartesian coordinate system: $\left(\dfrac{\partial y}{\partial \phi} = R\right)$, we obtain the horizontal shear of a zonal current, that would establish itself if air were exchanged meridionally under conservation of absolute angular momentum:

$$\frac{\partial \mathrm{u}}{\partial y} = f + \frac{\mathrm{u}}{R}\tan\phi\,. \tag{7}$$

In middle latitudes the Coriolis parameter, $f = 2\Omega \sin\phi$, is of the order of 10^{-4}/sec. The second term, produced by the latitudinal convergence of meridians, is of the order of $1.6 \cdot 10^{-5}$/sec for very strong jet streams (u = 100 m/sec). Normally, the second term amounts to less than 10% of the Coriolis parameter.
In dish-pan experiments, as well as on the equatorial side of well developed atmospheric jet streams[1], we commonly find shears conforming to eq.7, indicating that the conservation of angular momentum is a principle which the atmosphere tries to follow in generating jet streams. ARAKAWA (1951) has shown, that anticyclonic shears $\left(\dfrac{\partial \mathrm{u}}{\partial y} > 0\right)$ in excess of those given by eq.7 render a zonal current dynamically unstable.
The hydrodynamic equations have to be satisfied as well. A jet stream produced by

[1] It is assumed that the reader is familiar with the terminology of "jet streams". According to W.M.O. definition they are air currents with quasihorizontal axes, thousands of km long, hundreds of km wide, and several km deep. Wind speeds in the core of a jet stream should exceed 30 m/sec. Vertical gradients are of the order of 5 m/sec/km. Horizontal gradients are of the order of 5 m/sec/100 km.

meridional motions through the tendency for conservation of angular momentum would generate mean horizontal mass convergence. (This is strongly implied in the subtropical jet stream of Fig.1). This convergence will build up pressure forces which, in turn, will act on the flow, i.e., the dynamics of a jet stream strongly influence its structure and its behavior. We should not expect, therefore, to find anticyclonic shears as given by eq.7 near every jet stream on the weather map. Nevertheless, the *tendency* towards conservation of absolute angular momentum is instrumental in producing jet streams originally, and in developing strong anticyclonic shears.

(*4*) Wind speeds in the jet stream can build up only to a certain limiting value, beyond which cyclonic shears would be generated that produce dynamic instability. The resulting turbulence would tend to dissipate excessive kinetic energy in the jet core. This turbulence evidently puts a limitation on the latitude range over which air can travel meridionally under conservation of absolute angular momentum.

ARAKAWA (1951) has derived a criterion of limiting cyclonic shears:

$$-\frac{\partial u}{\partial y} = \frac{f}{2} + \frac{2u}{R} \tan \phi \tag{8}$$

by comparing the excess centrifugal force, constituting the turbulence generating force, of a meridionally displaced air parcel with the Reynolds stresses, representing the turbulence alleviating force. More refined stability criteria for zonal shear, taking into proper account the fact that a fluid motion is stable if its eddy kinetic energy decreases with time, have been derived by KAO (1964).

(*5*) Under given conditions of heat input at the equator and removal at the pole in a rotating "dish pan" or in the atmosphere, a simple meridional trade wind cell across the whole hemisphere will establish itself only if the resulting transport of momentum does not generate excessive shears. This will be the case if the Coriolis parameter, i.e., the rate of rotation of the system, is sufficiently small.

If the rotation rate is high, such as the earth's, the tradewind or Hadley cell can no longer extend over the whole hemisphere but will break down in subtropical latitudes (see Fig.1). Since the meridional circulation alone is no longer capable of transporting heat and momentum effectively across the latitude belt in which this breakdown occurs, horizontal eddies in the form of Rossby waves—i.e., "meanders" superimposed upon the jet stream belt—must carry out part of the required transport.

In dish pan experiments we find, that above some critical rate of rotation, the Hadley regime with a jet stream in polar latitudes breaks down. The jet stream shifts to lower latitudes and at the same time ceases to be a ring symmetrical about the pole. It assumes a wave pattern with the hemispheric wave number larger the faster the rate of rotation (FULTZ, 1960).

(*6*) Both experimental evidence and reasoning lead us to accept the existence of a belt of westerlies in subtropical latitudes, with strong shears on its cyclonic and anticyclonic sides. Thus, the formation of a jet stream—specifically of the "sub-tropical jet stream"—has been deduced without resorting to considerations of the temperature distribution and the resulting pressure gradients.

PALMÉN's (1954) circulation model (see Fig.1) contains a second jet stream above the strong temperature gradients of the "polar front." The Staff Members of the Department of Meteorology, University of Chicago (ANONYMOUS, 1947), together with ROSSBY

(1947), suggested a different mechanism responsible for the formation of this jet. They postulated the mixing of vorticity in the cold air lying over the polar cap of the earth, until a uniform absolute vorticity distribution is reached. Certain observational evidence supports these deductions, but the fact that the jet stream core (i.e. the region of strongest winds) is found in the warm air south of the frontal zone, rather than in the polar cold air north of it, remains unexplained by this theory.

As suggested by PALMÉN's (1954) circulation model, the air ascending northward over the polar front should be expected to attain large westwind components if its absolute angular momentum is conserved. The presence of an indirect circulation cell (Ferrel cell) between the two direct cells in polar and equatorial latitudes suggests the presence of two jet-stream systems, even without taking recourse to Rossby's mixing theory.

We have already mentioned the necessity of horizontal eddies in transporting momentum and heat across subtropical and mid-latitudes. In a regime of steady-state Rossby waves, such as may be generated in dish pan experiments, the required meridional and eddy transports can be accomplished by one jet-stream system. Even though in these experiments we cannot distinguish between subtropical and polar-front jet streams, an indirect circulation cell appears if the data are averaged around latitude circles (RIEHL and FULTZ, 1957, 1958).

If the rate of rotation of the dishpan is increased further, the regime of symmetric waves gives way to a sequence of westerly waves which form and dissipate together with individual jet maxima, similar to what is observed in the earth's atmosphere.

The state of tropospheric circulation in the atmosphere is even more complicated than suggested by the irregular Rossby waves in a dishpan. Air mass differences between arctic, polar, and tropical air generate several frontal zones; each frontal zone carries a separate jet stream (GIBSON, 1964). Thus, at times, we may find three or more jet streams in one meridional cross-section for a particular day and longitude.

So far we have concerned ourselves only with a physical explanation of the fact that jet streams exist in the troposphere. Differential heating and a tendency toward conservation of angular momentum evidently suffice to explain the gross features of tropospheric circulation. We have not included any considerations of the pressure or temperature fields.

(7) The appearance of a band of strong winds in the upper troposphere is closely associated with a baroclinic frontal zone underneath. Consequently, the existence of the jet stream is reflected in the thermal wind equation, assuming quasi-geostrophic conditions of flow throughout the troposphere.

The geostrophic wind equation may be written in the form:

$$V_g = -\frac{\alpha}{f}\nabla_h \mathrm{p}$$

which follows from eq.1 under conditions of steady ($\dot{V}=0$), horizontal ($\mathrm{w}=0$) and frictionless ($F=0$) flow. Eliminating the specific volume from eq. 9 by substituting from the equation of state:

$$\alpha = \frac{R\mathrm{T}}{\mathrm{p}} \tag{10}$$

and by using the hydrostatic equation in the form:

$$g = -RT\frac{\partial \ln p}{\partial z} \tag{11}$$

we derive the thermal wind equation for steady, horizontal, frictionless geostrophic flow:

$$\frac{\partial \boldsymbol{V}_g}{\partial z} = \frac{\boldsymbol{V}_g}{T} \cdot \frac{\partial T}{\partial z} - \frac{g}{fT}(\nabla_h T \times \boldsymbol{k}) \tag{12}$$

The correlation between temperature, pressure and wind fields, as expressed by eq.9 and 12 is the basis of the so-called "confluence theory" of jet-stream formation (NAMIAS and CLAPP, 1949). This theory states that confluence of air masses of different temperature accentuates the horizontal temperature gradients, leading to an increase of wind speeds and to jet stream formation aloft. Since, however, confluence of sufficient magnitude in the lower atmosphere is always associated with a pre-existing jet stream, this theory accounts for the intensification of a jet, but not for its original generation. This fact was well recognized by NAMIAS (1952) but overlooked by others (DAHLER, 1957, 1960).

Under the influence of solar radiation alone we should expect a rather broad and diffuse baroclinicity in the troposphere between equator and pole. If a simple meridional circulation cell could be held responsible for the tropospheric circulation, (moist) adiabatic cooling of the rising equatorial air in the upper troposphere and adiabatic warming of the sinking polar air would tend to decrease the meridional temperature gradient. There is no mechanism in the radiation budget of the atmosphere to produce sharp frontal zones as they are actually observed. These zones, therefore, must be a consequence of the jet streams and their dynamics, rather than their cause.

As has been pointed out by RAETHJEN (1958, 1961) and others (NEWTON, 1959a; REITER, 1961a, 1963a) atmospheric motions follow a *principle of adaptation* whereby the pressure field adjusts itself to the wind field and vice versa. This action tends to limit the ageostrophic components of large-sale motions and tends to satisfy the geostrophic (or the gradient) wind equation, to a close approximation:

$$V = \frac{rf}{2}\left[\mp 1 \pm \sqrt{1 + \frac{4V}{rf}}\right] \tag{13}$$

This adaptation is not complete and instantaneous. Ageostrophic components *are* present and *are* of importance in the atmosphere. It may suffice for the moment to state that an adaptation tendency does exist.

Let us review briefly our reasoning. The radiation budget of the earth generates a meridional temperature gradient. This, in turn, causes pressure gradients which tend to produce a large trade-wind cell. In the mean this cell cannot be maintained under the rotational conditions of the earth but breaks down into the 3-cell pattern shown in Fig.1, leading to the formation of jet-streams in temperate latitudes. If the original radiation-controlled temperature gradients, which caused the circulation, remained unchanged, these jet-streams would be strongly ageostrophic—in reality they are not.

We assume these jet streams are generated by a meridional circulation acting in concert with a tendency toward conservation of angular momentum and with an atmospheric adaptation mechanism. Thus, the originally diffuse meridional temperature gradient concentrates into frontal zones under the dynamic influence of the flow pattern. From the point of view of the global circulation of the atmosphere, the frontal zones and their strong horizontal temperature gradients become an effect of, rather than a cause for, the jet streams.

If we focus our attention on individual jet streams and their related wind and temperature fields, this postulate assumes a secondary philosophical importance. The geostrophic and gradient wind equations, as well as the thermal wind equation, state an equivalence of forces, but not the direction in which a causal chain should be followed. In other words, our basic dynamical equations enable us to judge the equilibrium of simultaneously acting forces, rather than to establish a sequence of events.

(8) The jet streams described in the foregoing not only are characterized by well-marked horizontal shears, but by strong vertical shears as well. A well-defined level of maximum wind in the atmosphere may, *in first approximation*, be identified with the tropopause. (In the case of individual jet maxima, the level of maximum wind may deviate significantly from the tropopause level as a result of the dynamics of the jet stream.) In the dish-pan the maximum "wind" level lies at, or close to, the free surface of the water. Jet streams in the upper stratosphere and mesosphere show an affinity for levels of significant change in lapse rate (MURGATROYD, 1957). We may, therefore, make the general statement that jet streams are "pause" phenomena. Several of these changes in lapse rate are of enough climatological significance to appear in mean soundings and to be represented in the "standard atmosphere" (see Chapter 2).

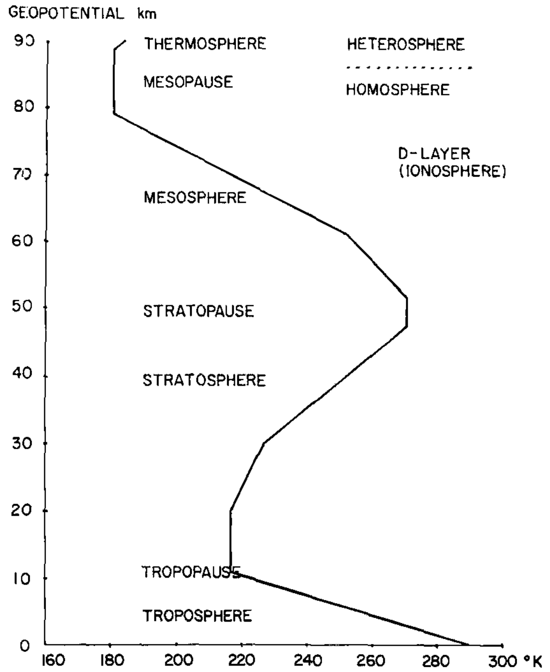

Fig.2. Temperature distribution and nomenclature after the *U.S. Standard Atmosphere 1962* (ANONYMOUS, 1962).

Fig.2 shows a schematic temperature distribution, together with the current nomenclature of atmospheric layers. According to this diagram, the lowest significant discontinuity occurs at the *tropopause*. Here we find the system of *tropopause jet streams*, whose existence—in part—we have justified in the foregoing.

Marked changes in lapse rate occur below the tropopause at frontal and subsidence inversions. Since the levels at which such inversions may be found vary over the whole depth of the troposphere, they are not evident in the "mean" sounding shown in Fig.2. Nevertheless, wind maxima associated with significant horizontal and/or vertical shears are frequently observed at such inversions, either in the form of a *low-level jet stream* (vertical as well as horizontal shears) or of an *inversion wind maximum* (large vertical shears only).

At higher levels we find jet streams associated with the stratopause. Even the discontinuity between the isothermal and the inversion portion of the stratosphere seems to be reflected in vertical wind profiles, sometimes showing a wind maximum (GODSON and LEE, 1958), sometimes a minimum. Jet streams in the ocean, like the Gulf Stream or the Kuroshio, lie close to the free surface (ISELIN, 1936; NEWTON, 1959b) and would qualify as "pause" phenomena.

We now restrict ourselves to a discussion of the tropopause as a jet stream controlling surface, realizing, however, that similar reasoning could be applied to jet streams occurring elsewhere under similar geophysical conditions. If we accept the idea, that the mean tropospheric lapse rate is produced by vertical mixing processes, while the mean isothermal state of the stratosphere is indicative of predominant radiation processes, we have no difficulty in recognizing the tropopause as a "lid" on the vertical and meridional circulations shown in Fig.1. In view of the latitude dependence of radiation absorbed at the ground we should expect a similar functional relationship for vertical mixing processes in the troposphere, hence a tropopause sloping from the equator to the pole.

An over-simplification in this concept becomes apparent if we consider winter conditions, when no radiation is received at high polar latitudes. According to this primitive model of the atmosphere, there should be no troposphere present in the polar-night region. Actual observations show this is not the case. Evidently horizontal advection and exchange processes have sufficient strength to render our primitive model invalid. Nevertheless, we may find the tropopause over polar regions as low as 8 km, and in tropical regions as high as 18 km, indicating a certain convective control of tropospheric depth.

The thermal wind equation (eq.12) explains the connection between maximum wind level and tropopause, if the latter shows a general slope from the equator to the pole. The discontinuity in vertical lapse rate at the "pause" will, under these conditions, cause a reversal of the horizontal temperature gradient. According to eq.12, a level of maximum or minimum winds $\left(\frac{\partial V_g}{\partial z} = 0\right)$ should coincide approximately with the level at which $\nabla_h T = 0$ (if the first term on the right-hand side of eq.12 is neglected).

The level of maximum wind (LMW) should only in first approximation be identified with the tropopause level. Actually, one should find the LMW *above* the tropopause over the cold polar air, *below* the tropopause in warm subtropical air. This conclusion is very well substantiated from observational evidence.

Fig.3 shows a cross-section through a jet stream over the U.S.A. It illustrates very well a number of peculiarities associated with the tropopause–jet stream relationship. For the stations Green Bay (GRB), Wisc.; and Peoria (PIA), Ill., abnormally high tropopause pressures (<400 mbar) have been coded (heavy black dots). The stations Columbia (CBI), Mo.; Topeka (TOP), Kans.; and Oklahama City (OKC), Okla., on the other hand show

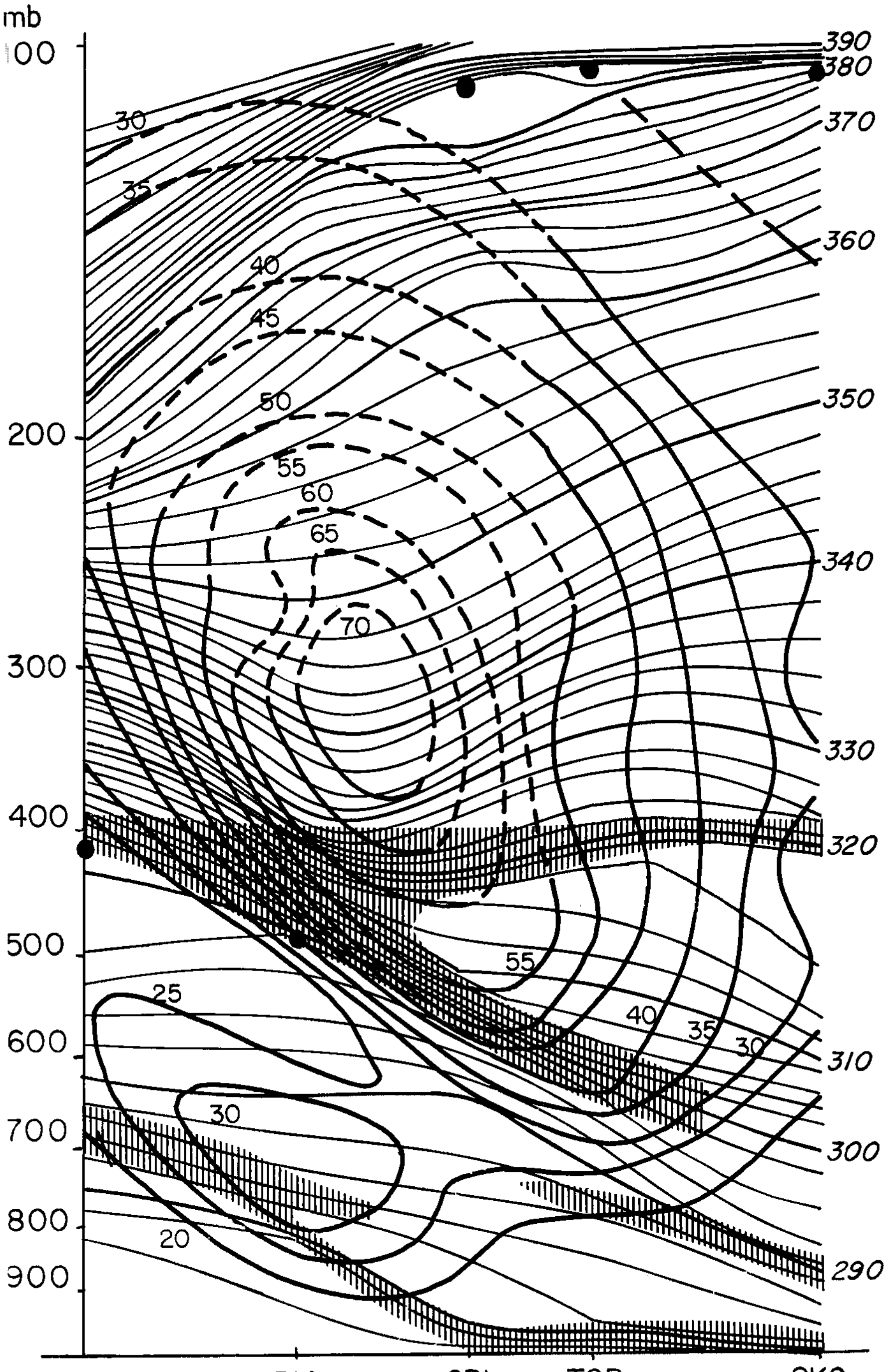

Fig.3. Cross section through the atmosphere from Green Bay (GBR) (Wisc.) to Oklahoma City (OKC) (Oklahoma); 22 November, 1962, 12h00 G.M.T. Heavy full and broken lines: isotachs (m/sec—vertical numbers); thin lines: potential temperature (°K—slanting numbers). Vertical hatching indicates stable layers. Heavy dots mark the coded tropopause levels. (After REITER and MAHLMAN, 1964.)

tropopause pressures near 100 mbar, as they would be characteristic for the tropical atmosphere. Over the latter three stations, a discontinuity of lapse rate is evident near the 400-mbar level, which was not considered as a tropopause.

The definition of a "tropopause" is somewhat arbitrary in nature as is demonstrated by the preceding discussion. According to current radiosonde coding regulations, the tropopause is the bottom of a stable layer in which the lapse rate is less than 0.2°C/100 m and the layer has to be at least 2 km thick. Furthermore, in accordance with these coding procedures, the temperature sounding is approximated by a straight line, as long as this line does not deviate from the mean sounding by more than 2°C, and as long as the mean temperature between standard isobaric surfaces (which affects the thickness and height computations) is conserved.

As a result, it is not surprising that the occurrence of tropopauses shows a rather odd frequency distribution (DEFANT, 1958), favoring standard isobaric surfaces and the 10-mbar intervals in between.

Returning to Fig.3, we see that in spite of all these shortcomings, the level of maximum wind tends to lie above the polar tropopause with low potential temperatures, and below the tropical or subtropical tropopause—whatever the case may be—with high potential temperatures. We note also that slightly poleward of the jet-stream core the surface of the tropopause is ruptured. This phenomenon is called the "tropopause break" or "tropopause gap." Its association with the jet stream has been used successfully in tracing the position of jet streams from analyses of tropopause heights, pressures, or temperatures, and by watching for belts in which these parameters show a sharp discontinuity (DEFANT and TABA, 1958a, b, c). The tropopause break is evidently caused by the dynamics of the jet stream, specifically by vertical motions in the jet-stream region. Since the tropopause acts as a "lid" on convective motions induced by heating of the ground, we should expect the maximum poleward flux of mass, heat, and momentum below, but near, the tropopause, as indicated in Fig.1. From the point of view of large-scale mean motions we may consider the anticyclonic side of jet-streams formed near the tropopause to be the "active" side (shears are generated here by the tendency to conserve angular momentum), and the cyclonic side to be the "passive" side (shears are generated by Reynold's stresses and drag from the high-speed jet core, following ARAKAWA's (1951) argument). With a sloping tropopause, intersecting the level of maximum wind as well as the isentropic surfaces, one should expect that turbulent mixing processes, which were postulated to generate the cyclonic shears, might provide an exchange of tropospheric and stratospheric air masses in the region where the LMW intersects the tropopause. If these mixing processes were strong enough, a sharp and well-defined tropopause might not be found at all in the area of strong cyclonic shear.

The dynamics of large-scale circulations and of jet streams

Conservative properties

The hydrodynamic principles governing atmospheric motions have been studied closely only for tropospheric flow patterns. They are universally applicable in the same form, however, as long as we may neglect electromagnetic forces acting in an ionized medium. Up to ionospheric heights, therefore, essentially the same system of equations is valid. In studying the laws of atmospheric motion we try to define conservative properties which are easily measured, and which enable us to follow the movement of individual air parcels in space and time. As we shall see, several of these properties are conserved only under restricting conditions. The term "quasi-conservative" is, therefore, more befitting for these.

In utilizing "conservative properties" for tracing atmospheric motions one usually encounters a major problem in the definition of boundary conditions. A property characteristic of an air parcel will be conserved only if the air parcel may be considered a closed system, i.e., if no exchange of this property takes place across the boundaries of this air parcel. This rather sweeping assumption appears well justified, as long as no large gradients of the property are observed near the air parcel under consideration. If sizeable gradients are present, flux or mixing processes will gradually change the characteristic parcel property. Still, we may consider the property "quasi-conservative" for time periods significantly shorter than the time scale involved in these fluxes. As an example, potential temperature may be taken as a conservative quantity in the absence of condensation processes and of turbulent mixing, even though adiabatic processes are never actually realized in the atmosphere because of ever-present radiation fluxes. Under normal conditions these fluxes are very slow-acting, however, so that at least for time periods commensurate with synoptic observation intervals, and for accuracies within the limits of our upper-air observation systems, dry-air motions may be considered adiabatic.

Several of the more important conservative properties of air parcels[1] are discussed in the following paragraphs. In these discussions no attempt is made to present detailed derivations of the functional relationships used. For such detail the reader is referred to current texts on dynamic meteorology.

Conservation of mass

The continuity equation:

$$\nabla\cdot(\rho V)=\rho\nabla\cdot V+V\cdot\nabla\rho=-\frac{\partial\rho}{\partial t} \tag{14}$$

states the fact that mass is conserved during atmospheric flow processes. Imports and exports across the boundaries of the volume containing the air parcel will have to be compensated by density changes within the volume. Substitution into the pressure tendency equation at the level H yields the statement that pressure changes at a given level are produced by mass divergence or convergence in the air column above this level:

$$\left(\frac{\partial \mathrm{p}}{\partial t}\right)_H=\int_H^\infty\frac{\partial\rho}{\partial t}\,\mathrm{d}\Phi=-\int_H^\infty\nabla\cdot(\rho v)\mathrm{d}\Phi \tag{15}$$

where $\mathrm{d}\Phi=g\cdot\mathrm{d}z$ is the earth's gravitational potential.

Since the actual magnitude of divergence in the atmosphere, especially near the ground and near jet-stream level, calls for pressure changes almost two orders of magnitude larger than those actually observed, a *compensation principle* has to be active in the atmosphere. Divergence aloft is to a large degree compensated by convergence near the ground and vice versa. The small residual of vergences in this primitive two-layer model

[1] The term air "parcel" is used instead of air "mass." Recent investigations, mainly in connection with radioactive fallout, have brought out the fact that "air masses," formerly considered to be homogeneous within relatively large anticyclonic pressure systems, may show large variations in their radiochemical properties. The old concepts of "air masses" as large homogeneous bodies of air, therefore, may be misleading at times. The concept of atmospheric fronts constituting "air mass boundaries" also needs revision, as will be pointed out in the text.

of the atmosphere accounts for the observed pressure tendencies. Theoretically, a level of *non-divergence* should exist somewhere in the middle troposphere, dividing the two compensating atmospheric layers. Statistical evidence (LANDERS, 1955, 1956) shows, that it is more appropriate to speak of a *layer of minimum divergence*, which on the average is located near the 600-mbar level. The compensation principle was first discovered by DINES (1912, 1919, 1925) and independently by SCHEDLER (1917) from stratospheric and tropospheric temperature statistics.

For an incompressible fluid the continuity equation (eq.14) reduces to the statement that the horizontal divergence D_h has to be compensated by a corresponding change in the thickness Δp of the layer over which D_h is measured, and which is contained between two physical surfaces (e.g., between two isentropic surfaces under adiabatic flow conditions):

$$D_h \equiv \frac{\partial u}{\partial x} + \frac{\partial v}{\partial y} = -\frac{\partial \omega}{\partial p} \tag{16}$$

The vertical velocity in a coordinate system with pressure as vertical coordinate is given by:

$$\omega = \frac{dp}{dt} \tag{17}$$

Thus:

$$\bar{D}_h = -\frac{1}{\Delta p}\frac{d\Delta p}{dt} \tag{18}$$

where $\bar{D}_h$ stands for the *mean* horizontal divergence in the layer Δp. It follows that:

$$\frac{\partial D_h}{\partial p} = -\frac{\partial^2 \omega}{\partial p^2} \tag{19}$$

For the level of non-divergence eq.16 indicates that vertical velocities should have extreme values. The level of extreme divergence at jet stream altitudes should coincide with an inflection point in the vertical velocity profile of an incompressible atmosphere (eq. 19).

Conservation of energy

Scalar multiplication of eq.1 by $\boldsymbol{V}$ yields, after manipulation:

$$\frac{d}{dt}\left(\frac{V^2}{2} + gz\right) = -\alpha \boldsymbol{V}\cdot\nabla p + a\boldsymbol{V}\cdot\boldsymbol{F} \tag{20}$$

This equation shows that changes in kinetic ($V^2/2$) and potential (gz) energy per unit mass of an air parcel should be reflected by ageostrophic flow across isobars ($\boldsymbol{V}\cdot\nabla p \neq 0$) and/or by frictional dissipation. The latter would convert energy of motion into energy of heat. Following a derivation by DANIELSEN (1961), with Θ as an explicit variable and neglecting frictional effects, we may obtain from the First Law of Thermodynamics and Poisson's equation, the expression:

$$c_p \frac{T}{\Theta}\frac{d\Theta}{dt} = \frac{d}{dt}\left(\frac{V^2}{2}\right)_\Theta + \frac{\partial}{\partial\Theta}\left(\frac{V^2}{2}\right)\frac{d\Theta}{dt} + \left(\frac{dM}{dt}\right)_\Theta + \frac{\partial M}{\partial\Theta}\frac{d\Theta}{dt} - \left(\frac{\partial M}{\partial t}\right)_\Theta \tag{21}$$

where $M = gz + c_pT$ is the Montgomery stream function (MONTGOMERY, 1937). Under the hydrostatic assumption $\frac{\partial M}{\partial \Theta} = c_p \frac{T}{\Theta}$, we obtain by integration with respect to time:

$$\int \left(\frac{\partial M}{\partial t}\right)_\Theta dt = (M_2 - M_1)_\Theta + \left(\frac{V_2^2}{2} - \frac{V_1^2}{2}\right)_\Theta + \frac{\partial}{\partial \Theta}\left(\frac{V^2}{2}\right)(\Theta_2 - \Theta_1) \tag{22}$$

where subscript 1 indicates initial values and subscript 2 indicates final values.
This form of the energy equation lends itself conveniently to the construction of trajectories of air motion. The total change of enthalpy (c_pT) and of potential energy (gz) of an air parcel along its path—given by the first term on the right-hand side of eq.22—appears in part as a change in the kinetic energy of the parcel (2nd and 3rd terms on right-hand side) and in part as field changes along the path of the parcel (left-hand side of equation). The last term in this equation incorporates diabatic effects, e.g., condensation of water vapor.
The MONTGOMERY (1937) stream function also satisfies the equation for frictionless motion on an *isentropic* surface:

$$\dot{\boldsymbol{V}} = -\nabla M + f\boldsymbol{V} \times \boldsymbol{k} \tag{23}$$

In applying the foregoing to tropospheric motions, specifically to motions in the vicinity of the jet stream, the advantage of the Montgomery stream function analyses over isobaric analyses becomes immediately obvious. The latter—together with temperature analyses—imply the existence of strong vertical motions in regions, where the cross-isothermal wind component is stronger than the speed C of the isotherm:

$$w = \frac{1}{\Gamma - \gamma}\left(\frac{\partial T}{\partial t} + V\frac{\partial T}{\partial s}\right) \tag{24}$$

Γ being the dry-adiabatic lapse rate, and γ the actual lapse rate. Since:

$$\frac{\partial T}{\partial t} = -C\left(\frac{\partial T}{\partial s}\right) \tag{25}$$

$$w = -\frac{1}{\Gamma - \gamma}(V - C)\frac{\partial T}{\partial s} \tag{26}$$

This fact is frequently overlooked. The meteorological profession has become "brainwashed" during more than a quarter-century of isobaric upper-air analysis.
In viewing sharp upper troughs, for instance, we tacitly assume that the air moves around the bend. The curvature of the contour lines is used in first approximation to yield the streamline curvature. With a correction for the movement of the system an approximate trajectory curvature is obtained. This then, together with the geostrophic wind speed derived from contour spacing, is used to compute the gradient wind (see STALEY, 1961). We hardly ever stop to think that air parcels in sharp troughs do not follow the curvature indicated by the contour lines, but they move—in the absence of condensation and sublimation processes—along isentropic surfaces, as described by eq.22 and 23. Thus, isobaric and isentropic trajectories will yield completely different impressions of air motions. In extreme cases the sense of curvature may even reverse its sign in going from one method to the other (DANIELSEN, 1961).
What this means in terms of jet-stream structure may be illustrated with the following example (REITER and NANIA, 1964). Fig.4 and 5 show 250-mbar isotach and isotherm

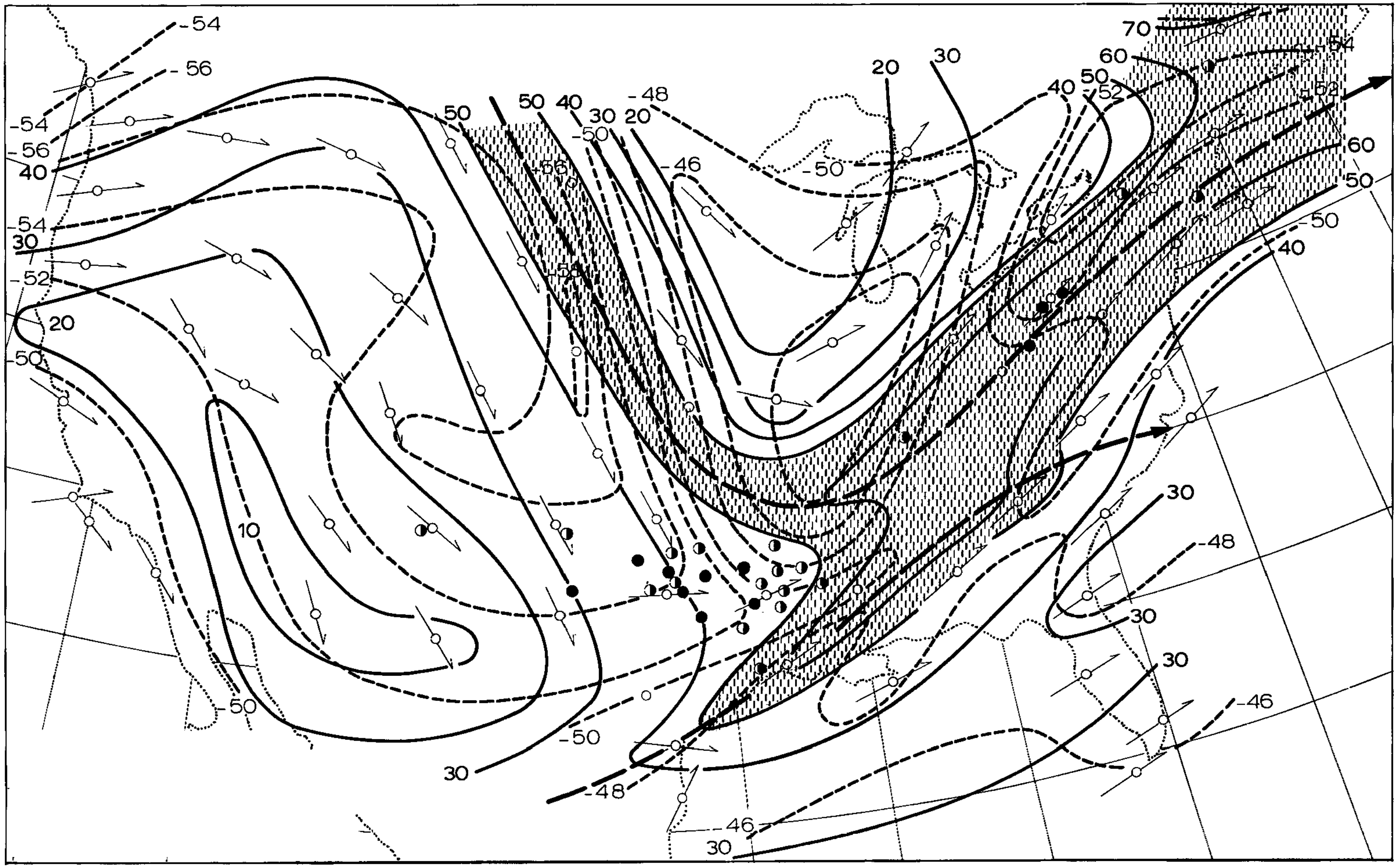

Fig.4. Isotachs (m/sec, solid lines, heavy numbers) and isotherms (°C, dashed lines, light numbers) of the 250-mbar surface, 13 April 1962, 00h00 G.M.T. Regions with speeds > 50 m/sec are shaded. Half-filled circles stand for aircraft reports with moderate CAT (Clear Air Turbulence), heavy dots stand for severe CAT. (Numerous reports of light CAT have not been entered.) Jet axes indicated by heavy dashed lines and arrows. (After Reiter and Nania, 1964.)

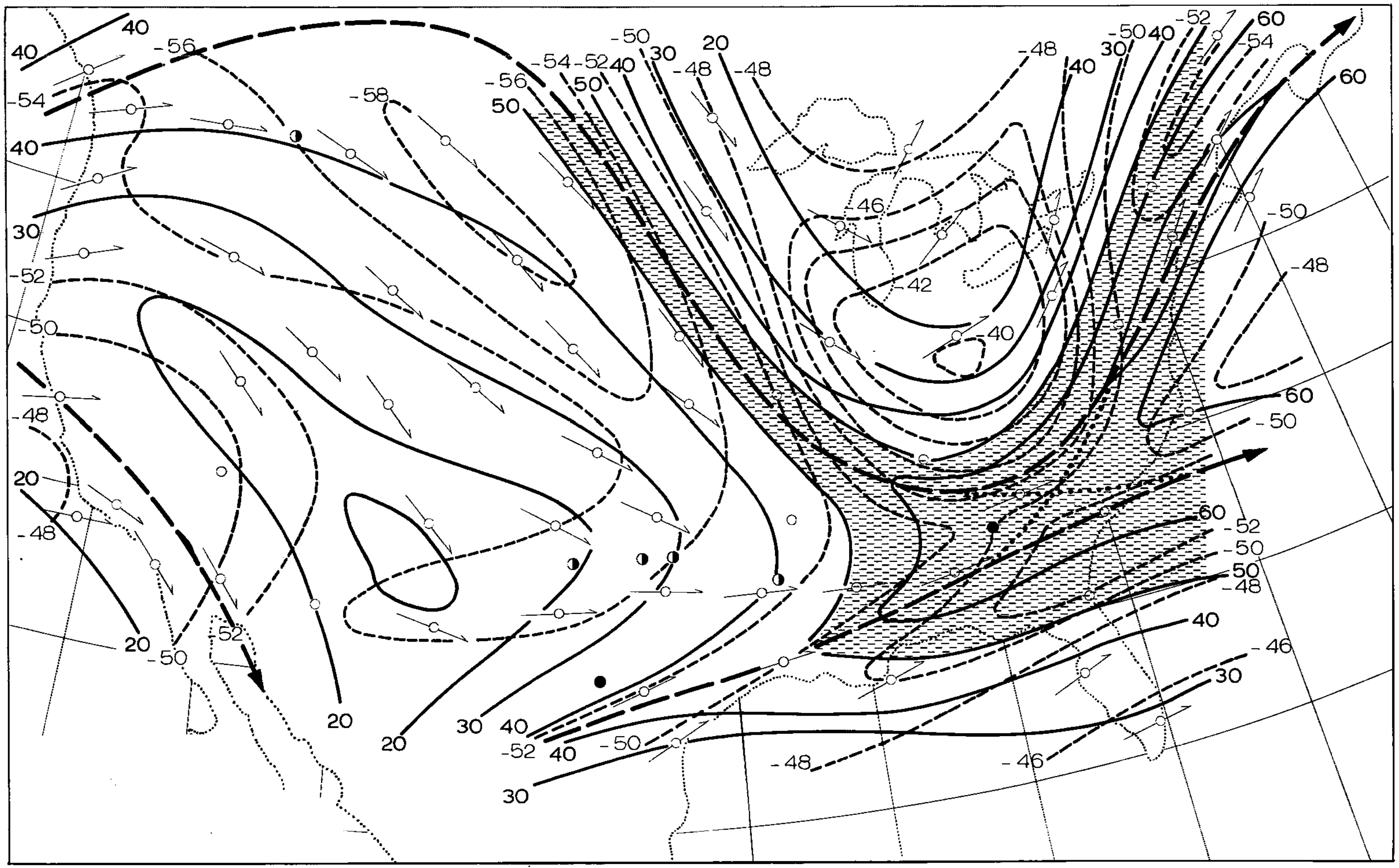

Fig.5. Same as Fig.4. except 13 April 1962, 12h00 G.M.T.

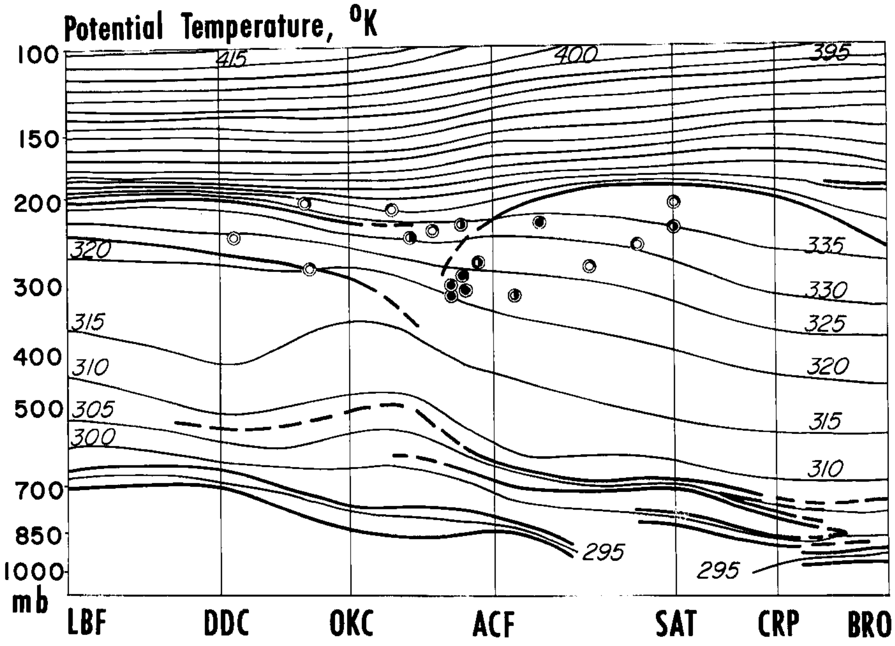

Fig.6. Cross section through the atmosphere from North Platte (LBF) (Nebr.); to Brownsville (BRO) (Texas); 13 April 1962, 00h00 G.M.T., same map-time as Fig.4. Light solid lines: potential temperature (°K). Heavy lines: tropopauses and boundaries of stable layers. CAT observations in the vicinity of the cross-sectional plane: open inner circles = light CAT; half-black inner circles = moderate CAT; black inner circles = severe CAT. The black portions of the outer rings indicate the time of CAT encounter (plus or minus 6 h from map time correspond to a black semi-circle to right or left of inner circle). (After REITER and NANIA, 1964.)

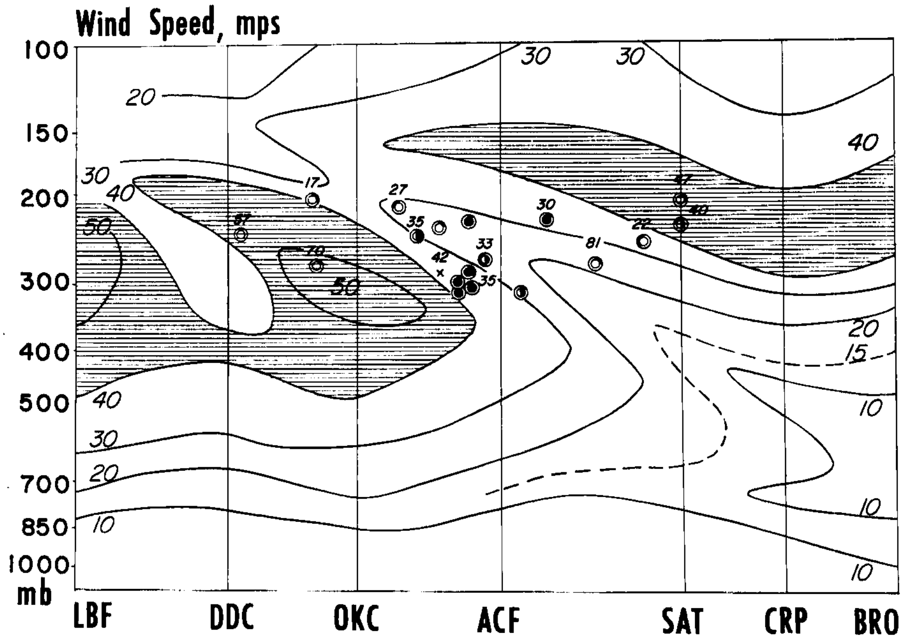

Fig.7. Same as Fig. 6, except wind speeds in m/sec. Aircraft reports are entered numerically next to CAT observations, x stands for wind report without turbulence. Regions with speeds >40 m/sec are shaded. (After REITER and NANIA, 1964).

analyses of 13 April 1962. At 00h00 G.M.T. severe clear-air turbulence was abundantly encountered over the southern U.S.A. (see p.198). The upper-flow pattern indicates the merger and subsequent splitting of two jet-streams. Following classical nomenclature one would call the southern branch a "subtropical jet stream," and the northern branch a "polar-front jet stream" (see p. 146). Most turbulence reports stem from a region where an abrupt shift in wind direction from northwest to west-southwest is apparent.
Fig.6–8 show a series of cross sections through the turbulence area. The two cores of high wind speeds (Fig.7) are associated with quite different wind directions (Fig.8). A zone in which the wind backs sharply with height (by about 70° within a layer of approximately 100 mbar or $2\frac{1}{2}$ km) and which seems to contain the moderate and severe cases of CAT, is aligned with the sloping isentropic surfaces (Fig.6).

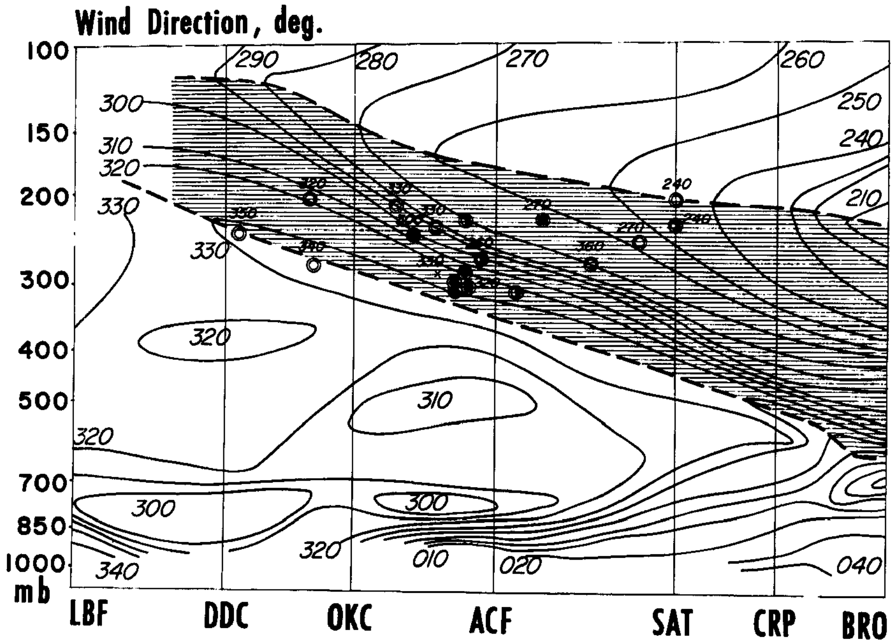

Fig.8. Same as Fig.6 and 7, except wind directions (degrees). Maximum and minimum directions are indicated by heavy dashed lines. Shaded area marks region of strong backing of wind with height. (After REITER and NANIA, 1964.)

It is quite apparent from these diagrams that the air in this two-branched jet-stream system does not follow around the strong trough indicated on the 250-mbar surface (Fig.4). Instead, the air in the northwestern jet branch descends and "slides in" underneath the southwestern branch. The air in the latter is rising. This is properly indicated by the temperature advection in Fig.4, especially if we consider that the isothermal pattern remains nearly stationary during the subsequent 12 h (Fig.5).
Fig.9 shows isentropic trajectories traced forwards and backwards from the trough region for a 12-h period. The air in the northwesterly jet branch descends quite markedly —parcels located near the jet core by as much as 190 mbar in 24 h. At the same time the cyclonic curvature on the 320°K isentropic surface is not nearly as sharp as on the isobaric map (Fig.4).

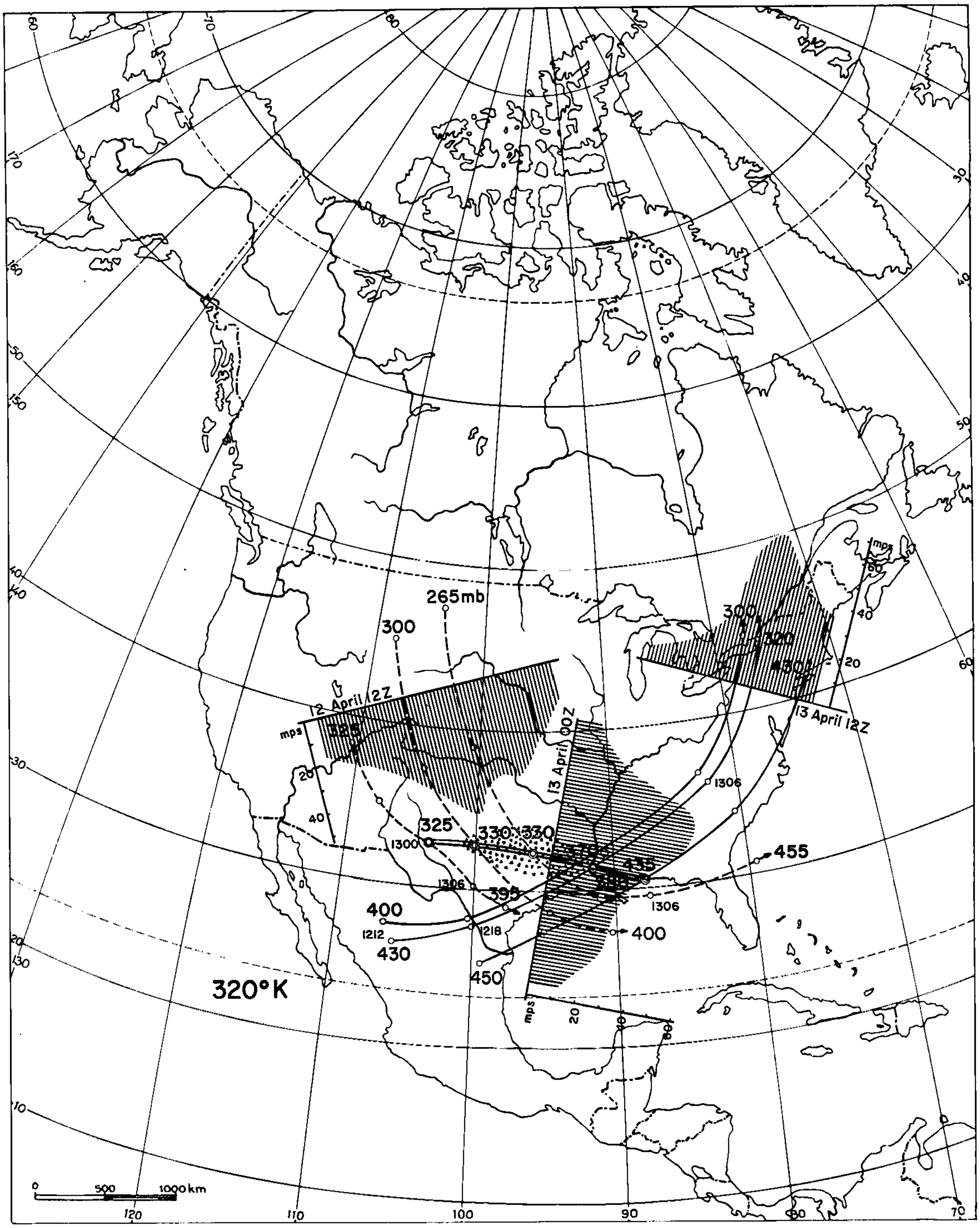

Fig.9. Trajectories along 320°K isentropic surface, tracing air motion backward and forward from the locations at 13 April 1962, 00h00 G.M.T., marked by double circles. The single circles give trajectory positions at 6-h intervals. Dashed trajectories belong to the northwestern jet branch, solid trajectories to the southwestern one. The CAT region of Fig.4 is marked by irregular shading. Wind profiles along isentropic surface, with scale in m/sec, are entered along the solid base lines which run approximately normal to the upper flow. The profiles have been constructed for map times as indicated. Note the extremely strong cyclonic shears in the profile of 13 April, 12h00 G.M.T., characterizing the warm-air flow from the southwest. (After REITER and NANIA, 1964.)

The air in the southwesterly jet branch rises gradually—again more rapidly in the jet core. It overrides the air from the northwest. Thus, from this diagram it appears that the "subtropical" jet stream should be north of the "polar front-jet" downstream from the merger zone. Even though trajectories may be slightly in error in this region due to possible moist-adiabatic processes, the shortcomings of the widely accepted nomenclature become quite apparent. If we were to apply the foregoing reasoning, jet axes should be drawn as indicated by dotted lines in Fig. 5, symbolizing a crossing-over of the flow rather than a side-by-side confluence and subsequent diffluence.

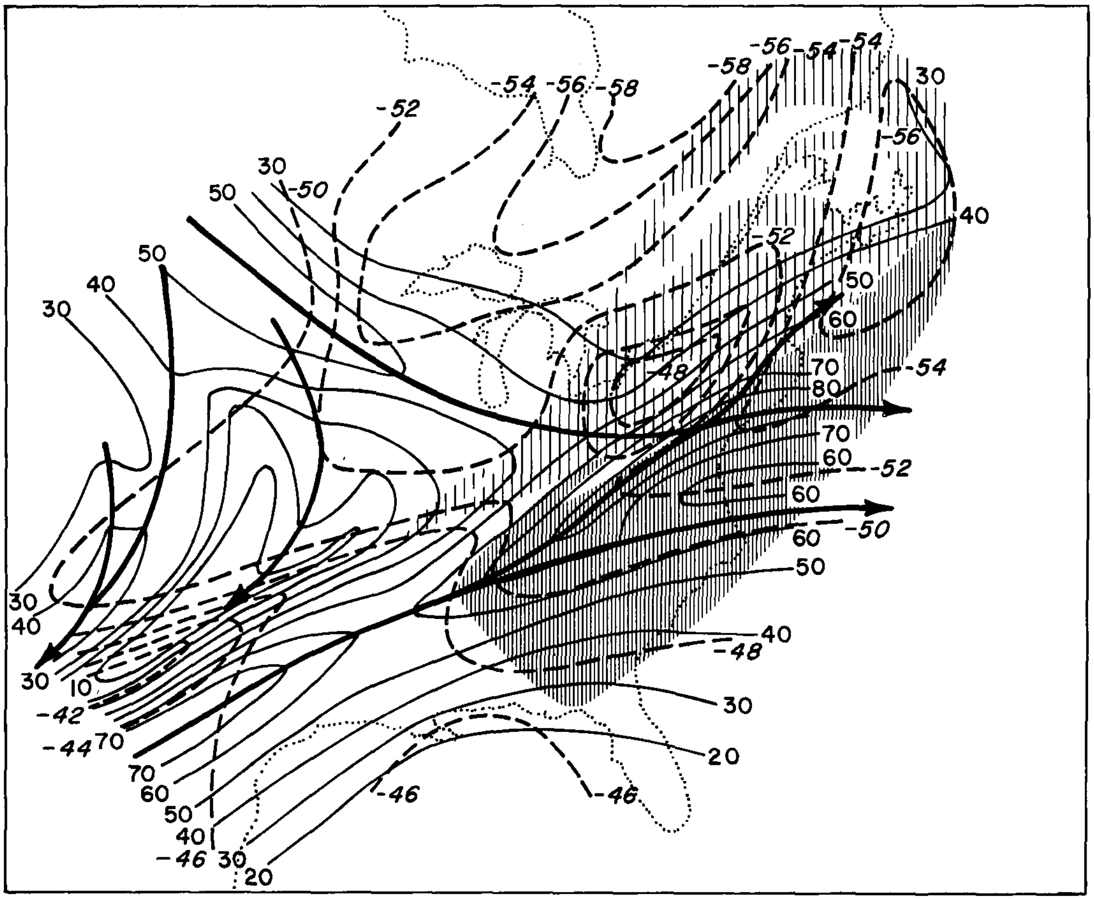

Fig.10. 250-mbar isotachs (m/sec, solid lines, vertical numbers) and isotherms (°C, dashed lines, slanting numbers); 20 November, 1962, 12h00 G.M.T. High and low level clouds according to "Tiros VI" observations (Fig.11) entered with dense and light shading. Note the similarity of the flow pattern with the one shown in Fig.4 and 5. The region of warm advection (rising motion) agrees well with the observations of high-level clouds. The abrupt edge of the cirrus-cloud bank is located near the axis of coldest temperatures, indicating the intersection of the tropopause with the 250-mbar surface.

Recent interpretations of satellite pictures corroborate these conclusions. Shadow bands which are sometimes cast on lower clouds by a high-level cloud deck (OLIVER et al., 1964), show that the flow of moist air at high levels associated with the southwestern branch of two jet streams crosses over into the northeastern branch. Fig.10 shows isotachs of the 250-mbar surface with superimposed nephanalyses of 20 November 1962, 12h00 G.M.T. "Tiros VI" pictures at 13h55 G.M.T. (Fig.11) as well as "Tiros V" photo-

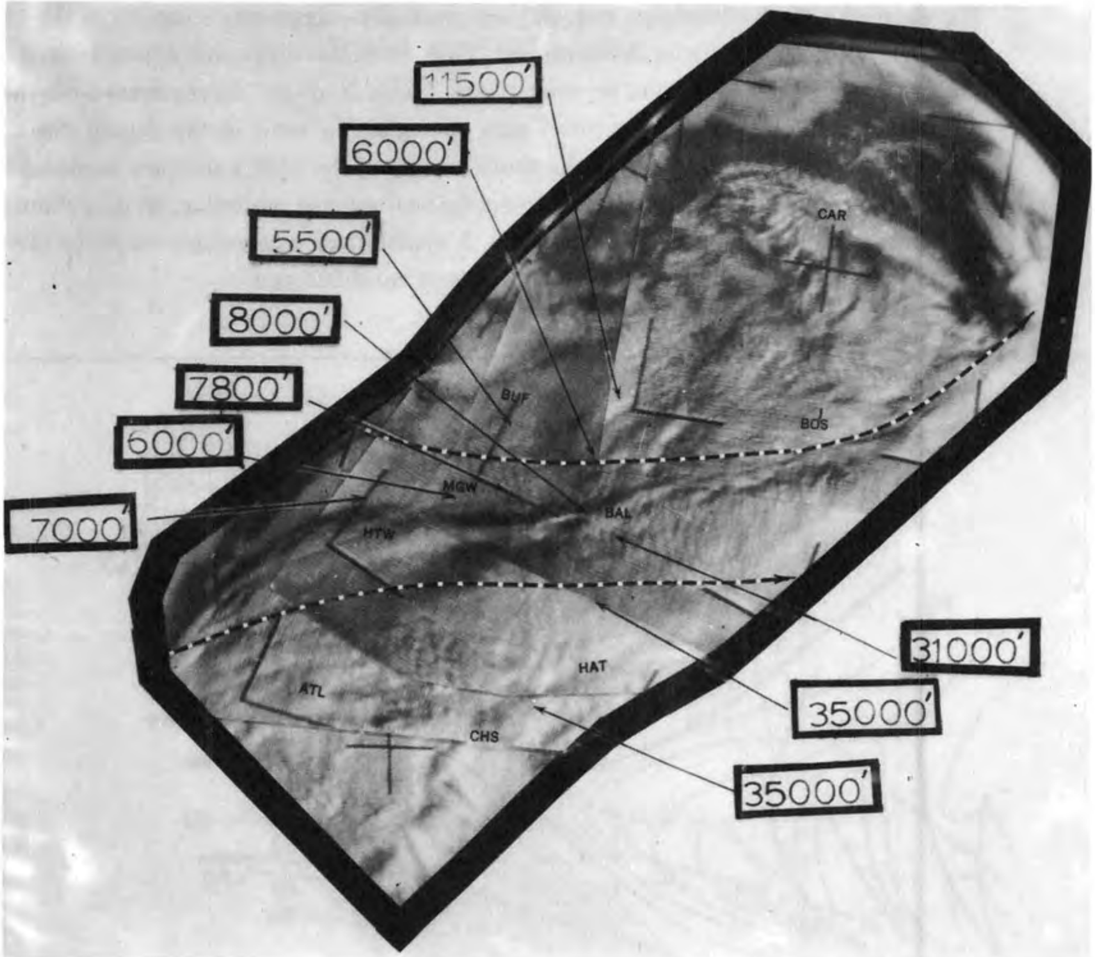

Fig.11. Mosaik of pass 0922, "Tiros VI", 20 November, 1962, 13h55 G.M.T., i.e., approximately 1 h after the map time of Fig.10. Code letters of radiosonde stations have been entered in the photograph. Cloud heights are given in feet, as reported by pilots within 1 h of picture time. Dashed lines are jet axes at the 200-mbar level. Note the dark streak, interpreted as a shadow band, emerging from the jet axis in the lower left corner of the picture, running through stations HTW and BAL, and merging with the northern jet branch in the upper right corner of the photograph. (After OLIVER et al., 1964.)

graphs at 14h48 G.M.T. (not reproduced here) show such a "shadow band" cast by a high-level cirrus deck. Similar distributions of cirrus crossing from the southern to the northern jet stream have been observed by KADLEC (1963, 1964).

With strong vertical motions present in the vicinity of upper troughs, jet streams should be more effective agents in the mixing of the atmosphere than would be indicated by isobaric charts (see Fig.4). Truly enough, we find that sinking processes as outlined above carry substantial amounts of stratospheric air into the troposphere (REITER, 1963b; REITER and MAHLMAN, 1964; MAHLMAN, 1964; DANIELSEN, 1964a, b). It has been estimated that in a jet stream of average intensity, associated with cyclogenesis and anticyclogenesis of average intensity, air masses of the order of $0.6 \cdot 10^{12}$ metric tons may be carried quasi-adiabatically from tropopause level to the ground in a matter of approximately 2–3 days. At least as much air, probably more, is introduced from the stratosphere into the troposphere at potential temperatures too high to reach the ground without diabatic cooling processes. These exchange processes between stratosphere and troposphere, in

which the jet stream figures as a vital link, are of important consequence in the transport of radioactive debris and other tracer materials (see p.112).
So far, only the adiabatic downward transport of air has been studied in detail. Fig.4–9 suggest that jet stream systems may be equally important in the return flow of tropospheric air into the stratosphere. Unfortunately, routine humidity measurements at jet stream level are, until now, not sufficiently accurate to permit a satisfactory estimate of the diabatic last term in eq.22 and the construction of reliable trajectories. More research in this field—possibly with well-equipped research aircraft—is urgently needed.

Conservation of absolute vorticity

Simplifying the so-called vorticity equation and abbreviating $D = \nabla \cdot V$, we may write for frictionless flow ($F = 0$):

$$\frac{\mathrm{d}Q}{\mathrm{d}t} = -DQ + N + (Q \cdot \nabla) V \tag{27}$$

From this equation we see that the absolute vorticity is a conservative quantity $\left(\frac{\mathrm{d}Q}{\mathrm{d}t} = 0\right)$ *only*, if the following conditions are met simultaneously:

(*1*) The flow is non-divergent ($D = 0$).
(*2*) There are no solenoids in the surface along which the motion takes place. This is the case for adiabatic motions along isentropic surfaces, as well as for motions along isobaric surfaces ($\nabla p = 0$).
(*3*) There are no velocity gradients along the direction of the vorticity vector. If there are, this will lead to the tilting of vortex tubes, hence, to changes of vorticity.
Condition *2* is easily satisfied, if we consider motions over relatively short periods of time, during which diabatic effects are of only small consequence. Preferably, these motions should follow a *sinking* tendency. This will enable us to rule out the release of latent heat from condensation processes.
The third term on the right-hand side of eq.27, which led to condition *3*, usually assumes rather small proportions if one considers large-scale atmospheric motions. Standard procedure has been to neglect these "tilting" terms. NEWTON (1954) and others (REED and SANDERS, 1953) have shown such terms to be of significant proportions, if one deals with frontogenetic and cyclogenetic processes.
Flow patterns in the vicinity of jet streams will require specific consideration of the "tilting" terms. As is shown in Fig.12, the stable region underneath the jet core—frequently referred to as the "jet stream front"—may be a place of strong sinking motion. The existence of this stable baroclinic zone is dynamically linked to the jet stream. Equatorward of this stable region, within the warm air adjacent to the frontal zone, one frequently finds extensive cloudiness, indicative of ascending motions. The stable region itself is dry, commensurate with the sinking which it is undergoing (see Fig.19). Thus, underneath the jet core and in the vicinity of the jet-stream front one may expect values of $\frac{\partial w}{\partial y} < 0$ of significant magnitude. These will combine with values of $q_y = \frac{\partial u}{\partial z} - \frac{\partial w}{\partial x}$, mainly due to strong positive vertical shears $\frac{\partial u}{\partial z} > 0$ in this region. The

major effect of "tilting terms" underneath the jet core, therefore, should be to *reduce* the absolute vorticity of the flow in this region.

Although this agrees well with observations—air sinking in the jet-stream front loses some of its cyclonic vorticity and may even curve anticyclonically—the effect of the tilting terms is usually largely overshadowed by the divergence term, $-DQ$. This term is mainly responsible for the non-conservative nature of absolute vorticity, especially in the jet stream region.

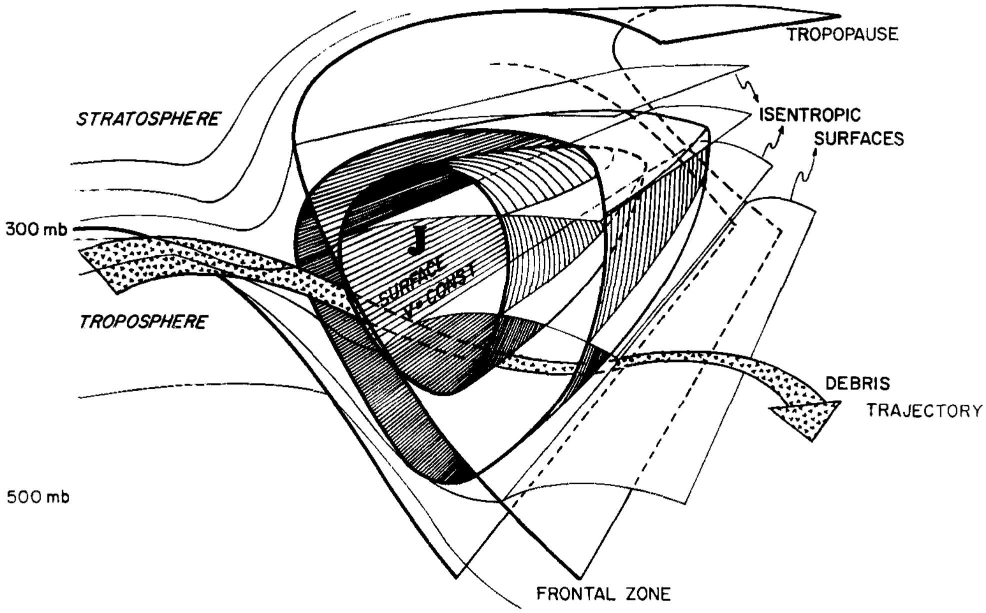

Fig.12. Schematic three-dimensional view of mass flow from stratosphere to troposphere near a jet stream. Isentropic surfaces are indicated by thin lines. Surfaces of constant wind speed, boundaries of the frontal zone, and the tropopause are marked by heavy lines.

For simplicity's sake let us consider the vertical component Q_z of absolute vorticity only. If we furthermore consider *adiabatic motions* on an *isentropic surface* (indicated by subscript "$_\Theta$"), no vertical motions through this surface will exist, hence there will be no "tilting terms" in an isentropic coordinate system. Eq.27 reduces to the simple form of:

$$\frac{\mathrm{d}Q_z}{\mathrm{d}t} = \frac{\partial Q_z}{\partial t} + \boldsymbol{V}_\Theta \cdot \nabla Q_z = -D_\Theta Q_z \tag{28}$$

We may now choose a moving coordinate system, so that:

$$\frac{\mathrm{d}}{\mathrm{d}t} = \frac{\delta}{\delta t} + (\boldsymbol{V}-\boldsymbol{C})\cdot\nabla \tag{29}$$

where $\delta/\delta t$ is the local change of a parameter in the coordinate system which moves with the velocity $\boldsymbol{C}$. If this system is chosen so that it moves with the vorticity pattern, then $\frac{\delta Q_z}{\delta t} = 0$ and:

$$(\boldsymbol{V}-\boldsymbol{C})\cdot\nabla Q_z = -DQ_z \tag{30}$$

Let V_r be the magnitude of the difference vector $(\boldsymbol{V}-\boldsymbol{C})$, i.e., the wind speed relative to the moving coordinate system, and let s_r express a relative streamline in this system, then:

$$V_r \frac{\partial Q_z}{\partial s_r} = -DQ_z \tag{31}$$

Positive vorticity advection, thus, will result in convergence ($D < 0$), negative vorticity advection in divergence ($D > 0$).
In the jet stream region: $|V| \gg |C|$. The propagation speed of jet maxima and their associated vorticity patterns usually is in the order of 10 m/sec while wind speeds frequently are in excess of 50 m/sec. Thus a good qualitative indication of vorticity advection may be readily obtained by comparing actual streamlines with the vorticity pattern, and neglecting the motion of the system in first approximation.
Expressing absolute vorticity in the form:

$$Q_z = \frac{V}{r_s} - \frac{\partial V}{\partial n} + f \tag{32}$$

where r_s is the radius of curvature of the streamlines, and n is the horizontal coordinate normal to the direction of flow (positive to its left), one sees that vorticity advection may be brought about by changes in stream-line curvature as well as of shear, and by motion towards a different latitude. The latter—producing changes in the Coriolis parameter—is of importance in the derivation of the so-called Rossby waves but is a secondary effect as far as the divergence distribution around a jet maximum is concerned.
As we have seen, strong anticyclonic shears should prevail near, and to the equatorial side of, jet streams generated under conservation of absolute angular momentum, whereas strong cyclonic shear will build up on their poleward side. Neglecting curvature for the moment, eq.32 would suggest a vorticity discontinuity, or at least a strong gradient: $\frac{\partial Q_z}{\partial n}$, in the jet axis. Thus, the jet axis should sharply divide two different vorticity advection regimes.
Since strongest shears are encountered near the jet maximum, and weakest shears prevail near the relative minimum of velocity along the jet axis, the distribution of absolute vorticity will show a regionally confined maximum poleward of the jet axis, and a confined minimum equatorward of the axis. Thus, the area about a jet maximum may be divided into four quadrants with different regimes of vorticity advection, and with conforming distribution of divergence and convergence. This is shown schematically in Fig.13. Surface pressure falls and cyclogenesis should be expected underneath the

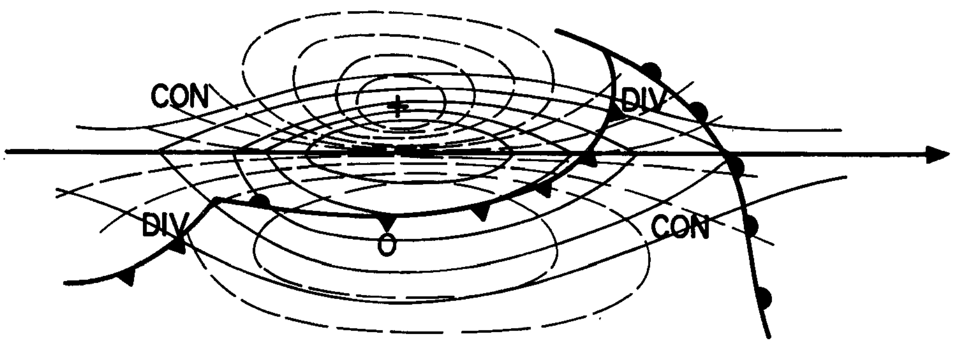

Fig.13. Schematic representation of surface fronts as well as of absolute vorticity distribution (dashed) and of divergence at the 300-mbar level in the vicinity of a jet maximum. Isotachs are drawn as full lines.

region of divergence at jet-stream level. Anticyclogenetic regions should be congruent with regions of upper convergence. The appropriate frontal systems have been entered schematically in Fig.13.

In reality, flow patterns are not as simple and clear-cut as indicated in this diagram. First of all, curvature vorticity, V/r_s, may enhance or offset the effects of shearing vorticity, $\left(-\frac{\partial V}{\partial n}\right)$. Generally speaking, cyclonic curvature of flow will render the vorticity advection pattern diffuse in the two quadrants on the anticyclonic side of the jet axis. Maximum divergence and convergence in such cases will occur close to the jet axis east and west of the trough, respectively (NEWTON and PALMÉN, 1963). Anticyclonic curvature of flow will tend to weaken the vorticity pattern in the two quadrants on the cyclonic side of the axis. In addition, horizontal shear conditions may be rather complicated. The jet-stream forming mechanism shown in Fig.1 may hold well under mean or steady-state conditions; individual jet maxima, however, are a manifestation of the non-steady character of the flow. We may expect, therefore, appreciable deviations from the idealized flow patterns previously described.

From case-studies of radioactive fallout we find that air from the lower stratosphere and from the tropopause region is moved to the ground underneath cyclogenetically active jet streams (STALEY, 1960; REITER, 1963b, 1964a; REITER and MAHLMAN, 1964; DANIELSEN, 1964a). This motion apparently does not occur in the form of a continuous "seepage," but rather in strong surges of downward transport. It has been reported on p.104, that large masses of air may be carried from tropopause level to the ground in a matter of approximately two days.

Fig.14 and 15 show the jet stream configuration on the 300°K isentropic surface of 22 November 1962, 00h00 and 12h00 G.M.T. Heavy radioactive fallout was observed between 24 and 27 November over the southern U.S.A. Fallout values exceeded 320 $\mu\mu$ curies/m^3 of dry air on 25 November (Fig.16). The atomic debris reaching the ground in the indicated area was contained within the southern branch of the splitting jet stream shown in Fig.14 and 15. The remarkable fact that debris in relatively high concentrations was encountered in an area of clearly defined extent promotes an interest in "air-body" dynamics rather than "air-parcel" dynamics. The contaminated "air-body" had apparently traveled from the Russian test site near Semipalatinsk at relatively high speeds within a jet stream. The source of the debris probably was the nuclear event of 17 November 1962 at that location. A certain amount of coherence will have to be attributed to the "air-body," if it traveled such a great distance and finally separated from the main jet stream as a discrete and large discharge towards the ground.

The still rather vague concept of "air-bodies" should not be confused with the concept of large "air masses" whose classification and utilization in forecasting was much in vogue in the forties (SCHINZE and SIEGEL, 1943)[1]. In the case of radioactive fallout shown in Fig.16, the contaminated air was embedded in a large anticyclonic system of rather uniform characteristics as established in the classical air mass types. The use of additional properties, such as radioactive contamination, or ozone concentrations, etc., evidently brings out more detail in atmospheric structure than is possible from a humidity and temperature classification only. It would appear, therefore, that "air-bodies" parti-

[1] SCHINZE's et al. (1943) air mass typification is based on the equivalent potential temperature, which enters as abscissa into his "thetagram". Pressure constitutes the ordinate of this diagram.

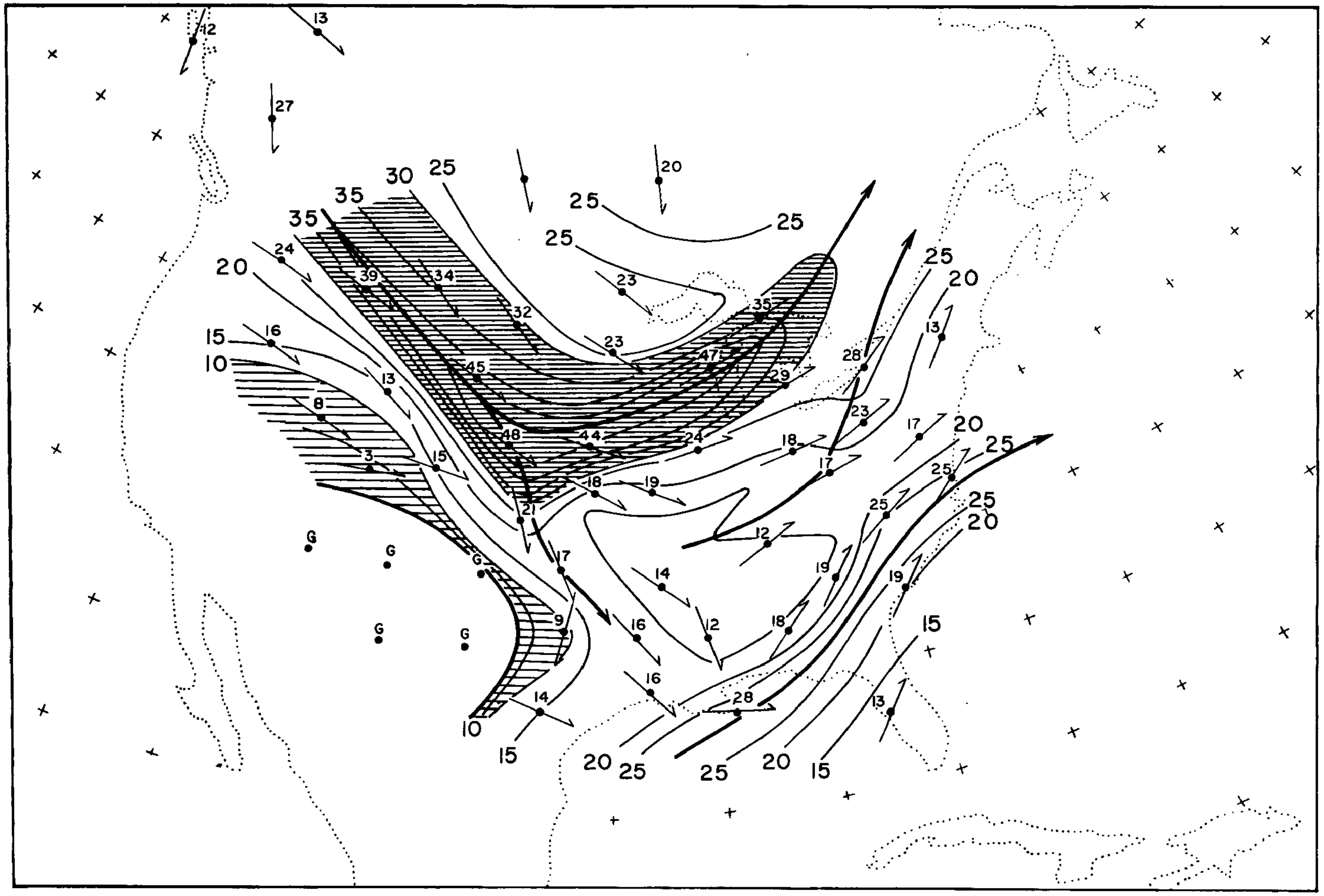

Fig. 14. Isotachs (m/sec) on the 300° K isentropic surface for 22 November, 1962, 00h00 G.M.T. Regions with speeds less than 10 m/sec and more than 30 m/sec are marked by different shading. Intersection of isentropic surface with ground is indicated by heavy line (*G* identifies stations with ground level warmer than 300° K). Jet axes are shown by heavy lines with arrows.

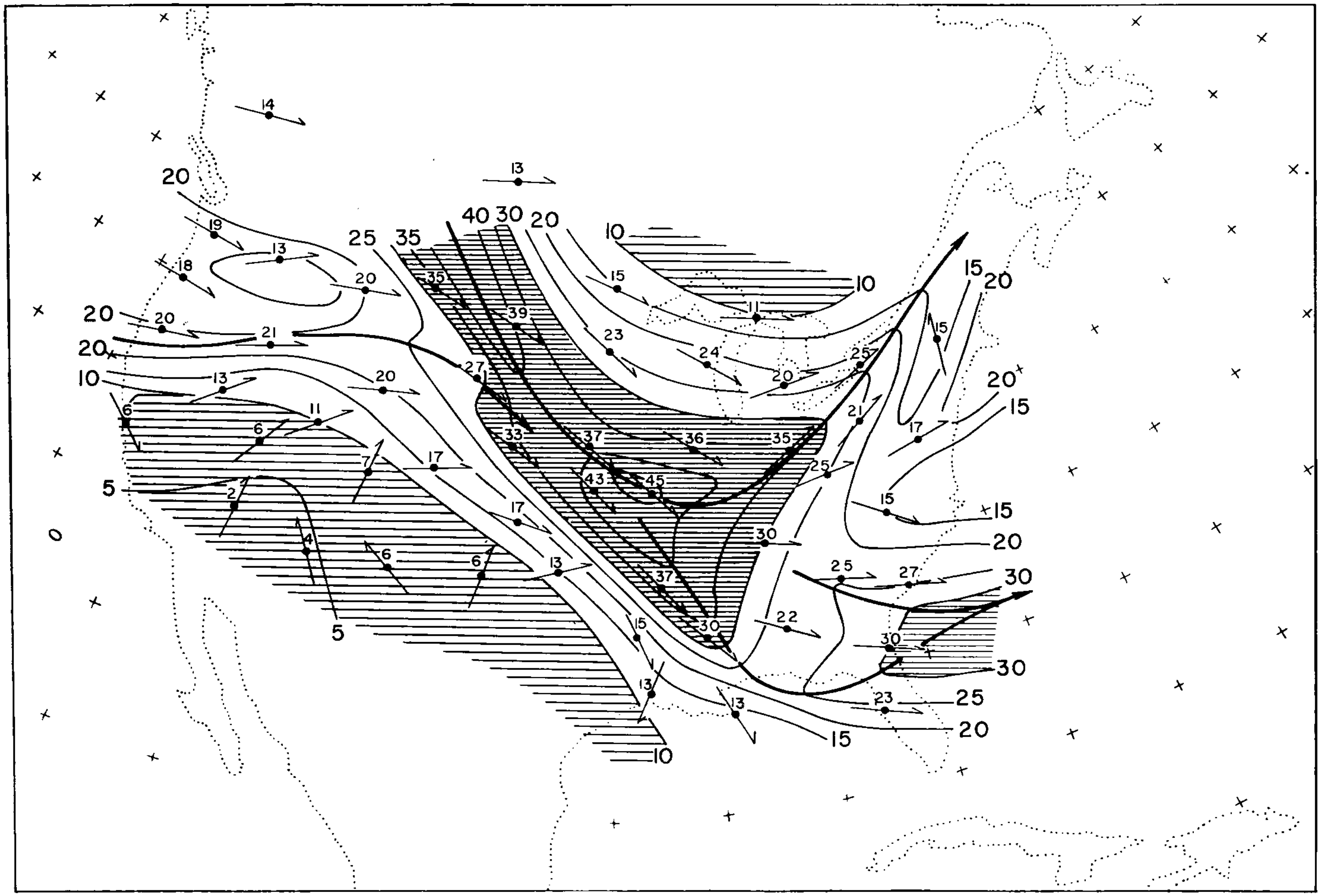

Fig.15. Same as Fig.14, but 22 November, 1962, 12h00 G.M.T.

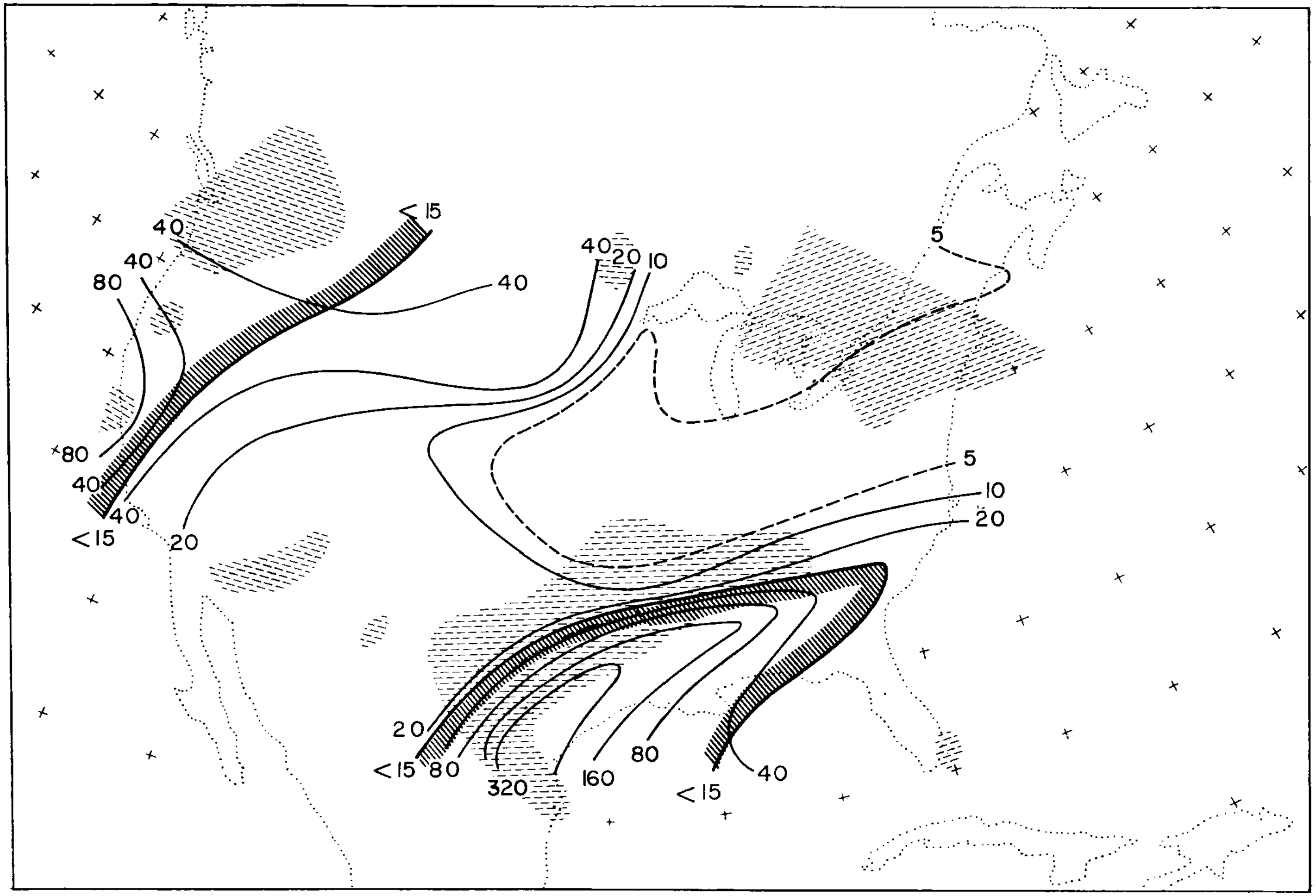

Fig. 16. Distribution of radioactive fallout on 25 November, 1962, over the contiguous U.S.A. Values are given in $\mu\mu$ curie m^{3} of dry air, as measured by the U.S. Public Health Service Radiation Surveillance Network. Average collection time in the central United States is 15h00 G.M.T., collection filters are exposed for 24 h. Line labelled < 15 and marked by a shaded band encloses area with debris age less than 15 days. Lightly shaded regions indicate precipitation during 24-h period ending 06h00 G.M.T. as reported in the *Daily Weather Maps* of the U.S. Weather Bureau. (After REITER and MAHLMAN, 1964.)

cipating in vertical exchange processes through the jet stream are on the average of much smaller extent than the classical "air-masses".

A satisfactory explanation of the so-called "cross-stream circulation," i.e., the mass exchange across the jet axis which is necessary to maintain the meridional transport of heat and momentum, hinges on finding a way by which air can cross the location of the strong vorticity gradient without having to undergo drastic vorticity changes in doing so. As we will see, potential vorticity also shows a steep gradient in, and on the cyclonic side of, the jet core, presenting an even more formidable barrier to cross-stream circulation, since potential vorticity is better conserved than absolute vorticity. Studies of fallout cases similar to the one described above indicate a solution to this problem (REITER, 1963b; REITER and MAHLMAN, 1964; MAHLMAN, 1964). Fig.12 shows a schematic cross-section through a jet stream. Debris originally located in the stratosphere on the cyclonic side of the upper current has been traced moving through the stable baroclinic zone underneath the jet core (the "jet-stream front"). It finally ends up on the anticyclonic side of the jet in a subsidence inversion (not shown in the diagram).

The air undergoing this sinking motion travels along an isentropic surface, thus conserving its entropy. Furthermore, horizontal shears and vertical stability within the stable layer are relatively large. Thus no discontinuity lines in absolute or potential vorticity will have to be crossed while the air passes from the cyclonic side to the anticyclonic side of the jet by "slipping through" underneath the jet axis. Since the surfaces of constant speed show nearly the same orientation in the stable layer as the isentropic surfaces, no strong accelerations or decelerations of air have to be postulated for this sinking process. As has been mentioned on p.104, it was estimated that $0.6 \cdot 10^{12}$ metric tons of tropopause, or lower stratospheric, air reached the ground during one such sinking process of quasi-adiabatic motion. It takes the air approximately 2 days to traverse the whole depth of the troposphere underneath a jet stream of moderate cyclogenetic activity. With several such jet maxima present around the hemisphere, and with subtropical, polar-front, and arctic-front jet streams acting at the same time, it was estimated that air equivalent to the mass of the stratosphere poleward of 45° latitude could easily be transported downward through the "tropopause gap" within one year.

With such a powerful transport mechanism acting in *one* direction, it is only natural to assume that jet streams are also instrumental in providing the return flow from the troposphere into the stratosphere. Such return flows have not yet been studied carefully, although they constitute a vital link in the understanding of atmospheric transport and exchange processes. The difficulty stems from the fact that the ascending return flow will be "contaminated" by diabatic precipitation processes. Trajectories, therefore, are difficult to construct. Moist layers with small ozone concentrations in the stratosphere might eventually be identified with tropospheric source regions.

From Fig.14 and 15 it is quite apparent that near a jet maximum, cyclonic shears may be weaker than anticyclonic ones when measured on an isentropic surface. Since air in the jet-stream region follows such isentropic surfaces more closely than isobaric ones, we evidently should revise our image of the jet-stream structure which has mainly been obtained from isobaric wind profiles. The "peaked" wind profile along an isobaric surface through the jet core gives way to a profile showing a "platform" of almost uniform winds along an isentropic surface through the "jet stream front". This platform of constant winds, again, suggests that a relatively large and coherent "air body" is transported within the stable layer. This would not become apparent at all from the strong *isobaric* wind shears that exist in the same layer.

Rossby waves

If we consider atmospheric motions close to the level of minimum divergence (LANDERS, 1955), i.e., slightly below, or at, the 500 mbar level, the absolute vorticity is more nearly conserved than near jet stream level. If we make the assumption that motions are isobaric ($N=0$) and that the tilting term in eq.27 may be neglected, then:

$$\frac{dQ}{dt} = 0 \tag{33}$$

i.e., the absolute vorticity is conserved.

For each parcel in the field of flow we may thus derive a trajectory which it should follow as long as its value of Q_z remains constant. Such "constant absolute vorticity-trajectories" (CAVT) were widely used in weather forecasting during the late forties, prior to the advent of high-speed numerical computation techniques. By comparing CAVT with actual flow patterns, major readjustments of the 500-mbar current were predicted if theoretical trajectories and actual contour patterns showed large discrepancies.

If the wave pattern is not stationary, and for small amplitudes where we may assume $V \cong u$, the well-known equation for Rossby waves is:

$$L = 2\pi\sqrt{\frac{u-C}{\beta}}$$

or:

$$C = u - \frac{L^2\beta}{4\pi^2} \tag{34}$$

where C is the propagation speed of the wave system (ROSSBY, 1945). Since C is a function of L, the waves should have dispersive properties, and a group velocity C_g may be defined as:

$$C_g = C - L\frac{dC}{dL} \tag{35}$$

From eq.34:

$$L\frac{dC}{dL} = -2\beta\left(\frac{L}{2\pi}\right)^2$$

and we obtain:

$$C_g = C + 2\beta\left(\frac{L}{2\pi}\right)^2 = u + \beta\left(\frac{L}{2\pi}\right)^2 \tag{36}$$

Thus it appears that in the westwind region the group velocity not only exceeds the wave speed, but also the mean speed of the westerlies. According to NAMIAS (1947) cyclone waves in middle latitudes propagate with a speed of approximately 10°–12° of longitude per day, (i.e., about 10 m/sec) while long waves move only about 1.5° of longitude

per day, on the average. The group velocity for an average wave length of 50° longitude is approximately 28° longitude per day ($\approx$28 m/sec) according to eq.36.
Such theoretical group velocities are in agreement with the observation that sometimes pressure systems downstream from a deepening trough intensify at a rate which could neither be explained by advection nor by simple wave propagation. In accordance with the laws of physics, the group velocity thus controls the downstream propagation of perturbation energy, if the latter is expressed by the square of the wave amplitude.

Jet maxima and quasi-inertial motions

The Rossby waves described in the preceding section have dealt with an oscillatory motion set off by a perturbation superimposed on a homogeneous zonal current under conservation of absolute vorticity. Another type of oscillation is generated by an imbalance between centrifugal and Coriolis forces:

$$\frac{V^2}{r} = fV$$

or:

$$V = fr \tag{37}$$

where r is the radius of the "inertial circle," assuming f to be a constant. The time, which it takes an air parcel to complete one revolution of the inertial circle, called the "inertial period," is:

$$T_i = \frac{2\pi}{f} \tag{38}$$

or half a pendulum day, the latter being defined as: $\frac{2\pi}{\Omega \sin \phi}$, the time which a Foucault pendulum requires to complete one cycle.
Let us assume now that the field of flow at jet stream level consists of a *geostrophic* basic current $\bar{u}$, and an ageostrophic component which—when considered in a coordinate system which moves with the basic current—would prescribe an inertial circle. Obviously, the particle trajectories in this flow would be cycloids with a wave length (RAETHJEN, 1961):

$$L_i = \frac{2\pi}{f}\,\bar{u} \tag{39}$$

Let us furthermore assume that the geostrophic basic zonal current has lateral shear (VAN MIEGHEM, 1951; KAO and WURTELE, 1959; NEWTON, 1959, 1964; RAETHJEN, 1961):

$$\bar{u} = \frac{\partial \bar{u}}{\partial y}\, y + \bar{u}_0 \tag{40}$$

where $\bar{u}_0$ is the geostrophic wind speed at $y=0$. By properly choosing our space and time coordinate origins we may show that:

$$y = A_y \sin (f\alpha t) \tag{41}$$

which yields for the inertial period of a shearing current:

$$T_i = \frac{2\pi}{f\alpha} \tag{42}$$

This expression reverts to eq.38 if no horizontal shears are present in the basic current. By differentiation of eq.41 we obtain:

$$v^* = \frac{dy}{dt} = f\alpha A_y \cos(f\alpha t) \tag{43}$$

For $t=0$ the perturbation component v_0^* is obtained from eq.43. The amplitude of the inertial oscillation:

$$A_y = \frac{v_0^*}{f\alpha} \tag{44}$$

thus is a function of the initial perturbation velocity, of geographical latitude. and of the horizontal shear in the basic current.
In the derivation of the above equations we have assumed that the geostrophic basic current remains unchanged under the action of perturbation motions. (See PETTERSSEN, 1956, Vol. 1; JOHANNESSEN, 1956). In other words, we have assumed that there is *no* adaptation mechanism which would allow an adjustment between pressure and wind fields. On the other hand, if there were *perfect* adaptation between the two fields, no inertial oscillations would be possible at all. Any ageostrophic perturbation velocity superimposed upon a geostrophic basic current would be absorbed immediately by a new, adjusted pressure field, and by a new geostrophic flow.
Clearly enough, neither of these two extremes holds in the atmosphere. A certain amount of adaptation is to be expected, but the mechanism is by no means perfect. Statistical investigations by NEWTON (1959a, 1964) revealed that actual inertial periods near the jet stream show widely scattered values, larger than the value given by eq.38. On the average, an actual period of *twice* the magnitude given by eq.38 seems to prevail. Jet maxima, therefore, seem to be a phenomenon of *semi-inertial* oscillations. If these statistical findings are applied to the derivation of eq.42, we find for the actually observed period in a non-shearing current $\bar{u}$:

$$T = 2T_i = \frac{4\pi}{f} \tag{45}$$

The wave length of semi-inertial oscillations should be:

$$L = \frac{4\pi}{f}\bar{u} \tag{46}$$

In Fig.17 these wave lengths are compared with those of stationary Rossby waves (eq. 34 with $C=0$) for various zonal speeds and as functions of latitude.
From eq.42 and 44 it is evident that the amplitudes of inertial oscillations depend on geographic latitude and on the lateral shear of the basic current. The amplitudes are, furthermore, dependent on the magnitude of the original ageostrophic disturbance, v_0^*. If we assume a frictionless atmosphere, horizontal sheets of inertial oscillations could be stacked atop each other without any interlocking mechanism, especially if vertical shears are not excessive.

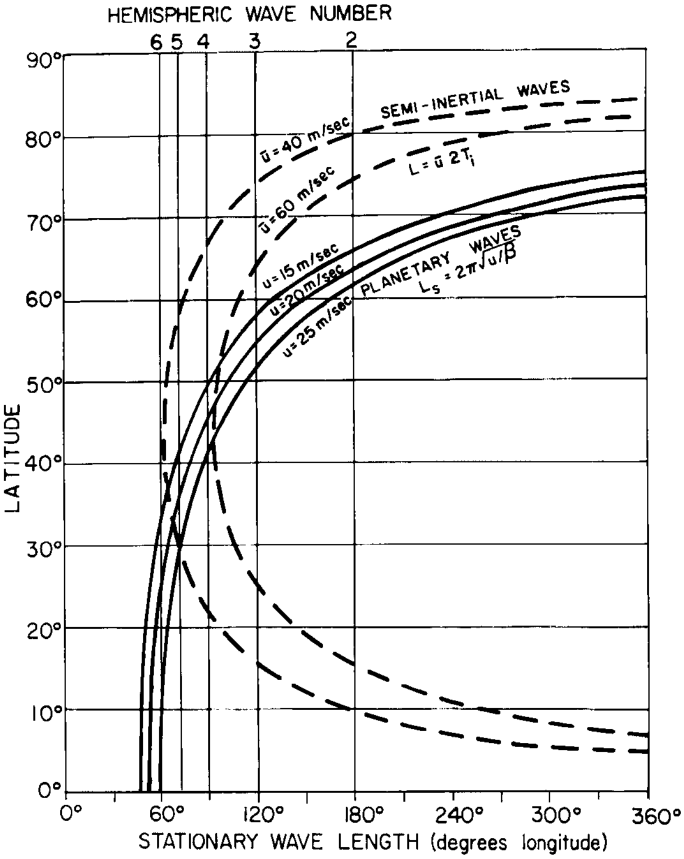

Fig.17. Wave length of planetary Rossby waves and of semi-inertial waves (abscissa) as a function of latitude (ordinate), at various wind speeds. (After NEWTON, 1964.)

Conservation of potential vorticity

Let us consider a theorem first derived by ERTEL (1942):

$$\frac{\mathrm{d}P}{\mathrm{d}t} = \frac{1}{\rho} \boldsymbol{Q} \cdot \nabla \frac{\mathrm{d}\psi}{\mathrm{d}t} + \frac{1}{\rho} \boldsymbol{N} \cdot \nabla\psi \tag{47}$$

where ψ is an arbitrary scalar function (ELIASSEN and KLEINSCHMIDT, 1957). Since the solenoidal vector N is perpendicular to both $\nabla\alpha$ and $(-\nabla p)$, the last term in eq.47 will vanish, if ψ is chosen to be a thermodynamic function of state (i.e., a function of p and α). Specifically, if $\psi = \Theta$, the potential temperature, we obtain the expression:

$$\frac{\mathrm{d}P}{\mathrm{d}t} = \frac{1}{\rho} \boldsymbol{Q} \cdot \nabla \frac{\mathrm{d}\Theta}{\mathrm{d}t} \tag{48}$$

which does not take frictional effects into account. In this case, P is called the *potential vorticity*. According to eq.48 it changes only if diabatic heating or cooling takes place. For adiabatic motion $\left(\frac{\mathrm{d}\theta}{\mathrm{d}t} = 0\right)$, $\frac{\mathrm{d}P}{\mathrm{d}t} = 0$.

Eq.48 offers a check on the accuracy of isentropic trajectories. Motions on an isentropic surface, which by definition are adiabatic, should conserve their potential vorticity.

Thus, if drastic changes of P are encountered along a trajectory, larger than those which could be explained by the frictional term or by neglected diabatic effects, the trajectories will have to be recomputed.

In applying the foregoing to atmospheric flow in the jet-stream region, we find that stratospheric air on the cyclonic side of the jet axis shows considerably higher values of P (by almost two orders of magnitude on the average) than tropospheric air on the anticyclonic side of the jet. Typical values of potential vorticity in stratospheric air on the cyclonic side of well-developed jet streams are of the order of 50 to $100 \cdot 10^{-9}$ g^{-1} cm sec degrees.

Since P is conserved in adiabatic air motions we are able to trace intrusions of strato-

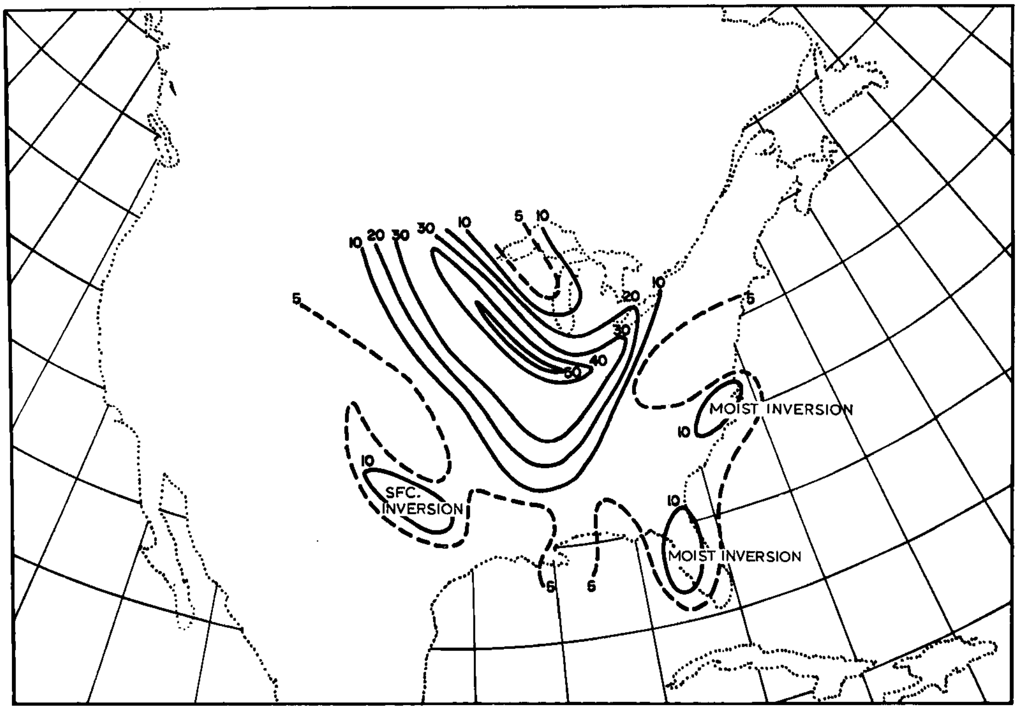

Fig.18. Potential vorticity (units 10^{-9} g^{-1} cm sec degree) of 300°K isentropic surface, 22 November, 1962, 12h00 G.M.T. (After REITER and MAHLMAN, 1964.)

spheric air into the troposphere by their high values of P relative to their surrounding (Fig.18). The schematic diagram of Fig.12 suggests a mechanism by which air can pass from the cyclonic to the anticyclonic side of the jet stream; it remains within a stable layer, which emerges from the "jet stream front" and—after descending to the lower troposphere—is classified as a "subsidence inversion" within the anticyclone. With the strong stabilities prevailing in such subsidence inversions, there is no difficulty in satisfying the condition of P=constant, even with decreasing absolute vorticity along the trajectory. Actually, both eq.48 and 28 are well satisfied by observations of strong sinking motions in the jet-stream region associated with radioactive fallout (REED and DANIELSEN, 1959; STALEY, 1960; REITER, 1963b; REITER and MAHLMAN, 1964). As the air at, and above, tropopause level enters the left rear quadrant of the jet maximum, it is subjected to horizontal convergence, and, according to eq.28, to an increase in vorticity. The latter, following eq.48, results in decreasing stability. The opposite is the case, as soon as the trajectories show divergence within the anticyclone.

Air motions from the stratosphere to the troposphere are well substantiated by aircraft measurements, which—even on the average, but much more so in individual cases—show relatively high values of ozone and low humidities in the "jet stream front." The British flight measurement of 8 May 1961, shown in Fig.19, may serve as an example

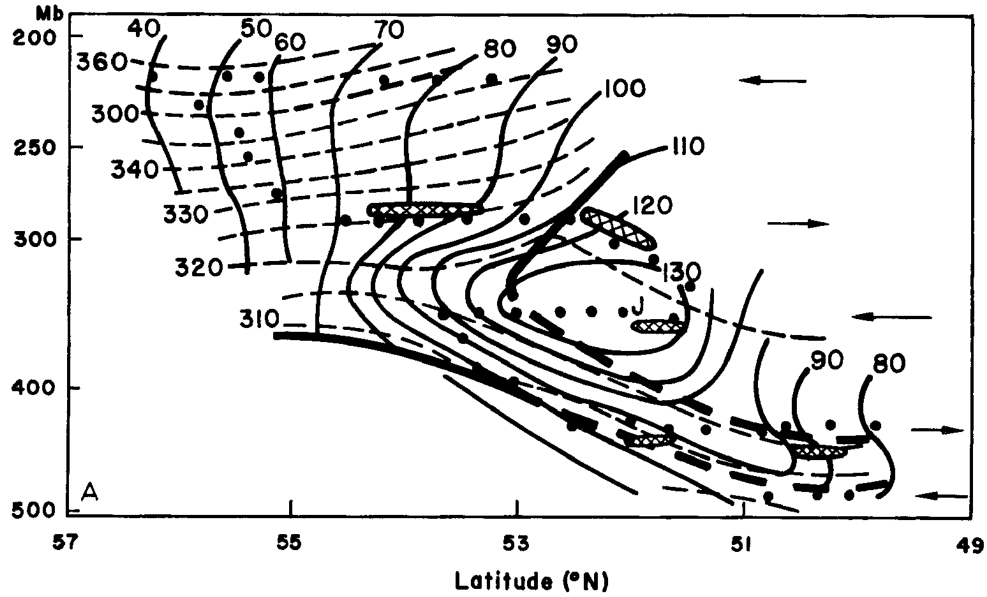

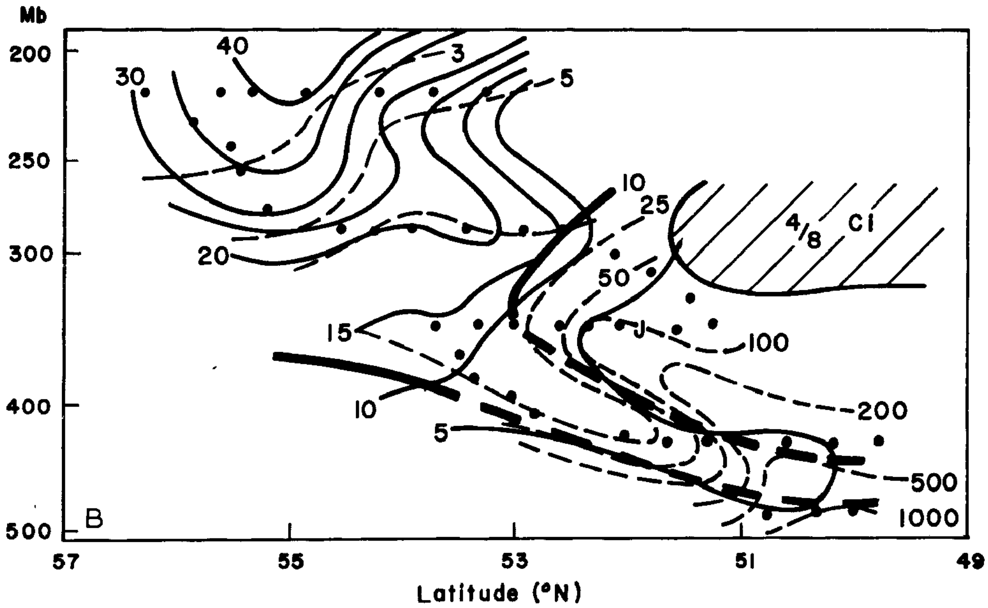

Fig.19. Flight measurements of 8 May 1961, between 50°N 1°W and 56°N 1°W, and 12h00 to 18h00 G.M.T.
A. Solid lines are isotachs (kt); dashed lines are potential isotherms (°K); hatched regions indicate slight and moderate CAT. Tropopauses and boundaries of stable layers are marked by heavy lines.
B. Solid lines indicate ozone-mixing ratio (mol/10^8 mol); dashed lines give values of humidity mixing ratio (μg/g). (After BRIGGS and ROACH, 1963.)

(BRIGGS and ROACH, 1963). Similar cases of dry air near cold fronts, which underwent strong sinking, are reported by MILES (1962).

As has been pointed out earlier, isobaric analyses may be quite misleading in the quantitative estimates of convergence. On an isobaric surface, the flow accelerates strongly in the entrance region of a jet maximum. Thus, in order to render convergence with: $\frac{dV}{ds} > 0$, the lateral confluence must be quite strong. This is shown in Fig.14, where two jet stream branches seem to merge along a convergence line. As we have seen in the discussion of this figure, these two jet branches are not joining in side-by-side flow, but rather, the northern one is submerging under the southern one. Similar conditions should be expected in the entrance region of less strongly developed jet maxima. The convergence in the left rear quadrant should express itself mainly in an isentropic "sliding" motion, which leads sheets of stratospheric air into the baroclinic "jet stream front," where they may sink along inclined surfaces of constant potential temperature.

The schematic diagram, Fig.12, indicates that values of $\frac{\partial V}{\partial s}$ may be considerably smaller along isentropic surfaces than along isobaric surfaces, because the isotach surfaces run almost parallel to the isentropic surfaces in the "jet stream front." Thus, air motion converging from the rear cyclonic side of the jet maximum towards the jet axis does not

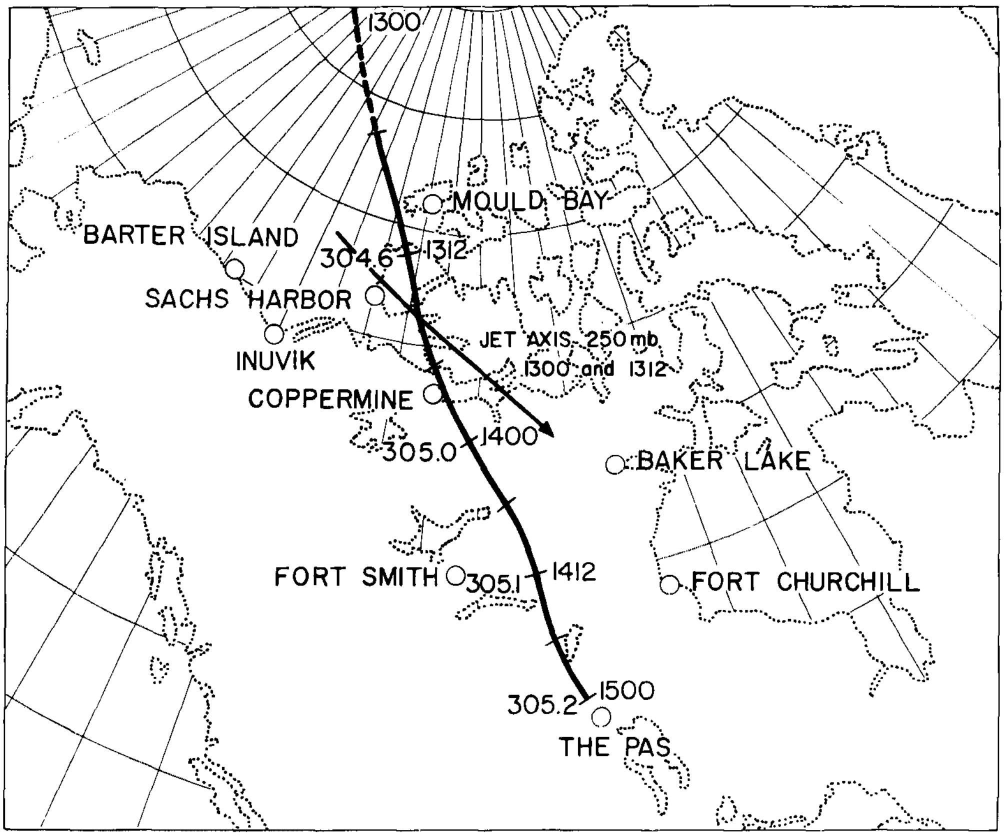

Fig.20. Isentropic trajectory along the 303°K surface, 13 September, 1961, 00h00 G.M.T. to 15 September, 00h00 G.M.T. Numbers to the left of the trajectory give the stream function value (10^7 erg/g), to the right the observation day and time. The jet axis of 13 September has been entered as a solid line with arrow.

have to cut across isotachs, but tends to maintain its speeds. This is also evident from the lengths of the isentropic trajectory segments in Fig.20. Radioactively contaminated air masses have been traced in this study, crossing the jet axis at almost constant speed and sinking from approximately 400 mbar to about 650 mbar at the same time. Deceleration is noticed only after the air has arrived in the region well to the anticyclonic side of the jet stream.

Inspecting Fig.14 and 15 we find very strong diffluence east of the trough line, which results in a splitting of the jet stream. One branch continues cyclonically in the middle and upper troposphere while the other branch follows an anticyclonically curved path and—as has been described on p.108—transports radioactive debris to eastern Texas and Louisiana (Fig.21). The convergence predicted from eq.28 for the right front quadrant

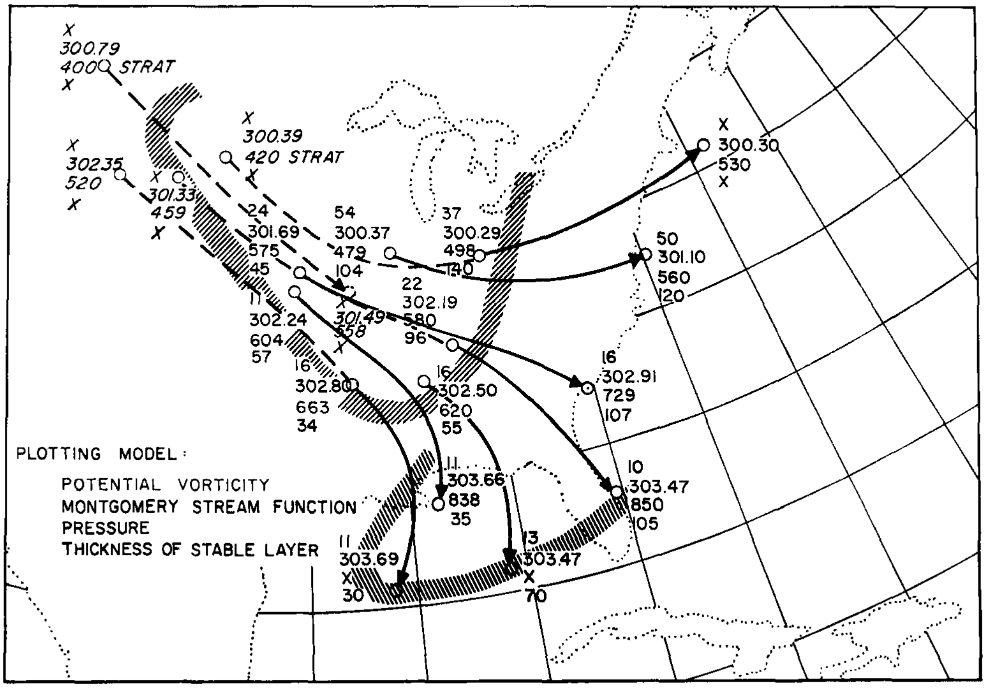

Fig.21. Trajectories on the 300°K isentropic surface. From 22 November, 1962, 00h00 G.M.T. to 12h00 G.M.T. (dashed lines); from 22 November 12h00 G.M.T. to 23 November 00h00 G.M.T. (full lines with arrows). Values of potential vorticity (units 10^{-9} g^{-1} cm sec degree), of Montgomery stream function (units 10^{7} cm^{2}/sec^{2}), of pressure (mbar) on the 300°K surface, and of thickness (mbar) of the stable layer within which the 300°K surface is contained are entered slanting numbers for 22 November 00h00 G.M.T. and vertical numbers for other observation times. The centres of the hatched bands mark boundaries at 22 November 12h00 G.M.T. and 23 November 00h00 G.M.T. of radioactively contaminated air that descended from tropopause level. (After REITER and MAHLMAN, 1964.)

seems to manifest itself mainly by decelerations along the trajectories: $\frac{\partial V}{\partial s} < 0$, as may be seen from Fig.14. In interpreting this figure one has to take into account the motion of the jet maximum. Thus, decelerations along trajectories will not be as strong as along stream lines. To what extent the diffluence and splitting of the jet stream shown in Fig.14 and 15 is enhanced, or maybe even caused, by strong horizontal shears and resulting dynamic instability near the jet maximum, has not yet been investigated.

Absolute vorticity increasing along the trajectory should lead to horizontal mass convergence according to eq.28. This, in turn, will lead to vertical stretching of an air column contained between two isentropic surfaces. Thus: $-\frac{\partial \Theta}{\partial p}$ should decrease along such trajectories, as required by eq.48.

To confirm this statement, let us again consider Fig.21. The trajectories emanating from the convergent right front quadrant of the jet maximum in Fig.15 indicate an increase in the thickness Δp of the stable layer, which conforms well with what has been said above. The trajectory terminating near Savannah, Ga., originates on the cyclonic side of the jet stream and remains there. The strong increase of the thickness Δp of the stable layer from 45 to 107 mbar along this trajectory is, at least in part, produced by the fact

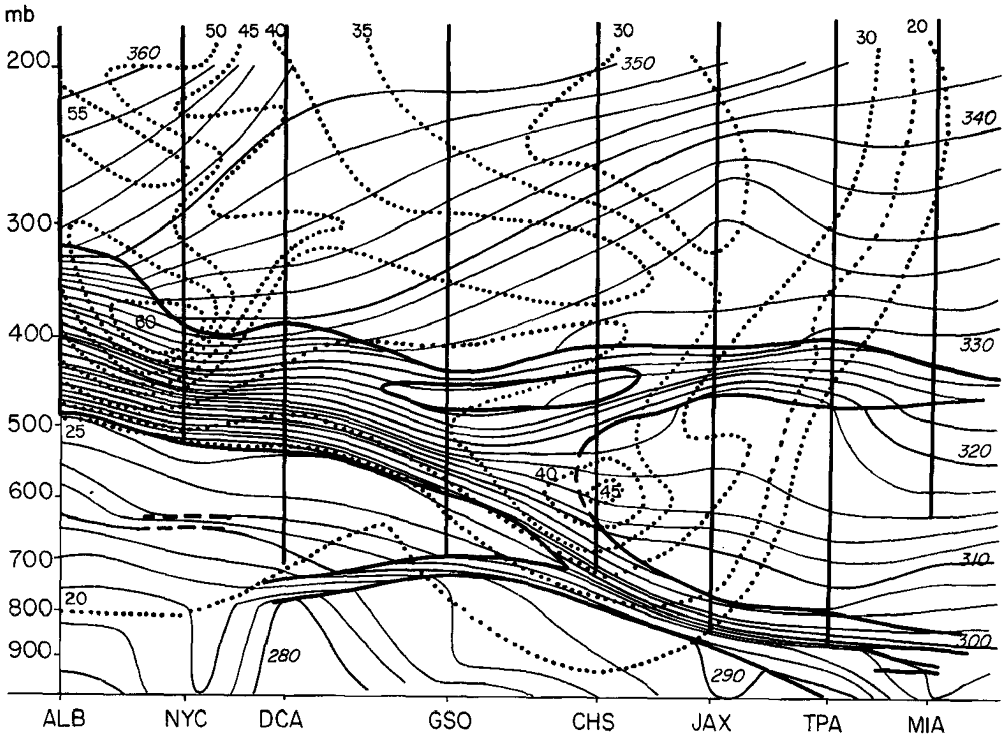

Fig.22. Cross-section through the atmosphere from Albany (ALB) (N.Y.) to Miami (MIA) (Fla.); 23 November 1962, 00h00 G.M.T. Thin lines—potential temperature (°K, slanting numbers); dotted lines—isotachs (m/sec, vertical numbers). Heavy lines indicate boundaries of stable regions. Heavy vertical lines over station locations mark the extent of "motorboating" humidity reports. (After REITER and MAHLMAN, 1964.)

that a stable layer, originally located below the contaminated region, merges with the latter, as may be seen from Fig.22. Nevertheless, from the vorticity theorem, eq.28, and the potential-vorticity expression, we should expect some increase in Δp between isentropic surfaces. The trajectory originates over the midwest close to the jet axis in almost straight flow, it terminates near Savannah with cyclonic shear. Thus, $\frac{dQ}{dt}$ seems to be positive along this trajectory. The two southwesternmost trajectories in Fig.21 show a decrease in Δp. They originate in an area with high potential vorticity (Fig.18), indicative of air coming from the stratosphere. Both these trajectories start in a region with only small horizontal shears. Their anticyclonic curvature increases, however, rendering $\frac{dQ}{dt} < 0$. Horizontal divergence, as well as increasing stability within the isentropic layer should result.

Two other problems have to be considered in connection with the downward transport of stratospheric air in the jet-stream region. One is the classical concept of ageostrophic motions on isobaric surfaces. In the preceding section we have seen that jet maxima may be considered as an effect of quasi-inertial oscillations, produced by ageostrophic flow. Speeds in the jet maximum itself should be supergeostrophic, and winds, therefore, should show a tendency to bank towards the high-pressure side of the flow. Statistical investigations by FAUST (1959, 1962) and others (HOLLMANN, 1959); ATTMANNSPACHER, 1961) seem to corroborate this conclusion. How can the convergence of stratospheric air into the rear quadrant of the jet maximum, and its intrusion into the troposphere on the anticyclonic side of the jet axis (see schematic diagram Fig.12) be brought into agreement with this concept?

Again the seeming discrepancy may be resolved easily by considering actual air flow along isentropic surfaces. The air in the jet core, which undergoes the strongest accelerations, is entirely of tropospheric origin. It ascends from lower levels merging with the flow in the upper troposphere. The potential vorticity of this flow will be relatively low. Ageostrophic components within this tropospheric jet core will match the observed accelerations. The air currents subsiding in the "jet stream front" and seemingly traversing the jet axis (by "slipping through" underneath the jet core) towards the anticyclonic side should *not* be considered in calculating ageostrophic components of flow on an *isobaric* surface. As we have seen, this descending air undergoes only minor speed changes near jet stream level. Later deceleration of this air agrees with its flow towards higher pressure, or higher stream-function values on an isentropic surface. Thus, if we consider air motions on "substantial" or "physical" surfaces rather than on isobaric surfaces, we find that the entire "entrance region" of a jet maximum does not have to be characterized by ageostrophic flow accelerating towards lower pressure or lower contour values. Only *tropospheric* air flowing into the jet core should show such components, while stratospheric air would behave differently, as explained above.

The second problem is concerned with the conservation of energy. Flow into a jet maximum is—through its acceleration—associated with increasing kinetic energy. The potential energy of this flow, therefore, should be decreasing. It is easily realized that air subsiding in the jet-stream front, and tropospheric warm air rising into the jet core, would provide such a conversion of potential into kinetic energy. If both, descending and ascending flow, are dry adiabatic, warming and cooling should destroy the horizontal temperature gradients. The ascending flow usually is, however, associated with cloud formation and precipitation, providing an additional energy source by converting latent into sensible heat (PALMÉN, 1958). Furthermore, we must remember that although the descending air starts its descent on the cyclonic rear side of the jet maximum, it travels rapidly through the jet stream as it moves downward and finally ends up on the anticyclonic side ahead of the core position aloft. Thus, any adiabatic warming which the air within the stable layer may have undergone would actually increase the meridional temperature difference relative to cold air that did not undergo appreciable sinking. Thus, while kinetic energy is consumed and potential energy is increased in this decelerating current, the frontal zone and its associated jet stream at the same time are provided with a propagation mechanism that moves them downstream.

Orographic sources of long-wave perturbations

The origin of certain major troughs and ridges in the upper tropospheric circulation shall be considered in this section. Their global distribution leads to large-scale climatological effects. SALTZMAN (1961) and others (SALTZMAN and PEIXOTO, 1957; SALTZMAN and FLEISHER, 1960a, b, 1961; SALTZMAN et al., 1961; SALTZMAN and TEWELES, 1964) have made extensive statistical studies of the wave characteristics of the tropospheric flow. According to these investigations, wave numbers 1 through 4 show certain geographic preferences as to their phase angle. In other words, these waves have a tendency to be stationary. They appear in monthly and seasonal mean charts of the upper tropospheric pressure or wind field. Wave number 1, according to Saltzman and others, shows a maximum in the kinetic energy of the zonal component the year around. It indicates the eccentricity of the circumpolar vortex whose centre in the Northern Hemisphere is located on the average along the 165th meridian at the 500-mbar level (LA SEUR, 1954). It favors this position as a result of the fact that the Himalayas and Rocky Mountains are not exactly 180° of longitude out of phase.

From mean 700 to 1,000-mbar thickness charts, indicative of the low tropospheric temperature distribution (ANONYMOUS, 1952), we see that the summer months are characterized by four to five troughs in middle and high latitudes. In winter (January) only three troughs are evident, with the ones over East Asia and over North America dominating. The reduction in wave number from summer to winter is consistent with eq.34 (for $C = 0$), considering the larger zonal speeds of the jet streams during the winter season. The two major troughs of winter occur on the lee side of the two major mountain ranges, the Himalayas and the Rocky Mountains, and are evidently produced orographically. The third trough over Europe, much weaker on the mean charts, may be considered a resonance effect between the two other major troughs. Its weakness is at least in part due to day-to-day shifts in its position. The two major troughs are considerably more stable in their location, thus they appear with greater amplitudes in the mean. Even July temperatures reveal remnants of these two orographic troughs. The summer pattern of stationary waves may be considered in resonance with orographic and continental effects.

Wave numbers 5 trough 8 in these statistical studies appeared to be associated with free planetary waves, wave numbers >8 with rapidly traveling small-scale cyclones and anticyclones. Since the position of such waves will change from day to day, their net effects on the monthly or seasonal mean pressure fields will cancel. They are of great importance, however, in the meridional transport of heat (enthalpy), angular momentum, and kinetic energy. Wave numbers 3 and 6 seem to contain maxima of kinetic energy of the v-component of flow. Since wave number 3 may be tied in with the earth's orography, as we have seen above, we may state that large mountain ranges play an important role in generating meridional transport processes in the atmosphere.

SALTZMAN and TEWELES (1964) found, furthermore, that in the *mean*, all waves feed their energy into the mean zonal motion. Thus, the general circulation with its large-scale perturbations does not have the characteristics of "turbulent" flow, in which energy would be drawn from the mean motion, and fed into the eddies. The two authors also found that wave number 2 and numbers 5–10 are sources of kinetic energy. The rest of the waves are sinks. Wave numbers 5–10 correspond to cyclones, which we know release potential energy. The energy source in wave number 2 would indicate that orographic effects, as well as the land-sea distribution, have a significant influence in maintaining the general circulation in its observed form.

WIIN-NIELSEN et al. (1963, 1964) have computed the effect of wave numbers 1–15 on the transport of heat and momentum at various latitudes and pressure levels for January, 1962, and 1963. Their findings, in essence, corroborate what has been said above and reveal the following interesting facts. Most of the sensible heat transport occurs at low levels (below 500 mbar) at latitudes of 45°–50°N. More than 50% of this transport is carried out by wave numbers 1–4, and a significant shift towards longer waves occur between 40° and 50°N, i.e., north of the mean jet-stream position. Part of this shift is due to the smaller circumference of latitude circles, hence smaller wave numbers for the same wave lengths at high latitudes. Momentum transports show maxima at high levels, as is to be expected from the large jet-stream velocities occurring there. Transports are directed northward south of 55°N, southward to the north of this latitude. Again, 50% of the transport is accomplished by wave numbers 1–4, 30% by number 5–8. Both momentum and heat transports show a minimum during July.

Zonal potential energy is converted to eddy potential energy at nearly all wave numbers. Maximum amounts of conversion are realized at "orographic" wave numbers 2 and 3 during January (BROWN, 1964). This is well in line with the experience of strong cold outbreaks in the lee of the large mountain ranges, especially over North America. During the transition months and in summer this conversion takes place at higher wave numbers. The zonal potential energy is replenished by the latitudinal distribution of the heat sources, which show maximum effectiveness during winter, minimum effectiveness during summer. Maximum heating occurs around 35°–40° latitude, maximum cooling takes place at higher latitudes. Relatively strong year-to-year variations in these amounts are indicated (BROWN, 1964).

The eddy transport of water vapor follows similar patterns (VAN DE BOOGAARD, 1964). Most of the transport occurs below the 850-mbar level, and it reaches maximum values near latitude 40°. Wave numbers smaller than 6 are the instrumental ones in carrying out the transport.

We can explain how orographic perturbations are generated with the aid of the potential vorticity theorem which, for simplicity's sake, we will state in the form used by ROSSBY (1940). If Δp is the thickness of a layer contained between two isentropic surfaces, the continuity equation yields the expression:

$$D_h = -\frac{1}{\Delta p}\frac{d(\Delta p)}{dt} \tag{49}$$

for the horizontal divergence. Upon substituting this term in the vorticity eq.28 for adiabatic flow, we obtain:

$$\frac{d}{dt}\left(\frac{Q_z}{\Delta p}\right) = 0 \tag{50}$$

Let us now assume that the atmosphere is incompressible, having a depth H_0 and is forced to flow over a mountain range of height h. Therefore, the flow has a channel of depth $H = H_0 - h$ available over the crest of the mountain range. Indicating undisturbed conditions away from the mountains with subscript "0", and omitting for brevity the subscripts "z" we may write:

$$\frac{q_0 + f_0}{H_0} = \frac{q + f}{H_0 - h} \tag{51}$$

and:

$$q = q_0 \frac{H}{H_0} - f_0 \frac{h}{H_0} + \Delta f \tag{52}$$

where $\Delta f = f_0 - f$. If we consider conditions in the jet axis, the relative vorticity may be written as $q = VK_s$, since the horizontal shears vanish. Assuming that an air parcel, originally located in the jet axis, remains there, we obtain from the analytic expression of curvature:

$$K = \frac{\dfrac{d^2 y}{dz^2}}{\left[1 + \left(\dfrac{\partial y}{\partial x}\right)^2\right]^{\frac{3}{2}}} = \frac{q_0}{V}\left(\frac{H}{H_0}\right) - f_0 \frac{h}{VH_0} + \frac{\Delta f}{V}$$

or:

$$d\left[\frac{\dfrac{dy}{dx}}{\left[1 + \left(\dfrac{dy}{dx}\right)^2\right]^{\frac{1}{2}}}\right] = \frac{q_0}{V}\left(\frac{H}{H_0}\right) dx - f_0 \frac{h}{VH_0} dx + \frac{\Delta f}{V} dx \tag{53}$$

Since $\dfrac{dy}{dx} = \tan \psi$, where ψ is the angle between the jet axis and the x-direction, the left-hand side of eq.53 yields d (sin ψ). The jet stream will cross the mountain range, if $90° > \psi > -90°$ or if $1 > \sin \psi > -1$.

A critical speed V_{cr} may be computed, for which the flow turns parallel to the mountain range, by imposing the condition $\sin \psi = \pm 1$. If V falls below this critical speed, the flow will turn back and will not cross the range. The critical conditions are:

$$V_{cr} = -\frac{q_0}{H_0}\int_x^{x+\Delta x} H dx + \frac{f_0}{H_0}\int_x^{x+\Delta x} h dx - \int_x^{x+\Delta x} \Delta f dx \tag{54}$$

For initially straight flow impinging on the mountain range, the first term on the right-hand side of eq.54 will be zero. BOLIN (1950), neglecting also the last term, arrives at a critical speed $V_{cr} = 20$ m/sec for a mean height of the mountain range $h = 2{,}000$ m, $\Delta x = 1{,}000$ km, the height of the atmosphere $H_0 = 10$ km, and $f_0 = 10^{-4}$/sec. Thus it appears that only mountain ranges of the dimensions of the Rocky Mountains or the Himalayas will deflect the upper current appreciably.

Conservation of potential vorticity, as considered in eq.51 provides an effective mechanism by which large scale perturbations are provided to the zonal westerly flow. Downstream from large orographic barriers the height H_0 of the atmosphere may essentially be considered constant. Thus, the trajectories of *constant potential vorticity* should —in first approximation—revert to trajectories of *constant absolute vorticity*. A pattern of waves as described by eq.34 with $C = 0$, should emerge downstream from the mountains. Both the Rocky Mountains and the Himalayas exert their influence according to eq.50; as the thickness of the atmospheric layer decreases in upslope motion, absolute vorticity will decrease at the same rate. Thus, the flow will acquire anticyclonic characteristics, mainly in its curvature. A high-pressure ridge should, therefore, be expected over the mountains. Conversely, a trough will develop in the upper flow to the lee of the mountains.

Downstream from these two mountain ranges, a hemispheric wave pattern will result having the following characteristics:

(*1*) Wave number one indicative of the eccentricity of the circumpolar vortex—due to the fact that the Himalayas and the Rocky Mountains are not located symmetrically with respect to geographic longitude;

(*2*) Wave number two as a result of the orographically induced, quasistationary troughs in the lee of these mountains; and

(*3*) Wave numbers three or four—depending on the mean speed of the circumpolar westerlies—a result of resonance Rossby waves.

In the Southern Hemisphere there is but one major orographic source of perturbations, the Andes. An additional factor in producing a certain asymmetry in the Antartic circumpolar vortex stems from the fact that the highest and coldest parts of Antarctica lie considerably distant from the pole.

The question whether mountain ranges or temperature differences between continents and oceans produce the quasi-stationary wave patterns in the upper flow has lead to much controversy in meteorological literature (SUTCLIFFE, 1951; ACADEMIA SINICA, 1958). Rather than to join sides in this dispute we may consider both causes instrumental in generating long-wave perturbations. Estimates from baroclinic models of the atmosphere show no clear preference for one effect or the other (SMAGORINSKY, 1953).

The thermal effects of land-sea distribution may be considered in two ways. If a coast line with its associated horizontal temperature contrast runs parallel with the mean direction of the upper flow, the baroclinicity of the troposphere will be strengthened or weakened—depending on the sign of the low-level temperature gradient. Thus, an intensification of southwesterly jet streams should be expected over the New England states during winter, when the continent on the average is colder than the ocean. A more striking example may be found during the summer months over North Africa, where the low-level meridional temperature gradient between the hot Sahara Desert and the relatively cool Mediterranean Sea seems to induce a great steadiness in the subtropical jet stream in this region.

In addition to these direct actions of horizontal temperature gradients on the upper flow, one may consider the dynamic effects of large temperature anomalies over continents and oceans. In a cold air mass the potential temperature surfaces will be elevated above their normal position. If—see eq.51—we assume a rigid "lid" on top of the atmosphere at height H_0, the upper flow will have to adjust to the presence of the cold air mass near the ground similar to air motion over a mountain range of large extent, giving rise to anticyclonic flow conditions. The inverse holds for flow over an abnormally warm region where isentropic surfaces in the lower troposphere are found below normal elevation and vertical air columns, therefore, should be expected to stretch as they are transported over this area. The flow, in this case, should tend to become more cyclonic. Normally, the temperature anomaly caused by continents and by oceans does not reach very high. An "effective elevation" of the ground may be computed by applying mean lapse rates of 0.6°C/100 m for winter and 0.4° C/100 m for summer to the observed surface temperatures, as shown by WIPPERMANN (1951). The relatively low pressures observed over the continents during summer and over the oceans during winter (MINTZ and DEAN, 1952) have been thought of as the result of a gigantic land and sea breeze phenomenon. During summer the air over the continents would be heated more than over the oceans. This would lead isobaric layers to stretch, causing a component in the pressure gradient aloft directed towards the surrounding oceans. Outflow of air along this gradient component would set in aloft, leaving a mass deficit in the total vertical air column over the continent, thus establishing the summer low pressure conditions mentioned above. We should, therefore, expect cyclonic conditions near the ground, and anticyclonic conditions aloft where the outflow takes place. While this model has simplicity as a merit, it does not take into account the dynamics of the upper current, expecially the effect of the Coriolis force which would prohibit simple inflow and outflow patterns on this large a scale.

Returning to our consideration of orographic influences we note that eq.53 indicates different trajectory curvatures for different initial values of vorticity, q_0. In first approximation, we might consider a jet stream impinging on a high mountain range, having a field of constant positive vorticity on the cyclonic side of the axis, and of constant negative (relative) vorticity on the anticyclonic side. In such a jet stream, trajectories originating on the cyclonic side should diverge from those originating on the anticyclonic side, while crossing the mountains. Thus, jet streams with a strong vorticity gradient should show a tendency to split when crossing a large orographic barrier. Fig.14 and 15 show such a splitting jet stream. Other, similar cases have been observed over the U.S.A. Unfortunately, upper air data are too sparse over the Pacific, to allow a conclusion as to whether or not the Rocky Mountains are responsible for this split.

A split in the jet stream is regularly observed over the Himalayas during the winter monsoon season. One branch, usually classified as the "polar front jet," flows north of the Plateau of Tibet and shows considerable latitudinal variation, while the other branch—the "subtropical jet"— is very steady and flows along the southern slopes of the Himalayan ranges. CHAUDHURY (1950) explains this splitting of the jet stream from the fact that during winter the plateau of Tibet acts as an elevated cold source, which tends to stabilize a baroclinic zone at its southern edge, where the subtropical jet is found. The other baroclinic zone lies between the plateau and the still colder air over Siberia.

The structure of jet streams

Scales of atmospheric motion

In several papers CHARNEY (1947, 1948) has pointed out the difficulties involved in integrating the atmospheric equations of motion in order to obtain a valid description and prediction of the movement of individual air parcels. These difficulties may be overcome, in part, by simplifying the equations and by neglecting certain terms which are thought to be of small consequence in describing the motion.

In doing so, one considers different scales of atmospheric motion; within each a particular set of simplifications is appropriate. So, for instance, if we deal with horizontal motions on a scale of $\geqq 10^6$ m, or vertical motions on a scale $\geqq 10^4$ m, the atmospheric flow may be considered frictionless in first approximation, and the geostrophic assumption usually entails errors which are one order of magnitude smaller than the flow velocities themselves (see also REITER, 1961a, 1963a).

As has been shown by Charney and others, the Coriolis force plays a dominant role in these *macro-scale* motions. The geostrophic assumption effectively filters out the non-geostrophic wave motions of smaller scale, such as gravitational waves and gravitational shearing waves. The wave equations of these do not contain the Coriolis parameter. Typical wave lengths for such waves are $< 10^4$ m in the horizontal, and thus belong to the *micro-scale* of the flow. (Again the corresponding vertical scale may be assumed two orders of magnitude smaller than the horizontal scale.)

Between these two scales, from approximately 10^4–10^6 horizontal metres, we have the *meso*-scale, as yet poorly understood in its structure and its role in the free atmosphere.

The macro-structure of jet streams

The large-scale structure of jet streams has been described in great detail in various monographs (REITER, 1961a, 1963a; RIEHL, 1962). Most of these details have been derived from analyses on isobaric surfaces, and, therefore, remain somewhat deficient in defining the true characteristics of the upper flow. Nevertheless, since one major "consumer" of meteorological information is commercial and military aviation, isobaric jet-stream structure gave, and still gives, invaluable information. With the development of high-flying jet aircraft and of supersonic aircraft a shift in emphasis may be anticipated away from this classical method of presenting upper-air "weather."

In order to accommodate these modern trends in aviation technology, we shall describe briefly the macro-structure of jet streams in terms of recent research results.

The macro-meteorological aspects of tropospheric flow patterns concern themselves with gross vertical wind profiles (vertical scale 10 km), and with horizontal features of the magnitude of planetary waves, including jet maxima and minima (scale $> 10^3$ km).

Vertical macro-scale

Inspection of individual wind soundings usually reveals a striking amount of fluctuation and detail (see Fig.23). As has been pointed out earlier (REITER, 1958a), some of these fluctuations may be due to instrument errors, especially when the frequency of the fluctuation corresponds closely to the frequency of measurement and of smoothing. This was the case with the GMD-1 equipment widely used for upper-wind measurements until the late 1950's.

The modern and highly accurate FPS-16 radar shows small-scale fluctuations in vertical wind profiles with a thickness of the order of 2 km. These fluctuations are beyond any doubt real and are not introduced by the instrumentation. They qualify, however, as meso-structure and should—as far as the atmospheric macro-structure is concerned—be regarded as "noise."

Objective ways have been devised to eliminate this "noise," and to arrive at smoothed vertical wind profiles which will be representative for an area and a time interval commensurate with the average distance between radiosonde stations and with the synoptic observation interval. Harmonic analysis of rawinsonde measurements yields such wind profiles in desired quality (RIEHL, 1961). These computation procedures can easily be adapted to electronic computer techniques (REITER et al., 1962; REITER and WHITE, 1964).

Since the stratospheric portions of rawin soundings may show large fluctuations in wind speeds, especially in the vicinity of jet streams, the very last reported wind value of a sounding may not be considered representative for a harmonic analysis. (These fluctuations may either be real or introduced by the instrument at low elevation angles.) Therefore, an artificial terminal point of the sounding is computed by taking the arithmetic mean value over the last nine reported wind values. Between the surface wind $A = V_1$ and this terminal point the harmonic "zero" is given by the straight-line wind profile:

$$B = \frac{\dfrac{V_{n-8} + V_{n-7} + \ldots + V_n}{9} - V_1}{n-4} \tag{55}$$

where n is the number of wind observations in the sounding. The harmonic analysis will be concerned only with the residual wind values, G, which exceed this straight-line profile, and which are given by:

$$G_{j+1} = V_{j+1} - A - B \cdot t_j \;; \qquad j = 0, \ldots, n-5 \tag{56}$$

where V_j is the original wind value reported at minute j and t_j is the time in minutes, if observations are available at one-minute intervals.

Harmonic analysis yields:

$$C_i = \frac{2}{n-5} \sum_{j=0}^{n-5} G_{j+1} \sin\left(\frac{\pi \cdot i \cdot j}{n-5}\right); \qquad i = 1, \ldots, 9 \tag{57}$$

Experiments have shown, that wind profiles are smoothed well if the number i of harmonics used in their representation is limited to 9. In rare cases, where nine harmonics still would produce multiple peaks in the vertical wind profiles, a smaller number (as small as six) may have to be used in computing a smoothed profile. Scanning techniques may conveniently be built into a machine program to identify such cases.

The smoothed wind values, using the first 9 harmonics, are given by:

$$V_{j+1} = A + B \cdot t_j + \sum_{i=1}^{9} C_i \sin\left(\frac{\pi \cdot i \cdot j}{n-5}\right) \tag{58}$$

Fig.23 shows two examples of vertical wind profiles, one for high wind speeds (baroclinic case) and one for low speeds (barotropic case). The dashed lines indicate the smoothed profiles obtained by harmonic analysis as outlined above.

As may be seen from this diagram, wind speeds reported from the actual measurements for any particular pressure level, say 300 mbar, may be contaminated by the vertical meso-structure, thereby leading to a certain amount of wind variation in the horizontal. This becomes especially apparent in the "fingery" structure of jet streams reported from aircraft research flights (REITER, 1961a, 1962, 1963a). This "contamination" is less serious if wind values are considered on isentropic surfaces. (As shall be shown below, meso-structural details have a tendency to orient themselves along isentropic surfaces. They appear to be spread out along such surfaces over a relatively large area, thus the

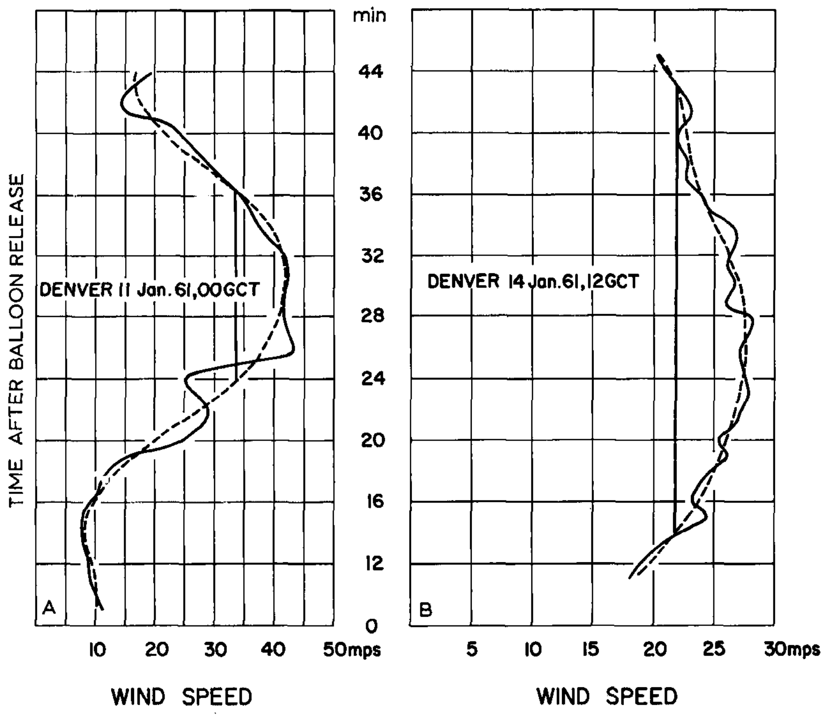

Fig.23. Examples of "baroclinic" (A) and "barotropic" (B) wind profiles over Denver, Colo. Solid line shows original wind measurements. Dashed line shows wind profile after harmonic analysis. Heavy vertical line indicates extent of layer of maximum wind (LMW). (After REITER and WHITE, 1964.)

sign of the meso-scale "noise" has a tendency to be the same over neighbouring stations at the same isentropic surface.)

In order to eliminate the "noise" contained in wind reports at specific pressure *levels*, experiments have been conducted with wind parameters integrated over a *layer*. Specifically, the concept of the layer of maximum wind (LMW) shows promise (REITER, 1958a). The U.S. Weather Bureau has adopted some of these concepts in its daily transmission of maximum wind charts.

Fig.24 shows the definition of the LMW. Its thickness: $\Delta h = h_2 - h_1$, includes the layer in which winds are within 80% of the peak wind, V_{max}. The mean height, $\bar{h} = (h_1 + h_2)/2$, may deviate from the height, h_{max}, at which the peak wind occurs, if the vertical shear above the wind maximum differs from that below the maximum. Usually these differences are small and may be neglected, i.e., one may assume shear distributions to be symmetric about the maximum wind level.

Four parameters—maximum wind (or mean wind of the LMW, i.e., approximately 0.9 V_{max}), mean wind direction in the LMW, thickness, and height of the LMW—define the smoothed field of flow at jet stream level as well as the mean vertical shear distribution about this level. All four parameters may be obtained by electronic computer techniques from the vertical wind profiles smoothed by harmonic analysis.

Horizontal macro-scale

These same considerations hold for the horizontal macro-structure of jet streams. If one is concerned with the large-scale features of flow only, the "noise" in upper-wind

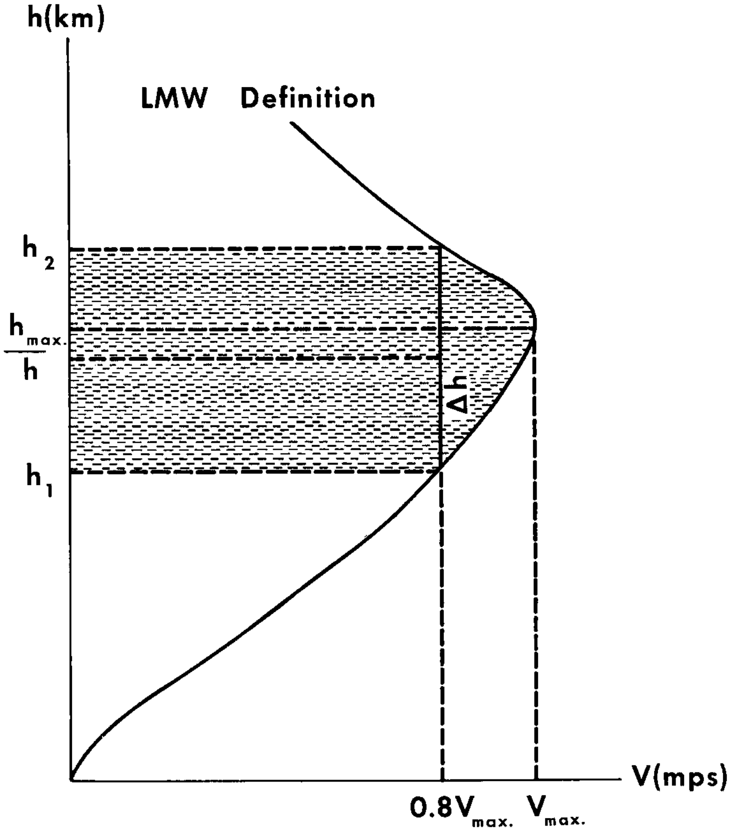

Fig.24. Definition of the layer of maximum wind. For explanation, see text. (After REITER and WHITE, 1964.)

measurements must be effectively eliminated. This may be done in various ways by objective analysis techniques.

One such technique has been tested successfully at the U.S. Weather Bureau. Devised by BERTHORSSON and DÖÖS (1955; see also DÖÖS, 1956; DÖÖS and EATON, 1957; CRESSMAN, 1959), it utilizes a "first guess" in estimating the wind field on an isobaric surface. The geostrophic wind approximation may serve as such a starting point. By means of actual observations at individual stations this "first guess" receives corrections which, when interpolated to surrounding grid points, yield quite reliable wind vectors over the grid. Curve plotters may be programmed so that isotachs are automatically drawn from this digital grid-point information.

Such objective analysis procedures involve a certain degree of smoothing in the upper-wind data, which is of advantage when "noise" in the wind measurements should be eliminated. This "noise," whether actually present in the atmosphere, or introduced by the instrumentation, or produced by the data extrapolation to grid points, affects the precision of objective machine forecasts adversely. In addition, so-called truncation errors (mainly produced by replacing differentials with finite differences in the basic equations) produce mathematical instability, i.e., artificial amplification of disturbances in the flow with time. Both "noise" and truncation errors magnify numerical forecast errors.

The LMW concept seems to eliminate successfully a large part of the "noise" from vertical wind profiles. Objective analysis techniques, introducing additional horizontal smoothing to the LMW data, may be applied. EDDY (1963) reports on such a technique, whereby LMW and tropopause analyses are constructed objectively, using a barotropic 500-mbar prognostic chart as "first guess."

REITER and WHITE (1964) report results obtained by a different analysis technique. A quadratic function is fitted to station data, so that the root-mean squared departure of the latter from the values given by the function is a minimum (BAER, 1962). The function thus derived permits extrapolation of station data to grid points. Again, the computation procedure can be programmed for high-speed electronic calculators. Fig.25, 26,

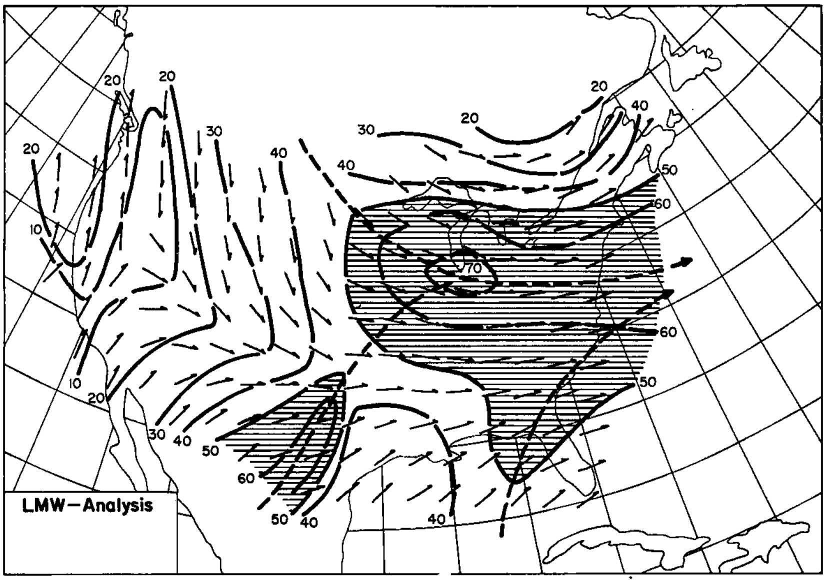

Fig.25. Objective analysis of LMW speeds (m/sec; areas with speeds >50 m/sec are shaded) and directions (thin arrows at grid points), for 23 January, 1961, 00h00 G.M.T. Heavy dashed lines with arrows indicate jet axes. (After REITER and WHITE, 1964.)

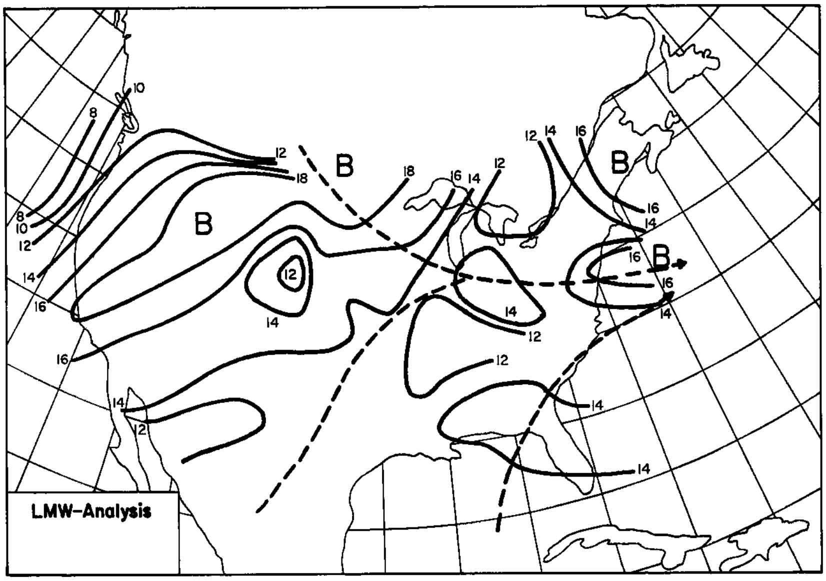

Fig.26. Objective analysis of LMW heights (km, same observation time as in Fig.25). B = barotropic regions. (After REITER and WHITE, 1964.)

and 27 show the distribution of LMW parameters obtained with this method. ("Barotropic regions" in these diagrams are areas in which vertical shears are small enough to produce thicknesses of the LMW > 6 km, or in which the height of the LMW was > 18 km in the original wind soundings.) Apparently the "quadratic-function technique" is less capable of eliminating noise in the data, than the "first guess" technique (see EDDY, 1963).

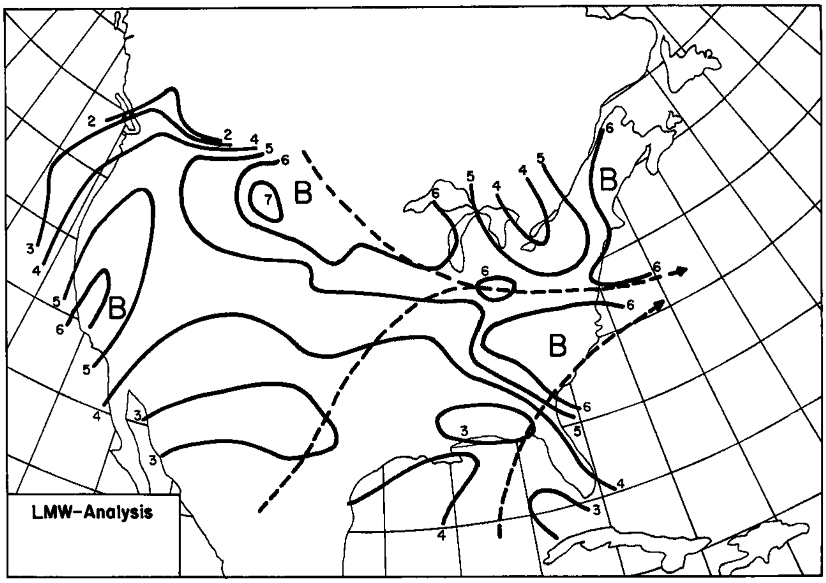

Fig.27. Objective analysis of LMW thickness (km, same observation time and notation as in Fig.25 and 26. (After REITER and WHITE, 1964.)

The meso-structure of jet streams

Recent exploration of the vertical meso-structure of tropospheric and lower stratospheric flow has produced new results that will be described in some detail in the following paragraphs. A general outline of horizontal meso-structure will suffice here. For a detailed discussion of horizontal structure the reader is referred to REITER (1961a, 1963a).

According to the scale considerations described earlier, disturbances superimposed upon the smoothed vertical wind profiles, and ranging in thickness from 10^2 to 10^3 m should be considered here. Fluctuations within this range have been measured with GMD-1 systems (REITER, 1958a; SAWYER, 1961), and have sometimes been interpreted as possible causes for clear-air-turbulence (CAT)(CLEM, 1955).

In dealing with such fluctuations one should be keenly aware of the signal-to-noise ratio that the instrument is capable of resolving (PASQUILL, 1962). In the case of radio theodolites, such as the GMD-1, low elevation angles exaggerate small errors in angle measurement made at great distances between target and theodolite. Such conditions are especially prevalent near jet streams, where the balloons drift off rapidly. In order to overcome the handicap of low elevation angle, the Japanese have instituted a "relay system". A balloon is released at one station (Honjo); after it has drifted out of range, it is tracked from a second station (Tateno) (ARAKAWA, 1959). This relay method can be put to effective use only if the direction of upper winds is very steady, as is the case over East Asia during winter. Under more variable weather conditions mobile balloon launching units might conceivably improve the quality of upper-wind measurements at tropopause height by keeping the elevation angle at which the balloon is being tracked at relatively high values.

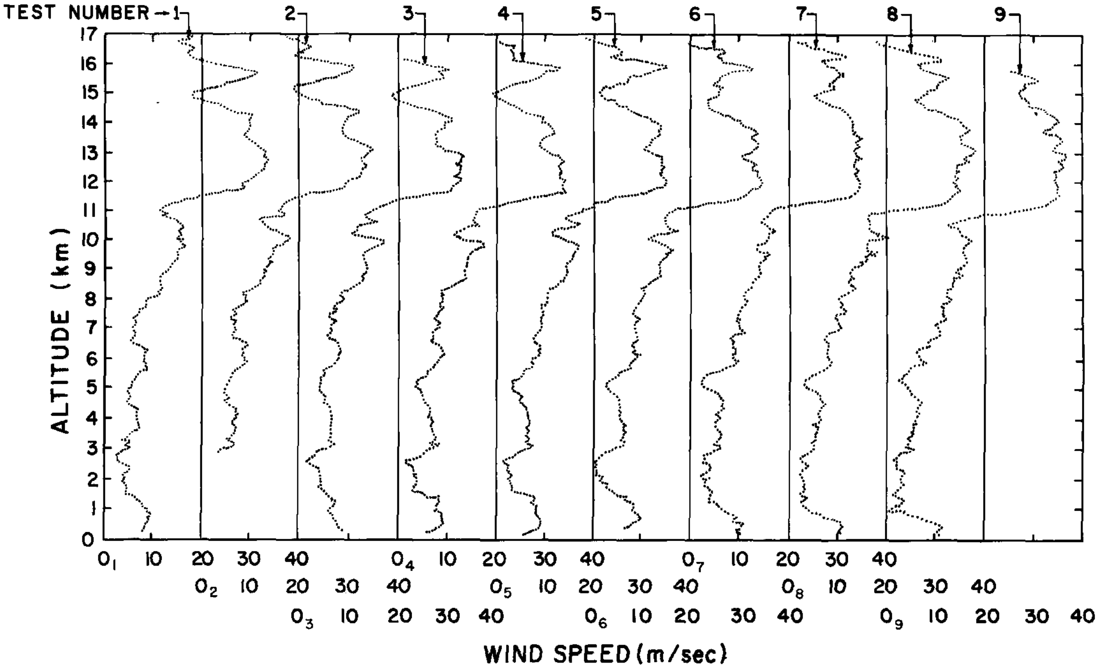

Fig.28. Vertical wind profiles measured at approximately 45-min intervals by FPS-16 radar over Cape Kennedy on 3 January 1963. A shifting scale has been used for the indication of wind speeds (m/sec) along the abscissa. (After SCOGGINS and VAUGHAN, 1963.)

In view of the fact that most of the wind fluctuations reported by the GMD-1 radio theodolites had vertical wave lengths corresponding to 1–2 min of ascent time, these fluctuations had to be rejected as not significant. Balloon positions are routinely obtained at 1-min. intervals, and then a mean wind is obtained for overlapping 2-min. intervals. Accordingly, the most frequently observed fluctuations in the vertical wind profiles correspond to either the measurement or the smoothing intervals (REITER, 1958a, 1961a, 1963a).

The use of radar instead of radio theodolites greatly enhances the quality of upper-wind measurements, even at low elevation angles. Some of the new instruments, such as the FPS-16, are almost too accurate to measure winds. It turns out, that with these instruments, one is able to discern the erratic path which a balloon describes due to the turbulence generated by its own ascent. Fig.28 shows a series of upper-wind measurements taken with FPS-16 equipment over Cape Kennedy at approximately 45-min intervals (SCOGGINS and VAUGHAN, 1963). Wind values were obtained every 0.1 sec during these balloon runs. They were then averaged over 25 vertical m, or 3-sec periods. Each of the smoothed values obtained is represented by a dot in Fig.28. The relatively wide scatter of data points in the troposphere is produced by the aforementioned aerodynamic behavior of the balloons. Above a certain height, which depends on the critical Reynolds' number, the data points in the wind profiles follow a very smooth pattern.

From the series of balloon ascents shown in Fig.28, as well as from other similar case studies (REITER, 1963d; WEINSTEIN and REITER, 1965), it may be seen that certain *meso-scale* features in the vertical wind structure persist for a considerable time. They are quite definitely *not* caused by instrumental errors, but are really present in the atmosphere, both fluctuations in wind speed as well as in wind direction. Similar fluctuations are encountered in the wind measurements of the rocket sonde network. Even though these measurements are less accurate than those taken with the FPS-16 system, the time-persistence of some of the observed details speaks in favor of their real existence.

What may be the physical cause of these meso-structural details in the wind profiles? HINES' (1960) model of gravitational waves, which is based on flow conditions in a stable atmosphere, has certain merits. A vertical succession of layers, in which gravity waves are out of phase, separated by nodal surfaces, might conceivably produce wind profiles similar to the ones observed. In view of the time-persistence of these features in the wind profiles we would have to postulate that these oscillations are standing rather than traveling gravity waves. Theoretical treatments of such waves—mainly produced by orographic obstacles, and therefore commonly referred to as "lee waves"—have been offered by LYRA (1940, 1943), QUENEY (1947, 1948), SCORER (1949), and others.

If one plots balloon positions at which an identifiable wind speed anomaly is observed, one finds the anomaly spread out over a fairly large region, larger than one wave length in a lee-wave formation. The gravitational-wave model, therefore, does not seem to be generally applicable to these *meso-scale* perturbations.

SAWYER (1961) suggests that the observed wind fluctuations may be quasi-inertial oscillations. Thus they could extend over an area which may extend several hundred miles along the axis of the mean flow. Sawyer's hypothesis is very plausible, indeed. If the layers of observed wind-speed anomalies are of sufficient vertical extent, frictional interaction will be relatively small. On the other hand, the alternating positive and negative vertical wind shears do not seem to be reflected in the temperature soundings (REITER, 1963d). The wind fluctuations, therefore, should be characterized by strong ageostrophic components of flow. These, however, would lead to quasi-inertia oscillations, if the changes in the basic (geostrophic) field of flow are smaller than the ageostrophic component itself.

Following SAWYER'S (1961) derivation, we consider the equations of motion:

$$\frac{\mathrm{d}\boldsymbol{V}}{\mathrm{dt}} - f\boldsymbol{V}\cdot\boldsymbol{k} = \mathrm{g}\nabla \mathrm{z} + \mathrm{K}\frac{\partial^2 \boldsymbol{V}}{\partial \mathrm{z}^2} \tag{59}$$

where the last term in eq.59 is a simplified expression for the frictional forces. Explicitly we may write:

$$\frac{\partial \mathrm{u}^*}{\partial t} + \bar{\mathrm{u}}\frac{\partial \mathrm{u}^*}{\partial x} + \omega^*\frac{\partial \bar{\mathrm{u}}}{\partial \mathrm{p}} - f\mathrm{v}^* = -\mathrm{g}\frac{\partial \mathrm{z}^*}{\partial x} + \mathrm{g}^2\rho^2\mathrm{K}\frac{\partial^2 \mathrm{u}^*}{\partial \mathrm{p}^2}$$

$$\frac{\partial \mathrm{v}^*}{\partial t} + \bar{\mathrm{u}}\frac{\partial \mathrm{v}^*}{\partial x} + f\mathrm{u}^* = -\mathrm{g}\frac{\partial \mathrm{z}^*}{\partial y} + \mathrm{g}^2\rho^2\mathrm{K}\frac{\partial^2 \mathrm{v}^*}{\partial \mathrm{p}^2}$$

$$\frac{\partial u^*}{\partial x} + \frac{\partial v^*}{\partial y} + \frac{\partial \omega^*}{\partial p} = 0$$

$$\left(\frac{\partial}{\partial t} + \bar{u}\frac{\partial}{\partial x}\right)\frac{\partial z^*}{\partial p} = -B\omega^* \tag{60}$$

Sawyer's derivation makes use of the following assumptions:
(*1*) Hydrostatic conditions;

$$\frac{\partial z}{\partial p} = -\frac{1}{g\rho} = -\frac{R\Theta p^{(\varkappa-1)}}{g\cdot 1000^{\varkappa}}. \tag{61}$$

(*2*) Small perturbations (indicated by asterisk) superimposed upon a shearing basic flow ($\bar{u}$) in the x-direction, so that the components of total flow are given by:

$u = \bar{u} + u^*$,

$v = v^*$,

$\omega = \omega^*$,

and

$$z = \bar{z}(y, p) + z^*(x, y, p) \tag{62}$$

Furthermore, $\omega = dp/dt$, and $\varkappa = (c_p - c_v)/c_p$.
(*3*) Adiabatic conditions of flow and steady state $\left(\frac{\partial}{\partial t} = 0\right)$. Since $V\cdot\Theta = -\omega\frac{\partial\Theta}{\partial p}$, we obtain by differentiation of eq.61:

$$V\cdot\nabla\left(\frac{\partial z}{\partial p}\right) = \frac{R\cdot p^{\varkappa}}{gp\cdot 1000^{\varkappa}}\cdot\omega\frac{\partial\Theta}{\partial p} = -B\omega, \tag{63}$$

where $B = -\frac{R}{gp}\left[\frac{\partial T}{\partial p} - \left(\frac{\partial T}{\partial p}\right)_{\Theta}\right]$, the subscript indicating the dry adiabatic lapse rate with Θ = const. Assuming a sinusoidal perturbation in the x, y, p and t directions:

$$u^* = u_0 \exp\left[i(\lambda(x - ct) + \mu y + \nu p)\right] \tag{64}$$

where u_0 is the amplitude of the perturbation. Using similar expressions for v^*, ω^*, and z^*, eq.60 yields:

$$i\lambda(\bar{u}-c)u_0 + \omega_0\cdot\frac{\partial\bar{u}}{\partial p} - fv_0 = -ig\lambda z_0 - g^2\rho^2 K\nu^2 u_0$$

$$i\lambda(\bar{u}-c)v_0 \qquad\qquad + fu_0 = -ig\mu z_0 - g^2\rho^2 K\nu^2 v_0$$

$$\lambda u_0 + \mu v_0 + \nu\omega_0 = 0$$

$$\nu\lambda(\bar{u}-c)z_0 = B\omega_0 \tag{65}$$

By eliminating u_0, v_0, ω_0, and z_0, we may solve for $(\bar{u}-c)$. The abbreviation $A = i\lambda(\bar{u}-c) + g^2\rho^2 K\nu^2$ allows us to write eq.65 as a determinant,

$$\begin{vmatrix} A & -f & \frac{\partial \bar{u}}{\partial p} & ig\lambda \\ f & A & 0 & ig\mu \\ \lambda & \mu & \nu & 0 \\ 0 & 0 & B & i\nu(A-g^2\rho^2K\gamma^2) \end{vmatrix} = 0 \tag{66}$$

from which one obtains:

$$\nu(A-g^2\rho^2K\nu^2)\left\{(A^2+f^2)\nu+\frac{\partial \bar{u}}{\partial p}(f\mu-A\lambda)\right\}+gAB(\lambda^2+\mu^2)=0 \tag{67}$$

In the absence of friction ($K=0$) and of wind shear $\left(\frac{\partial \bar{u}}{\partial p}=0\right)$, two solutions for A are obtained from eq.67:

$$A=0$$

$$A=\pm\left(-f^2-\frac{gB(\lambda^2+\mu^2)}{\nu^2}\right)^{\frac{1}{2}} \tag{68}$$

The first solution, $A=0$, together with frictionless and shearless flow conditions, renders the following expressions from eq.65:

$$f v_0 = ig\lambda z_0$$

$$f u = -ig\mu z_0$$

$$\omega_0 = 0 \tag{69}$$

Thus, for $A=0$ the motion is geostrophic, no vertical components of flow are present, and $\bar{u}=c$, i.e., the disturbance pattern is advected with the basic current. This solution evidently is not relevant in explaining the strongly ageostrophic fluctuations found in detailed vertical wind profiles.

In evaluating the significance of non-trivial solutions, SAWYER (1961) assumes the following magnitudes for the various parameters entering the above equations:

Horizontal wave length; $L_{x,y}=400$ km:

$$\therefore\ \lambda=\mu=2\pi/L_{x,y}=1.6\cdot10^{-7}/\text{cm}$$

Vertical wave length; $L_z=1.5$ km, equivalent to $\Delta p \cong 50$ mbar:

$$\therefore\ \nu=\frac{2\pi}{\Delta p}=1.3\cdot10^{-4}g^{-1}\ \text{cm sec}^2$$

Approximately isothermal lapse rate; $gB=4.5\cdot10^{-3}$ cm^4 g^{-2} sec^2. (For adiabatic lapse rates $gB=0$.)

Shear of 2 m/sec/km:

$$\therefore\ \frac{\partial \bar{u}}{\partial p}=7\cdot10^{-3}g^{-1}\ \text{cm}^2\ \text{sec.}$$

Eddy diffusivity; $K=10^3$ cm^2/sec.

Coriolis parameter; $f=10^{-4}$/sec.

With these magnitude assumptions, the second solution for A (eq.68) becomes:

$$A = \pm 1.5 \cdot 10^{-4} i \ \text{sec}^{-1} \tag{70}$$

and $(\bar{u}-c) = \pm 10$ m/sec. Since the solutions for $(\bar{u}-c)$ are necessarily real, the oscillations will be stable.

The effect of eddy viscosity on the magnitude of A (assuming $\rho = 0.4 \cdot 10^{-3}$ gm/cm^3):

$$g^2 \rho^2 K \nu^2 \cong 2.6 \cdot 10^{-6}/\text{sec} \tag{71}$$

is much smaller than the contribution indicated by eq.70. Thus, the character of the motion should not be influenced drastically by friction of the magnitude assumed above. Neglecting viscous effects, but including vertical shear, we may write the solution:

$$A = \tfrac{1}{2}\left[\frac{\lambda}{\nu}\frac{\partial \bar{u}}{\partial p} \pm \left\{\frac{\lambda^2}{\nu^2}\left(\frac{\partial \bar{u}}{\partial p}\right)^2 - 4\left(f^2 + \frac{\partial \bar{u}}{\partial p}\frac{f\mu}{\nu^2} + \frac{gB(\lambda^2+\mu^2)}{\nu^2}\right)\right\}^{\frac{1}{2}}\right] \tag{72}$$

Comparison of eq.72 with 68 shows, that the consideration of vertical shear introduces a real part into A; consequently this may produce unstable waves. The destabilizing effect seems to be small, however—as is the case with viscous effects (eq.71)—if the estimated magnitudes are accepted:

$$\frac{\lambda}{\nu}\frac{\partial \bar{u}}{\partial p} = \frac{\mu}{\nu}\frac{\partial \bar{u}}{\partial p} \cong 8.6 \cdot 10^{-6} \ \text{sec}^{-1} \cong \tfrac{1}{12} f \tag{73}$$

We may, therefore, assume that even with frictional and shearing effects of the specified magnitudes, the waves will behave like stable oscillations, moving relative to the stream at $(\bar{u}-c) \cong 10$ m/sec. Slight damping or amplification may be present, depending on whether shear or eddy viscosity dominates.

Different conclusions would have to be reached if λ were much larger than μ, i.e., if the wave length measured *across* the current were much larger than the one measured *along* the upper flow. From SAWYER's (1961) observations this was not evident however, nor is it from Project Jet Stream flight measurements.

The Project Jet Stream measurements revealed the existence of meso-structural fluctuations in the wind and temperature fields along quasi-horizontal aircraft traverses through the jet stream (REITER, 1961b, c, 1962; REITER et al., 1961; KUETTNER and MCLEAN, 1961). These fluctuations seem to be remarkably persistent in time. Fig.29 shows two flight legs of flight No.12 which were flown at approximately the same pressure altitude. In spite of a time difference of more than one hour between the two flight legs the meso-structural details in winds and temperature remain well preserved. Wave lengths of the perturbations, measured across the current seem to range from 20 to 60 nautical miles. From these flights evidence was collected that meso-structural details in the upper wind field seem to orient themselves along isentropic surfaces, with the wave lengths measured *along* the flow being much larger than the ones *across* the flow (REITER, 1961d). Thus it appears that the assumptions underlying Sawyer's derivations are quite safe.

Returning to eq.65 we may substitute the last two equations into the first one as follows:

$$\underbrace{i\lambda(\bar{u}-c)u_0}_{A} - \underbrace{\frac{\partial \bar{u}}{\partial p}\frac{1}{\nu}(\lambda u_0 + \mu v_0)}_{B} - \underbrace{f v_0}_{C} + \underbrace{\frac{igB}{\nu^2(\bar{u}-c)}(\lambda u_0 + \mu v_0)}_{D} + \underbrace{g^2\rho^2 K \nu^2 u_0}_{E} = 0 \tag{74}$$

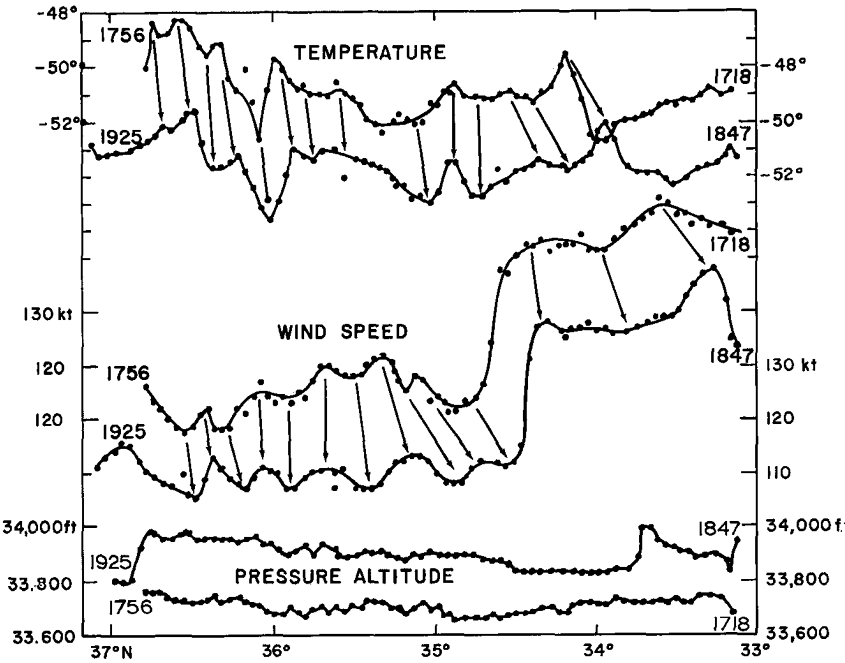

Fig.29. Aircraft measurements of temperature, wind speed and pressure altitude for two flight legs of Project Jet Stream Flight No.12, 18 January 1957, flown between Dayton, Ohio, and Charleston, South Carolina, along the same route but at different times. Ordinate values along left margin refer to flight leg between 17h18 and 17h56 G.M.T., values along right margin refer to flight leg between 18h47 and 19h25 G.M.T. (After REITER et al., 1961.)

Using the assumptions stated on p.137,the various terms in eq.74 have the following magnitudes in units of cm/sec^2:

A: inertial effects; $1.6 \cdot 10^{-4} u_0$

B: vertical advection (shear); $10^{-5} u_0$

C: Coriolis; $10^{-4} u_0$

D: thermodynamical effects; $0.4 \cdot 10^{-4} u_0$

E: frictional effects; $2.6 \cdot 10^{-6} u_0$.

Thus, inertial, Coriolis, and thermodynamic effects seem to be mainly responsible for meso-structural details observed in the wind soundings. The streakiness of the upper wind field, as revealed by the Project Jet Stream flights, in all probability is a manifestation of the same meso-structure.

Vertical wind profiles measured in jet streams would show stronger vertical shears $\frac{\partial \bar{u}}{\partial p}$ than the ones assumed on p.137. The vertical advection term B may become of significant magnitude under such conditions and unstable waves may result. If the vertical wave-length of the meso-structure were significantly smaller than the one assumed on p.137, frictional terms would gain importance.

Unfortunately, our present knowledge of the behavior of inertial oscillations in the atmosphere is rather limited. The speed of waves of synoptic scale may, of course, be determined from sequences of upper-air charts. Whether or not the meso-structural details behave in the same way is not known. SAWYER (1961) considers stationary waves ($c = 0$) possible. On the other hand, quasi-inertial wind oscillations leading to the formation of large-scale jet maxima may travel as fast as 20 m/sec. NAMIAS (1947) established a climatological mean-speed of short-wave troughs of 10 m/sec. The actual value of c for meso-structural details may lie anywhere between these two extremes.

Not only do we lack knowledge concerning the propagation speed of quasi-inertial meso-scale disturbances, but their horizontal extent along and across the current is also unknown. Single-station observations, as offered by the FPS-16 radar, indicate channels of ageostrophic departures of the same sign, oriented along the direction of the upper flow. From Project Jet Stream data one might conclude that the wave lengths of these disturbances are almost one order of magnitude smaller across the current than along its axis. An investigation of the three-dimensional orientation of meso-structural details and their change with time is still to be undertaken.

In the foregoing derivation $\frac{\partial \bar{u}}{\partial p}$ and $\bar{u}$ have been treated as quasi-constants, the latter varying only by a small fraction of its value over one vertical wave length. As has been pointed out above, under jet-stream conditions these assumptions may no longer be valid.

Furthermore, in eq.64 we have considered λ, μ, and $(x-ct)=(\bar{u}-c)t$ to be independent of p. In the case of simple inertial oscillations the wave length of the inertial wave, L_i, is a function of $\bar{u}$. It may be shown that:

$$\frac{\partial L_i}{\partial p} = \frac{2\pi}{f} \frac{\partial \bar{u}}{\partial p} \tag{75}$$

In the presence of vertical wind shears characteristic of jet streams we should, therefore, expect changes of the meso-structural, horizontal wave lengths with height.

With the present state of knowledge we cannot tell from one, single-station, balloon observation in which phase position the balloon is intercepting a certain meso-structural wind speed or direction anomaly. Consequently, no significant correlation should be expected between ν and u*, or between thicknesses of layers showing meso-structural wind anomalies of a positive or negative sign, and the amplitude of these anomalies (WEINSTEIN and REITER, 1965).

On the other hand, the *maximum possible amplitude* attainable by such oscillations will be limited by turbulence that would be generated by excessive vertical shears:

$$\frac{\partial u}{\partial p} = \frac{\partial \bar{u}}{\partial p} + \frac{\partial u^*}{\partial p} \tag{76}$$

Richardson's turbulence criterion:

$$Ri = \frac{K_T}{K_M} \frac{\frac{g}{T}\left[\frac{\partial T}{\partial z} + \left(\frac{\partial T}{\partial z}\right)_\Theta\right]}{\left(\frac{\partial u}{\partial z}\right)^2 + \left(\frac{\partial v}{\partial z}\right)^2} = \frac{K_T}{K_M} \frac{\frac{g}{\Theta}\frac{\partial \Theta}{\partial z}}{\left(\frac{\partial v}{\partial z}\right)^2} \tag{77}$$

may be taken as an indicator of limiting vertical shears. The "critical Richardson number," $Ri_{cr}=1$, below which turbulent conditions are assumed to set in, need not necessarily hold in the free atmosphere. Especially not, if K_T/K_M, the ratio of exchange coefficients of heat and momentum, is assumed to be different from unity (PETTERSSEN and SWINBANK, 1947; PANOFSKY and MCLEAN, 1964).

If we introduce eq.64 into 66, assuming $\mu = 0$, we obtain:

$$\frac{\partial u}{\partial p} = \frac{\partial \bar{u}}{\partial p} + iu_0 \left[\frac{\partial \lambda}{\partial p} (\bar{u} - c)t + \lambda \frac{\partial (\bar{u} - c)t}{\partial p} + v \right] \exp \{ i[\lambda(\bar{u} - c)t + vp] \} \tag{78}$$

From eq.78 one finds that strong shears are likely to occur where:

(*a*) $\frac{\partial \bar{u}}{\partial p}$ is large, i.e., near jet streams;

(*b*) where v is large, i.e., where the vertical wave length of meso-structural disturbances is small; or

(*c*) where the harmonic function over the distance Δp attains the extreme values of (-1) and $(+1)$ respectively, i.e., where meso-structural perturbations are "stacked" on top of each other $-180°$ out of phase.

In a vertically shearing current which possesses such quasi-inertial, meso-structural details in the vertical wind profiles, there should be confined regions in which wind anomalies separated by a thickness Δp, are superimposed out of phase. If their contribution $\frac{\partial u^*}{\partial p}$ renders $\frac{\partial u}{\partial p}$ in eq.78 supercritical according to the criterion expressed by eq.77, turbulence may result in those isolated regions and within those relatively thin layers.

In the following section this will be discussed in more detail. We may point out here, that in the troposphere with its relatively low values of stability, only moderate shears will be needed to render *Ri* subcritical, and to give rise to turbulence. It is not surprising, therefore, that in the FPS-16 wind profiles the stratosphere shows much more meso-structural detail than the troposphere. In the latter only deep layers with relatively small wind speed anomalies may be expected to survive the eroding effects of turbulence.

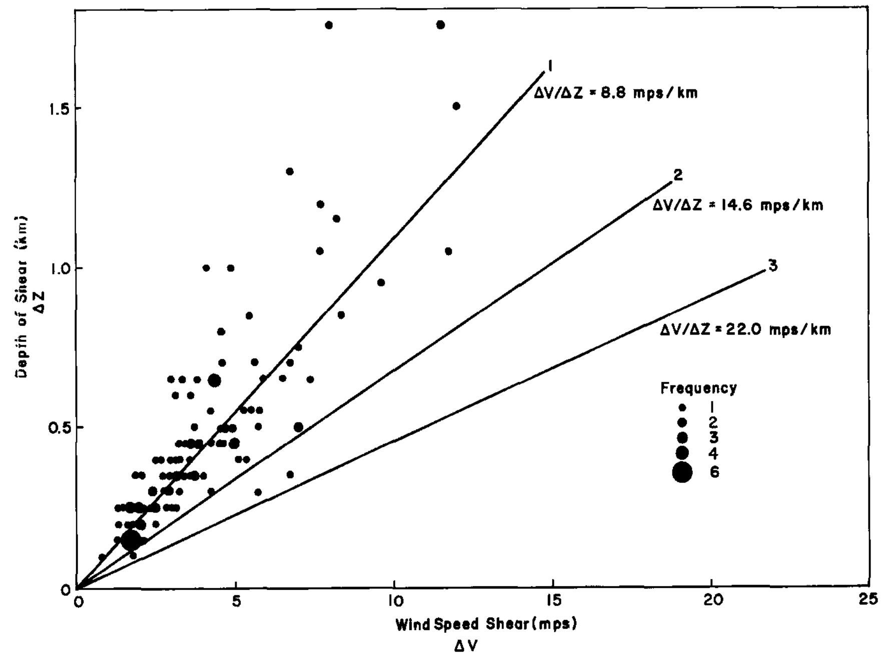

Fig.30. Maximum observed meso-structural wind shears (ΔV) in vertical wind profiles as a function of thickness (ΔZ) of shearing layer. Lines *1*, *2* and *3* indicate the mean correlation for all observations, the 97.5% probability of maximum shears, and theoretical shears for *Ri* = 1 under conditions of isothermal lapse rate and T = 73°C. (After WEINSTEIN and REITER, 1965.)

In the stratosphere, where the nearly isothermal lapse rates call for large Richardson numbers, meso-structural wind speed and direction fluctuations may survive for considerable periods of time, as shown by radar wind measurements (Fig.28), and as indicated from rocketsonde data.

Although we cannot obtain an indication of the wave lengths or phase relationships of wind anomalies within meso-structural layers from one single-station observation, we may utilize the above discussion to estimate the maximum possible meso-structural amplitudes under the given synoptic conditions. Since the speed fluctuations observed in vertical wind profiles affect vertically rising aerospace vehicles, the maximum possible turbulence action on these vehicles is readily computed if the response characteristics of the vehicles and their speed as a function of pressure or altitude are known.

Such an estimate of the maximum meso-structure may be made in two ways:

(*a*) We may proceed from eq.77 and select a suitable value for *Ri*, probably close to 1. $\left(\frac{\partial V}{\partial z}\right)$ in the denominator of that expression may be computed from $\frac{\Delta V}{\Delta z}$ or $\frac{\Delta V}{\Delta p}$, where Δz or Δp constitute $\frac{1}{4}$ of a vertical wave length of shearing layers. Under the given stability conditions maximum values ΔV will give maximum possible meso-structural speed anomalies as a function of Δz. (See appropriate line in Fig.30.)

If we have one balloon sounding available, and if the assumption is warranted that the layer depths of the meso-structural fluctuations will be conserved throughout the forecasting period[1], maximum possible speed amplitudes may be estimated from the correlation between ΔV_{max} and Δz shown in Fig.30.

(*b*) From time series of detailed balloon wind measurements one may regard each meso-structural wind layer separately. If the measurement series is long enough, it usually is not difficult to find at least one sounding among the series in which a particular speed fluctuation apparently attains maximum amplitude. We may assume that the balloon intercepted this particular layer at the time of the ascent close to its extreme amplitude (value of the harmonic function ± 1). ΔV_{max} may then be plotted as a function of Δz. Fig.30 shows, that such values obtained from actual data contain surprisingly little scatter. This may hopefully be taken as an indicator that the theoretical considerations described in the foregoing are valid.

Again, from individual soundings observed values of ΔV in their relationship with Δz may be extrapolated to ΔV_{max} for the same value of Δz, thus rendering the *maximum possible meso-structural agitation* of the atmosphere in this particular weather situation *if all meso-structural layers were encountered at a phase angle of* $\frac{(2n-1)\pi}{4}$, with $n = 1, 2, ..$:

The origin of meso-structural perturbations, as the ones discussed above, is still open to speculation. Ageostrophic components of flow, which seem to be responsible for this kind of atmospheric disturbance, may be generated in various ways. RAETHJEN (1961) and HÖFLICH (1961) suggest that convective motions in the troposphere are of importance. These motions would carry aloft a deficit of momentum, thus leading to subgeostrophic flow conditions. Ageostrophic flow, on a large scale, is observed in the entrance and

[1] In view of the long persistence of meso-structural details, as evident from FPS-16 measurement series especially in the stratosphere, this assumption appears safe for at least several hours and as long as no major changes in the upper-wind regime (such as the passage of the jet axis, or of a trough or ridge) are anticipated.

exit regions of jet maxima. In view of the dispersive properties of eq.75 this motion might generate a meso-structure superimposed upon the vertically shearing current. Orographic obstacles might also act as sources of ageostrophic motion (WEINSTEIN and REITER, 1965).

The micro-structure of jet streams

On p.128 we classified the microstructure as having perturbation wave lengths of $< 10^4$ m in the horizontal, and approximately two orders of magnitude less than this in the vertical. At present our knowledge of atmospheric fine structure in the jet-stream region depends almost exclusively on data collected by jet aircraft.

As an instrument platform, these aircraft with a cruising speed of about 200 m/sec have serious limitations. Certain portions of the turbulence spectrum of atmospheric motions have to be deduced from reactions of the aircraft (mostly from accelerometer measurements, but also from sensitive airspeed records or differential pressure probes) (BURNS and RIDER, 1965). These measurements are distorted by the response characteristics of the aircraft. The aircraft response may be corrected for mathematically, at least to a certain extent. Nevertheless, the aircraft itself and its aerodynamic properties constitute a "filter" which, at least at present, makes accurate atmospheric measurements in the upper range of the microstructure (wavelengths of about 0.5–10 km) very difficult (PASQUILL, 1962).

Atmospheric disturbances with a horizontal wave length of the order of 10^2 m may be detected from bumpy flight conditions. If such conditions are encountered in a cloud-free environment, the phenomenon is commonly known as "clear-air turbulence" (CAT). Severe cases of CAT may cause structural damage to aircraft (REITER, 1963b, 1964c). Even light and moderate cases adversely affect passenger safety and comfort and may reduce the useful life of an aircraft.

After more than a decade of research and measurements on this phenomenon, the physical nature of CAT still remains an open question. Statistical evidence has produced most of the large-scale correlations that can be developed. As shown in Table I (after COLSON, 1963), CAT seems to be more frequent near the jet-stream than away from it (BANNON, 1952). Cases of CAT have been reported, however, in association with relatively weak winds (REITER, 1964d). CAT seems to show a frequency maximum near the tropopause and near baroclinic stable layers, such as the "jet stream front," at least as far as presently available data from subsonic aircraft indicate (ENDLICH and MCLEAN, 1957; MCLEAN, 1962).

TABLE I

FREQUENCY OF CAT ENCOUNTERS OVER THE U.S.A. (%)

Season	≦150 miles to left of jet stream	≦150 miles to right of jet stream	No jet stream	Near trough	Near closed low	In mountain waves
Autumn	34	31	35	26	5	22
Winter	39	29	32	11	1	30
Spring	36	26	38	14	4	23
Summer	29	30	41	18	1	18

The observed frequency maxima of CAT over mountainous or hilly terrain (CLODMAN et al., 1960) indicate an effective perturbation input from orographic obstacles under proper atmospheric conditions. Thus, lee wave considerations such as those described by LYRA (1940, 1943), QUENEY (1947, 1948) and SCORER (1949) may be of value in locating potential CAT regions over mountainous terrain (REITER, 1960, 1963e,f, 1964b). In line with this reasoning there seem to be differences in the duration and intensity of CAT over oceanic and continental regions (CLODMAN et al., 1960); the latter show on the average higher frequencies but smaller extent of turbulent regions.

Cyclonic upper flow patterns, especially sharp troughs, also appear to produce more cases of CAT than straight or anticyclonic flow (see Table I). This may be due to the fact that confluence to the rear of troughs tends to produce shallow layers with strong vertical wind shears, mostly due to a turning of wind with height (ENDLICH, 1963, 1964; REITER and NANIA, 1964; REITER, 1964d; ENDLICH and MANCUSO, 1964), (see Fig.4–8).

All we know about the physical nature of CAT is that the aircraft receives jolts of certain intensity, produced by either vertical or horizontal gusts, or both, the former being more effective in producing accelerations than the latter, at least with the present aircraft types. These gusts may be produced by genuine atmospheric turbulence, or by short gravitational waves along a stable interface which is intercepted by the aircraft. If the wave lengths of these eddies correspond to resonance frequencies of the aircraft, they will be especially effective in generating CAT.

In both cases—CAT in stable shearing layers as well as in turbulent adiabatic layers—bumpy flight conditions more often seem to occur in relatively shallow layers rather than in deep air spaces,[1] especially when encountered in the stratosphere. One might, therefore, hypothesize that their common character—the relatively thin and layered structure of CAT—suggests a common physical cause.

Correlations of CAT cases with Richardson's number have produced contradictory statistics. The discrepancies in the correlations are mostly due to the fact that Richardson's numbers are computed over relatively deep atmospheric layers, while CAT is a small-scale phenomenon. Statistical treatment does not consider the principles of turbulence theory, whereby kinetic energy "cascades" from the mean flow into large disturbances, and through the various spectral ranges into viscous dissipation and generation of heat. As L. F. Richardson once put it: "Big whirls have little whirls that feed on their velocity, and little whirls have lesser whirls and so on to viscosity." Only if this cascade of energy is uninterrupted should we expect a significant correlation between large-scale flow patterns and CAT. Meso-scale features in the upper-flow pattern, on the other hand, should show a better agreement with CAT occurrence, because they produce a more immediate input into the small perturbations of clear-air turbulence.

This line of reasoning has been substantiated by measurements obtained over Australia (REITER, 1964d). In this instance efforts to forecast CAT were more successful when close attention was paid to shallow stable and shearing layers, as they became apparent from radiosonde observations, rather than by using established forecasting routines which give CAT warnings for an excessively deep air space.

Cases of moderate CAT were found over Australia with remarkably light wind speeds in regions where the winds turned rapidly with height. Cross-sections through the

[1] Deep adiabatic layers in the troposphere are usually accompanied with convective clouds. Turbulent flight conditions in these regions are to be anticipated and, therefore, would not qualify as CAT.

turbulent zone reveal that severe bumpiness was confined to a region where winds backed sharply with height. In these particular cases cold air was sinking underneath warm air, producing a stable stratification. SCHWERDTFEGER and RADOK (1959), on the other hand, have found CAT with destabilization of the atmosphere by differential temperature advection.

One particular observation of CAT over Australia deserves mentioning (REITER, 1964d). On 12 September 1963, the research aircraft encountered a patch of moderate CAT about 15 miles in diameter, embedded in a "smooth" environment. The CAT patch was first encountered over Lake Dutton (about 137°02'E, 31°48'S), a level salt flat northeast of Adelaide. In passing through the turbulent region, the aircraft marked its location with a smoke trail. In repeated passes the CAT patch was found again in penetrations from different directions, not significantly changed in intensity or extent. Aircraft traverses 1,000 ft. above and 2,000 ft. below the main turbulent level (32,000 ft.) showed appreciably less turbulence. The aircraft was able to stay with the turbulent patch for approximately 45 min, until it ran low in fuel. During this time the turbulent region drifted, as nearly as one could tell, with the mean wind of about 133 knots from 282°. In this and other cases of long-lived CAT, the meso-structure of the upper flow pattern must offer a continuous source of perturbation energy, which feeds into the smaller scales observed as turbulence.

In a preceding section the peculiarities of ageostrophic atmospheric layers, which may undergo some sort of quasi-inertial oscillations, have been discussed. It was suggested that the superposition of layers oscillating at different wave numbers may cause confined regions in which vertical wind shears (composed of mean shear plus perturbation shear) are quite strong (eq.78). Should these shears ever exceed those rendering critical Richardson numbers, turbulence might be expected within the layer and in the area. The relatively high frequency of CAT occurrence in the strongly shearing regions above and below the jet stream core corroborates this hypothesis. Further, according to eq.75, larger values of $\frac{\partial \bar{u}}{\partial p}$ would be associated with larger values of $\frac{\partial L}{\partial p}$. The latter would increase the number of places in a given area, where the perturbation velocities in vertically adjacent layers would be superimposed out of phase.

We may carry this purely speculative reasoning still farther. If turbulence were to result from meso-structural, vertically shearing instabilities, a (shallow) layer with adiabatic lapse rates—equivalent to the mean potential temperature of the vertically mixed air masses—bounded by two excessively stable (shallow) layers should result. At the same time the momentum of flow should be exchanged across the adiabatic layer, so that the meso-structural vertical wind shears would now be confined to the two adjacent stable layers. Since the *squared* vertical wind shear enters Richardson's criterion, and only the *linear* potential temperature lapse rate, the adiabatic mixing layer would be expected to spread vertically, until layers of opposing wind shear will limit the vertical momentum transfer.

A vertical succession of adiabatic and stable layers has been observed in detailed temperature soundings (DANIELSEN, 1959). The above reasoning brings up the question, in regions of strong vertical wind shears is the meso-structure observed in the temperature profiles generated by turbulent forces? Perhaps, observed meso-structure is not entirely the result of differential temperature advection.

More research, especially more sophisticated measurements, will be necessary before proof or disproof of the above speculations can be obtained. In view of increasing air traffic, and with our improved understanding of large-scale flow processes in the atmosphere, more attention must be devoted to the meso and micro-scales of atmospheric structure.

Climatology of tropospheric flow

In a preceding section it was pointed out that planetary long waves up to wave number 4 seem to be associated with the large mountain ranges and the land-sea distribution in the two hemispheres. These effects strikingly reveal themselves in the mean location of jet-stream systems (see Fig.36 and 37). Their dynamical properties, in turn, influence the sequence of weather patterns, and the meteorological parameters measured near the earth's surface. Thus, the mean conditions of tropospheric flow with their large-scale as well as their regional aspects constitute an integral part of dynamic climatology.

Tropospheric and tropopause jet-stream systems

In describing those jet-stream systems which are of great significance for tropospheric flow patterns, we shall adhere to classical nomenclature. It should be realized, however, that certain transition phases between individual jet-stream systems are possible. Each jet-stream is an integral part of the general circulation. It is not a self-contained entity, and its interactions with other jet-stream systems constitute the physical basis of large-scale transport processes in the atmosphere.

Jet streams occurring at or near tropopause level have been classified into two major groups: those which are associated with a low-tropospheric baroclinic zone, i.e., a "front," and those whose baroclinicity is confined to the upper troposphere. The main representative of the former type is the *polar-front jet* (PFJ) stream. Jet streams associated with maritime or arctic fronts shall be discussed in conjunction with the PFJ, since their characteristics are rather similar. The latter type is represented by the *subtropical westerly jet stream* (STJ) and the *tropical easterly jet stream* (TEJ).

In the lower troposphere, associated with an inversion or with a frontal discontinuity in temperature lapse rate, one sometimes encounters a more or less pronounced wind maximum in the form of a *low level jet stream* (LLJ) or an *inversion wind maximum* (IWM).

Frontal jet stream

The classical treatment of air mass properties (SCHINZE and SIEGEL, 1943), in vogue in the German meteorological services of the 1930's and 1940's, has been extended recently by the Canadian Meteorological Service, incorporating modern aspects of upper flow patterns (GALLOWAY, 1958, 1963; MCINTYRE, 1958). Since a jet-stream system may be associated with each major frontal system in the atmosphere, we find the *polar front jet* (PFJ) with its core near the 300 mbar level over the polar front which separates maritime tropical air (mT) from maritime polar air (mP); the *maritime-front jet* (MFJ) over the maritime front separating mP from maritime arctic air (mA); and the *arctic front jet*

(AFJ) over the arctic front separating mA from continental arctic air (cA) (SEREBRENY et al., 1962). In some of the cases analyzed, following the Canadian three-front concept, the surface frontal positions are very close together, and one might argue whether or not a clear distinction can be made between individual air mass boundaries (GALLOWAY, 1963).

The upper-flow pattern, as evident from the 300-mbar chart, indicates a very distinct "fingery" structure of the jet stream, especially in the entrance and exit regions of the main speed maximum. Such a detailed structure of the jet stream is rather common (NEWTON, 1959b; SEREBRENY et al., 1962; REITER and NANIA, 1964).

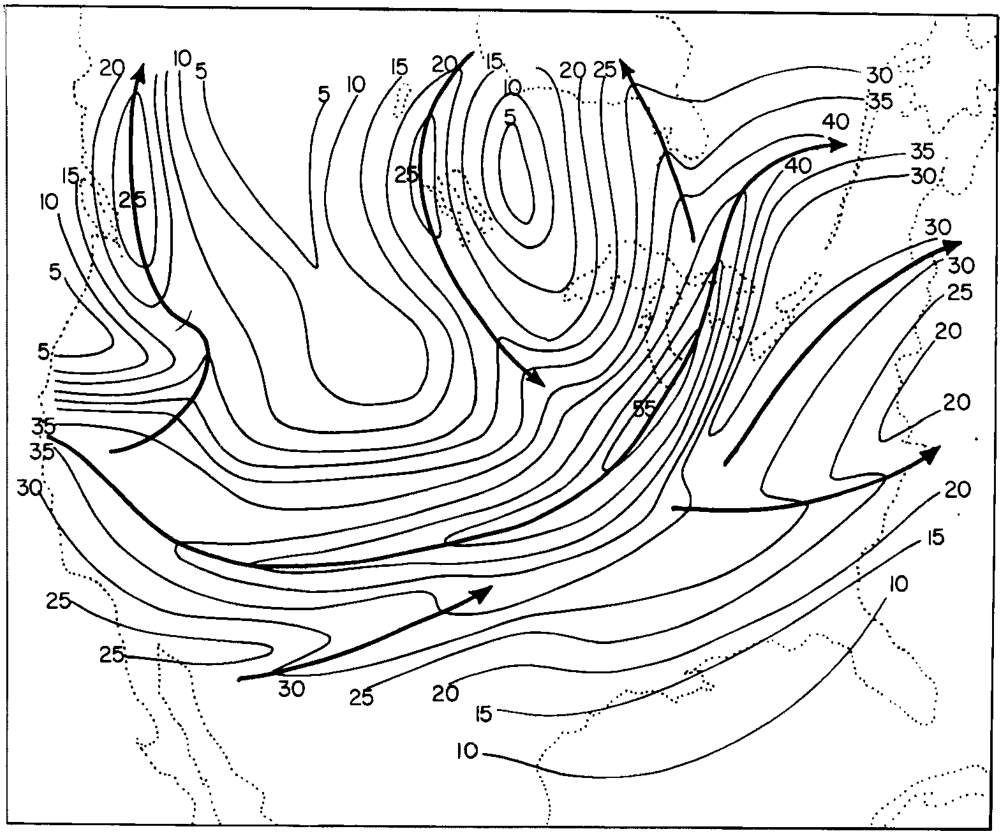

Fig.31. Isotachs (m/sec) on isentropic surface 315°K, 20 April, 1963, 00h00 G.M.T.

Isentropic analysis reveals the detailed structure of the jet stream even better. Fig.31 shows the flow on the 315°K surface on 20 April 1963, 00h00 G.M.T. around a deep cyclone over Minnesota. In comparison, Fig.32 shows a photograph of the same cyclone, taken by "Tiros V" a few hours earlier on the same day (April 19, 1924, G.M.T.). The high-speed band of the jet stream, in Fig.31, is contained within a stable layer, the "jet-stream front," as this layer has been called by ENDLICH and MCLEAN (1957). Again, we notice a "fingery" structure of the flow. It should be pointed out that the jet-stream flow analyzed in Fig.31, stretches over a wide range of pressures, from the stratosphere into the lower troposphere (Fig.33).

Inflow of moist air into the cyclone system occurs in the easternmost branch of this jet stream (Fig.33), where two parallel squall lines were observed on 19 April, 12 G.M.T. The "Tiros" photograph (Fig.32) indicates a well-developed cloud band in this region of moist air. Over the warm front the jet stream is fanning out; one branch flows anti-cyclonically around the ridge, while the other branch flows cyclonically into regions of high stability north of the cyclone location (ELIASSEN and KLEINSCHMIDT, 1957). Apparently it is this branch which provides inflow of moist tropospheric air masses into the stratosphere.

West of the cyclone a northerly jet-stream branch, containing dry stratospheric air, joins with the main flow in the stable layer. Such descending flow has been studied on

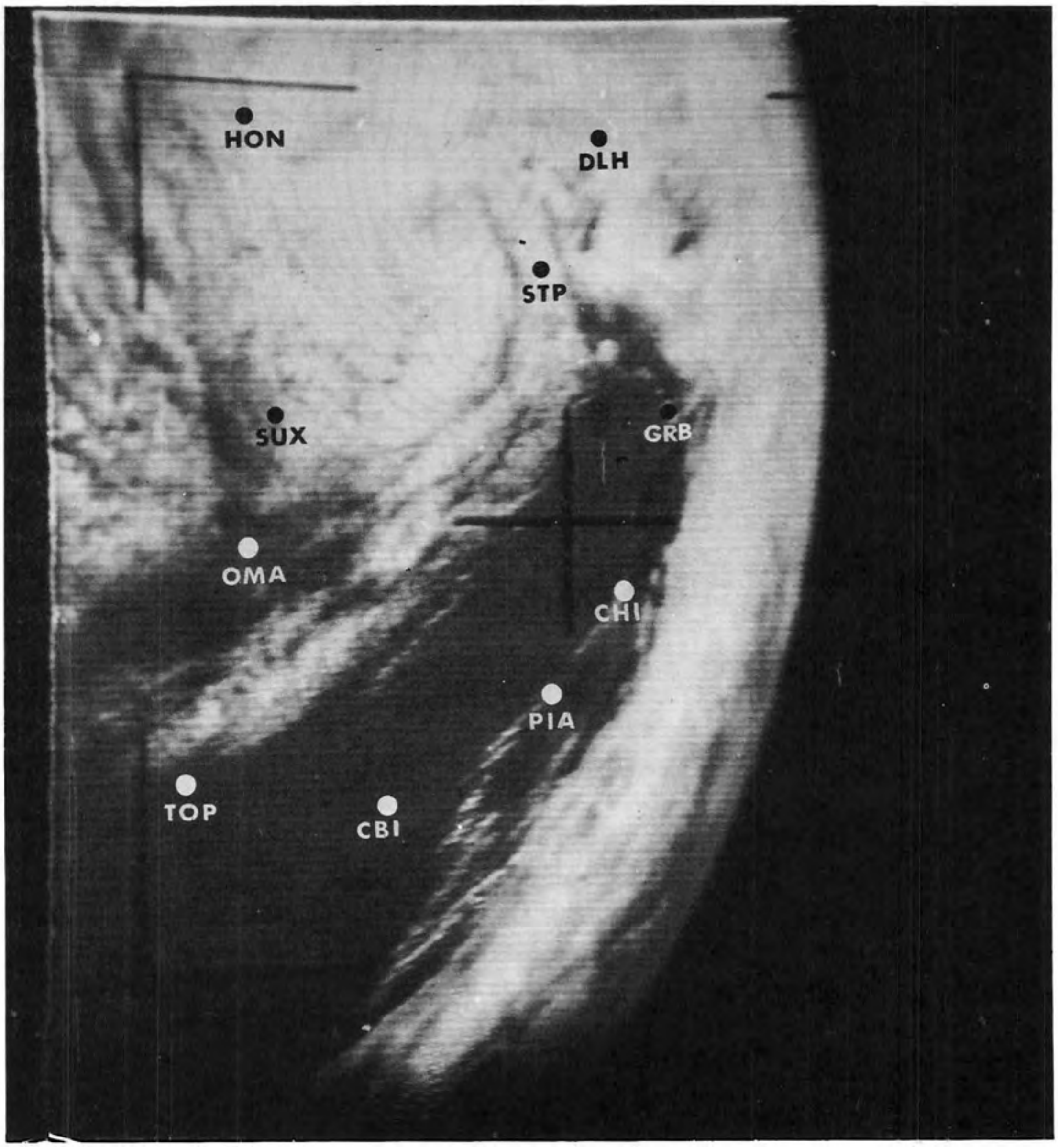

Fig.32. Cloud photograph, taken by "Tiros V", 19 April, 1963, 19h24 G.M.T. (U.S. Weather Bureau).

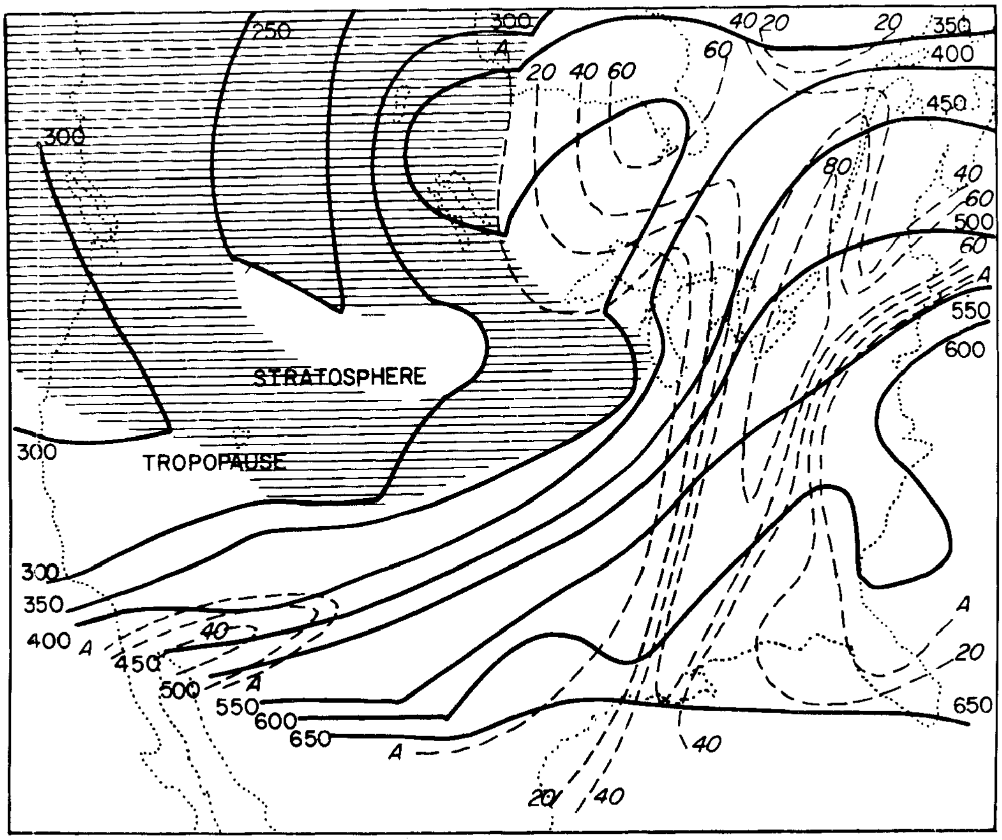

Fig.33. Pressure (mbar) and relative humidity (%, A indicates boundary of "motorboating", dry values) on the 315°K isentropic surface. Same observation time as Fig.31. Areas located in the stratosphere are shaded.

previous occasions in connection with the transport of radioactively contaminated stratospheric air (ELIASSEN, 1962; REITER, 1963b, 1964a; REITER and MAHLMAN, 1964; DANIELSEN, 1964a,b). This flow is indicated on the "Tiros" photograph by a cloud free band, seemingly spiralling into the cyclonic vortex (WIEGMAN et al., 1964). The upper flow, as seen from Fig.31, does not indicate a spiral motion, however. Low clouds near the center of the depression apparently are spreading out in part underneath the descending dry current, giving the impression of a spiral.

In essence, the identification of a jet-stream system with a frontal system makes use of the thermal-wind concept; baroclinicity in the troposphere leads to an increase of wind speeds with height, until the isopycnic level is reached. Frontogenetic or frontolytic processes will be accompanied by intensification or weakening of the associated jet-stream systems, as has been mentioned earlier. None of these systems, therefore, should be considered as permanent and hemispheric phenomena. Instead, they are in a continuous process of formation and dissipation, and with the modifications which the airmasses undergo as they travel with the tropospheric flow patterns, certain transitions of one jet-stream system into another will have to be expected.

With the close correlation between baroclinicity and wind field, the climatological preference of frontal zones for certain geographical regions reflects itself in upper-wind statistics (PETTERSSEN, 1950). So does the frequency of passage of cyclones and anticyclones, since both are closely correlated with the jet-stream aloft.

Baroclinic zones associated with cyclones and frontal-type jet streams allow for large-scale vertical motions along isentropic surfaces. Such motions, in turn, if directed upward, will lead to condensation and precipitation. Thus, the regions over which frontal-type jet streams are frequently found reflect themselves in mean global precipitation patterns. The water content of the air masses entrained into the jet stream circulation will naturally have a strong influence on the actual amount of precipitation associated with individual jet streams.

In preparing statistics on "mean jet stream" position and intensity one has to bear in mind that the flow in the vicinity of the jet core *is not* symmetrically distributed about the jet axis. This has been brought out in a number of studies (DAVIS, 1951; REITER, 1962; BRUNDIDGE and GOLDMAN, 1962; ENDLICH and MCLEAN, 1964). Fig.34 shows a

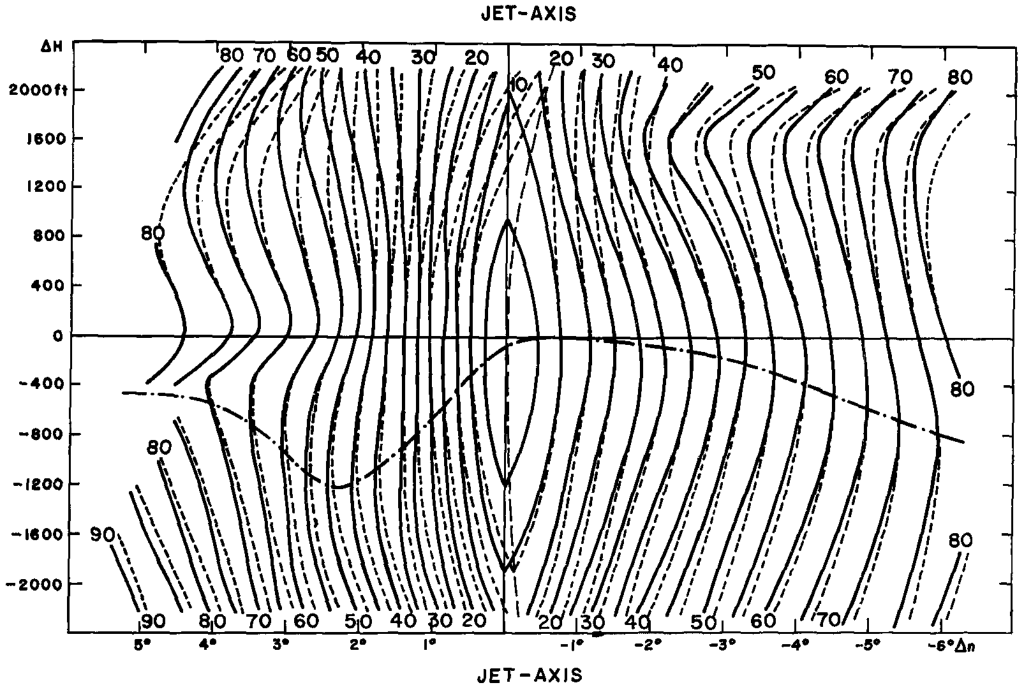

Fig.34. Isotachs (knots) of mean wind speed differences against speeds observed in the jet core, observed during 19 Project Jet Stream research flights. Dashed lines take into account the mean curvature of the jet axis in the vertical. Abscissa: lateral distance from jet axis in degrees of latitude. Ordinate: height interval (feet) measured from jet core level. Dashed-dotted line: level of maximum wind.

mean cross section, obtained from a number of research flights over the United States. Isotachs in this cross section are given as mean departures of speeds from the speed in the jet core. It is evident that in the vicinity of the jet axis the cyclonic shear—measured along isobaric or horizontal surfaces—exceeds the anticyclonic one. This fact has several implications.

At a particular geographic longitude, the position of the jet axis may show considerable latitudinal variations from day to day. Therefore, if one constructed mean monthly or seasonal cross sections along a particular meridian, a number of individual asymmetric jet streams would enter into these statistics with their axes at various latitudes. The averaging process produces a "mean jet stream" whose anticyclonic shears have a tendency to be larger than the cyclonic ones. Furthermore, the axis of the "mean jet stream" may coincide neither with the average nor with the median, nor with the most frequent position at which the individual jet axes are encountered (Davis, 1951; Reiter, 1963c). This is illustrated in Fig.35.

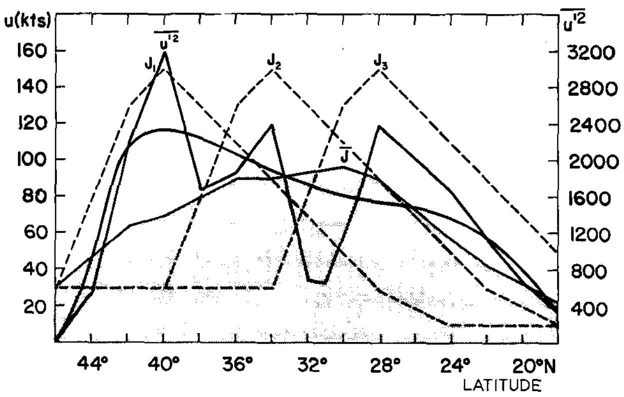

Fig.35. Averaging of three hypothetical zonal jet streams (J_1, J_2, J_3 shown by dashed lines). The shaded area indicates the mean jet stream, $\bar{J}$; the full jagged line gives twice the mean eddy kinetic energy of these three jet streams; and the smooth full line stands for a smoothed distribution of mean eddy kinetic energy.

Kao and Hurley (1962) have investigated the mean kinetic energy distribution of the geostrophic flow at the 300-mbar level, which coincides approximately with the maximum-wind level in the PFJ. In doing so, they considered separately the total and eddy kinetic energies, each averaged over one month. The mean eddy kinetic energy is defined as:

$$\overline{E^*} = \frac{\rho}{2}(\overline{u^{*2}}+\overline{v^{*2}}) \tag{79}$$

neglecting vertical motions. The quantities with asterisks indicate deviations from the mean flow, e.g.:

$$u^* = u - \bar{u} \tag{80}$$

where,

$$\bar{u} = \frac{1}{T}\int_{t-\frac{1}{2}T}^{t+\frac{1}{2}T} u(x,y,z,t)dt\,, \tag{81}$$

T being the time interval of averaging.

Fig.36 and 37 show the results of Kao's and Hurley's study. The distribution of total kinetic energy, expressed in units of kg/m/sec^2, reflects the position and intensity of the "mean jet stream," including the reservations voiced above. The strong jet stream over, and to the east of, Japan is clearly evident. Anticyclonic shears are very strong, in agreement with what has been said about the averaging procedure.

Statistics by Angell (1964), based on transosonde measurements between 140° and 180° E during the period 1957–1959, indicate mean wind speeds at the 300 and 250 mbar levels of approximately 103 knots in autumn, 123 knots in winter, and 101 knots in spring. These speeds are approximately 25 knots higher than mean speeds estimated

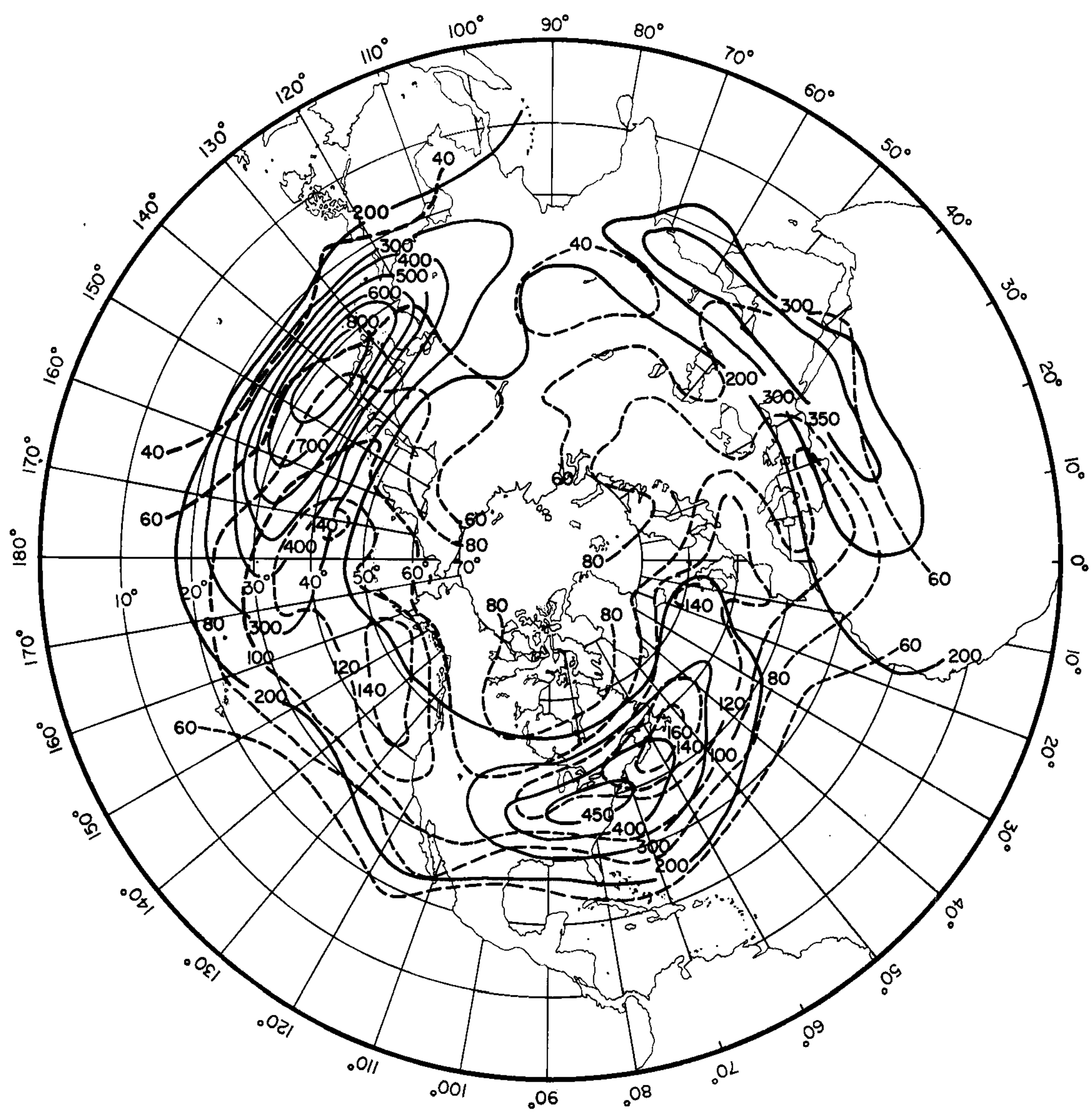

Fig.36. January distribution of mean total and eddy kinetic energies of the geostrophic wind in kg/m/sec², 300 mbar. —— = total kinetic energy; ------- = eddy kinetic energy. (After KAO and HURLEY, 1962.)

from conventional soundings. Premature termination of radiosonde ascents during days with excessively strong winds may be the cause of this low-wind bias.

The mean eddy kinetic energy in Fig.36 and 37 shows highest values north of, and downstream from, the Pacific and the North American mean jet maxima, especially during the winter season. The poleward shift of the maxima of mean eddy kinetic energy relative to those of mean total kinetic energy may be attributed, again, to the asymmetry peculiar to jet maxima. This effect is shown in Fig.35.

The eastward shift in the maxima of mean eddy kinetic energy seems to be hardly at all present over eastern Europe; it is well pronounced, however, over the Pacific and Atlantic regions (see Fig.36 and 37). To explain this fact, we recall that conservation of potential vorticity tends to generate anticyclonic flow over large mountain ranges, and a trough to their lee. East of this orographically generated trough there will be confluence between cold air from higher latitudes flowing around the trough, and warm air traveling

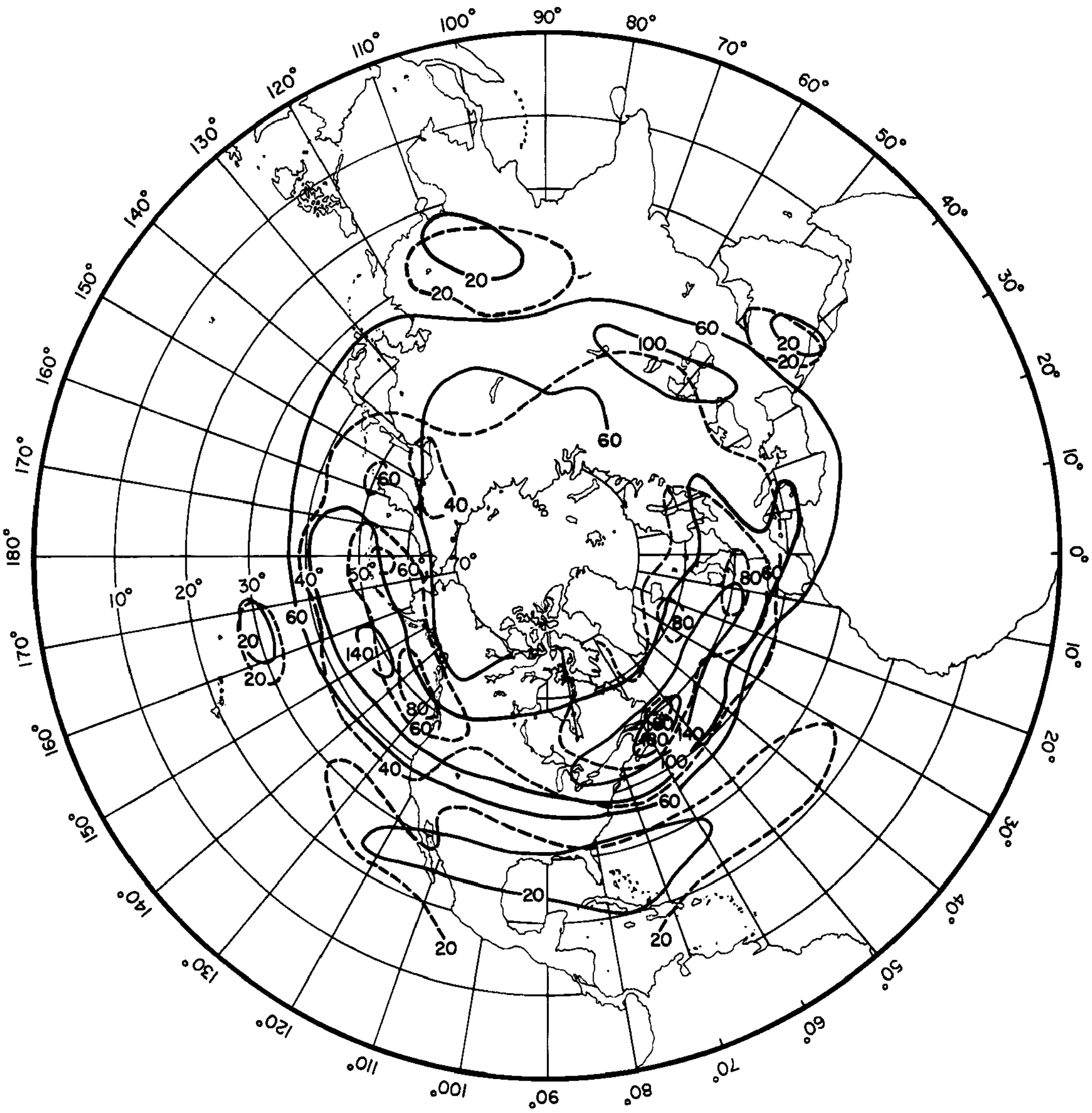

Fig.37. July distribution of mean total and eddy kinetic energies of the geostrophic wind in kg/m/sec^2, 300 mbar. —— = total kinetic energy; ------ = eddy kinetic energy. (After KAO and HURLEY, 1962.)

poleward around the subtropical anticyclone which is located downstream from the orographically generated trough. The northward flow around this anticyclone would tend to generate jet-stream velocities also from the point of view of conservation of absolute angular momentum.

One should expect that the influence of Himalayas and Rocky Mountains on the flow at jet-stream level should decrease with distance from these controlling sources. Thus, the mean eddy kinetic energy maxima, indicating the combined effects of intensity and steadiness of the flow, are additional evidence of the orographic control over the Pacific and North American jet maxima.

Neither KAO's and HURLEY's (1962) statistics, nor earlier ones by NAMIAS and CLAPP (1949), nor mean cross-sections, such as the ones presented by PETTERSSEN (1950) or CRUTCHER (1961), permit a clear separation between PFJ and STJ. This is, because at most longitudes the belts of latitudinal variation of PFJ and STJ overlap. The combined effect of both jet-streams produces a "mean jet stream" which—because of the asymmetry characteristics mentioned above—favors the latitude of the STJ. Only in regions where PFJ and STJ occurrence produces two distinct frequency maxima with enough latitudinal separation between them, should one expect separate "mean maxima" for each of these two jet streams. Such is the case for some mean cross-sections over the eastern United States, presented by KOCHANSKY (1955) and the *U.S. Weather Bureau* (ANONYMOUS, 1961). Mean cross-sections from the Southern Hemisphere for several individual months in 1960 also reveal distinctly separate cores for the PFJ and the STJ (PHILLPOT, 1962).

The subtropical jet stream

As has been pointed out on p.146, the main distinction between PFJ and STJ is that the latter is associated with a baroclinic zone which is confined to the upper troposphere and does not reach the ground. The horizontal characteristics of shear are very similar to the ones of the PFJ, and consequences have to be drawn from the observed asymmetries similar to the ones explained in the preceding discussion.

In Fig.1, and in the subsequent explanation of the origin of the jet stream, it has been pointed out that the STJ owes its existence to the tendency of atmospheric flow to conserve its angular momentum. The northward movement of air in the "anti-trades" aloft, thus, would give rise to strong westerlies as we observe them in the STJ.

This concept may serve very well when rationalizing the phenomenon of a *mean* STJ, encircling the hemisphere. When regarding individual jet maxima, especially over North America, another process will have to be considered in addition. Outbreaks of cold air in the lee of the Rocky Mountains, especially during late winter, follow in the wake of a cyclone and its associated PFJ. As this cold air flows southward it spreads out horizontally, and the originally baroclinic frontal zone assumes more and more the characteristics of a subsidence inversion. Even in this state, a jet-stream branch may be found over the core of the cold surface anticyclone. Although the history of such cases indicates that the cold outbreak was associated with a PFJ, one might be tempted to classify the jet branch over this cold anticyclone as an STJ, especially when it has moved far enough southward to become incorporated into the subtropical high-pressure belt. Thus, we have to allow certain transition mechanisms between PFJ and STJ, although they will add to the confusion which already exists in categorizing tropospheric jet streams. Such transition mechanisms will make proper allowance for a dual interpretation which one may give to the subtropical high-pressure belt. On the one hand, its dynamic origin may be postulated from the mass convergence aloft within the latitude belt of the STJ. On the other hand, one may follow individual cold anticyclones migrating southward, and observe their transformation and integration into subtropical high pressure regions.

The characteristics of the STJ have been studied extensively by KRISHNAMURTI (1961a, b). He finds this jet stream best developed during the winter season, when it forms a continuous belt around the globe. Fig.38 illustrates the mean STJ at the 200-mbar level during the winter of 1955–1956, with its characteristic three-wave pattern.

In the region of the PFJ we find wave number 3 dominant only for *mean conditions* (see Fig.36); analyses for individual days show much higher wave numbers. The reduction of the wave number in the averaging process has been attributed to the stationary effects

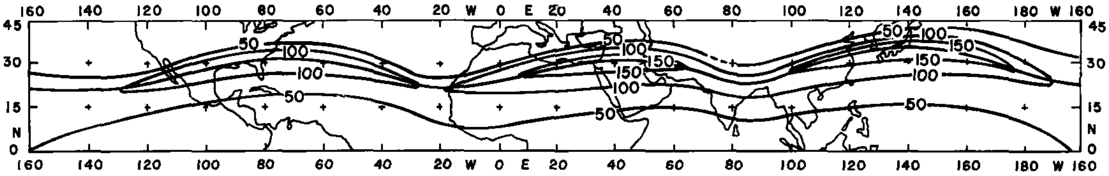

Fig.38. Mean subtropical jet stream for winter 1955–1956. Isotachs at 200-mbar level are drawn for every 50 knots. The mean latitude of the jet axis is 27.5°N. (After KRISHNAMURTI, 1961a.)

of mountains and of the land-sea distribution. In the case of the STJ of winter, Krishnamurti finds a well-established predominance of wave number 3 even on individual daily analyses. According to his study, these three waves in the STJ seem to be *out of phase* with the mean three wave pattern at 47.5°N, which corresponds to the mean latitude of the PFJ.

If we accept the hypothesis, that the waves in the mean flow of the PFJ region are orographically generated, these waves will cut into the subtropical high pressure belt and divide it into a cellular pattern. The STJ maxima, located in the *wave crests*, may be thought of as a consequence of northward flow east of the troughs, under conservation of absolute angular momentum. Thus, the wave crests of the STJ would be located in close proximity, but slightly east, of the troughs in the PFJ, the latter containing the mean PFJ maxima (Fig.36).

During summer the belt of the STJ is interrupted (RIEHL, 1962). Especially over the Asian sector of the Northern Hemisphere we find a quasi-permanent anticyclone occupying a large area over Tibet. The easterly flow to the south of this high-pressure region assumes jet-stream velocities (TEJ), and is associated with the Indian summer monsoon. The westerly flow is pushed rather far northward over Mongolia and Siberia. Mean wind speeds are also much weaker during summer in line with the decreased tropospheric temperature gradient between equator and pole, and the reversed temperature gradient in the higher levels of the stratosphere.

The winter STJ excels through its great steadiness. Core speeds vary only little from day to day. Some interdiurnal shifts in the latitudinal position of the jet axis are observed. They seem to have a minimum over Asia, where the flow in the STJ is strongly controlled by the mountain barrier of the Himalayas (see MOHRI, 1958, 1959; POGOSIAN, 1960; STEPANOVA, 1964).

From the preceding arguments on the dynamic origin of the STJ we have seen that the mean meridional mass circulation between equatorial regions and higher latitudes is instrumental in its generation. The rather steady trade winds near the surface constitute the return flow in this mass circulation "wheel" (see Fig.1). Data presented by PALMÉN

TABLE II

TOTAL NORTHWARD TRANSPORT OF ANGULAR MOMENTUM DURING JANUARY

Latitude	Transport by mean meridional circulation (10^{25} g cm^2 sec^{-2})	Transport by eddy exchange (10^{25} g cm^2 sec^{-2})	Ratio of the two modes of transport (%)
30°	6	56	11
25°	11	47	23
20°	14	32	44

and ALAKA (1952), and given in Table II, bear this out to some extent.

According to these data the role of horizontal eddies in transporting angular momentum increases drastically as we transgress the latitude of the mean position of the STJ. The same holds for heat transport. These data were essentially confirmed by TUCKER (1960) (see also SALTZMAN et al., 1961; DEFANT and VAN DE BOOGAARD, 1963.) As PRIESTLEY and TROUP (1964) have pointed out, one should be aware, that the absolute values of these transport quantities may be biassed by missing data under strong-wind conditions.

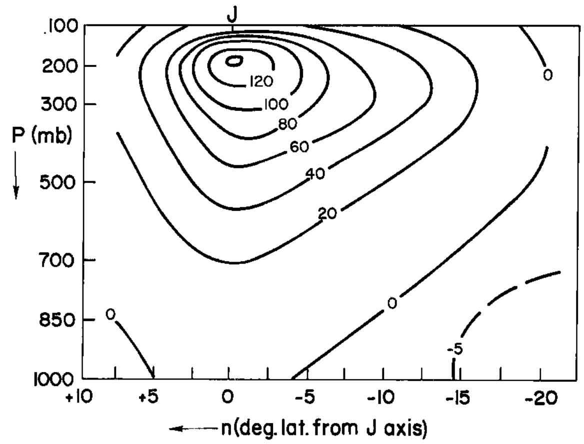

Fig.39. Monthly mean zonal wind (knots), December 1955, averaged around Northern Hemisphere in a curvilinear coordinate system (i.e., with coordinate origin in the axis of the STJ). (After KRISHNAMURTI, 1961a.)

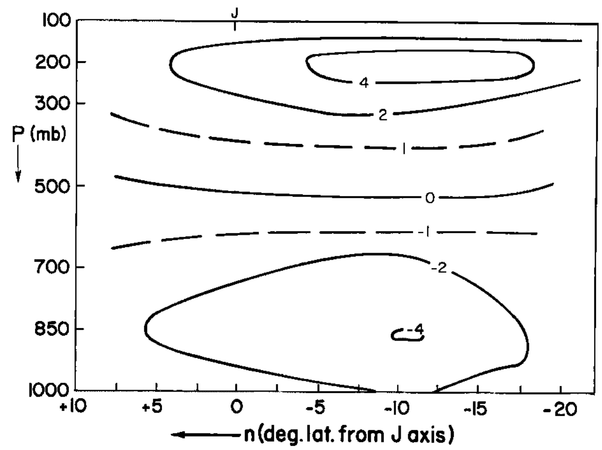

Fig.40. Monthly mean meridional wind (knots), December 1955, averaged around Northern Hemisphere in a curvilinear coordinate system (i.e., with coordinate origin in the axis of the STJ). (After KRISHNAMURTI, 1961a.)

These calculations were carried out in a Cartesian coordinate system, whose axes were pointed east and north, respectively. If one performs similar calculations by averaging motions in a "curvilinear" coordinate system whose x-axis follows the jet axis of the STJ, one automatically suppresses the influence of horizontal eddies on the transport of angular momentum and of other quasi-conservative quantities. The "meridional" mass circulation now becomes the dominant quantity, revealing a direct circulation with rising near the equator and sinking underneath the STJ. Fig.39 and 40 show the mean longitudinal and transverse components of motion in such a curvilinear coordinate system.

Fig.41 shows the magnitude of angular momentum transport in a curvilinear coordinate system. The role of the mean (transverse) mass circulation evidently is dominant. Standing eddies (the three quasi-stationary waves mentioned earlier) retain some influence in momentum transport, although it is relatively small near the jet axis. Transient eddies of a duration of less than 5 days (shaded area) become significant only more than 5° north of the jet axis, where the influence of transient vortices in the PFJ region makes itself felt.

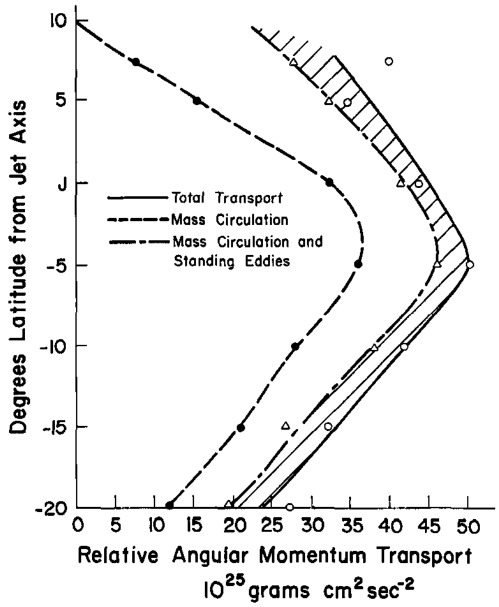

Fig.41. Relative angular momentum transport for winter 1955–1956. (After KRISHNAMURTI, 1961b.)

This brings up the disputed question of the relative importance of mean meridional vs. eddy transport. Dishpan experiments by RIEHL and FULTZ (1957, 1958) have, at least temporarily, brought about an "armistice" in this dispute. They were able to show conclusively, that the relative importance of the two modes of transport *depends on the coordinate system* in which computations are performed. In a Cartesian system the influence of horizontal eddies appears in its full magnitude in the vicinity of the jet axis, while the mean meridional circulation may even be "indirect" there. This is caused by the fact that strongest sinking occurs in troughs equatorward from the location of strongest rising in the ridges. Averaging around latitude circles yields sinking to the south and rising to the north of the mean jet axis, thus simulating an indirect mass circulation about the jet stream. Since an indirect circulation means generation of potential energy at the expense of kinetic energy, all kinetic energy will have to be provided by the horizontal eddies in this coordinate system.

Evidence for the importance of eddy terms is produced by the fact that jet maxima in the STJ tend to appear in the wave crests, following a trend of conservation of angular momentum. As for the polar-night jet stream, the indirect meridional circulation cell is difficult to reconcile with the fact that individual jet maxima evidently draw their kinetic energy from the potential energy which is released by the sinking of cold, and the rising of warm air.

The studies by RIEHL and FULTZ (1957, 1958) have clearly established the fact that only the *total* transports of momentum and heat are of real significance in estimating the effectiveness of the general circulation. In breaking the total transports down into eddy and mass circulation modes, we have to specify the coordinate system of reference as well. We may reach opposing conclusions depending on the choice of coordinates.

In analogy, we may consider transport processes of the above nature as vector quantities. If we wish to consider the relative importance of the two vector components as which we may regard eddy and mean mass transport, obviously we must make a statement as to the nature of the coordinate system, too.

The tropical easterly jet stream

In the preceding section it has been demonstrated that the dynamic origin of the subtropical high-pressure cell, as well as of the STJ, may be explained in terms of a Hadley cell, which transports mass as well as westerly angular momentum poleward. If there were no horizontal eddies superimposed upon this circulation cell, we would expect but a single subtropical jet stream belt of uniform flow in both the northern and the southern hemisphere.

In reality, however, we find that the subtropical high-pressure belt is broken up into individual cells (e.g., the Bermuda high, the Azores high, etc.), mainly by the action of long-wave troughs in extratropical latitudes. As has been pointed out, these troughs are closely related to large-scale orographic features, such as the Himalayas and the North and South American Andes.

Wherever large troughs permeate the subtropical high-pressure belts of either hemisphere, a mass-flow towards the equator occurs in the upper troposphere on the eastern edge of the high pressure cells. The tendency of *conservation* of *angular momentum* will deflect this flow towards the west, and a high-level easterly wind regime will result.

While this easterly wind regime is characteristic of tropical latitudes in both hemispheres, wind velocities have been observed to attain jet stream speeds (TEJ) only in the Northern Hemisphere over southeastern Asia and India, over Africa (SCHERHAG, 1948; VENKITESHWARAN, 1950; JENKINSON, 1955; KOTESWARAM, 1958; FLOHN, 1964; STEPANOVA, 1964) and in isolated instances over the Caribbean Sea (ALAKA, 1958).

The tendency of conservation of absolute angular momentum, to which the TEJ seems to owe its existence, may be seem from Fig.42 which gives easterly wind components over India and Thailand on 25 July 1955, at the 200 and 100 mbar levels. The latter lies close to the tropopause and the maximum wind level in these regions. Thus the TEJ may be considered a "tropopause jet stream", similar to PFJ and STJ. Since the TEJ is closely associated with the subtropical high-pressure cells, it has sometimes been discussed in conjunction with the STJ system (RIEHL, 1962). In view of its isolated regional and seasonal occurrence, separate treatment is preferred, however. An additional reason for this is given by the following consideration.

As stated above, the TEJ is associated with *breaks* in the subtropical high-pressure belt. Its existence cannot be explained by a meridional trade wind cell, but by horizontal eddies superimposed upon this cell. Thus, the STJ is a phenomenon, feeding on the mean meridional circulation, and, to some extent, on northward *eddy* angular momentum transport (see Table II on p.155), the latter accounting for jet maxima in the STJ system

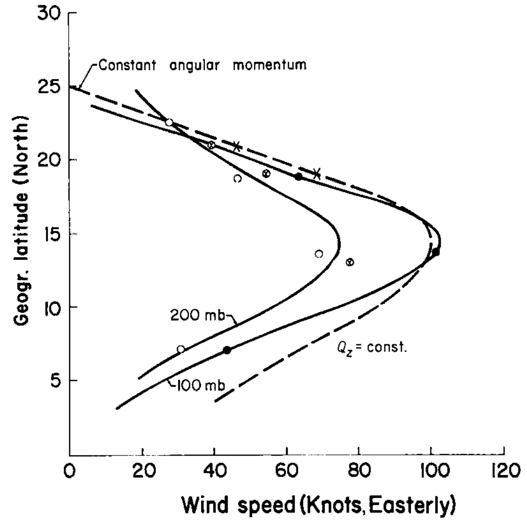

Fig.42. Meridional wind profile of east-wind component over India and Thailand, 25 July, 1955, at 200 and 100 mbar, together with theoretical wind profiles of constant angular momentum and constant absolute vorticity (dashed). (After KOTESWARAM, 1958.)

(BERSON and TROUP, 1961; KRISHNAMURTI, 1961a, b). The TEJ, however, draws mainly on southward eddy angular momentum transport and does not appear in mean meridional circulation considerations (see Fig.1).

A TEJ with great steadiness can only be found in the Northern Hemisphere during summer, confined to the longitude sector between Philippines and West Africa (Fig.43). This

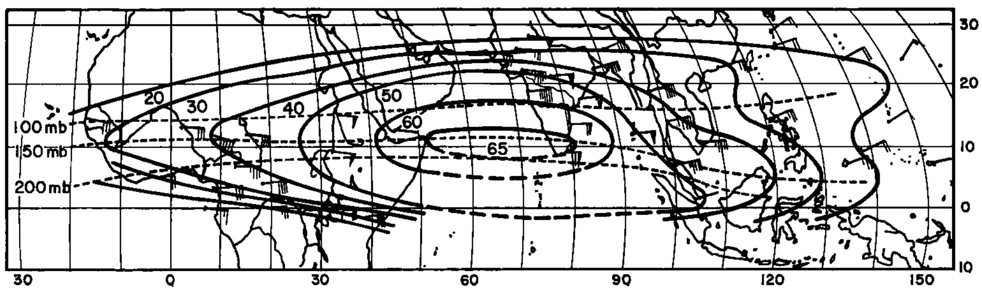

Fig.43. Resultant winds and isotachs (knots) at 150 mbar, July–August, together with jet axes at 200 and 100 mbar. (After FLOHN, 1964.)

peculiarity obviously has to do with the location and steadiness of the subtropical high-pressure systems. During the winter seasons of both hemispheres the subtropical high-pressure belt has relatively small meridional extent and is located close to the equator (SCHERHAG, 1948). Thus not enough southward angular momentum transport is provided to allow a steady wind regime at jet stream velocities to develop.

During summer the anticyclones over Tibet and over the Sahara are among the most stationary features of the general circulation. While easterly jet-stream velocities may be encountered spasmodically over other parts of the globe (BOND, 1953; ALAKA, 1958) only these two anticyclones are capable of serving as roots of a steady tropical jet-stream regime.

The physical reason for this steadiness has been pointed out by FLOHN (1950, 1957a, 1958, 1963) and others (CHAUDHURY, 1950; RAMAGE, 1952; FLOHN et al., 1959; REITER and HEUBERGER, 1960; REITER, 1959, 1961a, 1963a). The Plateau of Tibet, which lies within the range of migration of the subtropical high-pressure belt during summer, acts as an elevated heat source, generating higher temperatures there than in the free air over India at the same pressure level (Fig.44). While this effect may be smaller than originally thought, and while it may not suffice to *generate* a strong and steady anticyclone (RANGARAJAN, 1961) it certainly may help to *attract* the subtropical high to this *quasi-permanent* location before the "burst" of the summer monsoon.

Once the monsoon is established, the release of latent heat from precipitation will help to maintain the warm anticyclone (BERSON, 1961; DAS, 1962). In this respect it appears significant that a warm core is shown in Fig.44 between 10 and 15 km, i.e., in the upper

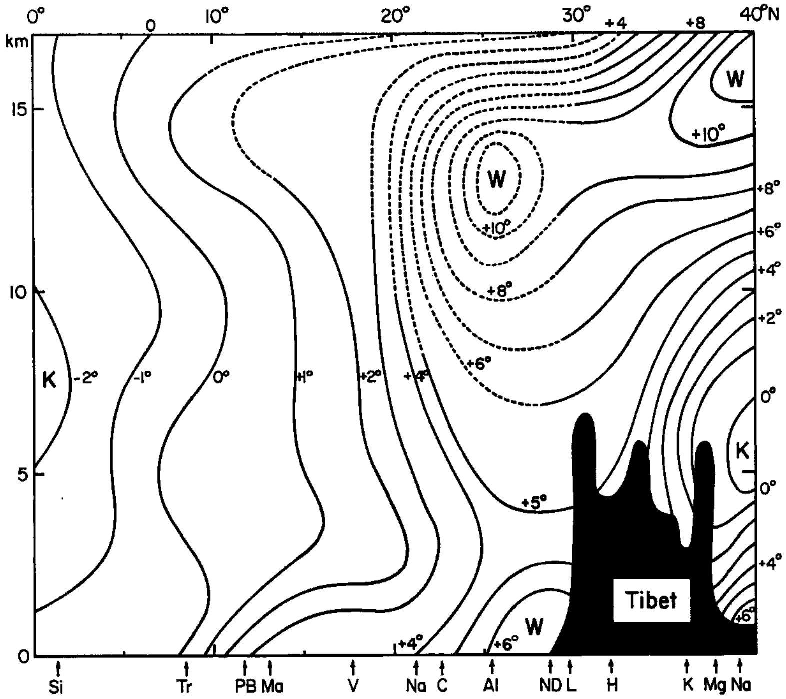

Fig.44. Meridional cross section along 78°E of mean temperatures (July–August 1957–1962) in terms of deviations from mean conditions over the equatorial Pacific (7–10°N). Dashed lines indicate possible bias by different types of radiosondes. (After FLOHN, 1964.)

troposphere, over northern India, *south* of the slopes of the Himalayas. This agrees well with findings by RANGARAJAN (1961). RIEHL's (1963) numerical estimates on mass circulation and release of latent heat in the monsoons of South and Southeast Asia show that the latter may be at least as effective in driving the circulation against frictional dissipiation, as conversion of potential into kinetic energy in extratropical eddies. The effect of the Plateau of Tibet on the general circulation, thus, does not have to be stretched as far as to explain the *existence* of the observed anticyclone and its associated TEJ, but only its *persistence* and its steadiness.

The dynamic effects of the general circulation, and the local thermal effects of the underlying surface and of precipitation may be visualized as acting together to produce the observed monsoon circulation. Similar effects may be found in other locations, e.g., where apparently the low-tropospheric temperature gradients between Sahara and Mediterranean Sea have a steadying influence on the wind field. The PFJ over the northeastern U.S.A. during winter is also enhanced in its intensity by the contrast between a cold continent and a warm ocean.

During winter the high plateau of central Asia acts as a cold source, stabilizing the flow in a similar fashion as during summer, but in reversed direction (CHAUDHURY, 1950; FLOHN, 1957b).

While certain variations of intensity of the TEJ have been observed between successive years, and even within one summer season (FLOHN, 1964), no 26-month cycle like the one which seems to prevail in the equatorial stratosphere (EBDON, 1960; REED et al., 1961, 1962; SHAPIRO and WARD, 1962; SHAPIRO, 1964; NEWELL, 1964; ANGELL and KORSHOVER, 1964) has been found so far. At this time, the possible causes for such a cycle are still open for speculation—and wind data entering the statistics of the TEJ will be open to improvement. Yet, the apparent downward propagation of this cycle from higher levels suggests that its physical sources are located appreciably above the tropopause level. The TEJ on the other hand is tied to the tropospheric circulation, and its main energy sources are the differential heating of the earths' surface, and the release of latent heat.

Fluctuations in the TEJ, once better observed and understood, may in due time serve to explain the short-term as well as the interannual changes of the monsoon regimes over Asia and Africa. Even at this point, where our knowledge of the high-tropospheric circulation patterns over these parts of the globe emerge only slowly in some detail, the dynamic influence of the TEJ on surface weather patterns may easily be recognized.

The monsoons of India, Southeast Asia, and Africa

It was realized already by WAGNER (1931) that the weather patterns associated with the Indian monsoon cannot be described simply by a "chimney effect," whereby air is heated over the continent and rises, being replaced near the ground by moist maritime air masses. RODEWALD (1936) was among the first to point out correlations between weather systems north of the Himalayas, and those causing monsoonal precipitation along the southern slopes of the Himalayas.

YIN (1949) was able to associate the disappearance of the subtropical jet stream south of the Plateau of Tibet with the onset of the Indian summer monsoon. These findings have been confirmed by YEH et al. (1959) and others (MURAKAMI, 1958; KOTESWARAM and BHASKARA RAO, 1961a). Fig.45 shows a 5-day mean cross-sections along 90° E during the transition period from winter to summer circulation patterns. The retreat of the westerlies over northern India coincides with the "burst" of the (southwesterly) summer monsoon. The monsoon flow, as may be seen from the lowest diagram in this figure, occupies but a relatively shallow layer. Yeh's study showed that similar changes in circulation, i.e., northward retreat of the westerly jet stream systems and advance of the tropical easterlies, could also be observed in other sectors of the Northern Hemisphere (see also SUTCLIFFE and BANNON, 1956). Thus, the shift in wind systems leading to the onset of the Indian monsoon is by no means uniquely confined to Asia, as has been mentioned earlier. It is the relatively high steadiness of the ensuing wind system that is a striking characteristic of the monsoon. The "burst" of the monsoon may occur in several

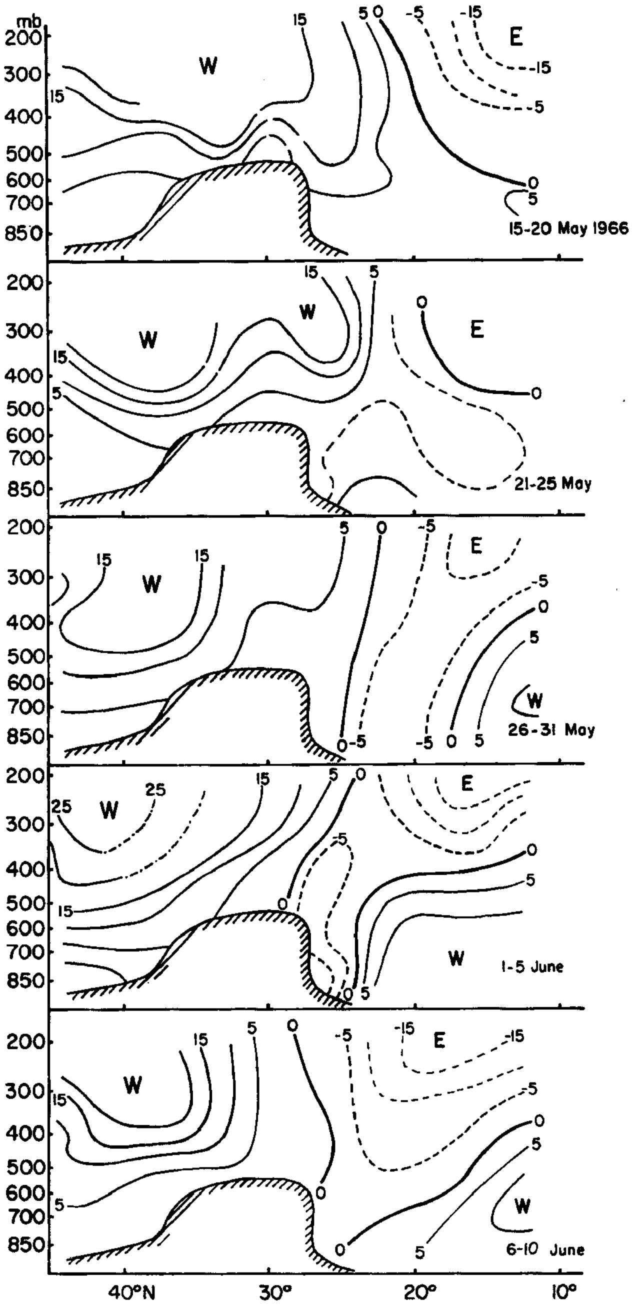

Fig.45. Five-day mean cross sections of the observed zonal winds(m/sec) along 90°E from May to June 1956. (After YEH et al., 1959.)

stages with interspersed "breaks." The re-appearance of the westerlies south of the Himalayas impedes the advance of the monsoon. (CHAKRAVORTTY and BASU, 1957; RAMASWAMY, 1962). The retreat of the Indian summer monsoon is heralded by a break-through of a westerly jet-stream south of the mountain range (REITER and HEUBERGER, 1960).

Almost simultaneously with the onset of the Indian summer monsoon, the "Mai-Yu" (Chinese) or "Bai-u" (Japanese) season brings the "plum rains" to the Yangtze Valley and somewhat later to Japan and Korea (DAO and CHEN, 1957; NEYAMA 1963). With the northward shift of the intertropical convergence zone over the Indian subcontinent, a cyclonic shear line establishes itself over China, giving rise to the rainy season there. A similar, but less pronounced interplay between high tropospheric easterlies and westerlies, and the onset of a monsoon-like precipitation regime has been observed over northern Australia (TROUP, 1961).

The rainy season in central Africa also bears the character of a monsoon; southwesterly

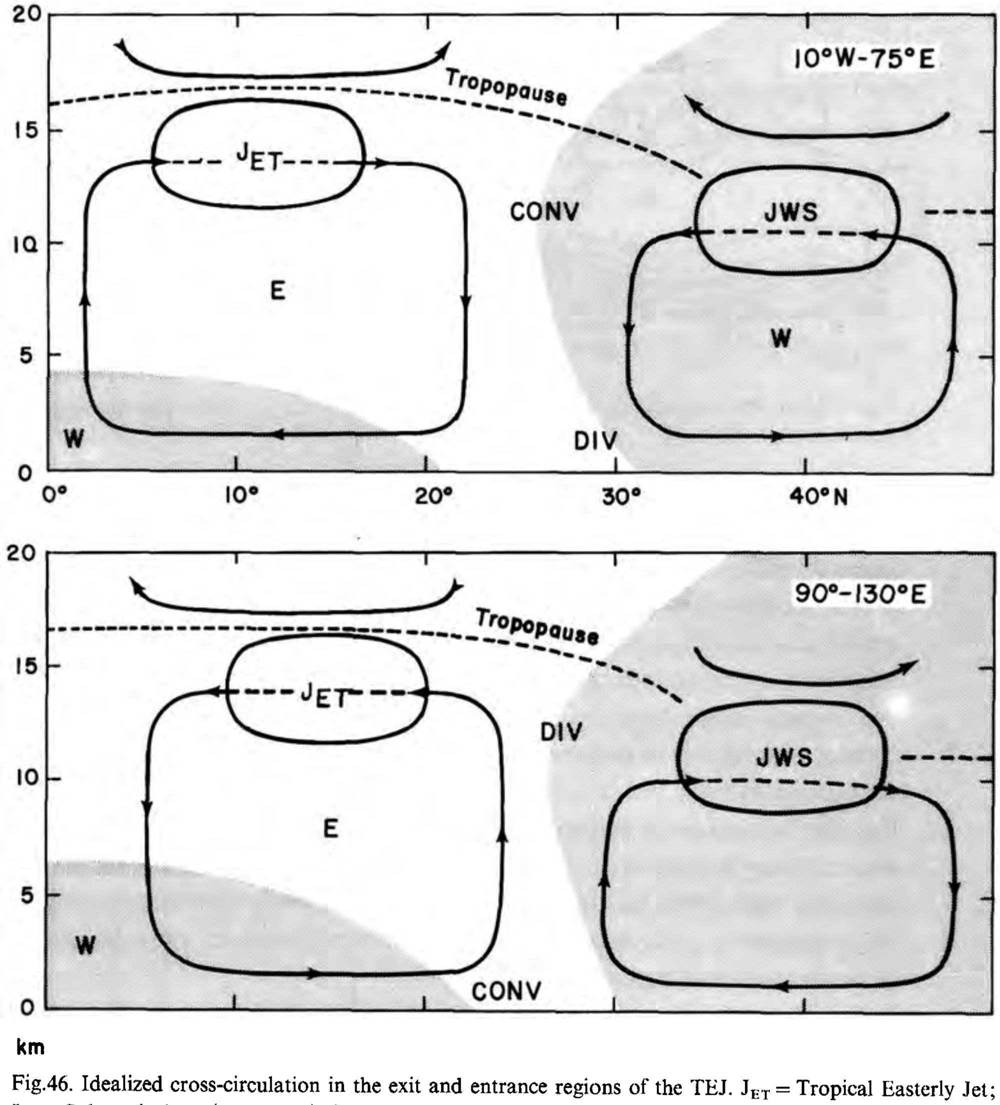

Fig.46. Idealized cross-circulation in the exit and entrance regions of the TEJ. J_{ET} = Tropical Easterly Jet; J_{WS} = Subtropical Jet (Westerlies). (After FLOHN, 1964.)

winds near the earth's surface carry moist oceanic air into the interior. The overlying easterlies with their jet-stream character and their traveling disturbances produce the high-level divergence fields that trigger off strong precipitation systems. The African monsoon, its dynamics and its energy budget, have not yet been studied in great detail. A more complete understanding of these seasonally controlled weather patterns was not achieved until the exploration of the tropical easterly jet stream had made progress (KOTESWARAM, 1958). Fig.46 shows schematically the vertical motions induced by the interaction of STJ and TEJ. The upper diagram in this figure corresponds to the exit region of the TEJ, thus to a cross-section running approximately through central Africa. The lower diagram cuts through the entrance region of the TEJ, and should be considered approximately along a meridian through the Philippines.

The mean July precipitation (Fig.47) is in excellent agreement with vertical motions that can be deduced from Fig.46. Thus it appears, that the Indian summer monsoon is strongly controlled by the TEJ, and by disturbances superimposed upon the mean flow. It has been pointed out that the baroclinicity associated with the TEJ is confined

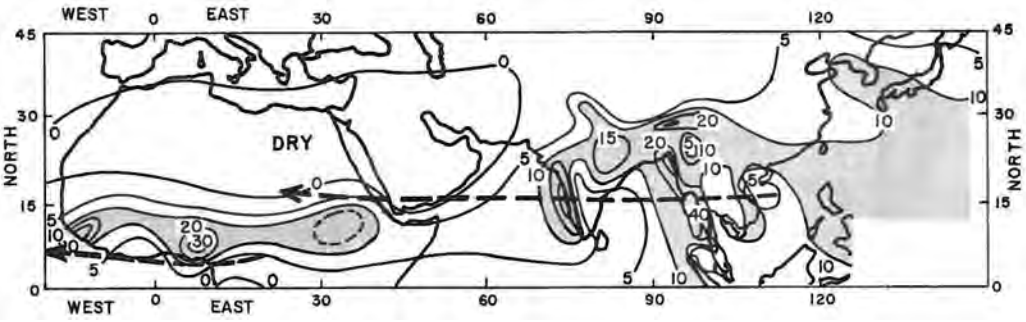

Fig.47. Mean July precipitation (inches) and position of the easterly jet stream during August 1955. (After KOTESWARAM, 1958.)

to the upper troposphere. No organized vertical motion along inclined isentropic surfaces, therefore, should be expected in the lower troposphere. Consequently, the monsoonal precipitation systems are of a non-frontal character.[1] They are associated with strong convective systems, due to a destabilization of deep tropospheric layers.

Inasmuch, as thermal advection plays an important role in the maintenance of monsoon depressions—aside from the release of latent heat of condensation—they do bear a certain resemblance to extratropical lows. Their most significant feature seems to be a strong asymmetry in the distribution of heavy rain, which falls mainly in the left forward (i.e., the SW) quadrant, as long as the depression continues on a westerly or northwesterly course. Heavy rains of up to 5 or 10 inch a day may be observed as far as 250 miles to the left of the track, while hardly any rain falls to the right of a westward moving depression. After recurvature, the heavy-rain area shifts to the northern and northeastern sectors (KOTESWARAM and BHASKARA RAO, 1961b).

It should be kept in mind that not all precipitation falling over India and Pakistan is "monsoonal" in character. Especially during the transition seasons between summer and winter moonsoon, precipitation may be associated with disturbances traveling in the westerlies (STJ) south of the Himalayas (RAMASWAMY, 1956; REITER and HEUBERGER, 1960). The actual monsoon rains, on the other hand, occur along the low pressure trough of the intertropical convergence zone which, in turn, is associated with the TEJ. Thus, if one attempts to draw conclusions on the variability of the monsoon from one year to another by examining rainfall records only, extreme care should be exercised in separating STJ from TEJ disturbances (RAMDAS et al., 1954).

[1] The "burst" of the monsoon over the Indian subcontinent and over western Africa may at times be traced from day to day in its northward advance in a "frontlike" fashion (BOSSOLASCO, 1953; RAMDAS et al., 1954). Nevertheless, the baroclinic stable layer characterizing a front is missing.

The low level jet stream

Studies by BLACKADAR (1957), FAY (1958) and others (see WEXLER, 1961; GERHARDT, 1962, 1963; IZUMI, 1962, 1964; HOECKER, 1963; IZUMI and BARAD, 1963; BONNER, 1965) revealed the relatively frequent existence of a low level velocity maximum in the vertical wind profiles. From these investigations it became apparent that such maxima are associated with temperature inversions. They are a rather widespread phenomenon and —although vertical shears may be at least as large as in tropopause jet streams— horizontal shears usually are quite small. It would be more appropriate, therefore, to classify these occurrences as "inversion wind maxima" (IWM), rather than as "low level jet streams" (LLJ) (MEANS, 1962).

Blackadar was able to explain the IWM as an inertial oscillation effect. During the late afternoon subgeostrophic flow conditions prevail underneath an inversion, because of surface friction and vertical mixing in the lowermost layers of the atmosphere. After convective mixing subsides, the subgeostrophic flow will accelerate in order to meet geostrophic (or gradient) wind conditions. The recovery, however, "overshoots" and a supergeostrophic wind maximum results. The oscillation has a period of $\frac{1}{2}$ pendulum day.

Conditions for the establishment of an IWM are, that vertical turbulent mixing is suppressed while formation of the wind maximum is in progress. The condition for this is, that Richardson's number increases with height—small Ri-numbers (usually < 1) indicate impending turbulence. If this condition was not met, the vertical shears, which are increasing during the formation of the IWM, would tend to generate turbulence and, thereby, destroy the wind maximum.

While the IWM is not a genuine jet-stream phenomenon, there are other types of low level flow which qualify as LLJ with respect to horizontal shears as well as maximum wind speeds. A number of studies on the LLJ, and its effects on severe weather have been summarized by REITER (1961a, 1963a). In these studies it has been pointed out that the vorticity distribution about the LLJ has similar effects upon divergence, convergence, and ensuing vertical motions, as the distribution about the PFJ. Violent convective activity should be expected where a low-level convergence area lies underneath a region of upper divergence (PITCHFORD and LONDON, 1962). Furthermore, squall-line formation seems to be associated with a deep, dry, but conditionally unstable layer on top of an inversion, with moist air underneath (see, for instance, SHOWALTER, 1943; BREILAND, 1958; BONNER, 1963; GERHARDT, 1963).

The formation of a LLJ is frequently witnessed to the east of the Continental Divide of the Rocky Mountains (WEXLER, 1961). An intense, moist current may be seen at the 850-mbar surface, importing humid air from the Gulf of Mexico. NEWTON (1956, 1959b) has studied such a case in some detail. He finds that the frictional influence on a low-level current moving along the slopes of the mountains would generate cyclonic vorticity through the term $(\nabla \times \boldsymbol{F})_z$. The vorticity thus generated may offer a significant contribution to orographic cyclogenesis.

When analyzed on the 850-mbar surface, as has been done in the above mentioned case study, the LLJ appears as an entity, separate from the tropopause jet stream. Recent analyses (REITER and MAHLMAN, 1964) have been carried out on isentropic surfaces. Allowing for errors contained in these analyses on account of possible moist-adiabatic

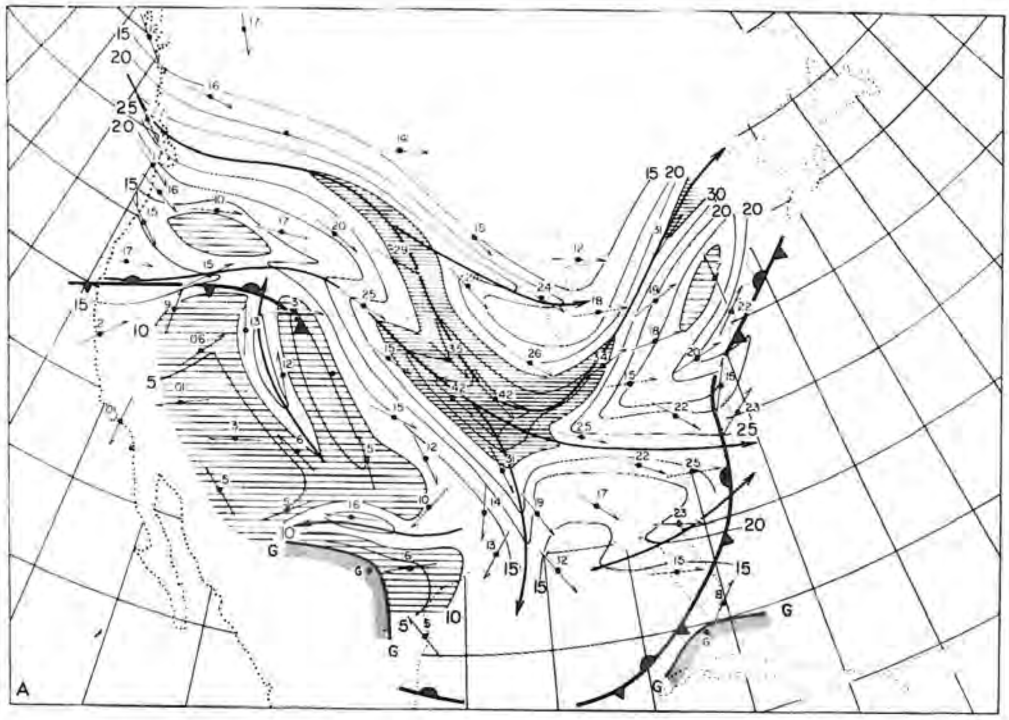

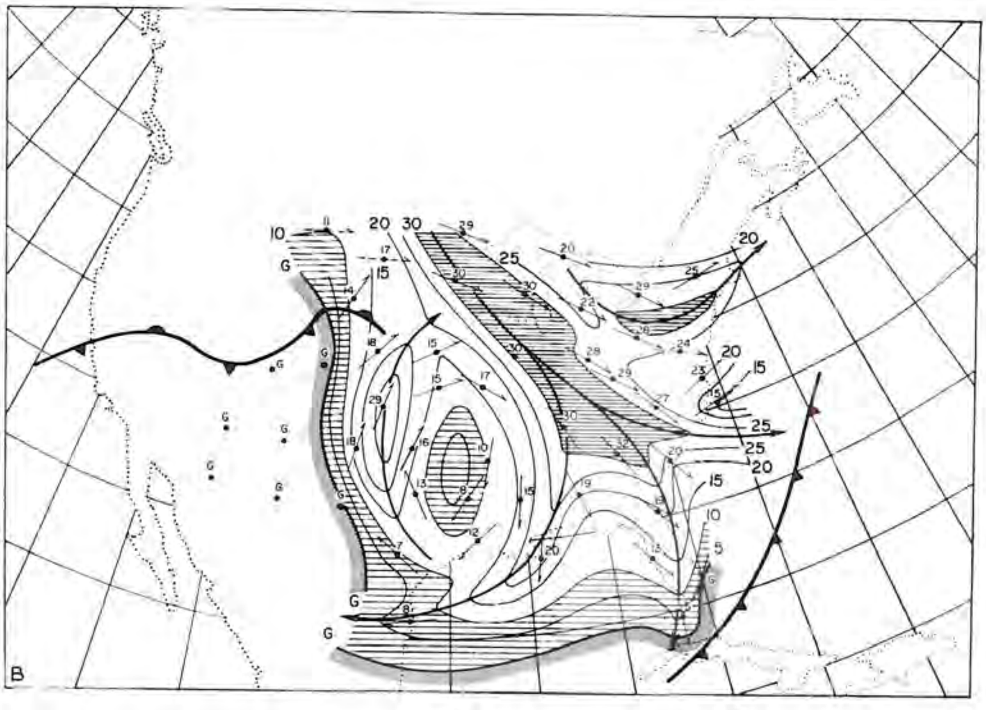

Fig.48. Isotachs (m/sec) on the 295°K isentropic surface for: A. 22 November 1962, 12h00 G.M.T.; B. 22 November 1962, 00h00 G.M.T.; and C. 23 November 1962, 12h00 G.M.T. Surface frontal systems have been entered. Regions with speeds <10 and >30 m/sec are shaded. Intersection of isentropic surface with ground marked by a broad band of hatching. (After REITER and MAHLMAN, 1964.)

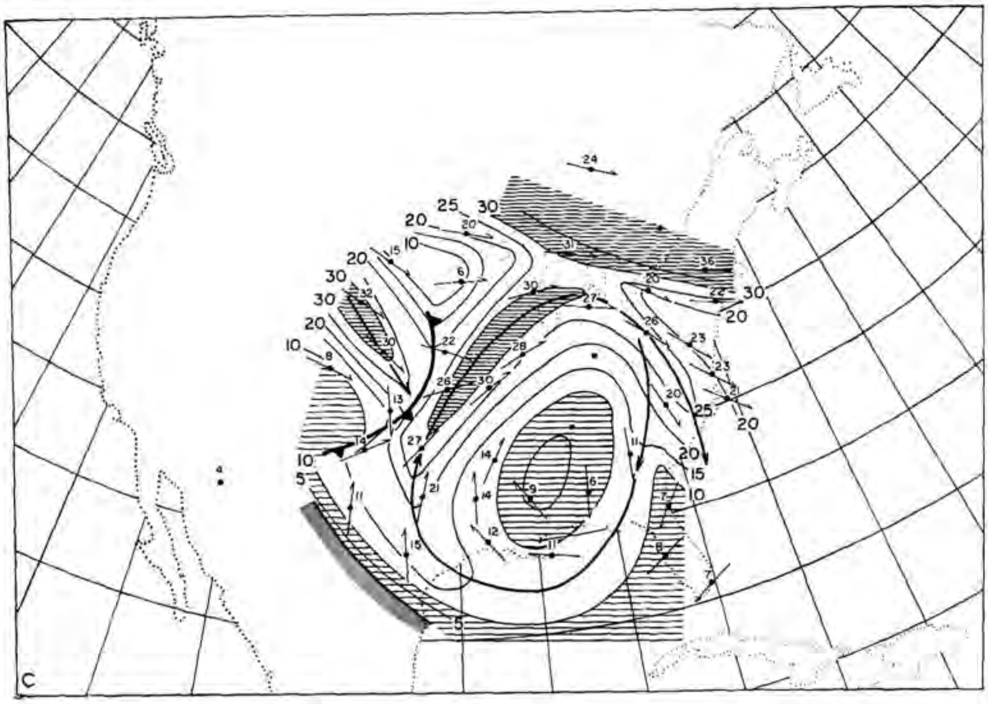

Fig.48 continued.

processes associated with cloud formation in the LLJ region, they indicate clearly a connection between the LLJ and PFJ. Fig.48 shows isotachs on the 295°K isentropic surface. The onset of a LLJ *west* of the Continental Divide may be seen on 22 November, 1962, 12h00 G.M.T., with Grand Junction reporting 12 m/sec, and Salt Lake City 13 m/sec. Twelve hours later the LLJ is well established to the east of the mountains, flowing ahead of an advancing cold front. Fig.14 and 15 show isotachs m/sec at the 300°K isentropic surface. On this slightly higher level, the LLJ, appeared only from 23 November 00h00 G.M.T. on (not reproduced here). There was no separate isotach maximum, however, on the 300°K surface, but a well-established branch that merged with the main jet stream over the Great Lakes region.

Fig.49 shows the isobaric pattern (in mbar) on the 295°K isentropic surface. Regions with $\frac{\partial p}{\partial s} > 0$ are marked by dense shading, with $\frac{\partial p}{\partial s} < 0$ by light shading. We see qualitatively (neglecting effects of local changes $\frac{\partial p}{\partial t}$) that the LLJ is associated with upward motion. Especially from 23 November, 00h00 G.M.T. on, we find that the air moving through the LLJ starts close to sea level and ascends beyond the 600-mbar level, there joining the main PFJ. If we made allowance for possible moist adiabatic effects, the air within the LLJ would reach even higher tropospheric levels. Fig.50 shows the relative humidity distribution (in %) on the 295°K isentropic surface. "Motorboating" reports are indicated by letter "A" and signify very dry conditions. From these analyses, we conclude that the LLJ constitutes a flow of moist air from the south.

Although research on the dynamics of the LLJ is far from completed, the above analyses would indicate the following tentative conclusions with regard to the North American area:

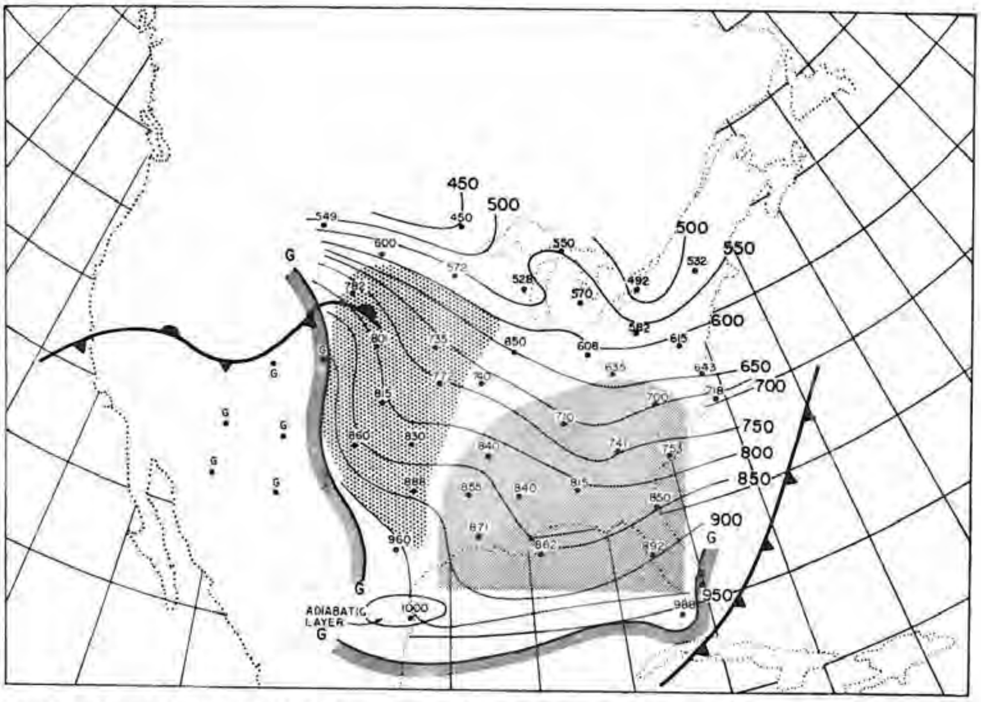

Fig.49. Isobars (mbar) on the 295°K isentropic surface, 23 November 1962, 00h00 G.M.T. Frontal systems as in Fig.48. Regions with $\partial p/\partial s < 0$ are marked with wide shading, those with $\partial p/\partial s > 0$ with dense shading. (After REITER and MAHLMAN, 1964.)

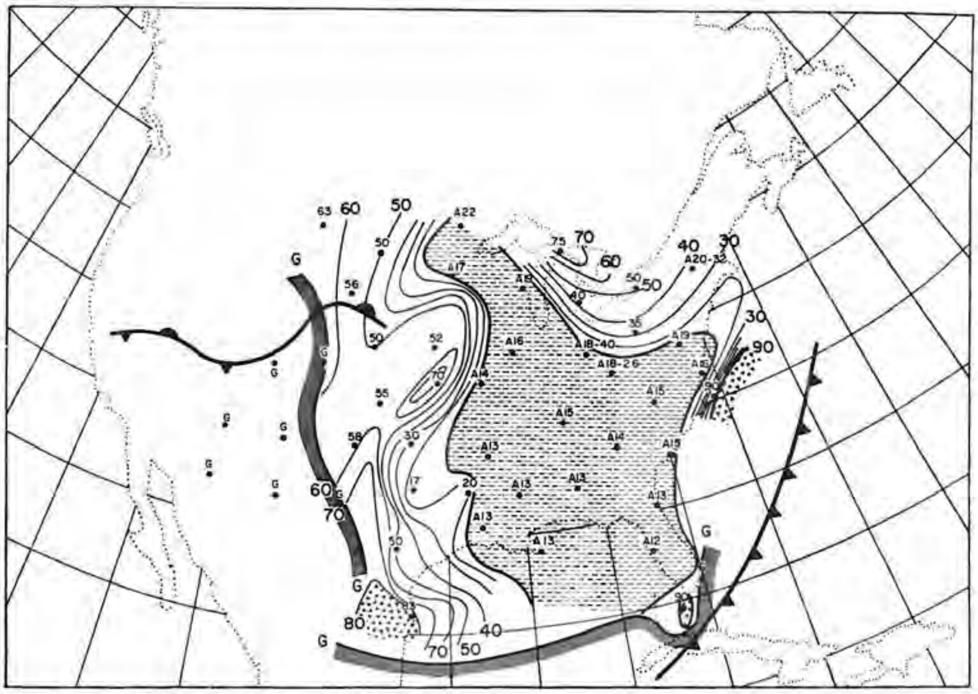

Fig.50. Relative humidities (%) on the 295°K isentropic surface, 23 November, 1962, 00h00 G.M.T. Frontal systems as in Fig.48 and 49. Areas with humidities >80% and with "motorboating" are marked by different shading. (After REITER and MAHLMAN, 1964.)

(*1*) Although the LLJ phenomenon seems to be best developed east of the Rocky Mountains, its origin may—at least in some cases—be traced back across the Continental Divide.

(2) The LLJ, at least at times, is not a separate entity, but constitutes a powerful inflow of mass and moisture into the North American tropopause jet stream system.

Centers of action and local circulation systems

Extratropical cyclones

A description and basic theory on cyclone formation may be found in almost any textbook on meteorology. Rather than duplicate here what is readily available elsewhere, we shall attempt to highlight a few important facts of cyclone development.
The original concept of a frontal cyclone, as developed by BJERKNES and SOLBERG (1921) and subsequently elaborated by many authors (see ANONYMOUS, 1960), considered a vortex which developed from an unstable and amplifying wave disturbance on the polar front. In its equilibrium state, the slope of a frontal surface is given by Margules' equation:

$$\tan \varepsilon = -\frac{f}{g} \cdot \frac{\rho V_g - \rho' V_g'}{\rho - \rho'} \tag{82}$$

where ε is the slope of the frontal surface, ρ is the density and V_g the geostrophic wind (parallel to the frontal surface). Primed quantities characterize conditions in the warm air. From this equation we may infer that a gradient of westerly wind speeds has to exist from the warm to the cold side of the front if the frontal surface is to remain stable. The Norwegian polar front theory of cyclone formation starts with a small disturbance in this balanced flow, acting on an originally straight west-to-east oriented frontal surface, and causing a slight intrusion of warm air into the "cold" side of the front. Under suitable conditions—later defined by CHARNEY (1947) and others as "baroclinic instability"—this small disturbance will grow into a wave. A "warm sector" will form, between a warm front and a cold front. As the latter "catches up" with the former, the occlusion process begins (see KREITZBERG, 1964). A trough of warm air aloft ("trowal") still signifies the presence of the warm air above the occluded front (KAMIKO, 1964a, b). Sometimes this "trowal" may extend into the warm sector (GALLOWAY, 1963). After the warm sector has been eliminated completely, a new polar front will form, and a slowly decaying vortex will remain for a while equatorward of this new frontal position. At times such vortices may exist for several days in the upper troposphere as "cut-off lows." The surface-pressure pattern underneath these upper cyclones may be quite diffuse. Forecasting the motion of cut-off vortices, together with their precipitation pattern, presents some difficulties, especially over Europe (HSIEH, 1949; HOLLMANN, 1952).
The "life cycle" of an extratropical cyclone, as outlined in the Norwegian theory, is well documented by satellite photographs (see e.g., LEESE, 1962; FRITZ, 1964; WIEGMAN et al., 1964). In interpreting such satellite pictures one should not jump to the conclusion that an "open wave" in the cloud formation necessarily corresponds to the warm sector of an unoccluded "wave cyclone". One should reason rather that the cloud free region corresponds to large-scale sinking motions in the troposphere. Such downward motions occur frequently *behind a cold front* rather than in the warm sector.

Although a great number of refinements have been added to the crude but effective Norwegian cyclone concept, two main difficulties remain:

(*1*) The original disturbance, causing the warm air to flow against the frontal surface, thereby generating a wave like indentation in the front, calls for convergence in the flow near the earth's surface. Such convergence, however, should be associated with a surface pressure rise rather than the observed pressure fall.

(*2*) The wave model of cyclone formation would call for precipitation in proximity to the surface fronts, where "forced lifting" along the inclined fronts occurs. While this is observed in a few "model cyclones," a great number of storms do not demonstrate these ideal characteristics.

Research on jet streams in the upper troposphere has helped to overcome these shortcomings. In Fig.13, and with the aid of the vorticity equation, the distribution of divergence and convergence patterns near the tropopause level has been explained. We have no difficulty in postulating a region of upper divergence in the left front quadrant of a jet maximum, which becomes superimposed upon a surface front. The pressure fall associated with the upper divergence actually will originate the perturbation, later causing the formation of a frontal wave with a warm sector. The cyclone will continue to deepen as long as the divergence at a higher level exceeds the convergence in the lower troposphere. It will start to fill, following the occlusion process, when the reverse is the case.

The existence of a low-tropospheric front is a necessary, but not a sufficient condition for frontal cyclogenesis. A high-tropospheric divergence area associated with a jet stream and its baroclinic "jet-stream front" has to act in unison with the low-level frontal zone (NEWTON, 1958). The latter can be explained as a transition zone of mixing between adjacent air masses. The "jet-stream front," however, is not produced by mixing, but by an intrusion of stratospheric air of high potential vorticity, as has been shown earlier.

Cloudiness and precipitation is associated with vertical motions in the troposphere, and these, in turn, follow the pattern of high-level divergence and low-level convergence (see NINOMIYA, 1962; LESTER et al., 1964; YAMAGUCHI, 1964). Considering this, we are not limited to the immediate vicinity of a surface front, but by the three-dimensional flow pattern in the troposphere. Although considerations up to, and beyond, jet stream level have rendered the "cyclone model" more complex than the original Norwegian concept, they provide a ready physical explanation for the "abnormal" behavior of certain cyclones and their precipitation regimes.

Because this improved cyclone model makes use of vorticity advection which provides the major cause for divergence and convergence, this cyclone theory is frequently referred to as the *vorticity–advection theory* of cyclone formation (PETTERSSEN, 1956). In certain ways it pays homage to the Austrian meteorological school of the years between the two world wars. They maintained that surface weather was controlled by steering mechanisms in the upper troposphere although the details of such mechanisms were not spelled out.

The close association between cyclogenesis and the jet stream aloft has been mentioned before. It was brought to light in a statistical study by PETTERSSEN (1950). According to his study the main regions of cyclogenesis coincide well with the most frequent position of the PFJ. Similar statistics, although not as reliable because of sparse observations, are available from the Southern Hemisphere (LANGFORD, 1957).

The relative importance of the terms in eq.83 may vary from storm to storm—this is indicated for instance by the fact that cloudiness and total precipitation amounts produced by individual cyclones vary considerably (see, e.g., NAGLE and SEREBRENY, 1962; RIEHL and GRAY, 1962; JORGENSEN, 1963; KREITZBERG, 1964). There also seem to be preferences according to geographic location; PETTERSSEN et al., (1962) have enumerated such differences as follows:

A. North Atlantic Ocean:

(*1*) Cyclone development at low levels commences under a more or less straight upper current (without appreciable vorticity advection) in the region where there is a maximum of baroclinicity.

(*2*) The upper cold trough develops simultaneously with the low-level cyclone, and the distance of separation between the upper trough and the low-level system remains sensibly unchanged.

(*3*) The effect of vorticity advection aloft is relatively small throughout the development, the major contribution coming from thermal advection.

B. North American continent:

(*1*) Cyclone development at low levels occurs normally when a pre-existing upper cold trough (with strong vorticity advection on its forward side) approaches a low-level baroclinic zone.

(*2*) The distance of separation between the upper trough and the low-level system decreases noticeably during the intensification period, and the axis tends toward a vertical position during the occluded stage.

(*3*) At the time of onset of the low-level development, the effect of vorticity advection aloft is predominant; the effect of thermal advection increases and becomes overwhelming during the later part of the development.

A comparison between items (*1*) above reveals, why the frontal concept, as well as the concept of "cyclone families" traveling along the same polar front, appealed to the Norwegian school, but was less applicable to North American conditions. The "vorticity advection" concept, on the other hand, was promoted by the "Chicago School", in line with conditions normally found over this continent.

The energy transformations taking place in a cyclone are as complex in nature as the cyclogenetic processes expressed in eq.83 and 84. On p.124 it has been mentioned that planetary wave numbers 5–10 are sources of kinetic energy. Cyclones which fall into this category of waves, therefore, constitute a major source of energy, contributing to the maintenance of the general circulation of the atmosphere.

PALMÉN (1958) made detailed estimates of such energy conversions in a tropical storm (hurricane "Hazel" of 1954) that had degenerated into an extratropical cyclone. Although certain energy contributions, such as the ones from the release of the latent heat of condensation, may have been higher in this case, his analysis permits valid conclusions concerning the effectiveness of cyclones as energy sources.

The following quantities were computed for this case:

Production of kinetic energy from potential energy: $18.9 \cdot 10^{10}$ kilojoule/sec.

Export of kinetic energy out of the cyclogenetically active area: $18.7 \cdot 10^{10}$ kilojoule/sec.

Dissipation of kinetic energy by friction: $2 \cdot 10^{10}$ kilojoule/sec.

Total kinetic energy of the cyclogenetically active area: $89 \cdot 10^{14}$ kilojoule.

Release of latent heat in this area: $155 \cdot 10^{10}$ kilojoule/sec.

Cyclones, especially in a well-developed stage, may be viewed as vortices embedded in a "steering current" (see ELIASSEN and KLEINSCHMIDT, 1957). This concept has brought about a large number of interesting studies on the interaction between vortex and mean current, and the possible modifications of the latter due to the action of the former. Several numerical investigations also have taken the approach of considering cyclones as unstable, baroclinic wave disturbances with growing amplitudes (see, for instance, KASAHARA et al., 1964).

The mean "steering current" is not given by the wind vector at jetstream level, but only by a fraction thereof. This is quite evident from the fact that jet maxima associated with surface cyclones travel slower than the wind itself (REITER, 1958a). (It is this very fact that produces the observed divergence and convergence patterns.) The steering is accomplished by the *mean* undisturbed tropospheric flow in which the vortex is embedded. As a first approximation to this mean flow one may take the geostrophic wind at the 500-mbar level (VEIGAS and OSTBY, 1963). The direction of the steering current, as a rule of thumb, is nearly parallel to the surface isobars in the warm sector of an "open-wave" cyclone which is not yet occluded.

Although vorticity advection gives a plausible explanation for surface pressure falls, the actual development of cyclones is far more complex. SUTCLIFFE (1947) and PETTERSSEN (1956) have indicated the physical considerations that would have to go into a quantitative estimate of cyclone formation. As a measure of such formation we may adopt the rate of change of vorticity at sea level or at the 1,000-mbar surface. Without developing the details of the mathematical derivation (see PETTERSSEN, 1956), the following expressions are given, in order to demonstrate the complexity of the parameters that enter into cyclone development:

$$\frac{\mathrm{d}Q_0}{\mathrm{d}t} = \mathrm{A}_Q + V \cdot \nabla Q_0 - \frac{\mathrm{R}}{f} \nabla^2 \left(\frac{g}{\mathrm{R}} \mathrm{A_T} + S + \mathrm{H} \right) \tag{83}$$

$$\frac{\partial Q_0}{\partial t} = \mathrm{A}_Q - \frac{\mathrm{R}}{f} \nabla^2 \left(\frac{g}{\mathrm{R}} \mathrm{A_T} + S + \mathrm{H} \right) \tag{84}$$

Eq.83 gives the rate of vorticity production in a moving air parcel, while eq.84 indicates the local rate of change of vorticity, indicative of cyclogenesis. At sea level or 1,000 mbar (indicated by subscript "0") the advection term $V \cdot \nabla Q_0$ is small, so that $\frac{\mathrm{d}Q_0}{\mathrm{d}t} \cong \frac{\partial Q_0}{\partial t}$.

A_Q symbolizes the vorticity advection at the level of non-divergence which normally lies slightly below the 500-mbar surface. $\mathrm{A_T}$ stands for the thickness advection between 1,000 mbar and the level of non-divergence, representing the effect of air masses of different temperature. S symbolizes a term containing static stability and vertical motion, and represents the local thickness changes due to wet and dry adiabatic processes. H represents an expression that accounts for thickness changes due to non-adiabatic processes which supply or remove heat from the system.

Vorticity and thickness advection are relatively easy to estimate from routine meteorological analyses. The other terms, containing adiabatic and non-adiabatic effects present considerably more difficulty. Naturally, this will influence adversely the quality of development predictions, since at times these effects may be appreciable (PETTERSSEN and CALABRESE, 1959; SPAR, 1960; DANARD, 1964; NITTA, 1964; PYKE, 1965).

PALMÉN concludes that 2–3.5 disturbances of the intensity of hurricane "Hazel" would be sufficient to maintain the kinetic energy of the general circulation poleward from 30° north against frictional dissipation—not counting the sizeable transport of kinetic energy across the latitude circle of 30° north. (MINTZ, 1955; PISHAROTY, 1955.)

Tropical cyclones

In the previous section it has been shown that the main source of perturbation kinetic energy of extratropical cyclones lies in the potential energy, which is released by sinking of cold air and rising of warm air. This vertical motion occurs mainly in the vicinity of baroclinic zones—the "frontal zones"—and near the jet stream which they are associated with. Sinking occurs—as we have demonstrated—along inclined isentropic surfaces. Rising motions are more difficult to trace because of the release of latent heat of condensation and sublimation. The conversion of latent into sensible heat may be a sizeable contribution in the *maintenance* of extratropical cyclones, but usually does not provide the *original* energy source for cyclone formation.

In tropical cyclones ("hurricanes" in the Atlantic, "typhoons" in the Pacific, and "cyclones" in the Indian Ocean) this is no longer the case and the release of latent heat becomes the original and dominant energy source which, together with sensible heat transported upward from the ocean surface, maintains the storm against frictional dissipation (PALMÉN and RIEHL, 1957; BERKOFSKY, 1960; KASAHARA, 1960, 1961; BARRIENTOS, 1964; OGURA, 1964). This is corroborated by the high negative correlation between sea surface temperatures and central pressure in hurricane Esther, indicating a deepening tendency over warm water with filling associated with cool water (PERLROTH, 1962).

Tropical cyclones originate over the tropical regions of the oceans where horizontal temperature gradients are small. Thus, release of potential energy in the troposphere cannot be considered as a main energy source. Only when tropical cyclones start to recurve poleward and eastward, may they draw on the potential energy of air-mass differences in the westerly "steering current." In doing so, however, they lose the characteristics of a tropical storm, and—in spite of their, at times, still violent nature—they are classified as extratropical cyclones.

Our present state of knowledge on hurricane formation and structure has been summarized by RIEHL (1954) and YANAI (1964). The detailed mechanisms that generate tropical cyclones are not yet fully explored. Tropical cyclones, in contrast to their extratropical counterparts, are so-called "warm-core" systems: Convective motions and release of latent heat by condensation processes characterize the early state of hurricane formation (KOTESWARAM and GEORGE, 1957). Such heat release produces strong warming in the middle and upper troposphere in the center of the disturbances (see Fig.51).

Two questions will have to be answered at this point:

(*1*) What mechanisms may generate organized convective motions?

(*2*) What processes will keep driving the "heat engine" by latent heat?

In answering the first question we note that even weak wave disturbances are associated with a definite vorticity pattern, mainly produced by changes in the curvature term V/r_s. The flow through such a vorticity pattern ($V \neq C$, where C is the wave speed) will produce a divergence and convergence distribution which, in turn, gives rise to vertical

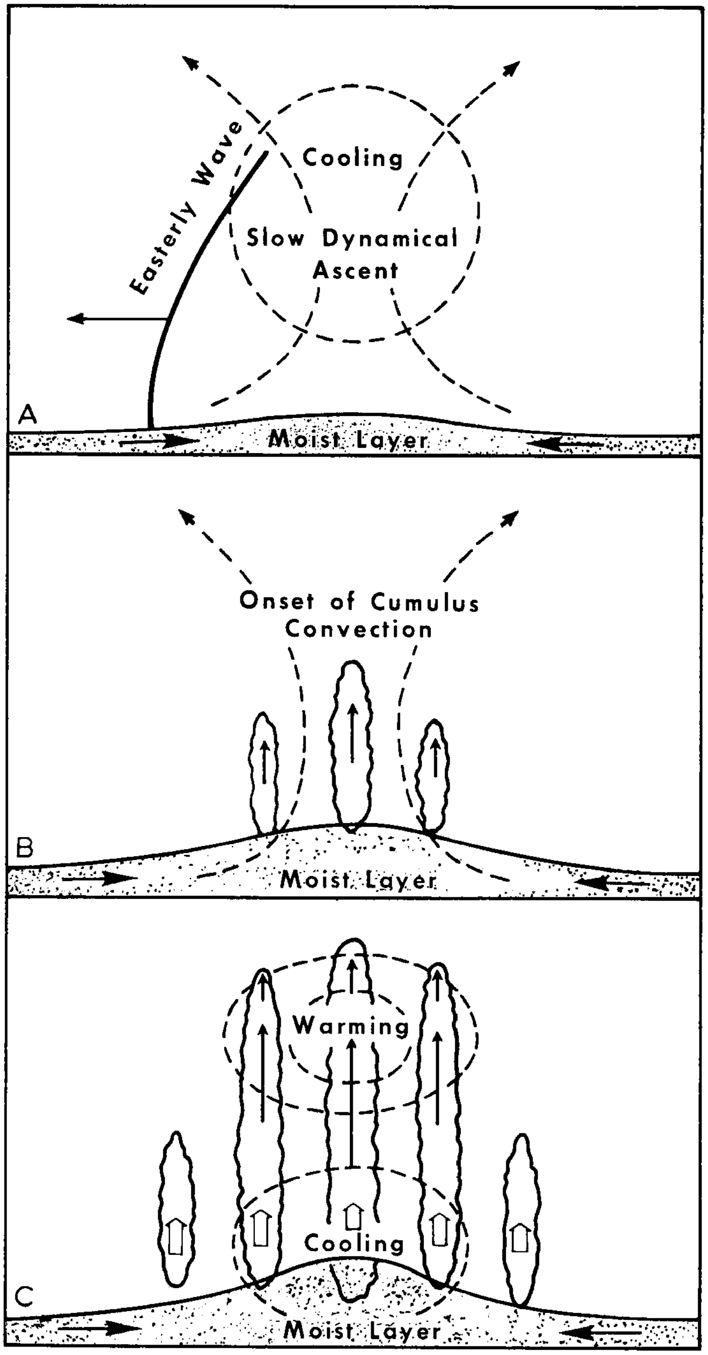

Fig.51. Postulated change of thermal structure during the formative stage ot a tropical cyclone due to cumulus convection (After YANAI, 1963a.)

motions and shower activity in well-defined areas (YANAI, 1963b; LANDERS, 1963). As is the case with extratropical cyclones, vertical motions are enhanced, if a divergent upper flow pattern is superimposed over low level convergence. Fig.52 shows time sections of relative vorticity over the Marshall Islands at 700 and 200 mbar, together with sections of vertical velocity ω at the 400 mbar level. Two wave disturbances with cyclonic vorticity at low levels and anticyclonic outflow at high levels later developed into typhoons ("Rita" and "Susan," 1958).

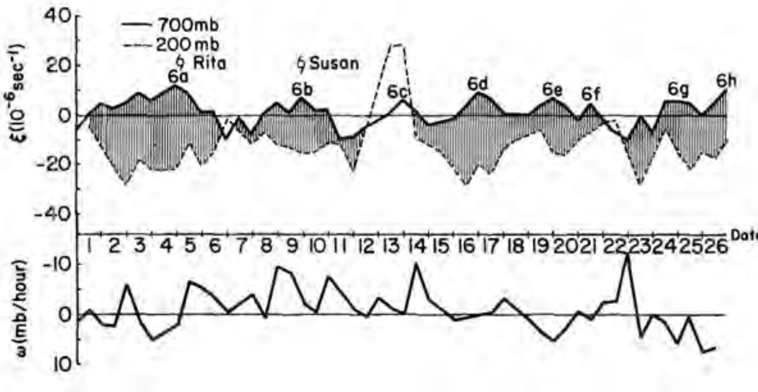

Fig.52. Time sections of vorticity at 700 mbar (solid) and 200 mbar (dashed) and of vertical velocity ($\omega = dp/dt$) at the 400-mbar level for June 1–26, 1958, computed for an area centered around Bikini Island. (After YANAI, 1963b.)

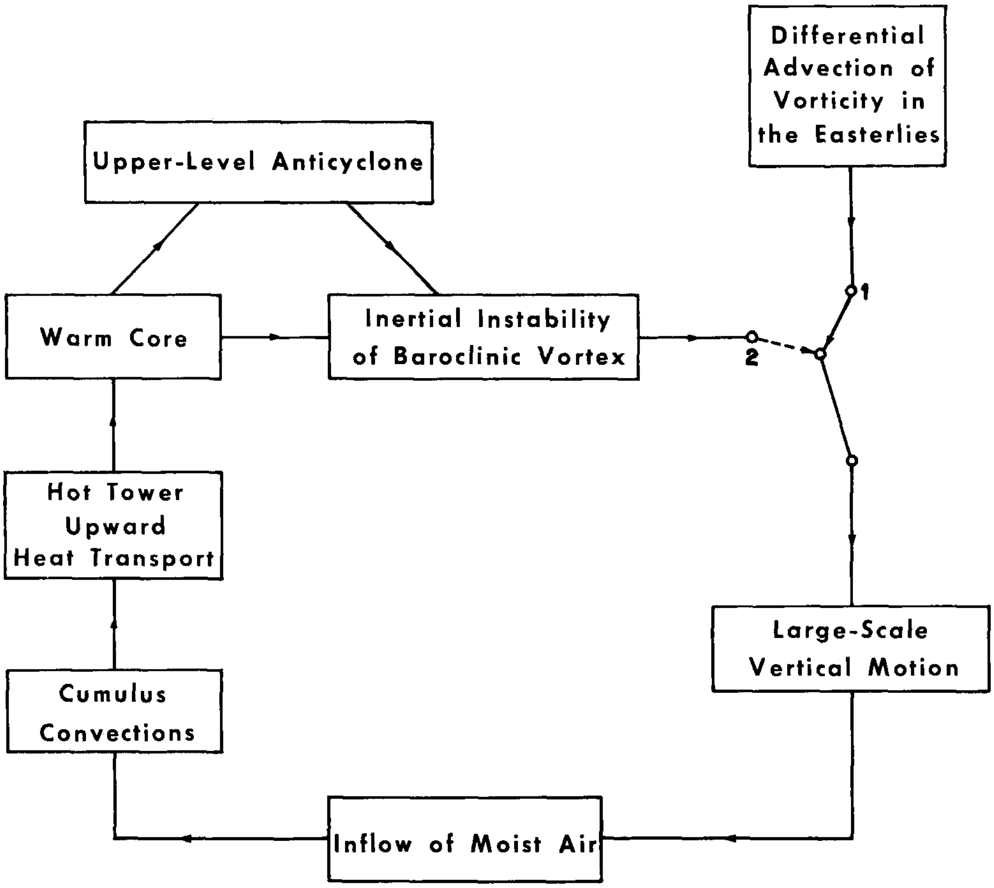

Fig.53. Hypothetical "chain of events" leading to hurricane formation. (After YANAI, 1964.)

As RIEHL (1951) has stressed earlier, anticyclonic outflow aloft is also important from the point of view of the second question. If air, rising under the release of latent heat of condensation, were to sink in the immediate vicinity of the convective system, it would do so dry-adiabatically, rendering the environment surrounding the convective cells warmer than the cells themselves. This, of course, would destroy the buoyant forces driving the convection, and the disturbance could no longer sustain itself. If, however, outflow aloft exports the rising (warm) air and lets it subside at some distance from the precipitation area, the disturbance will not destroy itself. A vorticity distribution like the one shown in Fig.52 seems to be a necessary condition for the formation of a tropical cyclone, but does not seem to be sufficient for the development of a wave into a cyclone. Further with respect to the second question, YANAI (1961a, 1963a, b; 1964) finds that warming must occur in the middle troposphere (see schematic Fig.51). Observational evidence is presented in Table III, again using data from the Marshall Islands area for June and July, 1958 (YANAI, 1963b).

Apparently the baroclinicity of a warm-core vortex once formed plays an important role in maintaining and deepening the disturbance. As discussed by YANAI (1961b, 1964), baroclinic instability along constant absolute angular momentum surfaces, or inertial instability along constant potential temperature surfaces, would maintain upward vertical motions and continuing release of latent heat within the vortex (see ALAKA, 1962). He envisions the "chain of events" presented in Fig.53. Development starts at point no.1 of the flow diagram. Once the development of the vortex has reached point no.2 in this diagram, repeated cycling through the loop will intensify the tropical cyclone in a self-sustaining mechanism, until the momentum absorption in the surface boundary layer and the supply of heat have reached an equilibrium state. Surface friction, the main "brake" on a cyclone, increases with wind speeds near the ground, hence

TABLE III

COMPARISON OF DEVELOPED AND NON-DEVELOPED DISTURBANCES

Year: 1958 date and time of vorticity max. at 700 mbar	Vorticity (10^{-6}/sec)			ω		Warming at 400 mbar relative to monthly mean values	Observation[1]
	700 (mbar)	200 (mbar)	difference	time of max. (400 mbar)	ω at 400 mbar (mbar/h)		
6/5/00Z	11.8	−22.1	33.9	6/5/12Z	−6.7	+1.1	Rita
				6/9/00Z	−9.5		Susan
6/10/00Z	6.8	−15.2	22.0	6/11/00Z	−7.5	+2.0	
6/14/00Z	5.6	28.2	−22.6	6/14/12Z	−10.2	−1.6	×
6/17/00Z	8.7	−19.5	28.2	6/18/00Z	−3.2	−2.6	×
6/20/00Z	7.4	−15.4	22.8	6/21/00Z	−0.6	−1.0	×
6/21/12Z	4.5	−7.3	11.8	6/23/00Z	−12.4	−2.5	×
6/25/00Z	6.1	−14.7	20.8	6/25/12Z	0.5	−2.8	×
6/27/00Z	10.7	−10.2	20.9	(6/28/00Z)	?	+1.0	Tess
7/2/12Z	6.8	12.5	−5.7	7/2/12Z	−2.8	+0.1	×
7/4/00Z	3.3	−27.6	30.9	7/4/00Z	−6.3	+2.3	Viola
(7/7/00Z)	(+)	(−)	?	(7/7/12Z)	?	+0.2	×
				7/9/12Z	−8.7		Alice
7/8/12Z	9.8	−21.2	31.0	7/11/12Z	−12.1	+1.7	
7/13/00Z	16.4	−13.9	30.3	7/14/00Z	−7.4	−0.8	×
7/16/18Z	6.0	−16.0	22.0	7/18/06Z	−0.1	−3.4	×
7/20/06Z	19.9	−18.5	38.4	7/20/06Z	−16.7		Doris
7/21/06Z	20.2	−24.0	44.2	7/22/00Z	−8.8	+2.5	
7/25/00Z	9.8	(−)	?	7/26/12Z	−6.5	−1.1	×
7/29/00Z	2.8	−16.1	18.9	?	?	−1.7	×

[1] × indicates no typhoon

also with horizontal pressure gradients (CASKEY, 1961; KASAHARA, 1961). In addition, however, lateral frictional forces may be quite large in hurricanes. GRAY (1962) computed such forces to be of the order of 10^{-1} to 1 dynes per unit mass, corresponding to pressure gradient forces of 1 mbar/5 miles (see also KRISHNAMURTI, 1961c).

The mature tropical cyclone shows a very distinct structure in its wind and temperature fields. An "eye" containing warm, dry and subsiding air can be seen in many radar and satellite pictures of tropical storms. Fig.54 shows a model temperature distribution about a tropical cyclone. More recent investigations (JORDAN, 1958) confirmed PALMÉN's (1948) early findings that the horizontal temperature gradients within the eye are concentrated near the eye walls. Furthermore, it appears that the deeper the depression in the center of the vortex, the warmer the temperature in the eye. This relationship becomes more pronounced at higher levels.

Relative humidities in the eye of a hurricane in the lower troposphere are low during the formative stages, high during the mature and dissipating stages of the storm, and appreciably higher than humidities in the mean tropical atmosphere (JORDAN, 1957, 1961). Lapse rates in the eye, after lowest sea-level pressure has been reached, are close to the moist

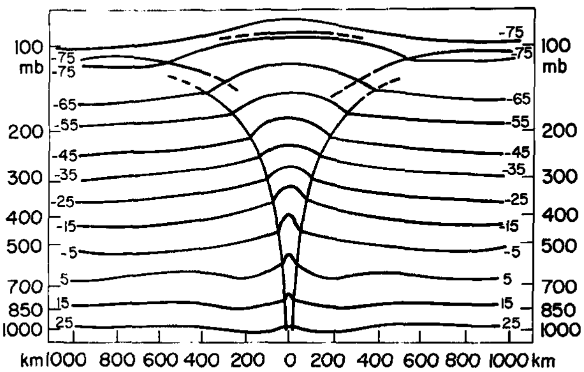

Fig.54. Vertical cross-section through a hurricane, September 17–20, 1947. Heavy lines mark the tropopause and the boundary of the eye of the storm. Thin lines are isotherms at intervals of 10°C. (After PALMÉN, 1948; JORDAN, 1958.)

adiabatic. This has prompted the conclusion that at least part of the descending air comes from the cloud walls surrounding the eye. Temperatures within the eye should be much higher than the ones normally observed at mid-tropospheric levels, if stratospheric air had descended dry-adiabatically to these heights. KUO (1957) concludes that sinking motion is confined to the center of the eye, while the air in the outer regions of the eye is dragged along by strong lateral mixing and undergoes outward and upward motion. LA SEUR (1957), on the other hand, postulates sinking near the rim of the eye.

Small tropical cyclones with relatively high central pressures at the surface may not possess an eye at all. Even in deep cyclones the eye does not appear to be a stable entity. It seems to form and dissipate, causing at times an erratic motion of the center of the storm (JORDAN, 1963). In mature storms large eyes of 30–50 miles in diameter have been observed.

The wall clouds surrounding the eye have been described as an awe-inspiring sight

(SIMPSON, 1952, 1954). Except for low-level clouds, skies within the eye may be clear or show cirrus or cirro-stratus (DUNN and MILLER, 1960). The cumulonimbi surrounding the eye may have steep, nearly vertical walls, or contain extending shelves of clouds. Their tops merge into a large cirrus shield, following the outflow at high-tropospheric levels (FUJITA and ARNOLD, 1963; GENTRY, 1964). In some storms cloud walls have been observed which were not completely closed. Strongest winds are found within the wall clouds, dropping off rapidly towards the center of the eye.

Another distinct feature of tropical cyclones are the cloud bands which follow a spiral arrangement about the center of the storm. From aircraft reconnaissance flights considerable variation in precipitation activity within these spirals has been found from day to day, with the main activity also shifting from sector to sector. Cloud bands may at times extend several hundred miles outward from the center. Convective activity within these bands increases towards the center (LA SEUR and HAWKINS, 1963). Fig.55 shows a composite picture of strong radar echos in hurricane "Cleo," on 18 August 1958, as observed from a research aircraft flying at 35,000 ft. The spiral arrangement of the precipitation areas is clearly evident.

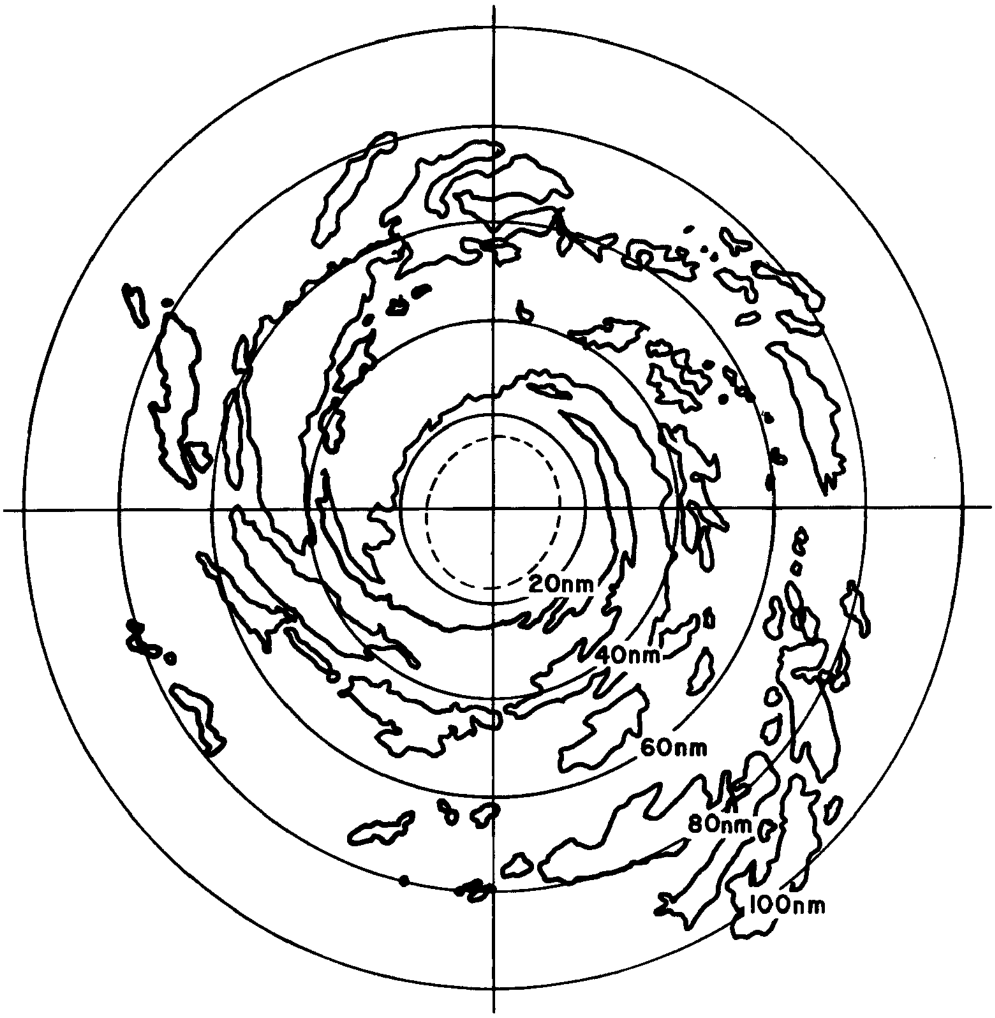

Fig.55. Composite diagram of stronger radar echoes observed from reconnaissance aircraft at 35,000 ft. pressure altitude, hurricane "Cleo", 18 August, 1958. (After LA SEUR and HAWKINS, 1963.)

The "hot towers" of the cumulonimbi from which the rain falls near the center of the storm play an important role in the vertical transport of latent heat in a tropical cyclone, although they comprise only a relatively small percentage of the total area of the cyclone (RIEHL and MALKUS, 1961). MALKUS et al. (1961) estimate the "hot tower" area to have been 1% of the total area within 200 miles from the center of hurricane "Daisy," 1958, in its formative stage, and 4% in its peak intensity stage. ACKERMAN (1963) arrives at the following percentage areas of "hot towers" for the same hurricane in its formative stage; 23% of the area within a 60-mile radius, 16% of the area within a 100-mile radius, and 2% of the area within a 200-mile radius.

These figures indicate the rapid decrease of convective activity in the spiral bands with increasing distance from the center of the storm. Thus, even in the region of *mean* upward motion the air is far from being saturated. This fact is of importance when considering the stability of the large-scale motion. While the atmosphere in tropical cyclones is gravitationally unstable with respect to small-scale cumulus motion, it remains gravitationally stable with respect to large-scale motions (CHARNEY and ELIASSEN, 1964). From a numerical model of a hurricane, KASAHARA (1961) finds that convective "bands" appear when latent heat releases are included in the computations, but are absent if this energy source is left out. KRISHNAMURTI (1962) obtains spiral bands of vertical motion by including *lateral* friction in a numerical model which allows for the fact that tangential velocities are not symmetrically distributed about a hurricane. They show a crescent-shaped maximum to the right of the center, viewing the vortex in the direction of its motion (HUGHES, 1952; JORDAN, 1952).

Detailed analyses of temperature and wind fields near hurricanes show a similarly striated pattern. Fig.56 and 57 are reproduced here as examples; they correspond in observation time to Fig.55. ("Relative isotachs" in Fig.57 give air motions with respect to a coordinate system that moves with the center of the storm.) Similar arrangements of warm and cold bands, as well as of high and low velocity streaks were found in other hurricanes (GENTRY, 1963).

From a climatological viewpoint, the frequency of hurricane and typhoon occurrence is of interest. For the period 1886–1958, JORDAN and HO (1962) find 15.3 and 4.6 storms per year, on the average, in the Pacific and Atlantic respectively. DUNN (1951) and RIEHL (1954) arrived at slightly higher frequencies by including weaker storms. The range of variation during the same time period was from 5–37 typhoons, and from 0–11 hurricanes in one year. The frequency variations between successive years are quite large, and no regular periodicity can be detected so far. These occurrence statistics, especially the ones over the vast areas of the eastern Pacific, may be subject to drastic revision as satellite surveillance becomes available. A study by SADLER (1964) indicates that even with only 30% of the eastern North Pacific area covered by "Tiros" pictures, in October 1962 only 5 tropical storms were detected in this region by conventional means, while 22 cyclonic systems revealed by "Tiros" appeared to have tropical character. Since estimates of intensity are difficult to make from "Tiros" photographs, all of the 22 storms may not have been of hurricane force.

Highest typhoon frequency is observed during August with 70% of all storms occurring in the months from July to October (ARAKAWA, 1963). In the Atlantic, 80% of the hurricanes occur between August and October, with the "peak season" in September (32%) (RIEHL, 1954).

Anticyclones

Research literature on anticyclones is less abundant than on cyclones by at least an order of magnitude. The obvious reason for this is that weather in anticyclones usually is fair because of the generally subsiding motion in the troposphere. The absence of violent and spectacular weather developments takes much of the "glamour" out of high-pressure regions. Nevertheless, they deserve interest; first of all, because anticyclonic flow and shear conditions may give rise to dynamic instability, and, secondly, because

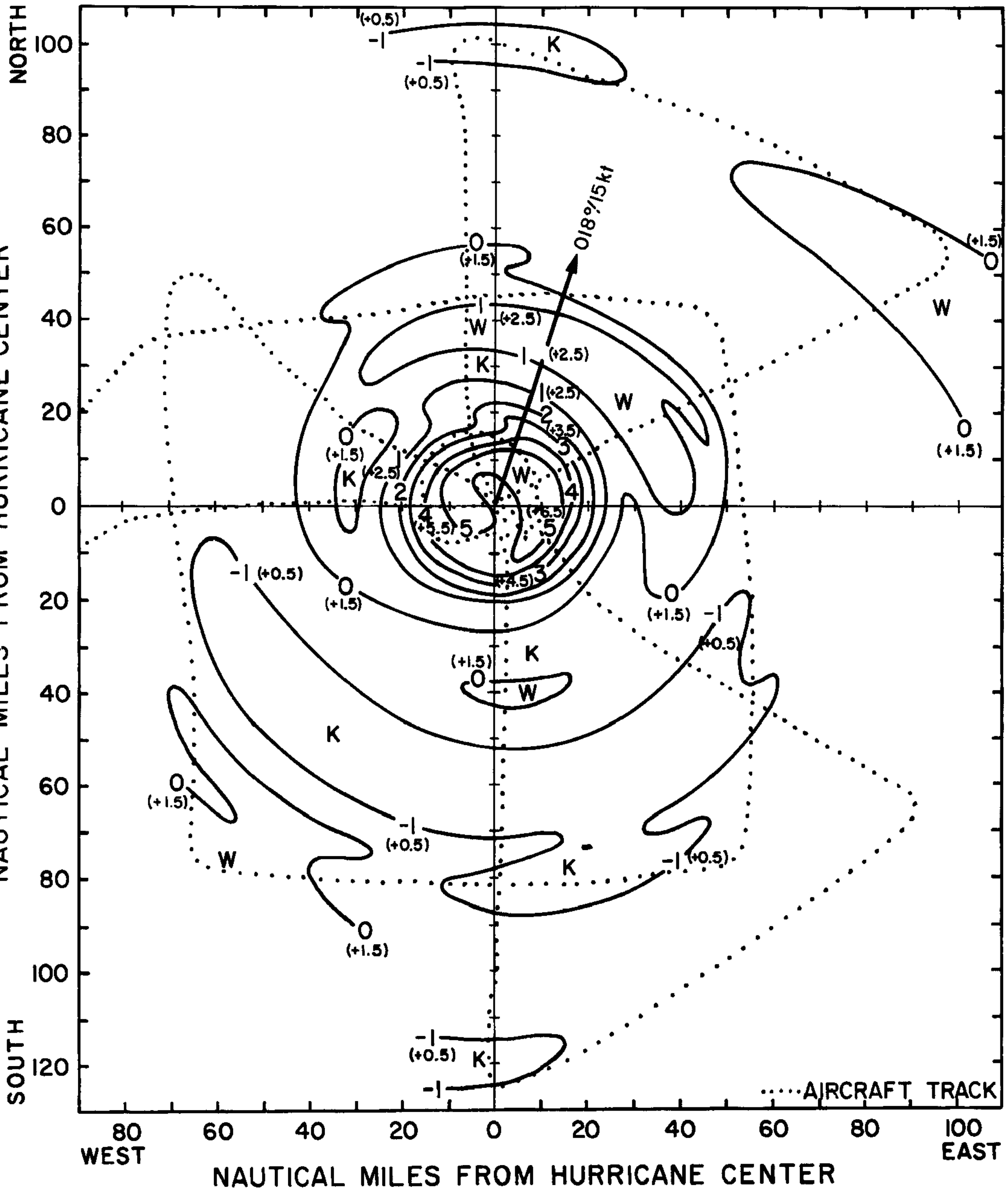

Fig.56. Temperature analysis, 500 mbar, hurricane "Cleo", 18 August, 1958. (After LA SEUR and HAWKINS, 1963.)

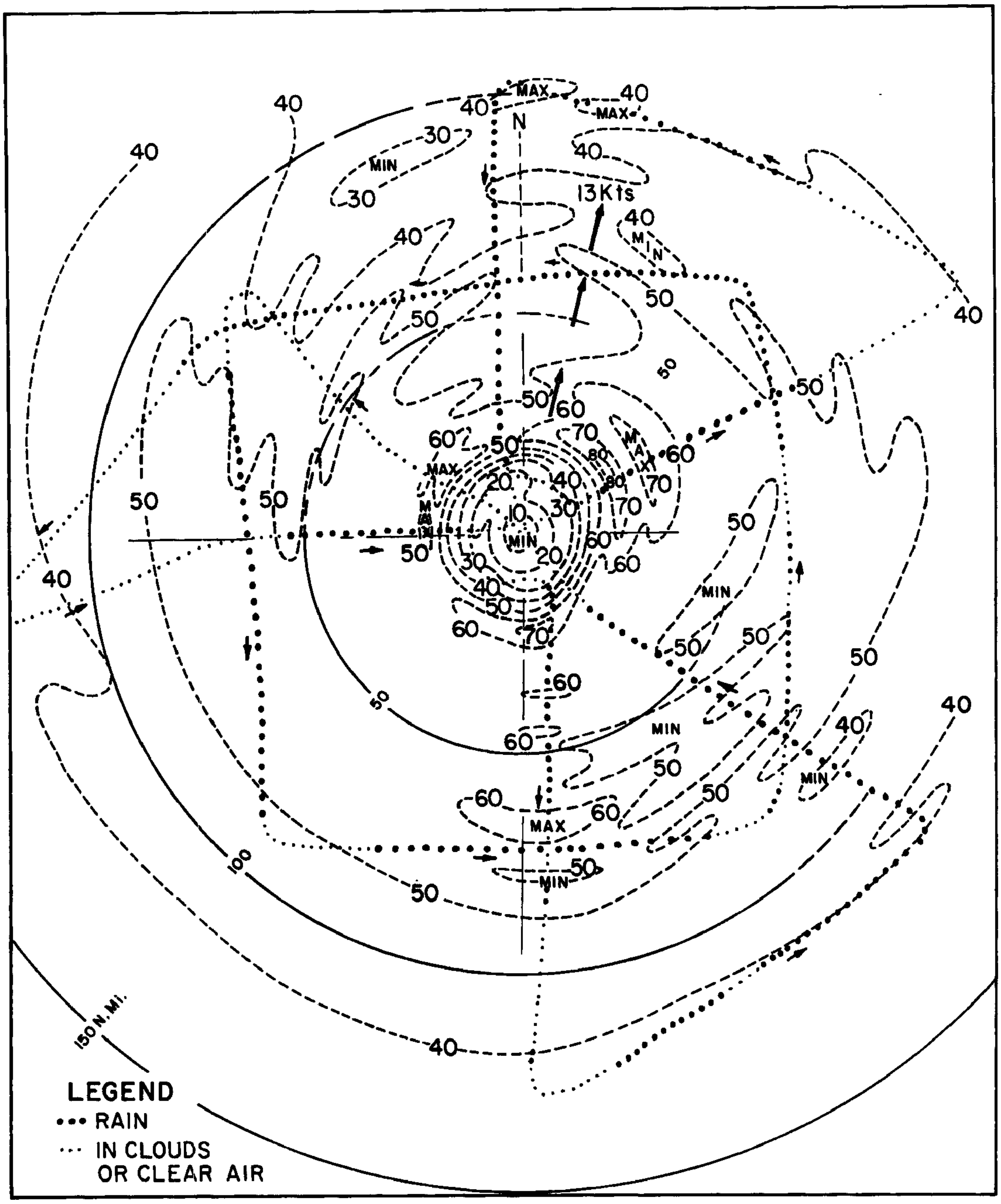

Fig.57. "Relative isotachs" (i.e., isotachs in a coordinate system moving with the storm centre) labeled in knots, at 500 mbar, hurricane "Cleo", 18 August, 1958. (After LA SEUR and HAWKINS, 1963.)

the vertical transport of air masses has gained considerable importance in times of nuclear and industrial air pollution.

In dealing with the dynamics of anticyclones we find, that the same factors that lead to cyclogenesis, also apply to anticyclogenesis. It turns out, however, that vorticity advection is of much smaller effect. In regions of cyclone development, the relative vorticity varies from 0 to about $3f$; in regions of anticyclogenesis it varies only between 0 and $-3/4f$, where f is the Coriolis parameter.

Although cyclones are associated with bad weather, it is the anticyclones which may cause instability of flow and thus lead to the amplification of disturbances in the mean flow. Limiting conditions for anticyclonic shear may be approximated by:

$$-\frac{\partial u}{\partial y}+f=0 \tag{85}$$

Anticyclonic curvature of flow also has a critical value beyond which dynamic instability results. The critical wind speed at a given radius of curvature is:

$$V_{max}=\frac{rf}{2} \tag{86}$$

or:

$$V_{max}=2V_g \tag{87}$$

where V_g is the geostrophic wind speed at a given pressure gradient. According to their vertical structure, we may classify high pressure regions very crudely into two categories: cold anticyclones and warm anticyclones.

In accordance with the hydrostatic equation pressure decreases more rapidly upward in cold and dense air, than in warm air. Thus, cold anticyclones transform into low-pressure regions already at mid-to upper-tropospheric levels. An example is the so-called "polar anticyclone" which occupies the polar basin and which is best developed during the winter season. From this reservoir of cold air, "cold domes" split off from time to time, and migrate southward with a jet maximum. The kinetic energy of the jet maximum is mainly drawn from the release of potential energy, resulting from the gradual collapse of the "cold dome." Rossby (1948) showed theoretically that in a mean westerly current, as we observe it in middle latitudes, cyclonic vortices have a tendency to migrate poleward, anticyclonic vortices favor an equatorward trend. Since cold anticyclones become low-pressure areas aloft, they form on the cyclonic side of the main westerly jet streams, and they migrate southward with appropriate shifts of the jet axis.

Migrating, cold anticyclones of the kind just described are associated with the large cold outbreaks of winter and early spring over the midwestern U.S.A. Such outbreaks follow in the wake of intense cyclones which tend to form to the lee of the Rocky Mountains. The air rushing southward behind the cold front may bring freezing temperatures as far south as Florida and Texas, causing serious concern for crops and livestock in this region. It is these cold outbreaks and their associated anticyclones which cause the mean winter isotherms to dip southward over the central U.S.A. and make the climate of Nebraska, Kansas, and Iowa, for instance, more severe than that of eastern Colorado.

Warm anticyclones give rise to anticyclonic flow conditions throughout the troposphere. Their intensity subsides gradually beyond the level of maximum wind. By their very nature, warm anticyclones are found equatorward of the PFJ. Although under certain flow conditions, such as the ones leading to "blocking highs" (Rex, 1950a, b, 1951; for more details see Reiter, 1961a, 1963a), we may find warm anticyclones at relatively high latitudes, their seasonal and global mean confines them to the location of the subtropical high-pressure ridge.

Whether anticyclones are cold or warm, they exhibit a common characteristic; anticyclonic flow, i.e., negative relative vorticity at the earth's surface. Since this vorticity is being destroyed by friction continuously, anticyclones become the major source of positive (cyclonic) vorticity. If we consider in crude approximation the flow above the friction layer to conserve its absolute vorticity, we see that anticyclones are an essential mechanism of the general circulation, without which a vorticity balance could not be maintained. Vorticity constantly produced by the polar and subtropical anticyclones is primarily consumed by the cyclone activity of the global west-wind belts. Thus, from the vorticity points of view, the anticyclones, in a broad sense, help to maintain the cyclones.

Similar considerations hold for the momentum budget. Easterlies, associated with the polar anticyclones and with the trade-wind belt of the subtropical high pressure ridges, are consumed by surface friction, which is equivalent to the generation of westerly angular momentum. This, in turn, is transported into the west-wind region (by a mean meridional circulation as shown in Fig.1, as well as by large horizontal eddies), where a balance of the momentum budget, again, is maintained through frictional dissipation. Small quasi-periodic and seasonal changes in the total momentum budget of the atmosphere, mainly caused by differences in the frictional characteristics of the "continental" Northern, and the "oceanic" Southern Hemisphere, are balanced by the momentum of the solid earth. Earth, atmosphere and oceans are a "closed system." Changes in the total angular momentum budget of atmosphere and ocean, therefore, reveal themselves in small changes in the rate of rotation of the earth, measured by the length of day (RUDLOFF, 1950).

The cold migrating highs exporting cold arctic air to lower latitudes underneath the rear convergent quadrant of a jet maximum, and the subtropical high-pressure ridge underneath the subtropical jet stream, fit relatively easily into our "model" concepts of atmospheric circulation. The warm blocking highs which, at times, barricade the course of the mid-latitude westerly jet-streams, on the other hand, still present a "pièce de résistance" in research on anticyclones.

From a number of case studies (REX, 1950a, b, 1951; NAMIAS, 1951; DEFANT and TABA, 1958a) the behavior of "blocking highs," their seasonal and geographical distribution. and their impact on weather patterns especially in the European sector has emerged quite clearly. It has also been shown that they play a major role in meridional transport of momentum, heat and water vapor because of the abnormally large amplitudes which they cause in the westerly flow of temperate latitudes. The maximum frequencies of occurrence are found in late winter and early spring, at a time, when the weakening of the tropospheric westerly jet stream, as well as the breakdown of the stratospheric polar-night vortex, require an efficient transport mechanism to carry westerly momentum into the Southern Hemisphere.

Statistics on blocking activity are less complete in the Southern Hemisphere. Yet there is evidence that in spite of the "zonal" character of the southern circulation, blocking highs are relatively frequently observed, especially east of the Australian continent (VAN LOON, 1956a, b). The Southern Hemisphere circumpolar vortex, in the mean, shows some excentricity towards the Australian sector. Thus, blocking seems to favor the regions downstream from the quasi-permanent troughs. It has been argued previously that the two deep troughs of the Northern Hemisphere are caused by orographic effects of the Rocky Mountains and the Himalayas. The ridges downstream from these troughs, which are susceptible to "blocking," thus appear to be orographically controlled as well. The land-sea distribution may have a significant effect, too. The excentricity of the Southern Hemisphere circumpolar vortex has been attributed to the Antarctic highlands, which act as a cold source.

The nature of the blocking high, an example of which is shown in Fig.58, indicates that warm air is advected northward on the west side of the "block," while cold air is transported southward on its east side. During the intensification of the blocking high one observes, in the mean, a slight retrogression towards the west. This indicates that meridional transports during this period are quite strong, causing an erosion of the block on its east side, and a continuous buildup on the west. During the decaying stage progression of the "block" towards the east is observed.

Cyclone tracks during a blocking weather situation split into two branches, one deviating far to the north, and one leading south of the "block" along a jet stream which crosses the elongated high-pressure ridge (Fig.58). This abnormal pressure pattern with its steering effect on cyclones causes rather significant anomalies in precipitation and surface temperature distributions (Fig.59 and 60).

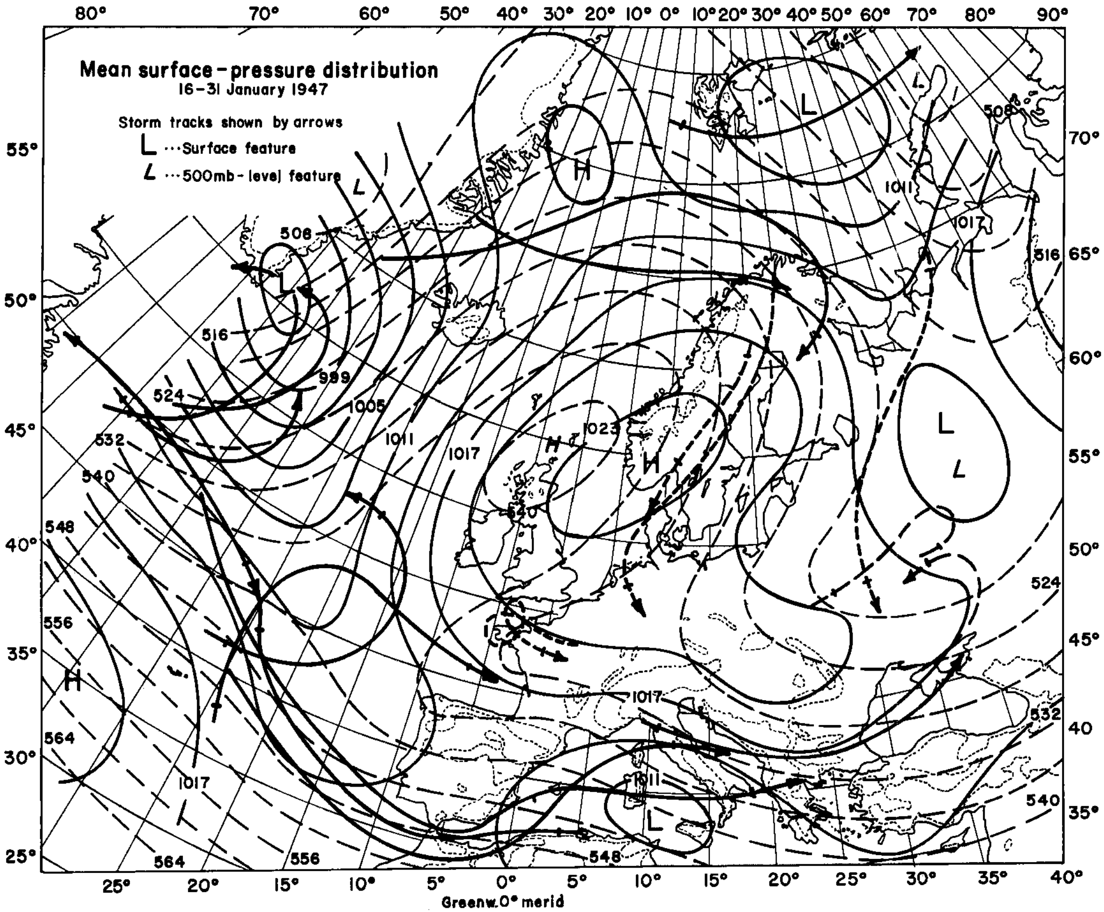

Fig.58. Mean surface pressure distribution over the Atlantic–European area during a wintertime case of strong Atlantic blocking action (16–31 January, 1947). Surface isobars are shown as thin solid lines, pressures given in mbar. The mean contour pattern at the 500 mbar level is shown by the thin long-dashed lines; contour heights given in dynamic decametres. Cyclone tracks at the surface are indicated by the heavy, solid and dashed arrows. Temperature advection may be estimated qualitatively by the advection of the pattern of thickness between surface and 500 mbar along the 500 mbar (geostrophic) streamlines. (After Rex, 1950b.)

REITER (1961a, 1963a) has argued that the annual mean atmospheric circulation during the Pleistocene may have resembled our present circulation during late winter and spring. Such a mean intensification of the circulation could have been caused by a mean temperature gradient between equator and pole larger than is presently observed in the yearly average. If such was the case, one should expect an increase in the annual number of blocking weather situations in the Atlantic sector over the present mean conditions. Sand-dune orientations in Europe, if properly interpreted, confirm this conclusion

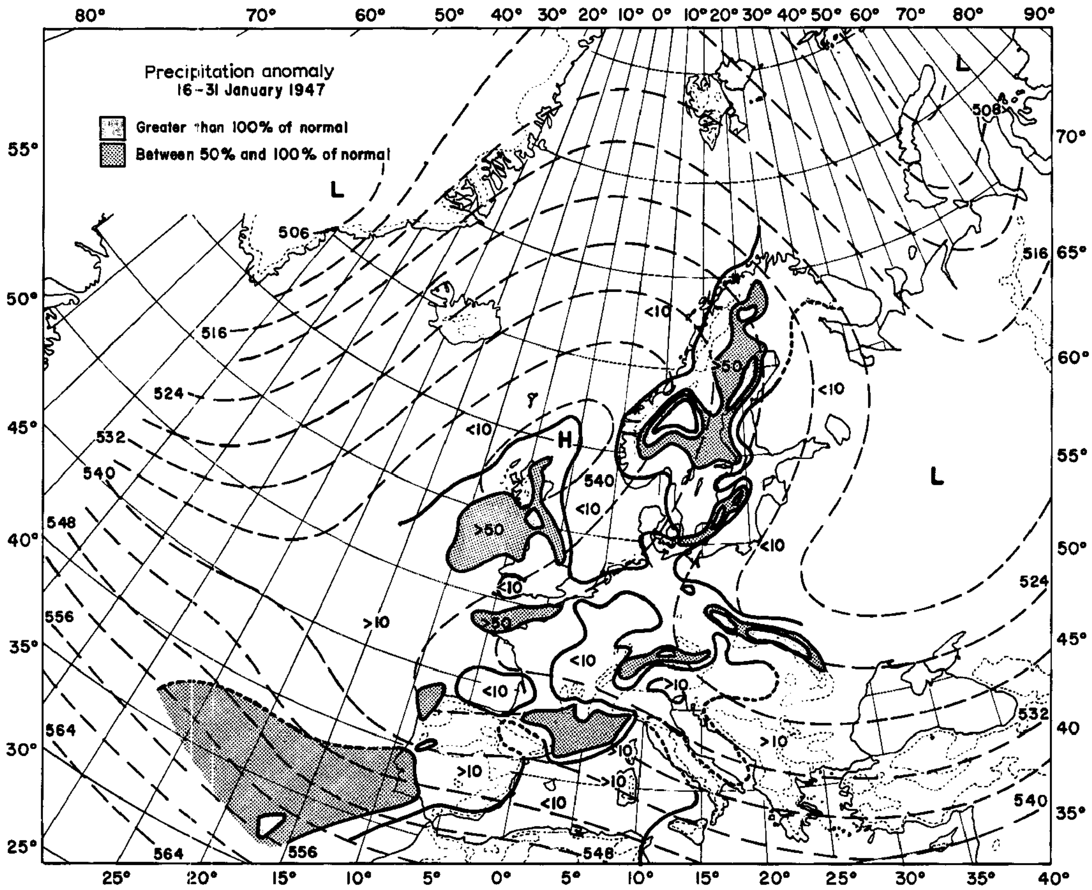

Fig.59. Isanomals of precipitation over the Atlantic-European area during a wintertime case of strong Atlantic blocking action (16–31 January 1947). Isanomal lines are given for 10, 50, 100 and 150% of normal and are shown as thin solid lines, except in areas of uncertain analysis where they are shown as thin short-dashed lines. Areas recording precipitation amounts greater than 50% of, but less than normal, are indicated by the shading. The mean contour pattern at the 500 mbar level is shown by the thin long-dashed lines; contour heights given in dynamic decametres. (After REX, 1950b.)

(Fig.61). Precipitation and temperature anomalies during such blocking situations would favor the formation of a large ice-shield over Scandinavia. The large positive temperature anomalies over the North Atlantic would encourage evaporation from these regions, and might also help to keep relatively large portions of this ocean ice-free. Cyclone tracks passing over Scandinavia would be aided by orographic effects in producing above normal amounts of precipitation (Fig.59). It should be noted that during such weather situations the European Alps also receive a slight excess of precipitation while central and eastern Europe remains relatively dry. A recent study by NAMIAS (1964) shows a deficit of precipitation along the Norwegian coast during periods of prolonged "blocking." However, the area over and to the lee of the Scandinavian mountains seems to be favored by wet weather.

Aside from these dynamic aspects of anticyclones, recent interest has been devoted to high pressure regions as potential areas of radioactive fallout. It has been mentioned earlier that stratospheric air is transported downward into the troposphere in the entrance region of a jet maximum (see p. 106). This air, which may be radioactively contaminated

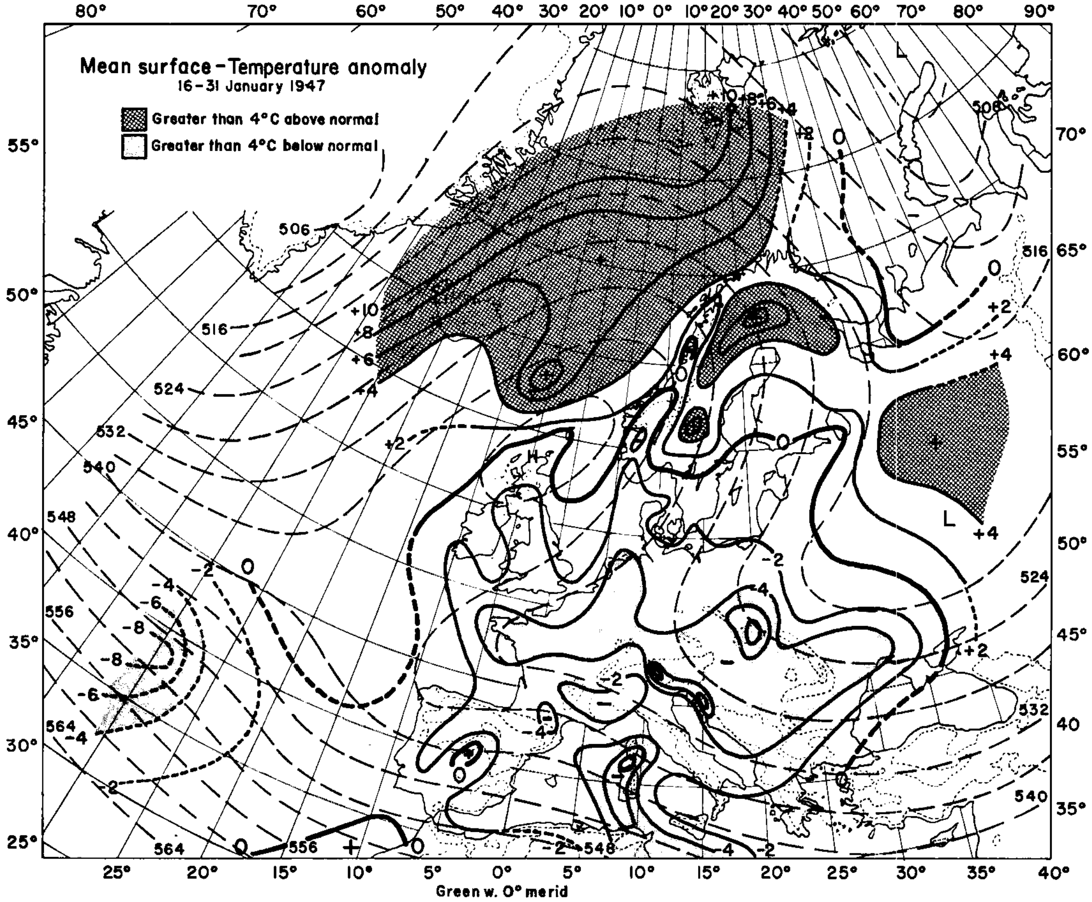

Fig.60. Isanomals of mean surface-temperature over the Atlantic-European area during a wintertime case of strong Atlantic blocking action (16–31 January, 1947). Isanomal lines are given for each 2°C above and below normal and are shown as thin solid lines, except in areas of uncertain analysis where they are shown as thin short-dashed lines; the isonormal line (zero anomaly) is shown as a heavy solid (or dashed) line. Areas recording mean temperatures more than 4°C above normal are indicated by the dark shading. The mean contour pattern at the 500 mbar level is shown by the thin long-dashed lines; contour heights given in dynamic decametres. (After REX, 1950b.)

travels through the "jet-stream front" in the upper troposphere, and finally ends up in an inversion over an anticyclone (REITER, 1963b; REITER and MAHLMAN, 1964; DANIELSEN, 1964a, b). The general subsidence within the anticyclone tends to increase the stability of the inversion. This is also in agreement with the principle of conservation of potential vorticity: decrease of absolute vorticity in anticyclonic flow increases the vertical stability. As a consequence anticyclones tend to show considerable detail in the vertical thermal structure (DANIELSEN, 1959).

Similar considerations hold for the subtropical high-pressure cells. It has been shown

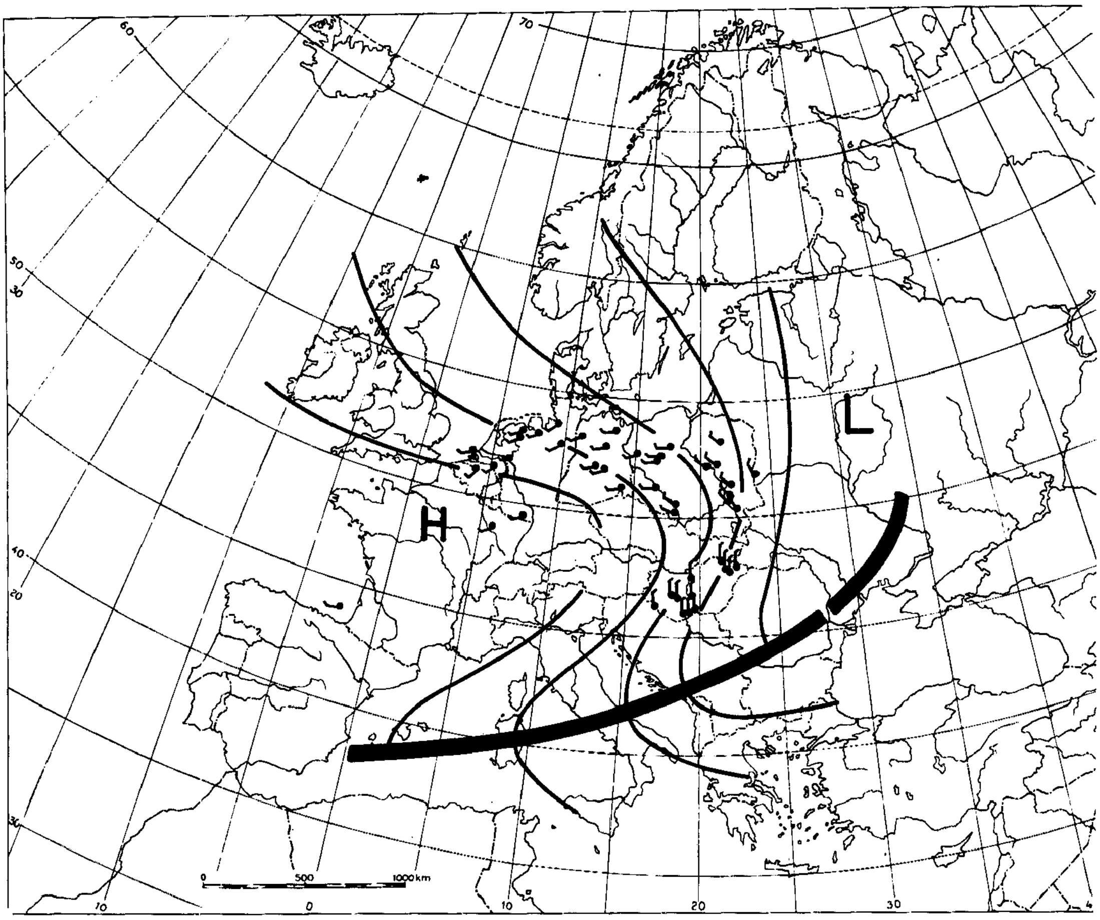

Fig.61. Winds (interpreted from sand-dune orientation) and pressure distribution during the pleistocene. Isobar pattern takes into account friction-induced flow across isobars. (After REITER, 1961a.)

that the trade-wind inversions are most intense, and occur at lowest levels, along the east sides of the subtropical anticyclones (e.g., over the eastern Atlantic close to the African coast). Stabilization is aided here by relatively cold ocean surfaces produced by upwelling water along the coast, and extensive stratiform cloud covers are frequently observed. At the same time the decrease of relative humidity from the bottom to the top of the inversion is largest in these regions. As the air travels westward in the trade-wind region, the inversion is pushed higher and is weakened by convective activity in the lowest atmospheric layers (for more details see RIEHL, 1954).

From the foregoing we must conclude that anticyclones are far more complex in nature than they may appear at a superficial glance. SCHINZE's and SIEGEL's (1943) air mass theories, which name the large anticyclones as source regions for air masses because of their rather homogeneous structure, thus should not be applied indiscriminately.

Local circulation systems

In describing local circulation systems in the troposphere we will confine ourselves to those, which are of general consequence, applicable to several regions on the globe.

A description of systems which apply only to specific locations will be left to the regional climatographies found in other volumes of this series. In rather broad terms we may classify the circulation systems with which we shall concern ourselves into two groups; first, local circulation systems, influenced by large-scale flow patterns, and second, local circulations produced by diurnal effects. Included in the first group are foehn and katabatic winds; in the second are land, sea, mountain, and valley breezes.

Foehn and katabatic winds

Foehn winds are dry and gusty downslope winds which occur under special weather conditions on the lee side of mountain ranges. The name of these winds is derived from the German. In the U.S.A. such winds are frequently called "chinook" winds (named after an Indian tribe, formerly inhabiting the Columbia River Valley).

The foehn phenomenon has been studied extensively in Europe (BILLWILLER and DE QUERVAIN, 1912; KANITSCHEIDER, 1932–1939; HANN and SÜRING, 1943; FREY, 1945; HOINKES, 1950; REITER, 1958b; VON FICKER, 1905, 1910). These winds are associated with a strong component of flow normal to the mountain range. On the windward side there is forced ascent up the slopes, the magnitude of which led to the distinction between "anticyclonic" and "cyclonic" foehn. The former is associated with convergence at higher levels and with general sinking motions in the troposphere. The forced ascent along the windward slopes under these conditions leads to relatively little cloudiness and precipitation, if any.

Cyclonic foehn is associated with upper divergence and general rising motions in the troposphere. These act in support of the upslope flow, causing heavy precipitation on the windward side. If the air forced to rise across the mountain range is conditionally unstable, thundershowers may occur along the ascending path. Such conditions are frequently witnessed over the Rocky Mountains during spring and early summer: A row of thunderstorms develops west of the Continental Divide with their cirrus anvils blowing across the divide in long "plumes," indicating a strong westerly current at tropopause level. The region immediately to the east of the divide remains free of precipitation, while another row of thunderstorms may be seen forming approximately 30–50 km east of the high mountain ranges.

The descending air motion on the lee side, causing the foehn winds, is associated with a gravitational lee wave (QUENEY, 1947, 1948). The flow is strongly ageostrophic, traveling from a high pressure ridge over the mountains across a steep pressure gradient into a trough to the lee of the mountains. Both, ridge and trough, are aligned parallel to the mountain range. The ascending motions on the windward side produce a tongue of relatively cool air, also parallel to the mountain range, while the dry adiabatic descent in the foehn current to the lee of the mountains causes a tongue of warm air.

As is evident from lee-wave theory, the forced ascent and descent do not have the same phase-relationship with respect to the underlying terrain at all levels in the atmosphere. Along the vertical coordinate we should find a wave number (SCORER, 1949):

$$l = \sqrt{\frac{g}{\Theta}\frac{\partial \Theta}{\partial z}\Big/ u^2 - \frac{1}{u}\frac{\partial^2 u}{\partial z^2}} \tag{88}$$

where Θ is the potential temperature, g the acceleration of gravity and u the component of flow normal to the mountain ridge. The theory yielding these results assumes simple terrain features, atmospheric stratification and wind profiles. Thus, certain discrepancies between observed lee waves and theoretical results have to be expected. (See Döös, 1961, 1962; SAWYER, 1962; KRISHNAMURTI, 1964.)

Maximum horizontal wind velocities should be expected along the axis of the pressure minimum which, as we have stated, runs parallel to the mountain range and slopes upward in space according to conditions prescribed by above equation. Beyond the pressure minimum the strongly ageostrophic flow starts to decelerate again. Strong chinook winds as an effect of mountain waves, therefore, should be experienced only at relatively short distances from the mountain range (order of magnitude 30 km).

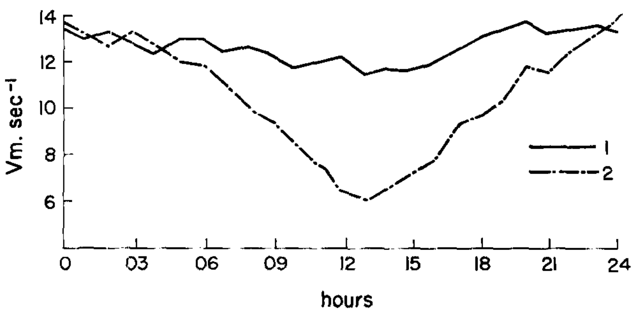

Fig.62. Diurnal variations of wind velocity in April 1956, Mirny, Antarctica. *1* = All observations combined; *2* = katabatic winds only. (After TAUBER, 1960.)

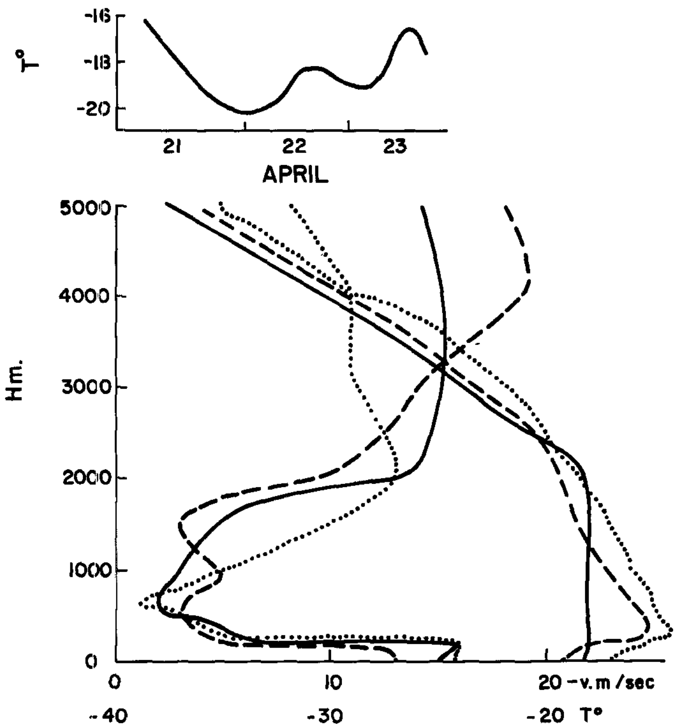

Fig.63. Distribution of temperature and wind velocity with height during the katabatic wind period 21–23 April, 1956, at Mirny, Antarctica. Lower left: curves of distribution of wind velocity. Lower right: curves of distribution of temperature. Upper diagram: change in surface temperature during the period 21–23 April. —— 21 April; - - - 22 April; . . . . . . 23 April. (After TAUBER, 1960.)

Effects of an irregular terrain may cause rather characteristic distributions in the intensities of mean winds and gusts of the foehn, as well as the time of their strongest development. So, for instance, one observes that the foehn winds may blow over the Inn valley in the Austrian Alps, while the bottom of the valley still experiences light drainage winds of cold air. When this cold air finally is removed, strongest winds are usually observed in the Inn valley, where an opening towards the Brenner Pass gives easy access for the southerly foehn winds.

The adiabatic descent in a foehn current has been attributed to a gravity-wave phenomenon, embedded in a broad current crossing the mountains. If the lowest layers of the atmosphere prior to foehn conditions were stably stratified, maybe even showing inversion lapse rates, their replacement by air descending adiabatically from the heights of the mountain crests will result in a marked warming. Thus, the name "foehn" or "chinook" is reserved for warm descending winds.

The "mistral" of the Rhone valley and the French Mediterranean coast, as well as the "bora" of the Adriatic coast of Yugoslavia, are gusty, "katabatic," strongly ageostrophic winds. They are associated with the passage of a cold front. Cold air then rushes through a gap in the mountain chain, and descends rapidly by its own potential energy. Wind speeds of 100 knots have been measured in bora gusts at Trieste. These katabatic winds are a considerable menace to coastal installations and to shipping.

If the atmospheric stratification near the ground prior to the arrival of a "bora" has been close to adiabatic, the wind appears as a cold wind. Thus, except for their differences in temperature and the added release of potential energy in descending post-frontal cold air, foehn and bora are rather similar phenomena. Actually, foehn winds close to the mountain crest may appear with the characteristics of a cold "bora." Only during their further descent along the mountain slopes will adiabatic warming produce the characteristics of a warm "foehn" when they arrive at the bottom of the valley.

Strong and gusty katabatic winds have also been reported from the shores of Antarctica (DZERDZEEVSKII, 1960; SHAW, 1962; STRETEN, 1963.) From the orientation of "sastrugi," i.e., snowdrifts shaped by wind erosion, MATHER (1960) concludes that katabatic winds near Mawson may extend as far as 400 miles inland. Under such conditions, the Coriolis force is expected to exert a certain influence on katabatic accelerations. In the region of Mirny, katabatic winds also have been observed far inland, as far as Pionerskaya, 375 km from the coast (TAUBER, 1960).

The characteristics of these katabatic winds agree well with those of the "bora" observed near Trieste (HANN and SÜRING, 1943). Fig.62 shows mean diurnal wind variations at Mirny during "bora" conditions. In agreement with the Trieste data, the bora is at its minimum intensity around noon. Fig.63 shows a vertical wind and temperature distribution for three cases of katabatic winds. The shallow layer of cold air involved in the "bora" flow is clearly evident, especially if one compares such situations with "normal" conditions (Fig.64).

Diurnal circulations

Diurnal circulation systems are generated by differential heating of adjacent regions. Discounting large-scale diurnal pressure waves between continents and oceans, and other tidal effects (see GODSKE et al., 1957), there remain land and sea breezes, as well as

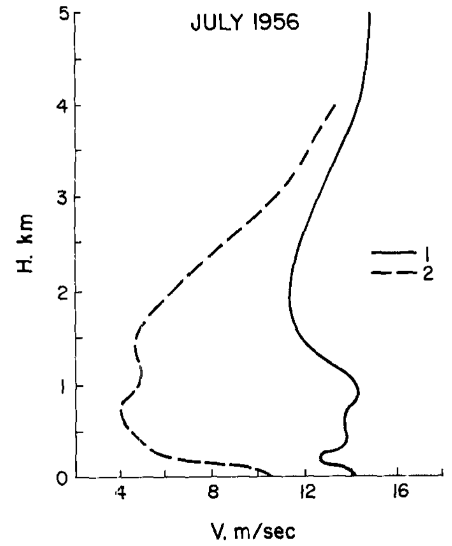

Fig.64. Average wind speed profiles at Mirny, Antarctica, for July, 1956. *1* = average wind speed profiles at all observation times (45 instances); *2* = for katabatic winds only. (After TAUBER, 1960.)

mountain and valley breezes to be discussed briefly. More extensive descriptions of these phenomena have been given by DEFANT (1951) and GODSKE et al. (1957).

In both instances, solar radiation generates a horizontal temperature gradient along isobaric surfaces, thus giving rise to isobaric-isosteric solenoids which set the observed circulation system into motion. In the case of the sea breeze, the coastal regions warm up more rapidly during the early morning hours than does the adjacent water surface. Air, thus warmed over land, expands, causing isobaric layers to stretch vertically. This process, in turn, establishes a pressure gradient aloft, which is directed from land to water. Air aloft starts to move and accelerates along this pressure gradient, causing pressure falls inland from the coast, and a pressure gradient with accompanying flow at the surface from the ocean to the land. A steady state of this circulation will be reached when balance between frictional forces and pressure gradients is achieved (CLARKE, 1961). At night the solenoidal circulation reverses, the ocean now being warmer than the land. The effects of land and sea breezes are quite obvious along the east coast of Florida, especially during the rainy season when a line of thunderstorms tends to form inland from the coast in late morning.

Mountain and valley breezes are generated in a similar way. During daylight hours the mountains act as an elevated heat source in comparison with the free air over the plains. Differential heating sets up a solenoidal field, giving rise to valley winds (i.e., winds directed upstream along the valley), as well as upslope winds along the sides of the valley. The latter are quite apparent if humidity conditions are favorable for the formation of cloud banks along the shoulders of the valley. During night time, cool drainage winds are directed down the slopes and out the valley (mountain winds).

List of symbols and abbreviations

A	constant used in harmonic analysis of wind profiles
B	half-width of jet stream; constant used in harmonic analysis of wind profiles
C	wave speed; propagation speed of temperature or pressure patterns
C_g	group velocity
C_i	variable in harmonic analysis of wind profiles
c_p	specific heat at constant pressure
c_v	specific heat at constant volume
D	three-dimensional divergence
D_h	horizontal divergence
E*	Eddy kinetic energy
F	frictional force
f	Coriolis parameter
G_a	absolute angular momentum
G_j	variable in harmonic analysis of wind profiles
g	acceleration of gravity
h	diabatic heat exchange per unit mass
K	eddy diffusivity
K_M	exchange coefficient of momentum
K_s	streamline curvature
K_T	exchange coefficient of heat; trajectory curvature
$\boldsymbol{k}$	vertical unit vector
L	wave length (planetary waves)
l	wave number (lee waves)
LMW	layer of maximum wind
M	$= gz + c_p T$, Montgomery stream function
$\boldsymbol{N}$	solenoidal vector
n	horizontal coordinate normal to flow; number of observation points (harmonic analysis of vertical wind profiles)
P	potential vorticity
p	pressure
$\boldsymbol{Q}$	absolute vorticity
Q_z	vertical component of absolute vorticity
$\boldsymbol{q}$	relative vorticity
R	earth's radius; gas constant
Ri	Richardson number
r	radius of curvature of trajectory
$\boldsymbol{r}_a$	radius vector of absolute motion
r_a	magnitude of radius of absolute motion
s	coordinate along streamline
T	temperature
T_i	inertial period
t	time coordinate
u	horizontal component of flow in the x-direction
$\bar{u}$	mean flow along x-direction
u*	perturbation flow along x-direction
$\boldsymbol{V}$	wind velocity (vector)
$\dot{\boldsymbol{V}}$	$= \frac{d\boldsymbol{V}}{dt}$ acceleration
V	total wind speed
$\boldsymbol{V}_g$	geostrophic wind vector
V_g	geostrophic wind speed
v	horizontal component of flow in y-direction
$\bar{v}$	mean flow in y-direction
v*	perturbation flow in y-direction;
w	vertical component of flow in z-direction
$\bar{w}$	mean flow in z-direction
w*	perturbation flow in z-direction
x, y, z	Cartesian coordinates pointing eastward, northward, upward

List of symbols and abbreviations *(continued)*

$\alpha = \frac{1}{\rho}$ specific volume

$\beta = \frac{\partial f}{\partial y}$ Rossby parameter

$\Gamma = \frac{-dT}{dz}$ dry adiabatic lapse rate

$\gamma = \frac{-\partial T}{\partial z}$ actual vertical lapse rate

ε slope angle of frontal surface

Θ potential temperature

$\kappa = \frac{c_p - c_v}{c_p}$, Poisson's constant

λ geographic longitude

ρ air density

Φ geopotential

φ geographic longitude

ψ scalar function (derivation of potential vorticity)

Ω earth's angular velocity

$\omega = \frac{d\lambda}{dt}$ zonal angular momentum relative to earth

$\omega = \frac{dp}{dt}$ vertical component of velocity along p-coordinate

References

ACADEMIA SINICA, 1958. On the general circulation over eastern Asia, III. *Tellus*, 10 (3): 299–312.

ACKERMAN, B., 1963. Some observations of water contents in hurricanes. *J. Atmospheric Sci.*, 20 (4): 288–298.

ADEM, J., 1962. On the theory of the general circulation of the atmosphere. *Tellus*, 14 (1): 102–115.

ALAKA, M. A., 1958. A case study of an easterly jet-stream in the tropics. *Tellus*, 10 (1): 24–42.

ALAKA, M. A., 1962. On the occurrence of dynamic instability in incipient and developing hurricanes. *Monthly Weather Rev.*, 90: 49–58.

ANGELL, J. K., 1964. A note on the magnitude of jet-stream winds east of Japan as derived from transosonde data. *Montly Weather Rev.*, 92 (5): 203–206.

ANGELL, J. K. and KORSHOVER, J., 1964. Quasi-biennial variations in temperature, total ozone and tropopause height. *J. Atmospheric Sci.*, 21 (5): 479–492.

ANONYMOUS, 1947. On the general circulation of the atmosphere in middle latitudes. *Bull. Am. Meteorol. Soc.*, 28; 255–280.

ANONYMOUS, 1952. Normal weather charts for the Northern Hemisphere. *U.S. Weather Bur., Tech. Papers*, 21: 74 pp.

ANONYMOUS, 1960. Cyclone and anticyclone. *Meteorol. Soc. Japan, Selected Meteorol. Papers*, 3.

ANONYMOUS, 1961. Monthly mean aerological cross sections, pole to pole along meridian 75° for the IGY period *U.S. Weather Bur., Publ.*

ANONYMOUS, 1962. *U.S. Standard Atmosphere 1962.* NASA, U.S. Air Force- -U.S. Weather Bur., Washington, D.C., 278 pp.

ARAKAWA, H., 1951. Possible heavy turbulent exchange between the extratropical tropospheric air and the polar stratospheric air. *Tellus*, 3 (3): 208–211.

ARAKAWA, H., 1959. The world's strongest winds as revealed by Tateno-relay-method soundings. *Bull. Am. Meteorol. Soc.*, 40 (7): 343–347.

ARAKAWA, H., 1963. Typhoon climatology as revealed by data of the Japanese Weather Service. *Proc. Inter-Regional Seminar Trop. Cyclones, Tokyo, 1962*, pp.31–36.

ATTMANNSPACHER, W., 1961. Nullschicht und Tropopause. *Geofis. Pura Appl.*, 48: 151–166.

BAER, F., 1962. Current status of numerical analysis. In: *Colo. State Univ., Atmospheric Sci. Tech. Papers*, 37: 15–21.

BANNON, J. K., 1952. Weather systems associated with some occasions of severe turbulence at high altitude. *Meteorol. Mag.*, 81: 97–101.

BARRIENTOS, C. S., 1964. Computations of transverse circulation in a steady state, symmetric hurricane. *J. Appl. Meteorol.*, 3 (6): 685–692.

BERGTHORSSON, P. and DÖÖS, B. R., 1955. Numerical weather map analysis. *Tellus*, 7 (3): 329–340.
BERKOFSKY, L., 1960. Prediction of hurricane formation. *Proc. Intern. Symp. Numerical Weather Prediction, Tokyo*, pp.375–386.
BERSON, F. A., 1961. Circulation and energy balance in a tropical monsoon. *Tellus*, 8 (4): 472–485.
BERSON, F. A. and TROUP, A. J., 1961. On the angular momentum balance in the equatorial trough zone of the Eastern Hemisphere. *Tellus*, 13 (1): 66–78.
BILLWILLER, R. and DE QUERVAIN, A., 1912. Registrierballonaufstiege in einem Föhntale. *Meteorol. Z.* 29 (5): 249–251.
BJERKNES, V. and SOLBERG, H., 1921. Meteorological conditions for the formation of rain. *Geofys. Publikasjoner, Norske Videnskapsakad. Oslo*, 2: 60 pp.
BLACKADAR, A. K., 1957. Boundary layer wind maxima and their significance for the growth of nocturnal inversions. *Bull. Am. Meteorol. Soc.*, 38: 283–290.
BOLIN, B., 1950. On the influence of the earth's orography on the general character of the westerlies. *Tellus*, 2 (3): 184–195.
BOND, H. G., 1953. Easterly jet streams over Darwin. *Weather*, 8 (8): 252–253.
BONNER, W. D., 1963. Thunderstorms and the low-level jet. *Univ. Chicago, Mesometeorol. Proj. Res. Papers*, 22: 20–33.
BONNER, W. D., 1965. Statistical and kinematical properties of the low-level jet stream. *Univ. Chicago, Satellite Mesometeorol. Res. Proj. Res. Papers*, 38: 1–54.
BOSSOLASCO, M., 1953. L'irruzione del monsone di SW in Somalia. *Geofis. Meteorol. (Genoa)*, 1(6): 97–99.
BREILAND, J. G., 1958. Meteorological conditions associated with the development of instability lines. *J. Meteorol.*, 15 (3): 297–302.
BRIGGS, J. and ROACH, W. T., 1963. Aircraft observations near jet-streams. *Quart. J. Roy. Meteorol. Soc.*, 89 (380): 225–247; 90 (386): 483–485.
BROWN, J. A., 1964. A diagnostic study of tropospheric diabatic heating and the generation of available potential energy. *Tellus*, 16 (3): 371–388.
BRUNDIDGE, K. C. and GOLDMAN, J. L., 1962. Model cross sections across the jet stream. *J. Appl. Meteorol.*, 1 (3): 303–317.
BURNS, A. and RIDER, C. K., 1965. Project TOPCAT power spectral measurements of clear air turbulence associated with jet streams. *Roy. Aircraft Estab., Tech. Rept.*, 65210: 11 pp.
CASKEY Jr. J. E., 1961. Further comments on distribution of surface friction in hurricanes. *J. Meteorol.*, 18 (3): 426–427.
CHAKRAVORTTY, K. C. and BASU, S. C., 1957. The influence of western disturbances on the weather over northeast India in monsoon months. *Indian J. Meteorol. Geophys.*, 8 (3): 261–272.
CHAPMAN, S., 1950. Upper atmospheric nomenclature. *Bull. Am. Meteorol. Soc.*, 31 (8): 288–290. Also *J. Geophys. Res.*, 55 (4): 395–399.
CHARNEY, J. G., 1947. The dynamics of long waves in a baroclinic westerly current. *J. Meteorol.*, 4 (5): 135–162.
CHARNEY, J. G., 1948. On the scale of atmospheric motions. *Geofys. Publikasjoner, Norske Videnskapsakad. Oslo*, 17 (2): 1–17.
CHARNEY, J. G. and ELIASSEN, A., 1964. On the growth of the hurricane depression. *J. Atmosph. Sci.*, 21 (1): 68–75.
CHAUDHURY, A. M., 1950. On the vertical distribution of wind and temperature over Indo-Pakistan along the meridian 76°E in winter. *Tellus*, 2 (1): 56–62.
CLARKE, R. H., 1961. Mesostructure of dry cold fronts over featureless terrain. *J. Meteorol.*, 18 (6): 715–735.
CLEM, L. H., 1955. Clear-air turbulence near the jet-stream maxima. *Bull. Am. Meteorol. Soc.*, 36 (2): 53–60.
CLODMAN, J., MORGAN, G. M. and BALL, J. T., 1960. High level turbulence. *N.Y. Univ., Res. Div., Final Rept., Contract No. AF 19(604)-5208*, 84 pp.
COLSON, D., 1963. Summary of high-level turbulence over United States, 1961–1962. *U.S. Weather Bur. Manuscript.* (Presented at Am. Meteorol. Soc. Meeting, New York, N.Y., January 21–24, 1963.)
CRESSMAN, G. P., 1959. An operational objective analysis system. *Monthly Weather Rev.*, 87 (10): 367–374.
CRUTCHER, H. L., 1961. Meridional cross-sections, upper winds over the northern hemisphere. *U.S. Weather Bur. Tech. Paper*, 41, 307 pp.
DAHLER, H., 1957. Zur Entstehung des Jet Stream und einige Folgerungen. *Meteorol. Rundschau*, 10 (3): 93–101.
DAHLER, H., 1960. Die Bedeutung der Temperaturadvektion für die Bildung und Verlagerung von Strahlström und Tropopause. *Z. Meteorol.*, 13 (9/10): 205–211.
DANARD, M. B., 1964. On the influence of released latent heat on cyclone development. *J. Appl. Meteorol.*, 3 (1): 27–37.
DANIELSEN, E. F., 1959. The laminar structure of the atmosphere and its relation to the concept of a tropopause. *Arch. Meteorol., Geophys., Bioklimatol., Ser. A.*, 11 (3): 293–332.

DANIELSEN, E. F., 1961. Trajectories: isobaric, isentropic and actual. *J. Meteorol.*, 18 (4): 479–486.

DANIELSEN, E. F., 1964a. Project Springfield report. *Defense Atomic Support Agency*, DASA 1517: 97 pp.

DANIELSEN, E. F., 1964b. Radioactivity transport from stratosphere to troposphere. *Mineral Ind. Penn. State Univ.*, 33 (6): 1–7.

DAO, SH.-Y. and CHEN, L.-SH. 1957. The structure of general circulation over continent of Asia in summer. *J. Meteorol. Soc. Japan, Anniv. Vol.*,: 215–229.

DAS, P. K.. 1962. Mean vertical motion and non-adiabatic heat sources over India during the monsoon. *Tellus*, 14 (2): 212–220.

DAVIS, N. E., 1951. The mean position of the jet stream. *Gt. Brit., Meteorol. Res. Comm., Meteorol. Res. Papers*, 615: 2 pp.

DEFANT, F., 1951. Local winds. In: *Compendium of Meteorology*. Am. Meteorol. Soc., Boston, Mass., pp. 655–672.

DEFANT, F., 1958. Die allgemeine atmosphärische Zirkulation in neuerer Betrachtungsweise. *Geophysica (Helsinki)*, 6 (3–4): 189–217.

DEFANT, F. and TABA, H., 1958a. The details of wind and temperature field and the generation of the blocking situation over Europe (Jan. 1–4, 1956). *Beitr. Physik Atmosphäre*, 31 (1–2): 69–88.

DEFANT, F. and TABA, H., 1958b. The strong index change period from Jan. 1 to Jan. 7, 1956. *Tellus*, 10 (2): 225–242.

DEFANT, F. and TABA, H., 1958c. The breakdown of zonal circulation during the period January 8 to 13, 1956, the characteristics of temperature field and tropopause and its relations to the atmospheric field of motion. *Tellus*, 10 (4): 430–450.

DEFANT, F. and VAN DE BOOGAARD, H. M. E., 1963. The global circulation features of the troposphere between the equator and 40°N, based on a single day's data. *Tellus*, 15 (3): 251–260.

DINES, W. H., 1912. Total and partial correlation coefficients between sundry variables of the upper air. *Gt. Brit., Meteorol. Office, Geophys. Mem.*, 2.

DINES, W. H., 1919. The characteristics of the free atmosphere. *Gt. Brit., Meteorol. Office, Geophys. Mem.*, 13: 47–76.

DINES, W. H., 1925. The correlation between pressure and temperature in the upper air with a suggested explanation. *Quart. J. Roy. Meteorol. Soc.*, 51: 31–38.

DÖÖS, B. R., 1956. Automation of 500 mbar forecasts through successive numerical map analysis. *Tellus*, 8 (1): 76–81.

DÖÖS, B. R., 1961. A mountain wave theory including the effect of the vertical variation of wind and stability. *Tellus*, 13 (3): 305–319.

DÖÖS, B. R., 1962. A theoretical analysis of lee-wave clouds observed by "Tiros I". *Tellus*, 14 (3): 301–309.

DÖÖS, B. R. and EATON, M. A., 1957. Upper air analysis over ocean areas. *Tellus*, 9 (2): 184–194.

DUNN, G. E., 1951. Tropical cyclones. In: *Compendium of Meteorology*. Am. Meteorol. Soc., Boston, Mass., pp.887–901.

DUNN, G. E. and MILLER, B. I. 1960. *Atlantic Hurricanes*. Louisiana State Univ. Press, Baton Rouge, La., 377 pp.

DZERDZEEVSKII, B. L., 1960. Certain features of weather in the coastal area of eastern Antarctica. In: *Antarctic Meteorology*. Pergamon, Oxford, pp.37–51.

EBDON, R. A., 1960. Notes on the wind flow at 50 mbar in tropical and subtropical regions in January 1957 and January 1958. *Quart. J. Roy. Meteorol. Soc.*, 86 (370): 540–542.

EDDY, A., 1963. A statistical model for the mid-latitude tropopause and jet-stream layer. *J. Appl. Meteorol.*, 2 (2): 219–225.

ELIASSEN, A., 1962. On the vertical circulation in frontal zones. *Geofys. Publikasjoner, Norske Videnskapsakad, Oslo*, 24 (4): 147–160.

ELIASSEN, A. and KLEINSCHMIDT, E., 1957. Dynamic meteorology. In: S. FLÜGGE (Editor), *Encyclopedia of Physics. 48. Geophysics II.* pp.1–154.

ENDLICH, R. M., 1963. The detailed structure of the atmosphere in regions of clear-air turbulence. *Stanford Res. Inst., Final Rept., Contract Cwb-10324*, 62 pp.

ENDLICH, R. M., 1964. The mesoscale structure of some regions of clear-air turbulence. *J. Appl. Meteorol.*, 3 (3): 261–276.

ENDLICH, R. M. and MANCUSO, R. L., 1964. Clear-air turbulence and its analysis by use of rawinsonde data. *Stanford Res. Inst., Final Rept., Contract Cwb-10624*: 1–55.

ENDLICH, R. M. and MCLEAN, G. S., 1957. The structure of the jet-stream core. *J. Meteorol.*, 14: 543–552.

ENDLICH, R. M. and MCLEAN, G. S., 1964. Studies of the climatology of winds, temperature, and turbulence in the jet stream. *Air Force Cambridge Res. Lab.*, AFCRL-64-834: 62 pp.

ERTEL, H., 1942. Ein neuer hydrodynamischer Wirbelsatz. *Meteorol. Zeitschrift*, 59 (9): 277–281.

FAUST, H., 1959. Nullschichteffekt und allgemeine Zirkulation. *Geofis. Pura Appl.*, 44: 257–264.

FAUST, H., 1962. The dynamical significance of null layers. *Weather*, 17 (9): 285–295.
FAY, R., 1958. A note on the mid-tropospheric wind maximum. *Bull. Am. Meteorol. Soc.*, 39 (7): 360–362.
FLOHN, H., 1950. Tropische und aussertropische Monsunzirkulation. *Ber. Deut. Wetterdienstes U.S. Zone*, 18: 34–50.
FLOHN, H., 1957a. Studien zur Dynamik der äquatorialen Atmosphäre, I. *Beitr. Phys. Atmosphäre*, 30: 18–46.
FLOHN, H., 1957b. Large-scale aspects of the "summer-monsoon" in South and East Asia. *J. Meteorol. Soc. Japan, Anniv. Vol.*: 180–186.
FLOHN, H., 1958. Recent investigations on the mechanism of the "Summer Monsoon" of southern and eastern Asia. In: *Monsoons of the World*, pp.75–88.
FLOHN, H., 1963. The tropical easterly jet and other regional anomalies of the tropical circulation. *W.M.O. Symp. Tropical Meteorol., Rotura, New Zealand, 1963.*
FLOHN, H., 1964. Investigations on the tropical easterly jet. *Bonner Meteorol. Abhandl.*, 4: 83 pp.
FLOHN, H., HOLZAPFEL, R. and OECKEL, H., 1959. Untersuchungen über die stratosphärische Ostströmung über der Sommerhalbkugel. *Beitr. Physik Atmosphäre*, 31: 217–243.
FREY, K., 1945. *Beiträge zur Entwicklung des Föhns und Untersuchungen über Hochnebel.* Inaugural Dissertation, Univ. Basel.
FRITZ, S., 1964. Pictures from meteorological satellites and their interpretation. *Space Sci. Rev.*, 3: 541–580.
FUJITA, T. and ARNOLD, J., 1963. The decaying stage of Hurricane "Anna" of July 1961 as portrayed by "Tiros" cloud photographs and infrared radiation from the top of the storm. *Univ. Chicago, Satellite Mesometeorol. Res. Proj., Res. Papers*, 28: 13 pp.
FULTZ, D., 1951. Non-dimensional equations and modeling criteria for the atmosphere. *J. Meteorol.*, 8 (4): 262–267.
FULTZ, D., 1960. Experimental models of rotating fluids and possible avenues for further research. In: R. L. PFEFFER (Editor), *Dynamics of Climate.* Pergamon, Oxford, pp.71–77.
GALLOWAY, J. L., 1958. Three-front model: its philosophy, nature, construction and use. *Weather*, 13 (1): 3–10.
GALLOWAY, J. L., 1963. The three-front model and the thunderstorm. *Weather*, 13 (2): 42–54.
GENTRY, R. C., 1963. Variation of wind and temperature in hurricane rain bands. *Natl. Hurricane Res. Proj., Rept.*, 8 pp.
GENTRY, R. C., 1964. Current hurricane research. *Weatherwise*, 17 (4): 180–185, 189.
GERHARDT, J. R., 1962. An example of nocturnal low-level jet stream. *J. Atmospheric Sci.*, 19 (1): 116–118.
GERHARDT, J. R., 1963. Mesoscale association of a low-level jet stream with a squall-line—cold-front situation. *J. Appl. Meteorol.*, 2 (1): 49–55.
GIBSON, T. T., 1964. Synoptic techniques in the Canadian Meteorol. Service. *Australian Meteorol. Mag.*, 45: 34–41.
GODSKE, C. L., BERGERON, T., BJERKNES, J. and BUNDGAARD, R. C., 1957. *Dynamic Meteorology and Weather Forecasting.* Am. Meteorol. Soc., Boston, Mass./Carnegie Inst., Washington, D.C., 800 pp.
GODSON, W. L. and LEE, R., 1958. High level fields of wind and temperature over the Canadian Arctic. *Beitr. Physik Atmosphäre*, 31 (1–2): 40–68.
GRAY, W. M., 1962. On the balance of forces and radial accelerations in hurricanes. *Quart. J. Roy. Meteorol. Soc.*, 88 (378): 430–458.
HANN, J. V. and SÜRING, R., 1943. *Lehrbuch der Meteorologie*, 5. Aufl. Keller, Leipzig. 1092 pp.
HINES, C. O., 1960. Internal atmospheric gravity waves at ionospheric heights. *Can. J. Physics*, 38: 1441–1468.
HOECKER, Jr., W. H., 1963. Three southerly low-level jet systems delineated by the Weather Bureau special pibal network of 1961. *Monthly Weather Rev.*, 91 (11–12): 573–582.
HÖFLICH, O., 1961. Convection fronts and development of pressure pattern in the jet stream. *Hamburger Geophysik. Einzelschr.*, 4: 91–186.
HOINKES, H., 1950. Föhnentwicklung durch Höhentiefdruckgebiete. *Arch. Meteorol., Geophys, Bioklimatol., Ser. A.*, 2 (1): 82–96.
HOLLMANN, G., 1952. Über Verlagerung und Wetterwirksamkeit von Kaltlufttropfen. *Z. Meteorol.*, 6 (1): 8–15.
HOLLMANN, G., 1959. Ueber die Nullschichteigenschaft von Flächen extremer Windstärke. *Meteorol. Rundschau*, 12 (6): 170–173.
HSIEH, Y. P., 1949. An investigation of a selected cold vortex over North America. *J. Meteorol.*, 6 (6): 401–410.
HUGHES, L. A., 1952. On the low-level wind structure of tropical storms. *J. Meteorol.*, 9 (6): 422–428.
ISELIN, C. O'D., 1936. A study of the circulation of the western North Atlantic. *Papers Phys. Ocean. and Meteorol.*, 4 (4): 101 pp.
IZUMI, Y., 1962. The low-level jet. Proceedings of the national symposium on winds for aerospace vehicle design. *Air Force Cambridge Res. Lab.*, AFCRL-62-273 (I) (1): 71–79.
IZUMI, Y., 1964. The evolution of temperature and velocity profiles during breakdown of a nocturnal inversion and a low-level jet. *J. Appl. Meteorol.*, 3 (1): 70–82.

IZUMI, Y. and BARAD, M. L., 1963. Wind and temperature variations during development of a low-level jet. *J. Appl. Meteorol.*, 2 (5): 668–673.

JENKINSON, A. F., 1955. Average vector wind distribution of the upper air in temperate and tropical latitudes. *Meteorol. Mag.*, 84: 140–147.

JOHANNESSEN, K. R., 1956. Some theoretical aspects of constant pressure trajectories. *U.S. Air Weather Serv. Manual*, 105–47: 86 pp.

JORDAN, C. L., 1957. Mean soundings for the hurricane eye. *Natl. Hurricane Res. Proj. Rept.*, 13: 10 pp.

JORDAN, C. L., 1958. The thermal structure of the core of tropical cyclones. *Geofysica*, 6 (3–4): 281–297.

JORDAN, C. L., 1961. Marked changes in the characteristics of the eye of intense typhoons between the deepening and filling stages. *J. Meteorol.*, 18 (6): 779–789.

JORDAN, C. L., 1963. Tracking of tropical cyclones. *U.S. Navy Weather Res. Facility*, NWRF 12-0763-075: 39 pp.

JORDAN, C. L. and TE-CHUNG HO, 1962. Variations in the annual frequency of tropical cyclones 1886–1958. *Monthly Weather Rev.*, 90: 157–164.

JORDAN, E. S., 1952. An observational study of the upper wind-circulation around tropical storms. *J. Meteorol.*, 9 (5): 340–346.

JORGENSEN, D. L., 1963. A computer derived synoptic climatology of precipitation from winter storms. *J. Appl. Meteorol.*, 2 (2): 226–234.

KADLEC, P. W., 1963. An in-flight study of the relation between jet streams, cirrus, and wind shear turbulence. *U.S. Weather Bur., Final Rept., Co tract No. Cwb-10356*, 48 pp.

KADLEC, P. W., 1964. A study of flight conditions associated with jet stream cirrus, atmospheric temperature change, and wind shear turbulence. *U.S. Weather Bur., Final Rept., Contract No. Cwb-10674*: 1–45.

KAMIKO, T., 1964a. Detailed structure of two subtropical frontal zones. *Australian Meteorol. Mag.*, 46: 54–75.

KAMIKO, T., 1964b. A developing subtropical depression and its frontal structure. *Australian Meteorol. Mag.*, 47: 1–14.

KANITSCHEIDER, R., 1932–1939. Beiträge zur Mechanik des Föhns. *Beitr. Physik Freien Atmosphäre*, 18: 27–49 (1932); 24: 26–44 (1938); 25: 49–58 (1939).

KAO, S. K., 1964. Turbulence criteria for a circumpolar vortex in a rotating gravity field. *Phys. Fluids*, 7 (5): 629–632.

KAO, S. K. and HURLEY, W. P., 1962. Variations of the kinetic energy of large-scale eddy currents in relation to the jet stream. *J. Geophys. Res.*, 67 (11): 4233–4242.

KAO, S. K. and WURTELE, M. G., 1959. The motion of a parcel in a constant geostrophic wind field of parabolic profile. *J. Geophys. Res.*, 64 (7): 765–777.

KASAHARA, A., 1960. The development of forced convection caused by the released latent heat of condensation in a hydrostatic atmosphere. *Proc. Intern. Symp. Numerical Weather Prediction, Tokyo*, pp.387–403.

KASAHARA, A., 1961. A numerical experiment on the development of a tropical cyclone. *J. Meteorol.*, 18 (3): 259–282.

KASAHARA, A., ISAACSON, E. and STOKER, J. J., 1964. Numerical studies of frontal motion in the atmosphere-I. *Courant Inst. Math. Sci., New York, Rept. Contract No.AT(30–1)-1480 and NONR.-285(55)*: 1–43.

KOCHANSKY, A., 1955. Cross section of the mean zonal flow and temperature along 80°W. *J. Meteorol.*, 12 (2): 95–106.

KOTESWARAM, P., 1958. The easterly jet-stream in the tropics. *Tellus*, 10 (1): 43–57.

KOTESWARAM, P. and BHASKARA RAO, N. S., 1961a. The structure of the Asian summer monsoon. *Proc. Symp. Monsoon Meteorol., Pacific Sci. Congr., 10th, Honolulu, 1961*: 35–56.

KOTESWARAM, P. and BHASKARA RAO, N. S., 1961b. Formation and structure of Indian summer monsoon depressions. *Proc. Symp. Monsoon Meteorol., Pacific Sci. Congr., 10th, Honolulu, 1961—Australian Meteorol. Mag.*, 41: 62–75.

KOTESWARAM, P. and GEORGE, C. A., 1957. The formation and structure of tropical cyclones in the Indian Sea area. *J. Meteorol. Soc. Japan, Anniv. Vol.*: 309–322.

KREITZBERG, C. W., 1964. The structure of occlusions as determined from serial ascents and vertically directed radar. *Air Force Cambridge Res. Lab., Res. Rept.*, AFCRL-64–26: 121 pp.

KRISHNAMURTI, T. N., 1961a. The subtropical jet-stream of winter. *J. Meteorol.*, 18: 172–191.

KRISHNAMURTI, T. N., 1961b. On the role of the subtropical jet-stream of winter in the atmospheric general circulation. *J. Meteorol.*, 18: 657–670.

KRISHNAMURTI, T. N., 1961c. On the vertical velocity field in a steady symmetric hurricane. *Tellus*, 13 (2): 171–180.

KRISHNAMURTI, T. N., 1962. Some numerical calculations of the vertical velocity field in hurricanes. *Tellus*, 14 (2): 195–211.

KRISHNAMURTI, T. N., 1964. Theory of two-dimensional mountain waves. *Rev. Geophys.*, 2 (4): 593–624.
KUETTNER, J. P. and MCLEAN, G. S., 1961. Instability and vertical motions in the jet stream. *Air Force Cambridge Res. Lab., G.R.D. Res. Notes*, 57: 15 pp.
KUO, H. L., 1957. Dynamics of convective vortices and eye formation. *Mass. Inst. Technol., Studies Atmospheric Gen. Circulation*, 2: 243–272.
LANDERS, H., 1955. A three-dimensional study of the horizontal velocity divergence. *J. Meteorol.*, 12 (5): 415–427.
LANDERS, H., 1956. Vorticity distribution and advection in the lower and middle troposphere. *J. Meteorol.*, 13: 511–520.
LANDERS, H., 1963. On the formation and development of tropical cyclones. *J. Appl. Meteorol.*, 2 (2): 206–218.
LANGFORD, J. C., 1957. Southern ocean analysis with special reference to the period December 1954 to March 1955. *Australian Meteorol. Mag.*, No. 16: 1–22.
LA SEUR, N. E., 1954. On the asymmetry of the middle-latitude circumpolar current. *J. Meteorol.* 11 (1): 43–57.
LA SEUR, N. E., 1957. An analysis of some detailed data obtained by aircraft reconnaissance of a hurricane. *Florida State Univ., Sci. Rept., Contract AF 19(604)-753*, 5: 25 pp.
LA SEUR, N. E. and HAWKINS, H. F., 1963. An analysis of hurricane Cleo (1958) based on data from research reconnaissance aircraft. *Monthly Weather Rev.*, 91 (10–12): 694–709.
LEESE, J. A., 1962. The role of advection in the formation of vortex cloud patterns. *Tellus*, 14 (4): 409–421.
LESTER, P. F., HALL, S. J. and THOMPSON, A. H., 1964. An investigation of the time variations in a subtropical jet-stream and the associated cloud patterns as shown by "Tiros I". *Texas Agr. Mech. Res. Found., Sci. Rept., Contract AF 19(604)-8450*, 7: 70 pp.
LYRA, G., 1940. Ueber den Einfluss von Bodenerhebungen auf die Strömung einer stabil geschichteten Atmosphäre. *Beitr. Physik Freien Atmosphäre*, 26: 197–206.
LYRA, G., 1943. Theorie der stationären Leewellenströmung in freier Atmosphäre. *Z. Angew. Math. Mech.*, 23 (1): 1–28.
MAHLMAN, J., 1964. Relation of stratospheric-tropospheric mass exchange mechanisms to surface radioactivity peaks. *Colo. State Univ., Dept. Atmospheric Sci., Tech. Papers*, 58: 1–19.
MALKUS, J. S., RONNE, C. and CHAFFEE, M., 1961. Cloud patterns in hurricane Daisy, 1958. *Tellus*, 13: 8–30.
MATHER, K. B., 1960. Katabatic winds south of Mawson, Antarctica. In: *Antarctic Meteorology*, Pergamon, Oxford, pp. 317–320.
MCINTYRE, D. P., 1958. The Canadian 3-front, 3-jet stream model. *Geofysica (Helsinki)*, 6 (3–4): 309–323.
MCLEAN, G. S., JR., 1962. The jet stream and associated turbulence. *Air Force Surv. AFCRL-62-273(I)*, 140: 221–233.
MEANS, L. L., 1962. Comments on "The low-level jet as related to nocturnal thunderstorms over midwest U.S.". *J. Appl. Meteorol.*, 1(4): 588–589.
MILES, M. K., 1962. Wind, temperature and humidity distribution at some cold fronts over S.E. England. 1. *Quart. J. Roy. Meteorol. Soc.*, 88 (377): 286–300.
MILES, M. K., 1963. Wind, temperature and humidity distribution at some cold fronts over S. E. England. 2. *Quart. J. Roy. Meteorol. Soc.*, 89 (381): 428–430.
MINTZ, Y., 1955. The mean geostrophic poleward flux of angular momentum and of sensible heat in the winter and summer of 1949. *Univ. Calif., Dept. Meteorol., Sci. Rept.*, 7 Contract AF 19 (122)-48: 12 pp.
MINTZ, Y. and DEAN, G., 1952. The observed mean field of motion of the atmosphere. *U.S. Air Force, Cambridge Res. Center, Geophys. Res. Papers*, 17: 65 pp.
MOHRI, K., 1958–1959. Jet streams and upper fronts in the general circulation and their characteristics over the Far East. *Geophys. Mag.*, 29 (1): 47–126; 29 (3): 333–412.
MONTGOMERY, R. B., 1937. A suggested method for representing gradient flow in isentropic surfaces. *Bull. Am. Meteorol. Soc.*, 18: 6–7.
MURAKAMI, T., 1958. The sudden change of upper westerlies near the Tibetan Plateau at the beginning of the summer season. *J. Meteorol. Soc. Japan*, 36 (6): 239–247.
MURGATROYD, R. J., 1957. Winds and temperatures between 20 and 100 km–a review. *Quart. J. Roy. Meteorol. Soc.*, 83 (358): 417–458.
NAGLE, R. E. and SEREBRENY, S. M., 1962. Radar precipitation echo and satellite cloud observations of a maritime cyclone. *J. Applied Meteorol.*, 1 (3): 279–295.
NAMIAS, J., 1947. *Extended Forecasting by Mean Circulation Methods.* U.S. Weather Bur. (Manuscript).
NAMIAS, J., 1951. The great Pacific anticyclone of winter 1949–1950. A case study in the evolution of climatic anomalies. *J. Meteorol.*, 8: 251–261.
NAMIAS, J., 1952. The jet stream. *Sci. Am.*, 187 (4): 26–31.
NAMIAS, J., 1964. Seasonal persistence and recurrence of European blocking during 1958–1960. *Tellus*, 16 (3): 394–407.

NAMIAS, J. and CLAPP, P., 1949. Confluence theory of the high tropospheric jet stream. *J. Meteorol.*, 6 (5): 330–336.

NEWELL, R. E., 1964. A note on the 26-month oscillation. *J. Atmospheric Sci.*, 21 (3): 320–321.

NEWTON, C. W., 1954. Frontogenesis and frontolysis as a three-dimensional process. *J. Meteorol.*, 11 (6): 449–461.

NEWTON, C. W., 1956. Mechanisms of circulation change during a lee cyclogenesis. *J. Meteorol.*, 13: 528–539.

NEWTON, C. W., 1958. Variations in frontal structure of upper level troughs. *Geophysika (Helsinki)*, 6 (3–4): 357–375.

NEWTON, C. W., 1959a. Axial velocity streaks in the jet stream: ageostrophic "inertial" oscillations. *J. Meteorol.*, 16: 638–645.

NEWTON, C. W., 1959b. Synoptic comparisons of jet stream and Gulf Stream systems. In: B. BOLIN (Editor), *The Atmosphere and Sea in Motion.* Oxford Univ. Press, London, pp.288–304.

NEWTON, C. W., 1964. Properties of partial inertial oscillations in the atmosphere, with particular relevance to waves in the jet-stream region. *Natl. Center Atmospheric Res.* (Unpubl. Manuscript.)

NEWTON, C. W. and PALMÉN, E., 1963. Kinematic and thermal properties of a large-amplitude wave in the westerlies. *Tellus*, 15 (2): 99–119.

NEYAMA, Y., 1963. Note on practical method of seasonal forecasting of Bai-u by aerological data at Marcus Island. *J. Meteorol. Soc. Japan, Ser. 2*, 41 (4): 247–254.

NINOMIYA, K., 1962. Investigation of a summer jet stream using TIROS and aerological data. *Univ. Chicago, Mesometeorol. Proj., Res. Papers*, 14: 26 pp.

NITTA, T., 1964. On the development of the relatively small scale cyclone due to the release of latent heat by condensation. *J Meteorol. Soc. Japan, Ser. 2*, 42 (4): 260–267.

OGURA, Y., Frictionally controlled, thermally driven circulations in a circular vortex with application to tropical cyclones. *J. Atmospheric Sci.*, 21 (6): 610–621.

OLIVER, V. J., ANDERSON, R. K. and FERGUSON, E. W., 1964. Some examples of the detection of jet streams from TIROS photographs. *Monthly Weather Rev.*, 92 (10): 441–448.

PALMÉN, E., 1948. On the formation and structure of tropical hurricanes. *Geophysica (Helsinki)*, 3: 26–38.

PALMÉN, E., 1954. Über die atmosphärischen Strahlströme. *Meteorol. Abhandl. (Berlin)*, 2 (3): 35–50.

PALMÉN, E., 1958. Vertical circulation and release of kinetic energy during the development of Hurricane Hazel into an extratropical storm. *Tellus*, 10 (1): 1–23.

PALMÉN, E. and ALAKA, M. A., 1952. On the budget of angular momentum in the zone between equator and 30°N. *Tellus*, 4 (4): 324–331.

PALMÉN, E. and RIEHL, H., 1957. Budget of angular momentum and energy in tropical cyclones. *J. Meteorol.*, 14 (2): 150–159.

PANOFSKY, H. and MCLEAN, J. C., JR., 1964. Physical mechanisms of clear-air turbulence. *Penn. State Univ., Dept. Meteorol., Rept.* 2: 22 pp.

PASQUILL, F., 1962. *Atmospheric Diffusion.* Van Nostrand, London, 297 pp.

PERLROTH, I., 1962. Relationship of central pressure of hurricane Ester (1961) and the sea surface temperature field. *Tellus*, 14 (4): 403–408.

PETTERSSEN, S., 1950. Some aspects of the general circulation of the atmosphere. *Centenary Proc. Roy. Meteorol. Soc., 1950*, pp.120–155.

PETTERSSEN, S., 1952. On the propagation and growth of jet-stream waves. *Quart. J. Roy. Meteorol. Soc.*, 78 (337): 337–353.

PETTERSSEN, S., 1956. *Weather Analysis and Forecasting*, 2nd ed. McGraw-Hill, New York, N.Y., 1: 446 pp.; 2: 266 pp.

PETTERSSEN, S. and CALABRESE, P. A., 1959. On some weather influences due to warming of the air by the Great Lakes in winter. *J. Meteorol.*, 16: 646–652.

PETTERSSEN, S. and SWINBANK, W. C., 1947. On the application of the Richardson criterion to large-scale turbulence in the free atmosphere. *Quart. J. Roy. Meteorol. Soc.*, 73: 335–345.

PETTERSSEN, S., BRADBURY, D. L. and PEDERSEN, K., 1962. The Norwegian cyclone models in relation to heat and cold sources. *Geofys. Publikasjoner, Norske Videnskapsakad, Oslo*, 24: 243–280.

PHILLPOT, H. R., 1962. Mean westerly jet streams in the Southern Hemisphere. In: *Antarctic Research—Geophys. Monograph*, 7: 128–138.

PISHAROTY, P. R., 1955. General Circulation Project. *Univ. Calif., Dept. Meteorol., Final Rept.*, 14: 6 pp.

PITCHFORD, K. L. and LONDON, J., 1962. The low-level jet as related to nocturnal thunderstorms over Midwest United States. *J. Appl. Meteorol.*, 1 (1): 43–47.

POGOSIAN, K. P., 1960. *Struinye Techeniia v Atmosfere.* (Jet streams in the atmosphere). Gidrometeorol. Izd., Moscow, 178 pp.

PRIESTLEY, C. H. B. and TROUP, A. J., 1964. Strong winds in the global transport of momentum. *J. Atmospheric Sci.*, 21 (4): 459–460.

PYKE, C. B., 1965. On the role of air-sea interaction in the development of cyclones. *Bull. Am. Meteorol. Soc.*, 46 (1): 4–15.

QUENEY, P., 1947. Theory of perturbations in stratified currents with applications to air flow over mountain barriers. *Univ. Chicago, Dept. Meteorol., Misc. Rept.*, 23: 81 pp.

QUENEY, P., 1948. The problem of air flow over mountains: A summary of theoretical results. *Bull. Am. Meteorol. Soc.*, 29 (1): 16–26.

RAETHJEN, P., 1958. Trägheitsellipse und jet-stream. *Geophysika, (Helsinki)*, 6 (3/4): 439–453.

RAETHJEN, P., 1961. Zur Dynamik des jet-stream. Disturbance of balance in the nonsteady jet stream. *Hamburger Geophysik. Einzelschr.*, 4: 1–90.

RAMAGE, C. S., 1952. Relationship of general circulation and normal weather over Southern Asia and the Western Pacific during the cool season. *J. Meteorol.*, 9 (6): 403–408.

RAMASWAMY, C., 1956. On the subtropical jet stream and its role in the development of large-scale convection. *Tellus*, 8 (1): 26–60.

RAMASWAMY, C., 1962. Breaks in the Indian summer monsoon as a phenomenon of interaction between the easterly and the subtropical westerly jet streams. *Tellus*, 14 (3): 337–349.

RAMDAS, L. A., JAGANNATHAN, P. and GOPAL RAO, S., 1954. Prediction of the date of establishment of southwest monsoon along the west coast of India. *Indian J. Meteorol. Geophys.*, 5 (4): 305–314.

RANGARAJAN, S., 1961. Thermal effects of the Tibetan Plateau during the Asian monsoon season. *Proc. Symp. Monsoon Meteorol., Pacific Sci. Congr., 10th, Honolulu, 1961*, pp.24–34.

REED, R. J. and DANIELSEN, E. F., 1959. Fronts in the vicinity of the tropopause. *Arch. Meteorol. Geophys. Bioklim., Ser.A.*, 11: 1–17.

REED, R. J. and ROGERS, D. G., 1962. The circulation of the tropical stratosphere in the years 1954–1960. *J. Atmospheric Sci.*, 19 (2): 127–135.

REED, R. J. and SANDERS, F., 1953. An investigation of the development of a mid-tropospheric frontal zone and its associated vorticity field. *J. Meteorol.*, 10 (5): 338–349.

REED, R. J., CAMPBELL, W. T., RASMUSSEN, L. A. and ROGERS, D. G., 1961. Evidence of a downward propagating annual wind reversal in the equatorial stratosphere. *J. Geophys. Res.*, 66 (3): 813–818.

REITER, E. R., 1958a. The layer of maximum wind. *J. Meteorol.*, 15 (1): 27–43.

REITER, E. R., 1958b. Klima von Innsbruck 1931–1955. (Anhang 1956 and 1957). *Statist. Amt Landeshauptstadt Innsbruck, Sonderveröffentl.*, 2: 68 pp.

REITER, E. R., 1959. Das Ende des indischen Sommermonsuns 1954 mit Daten der österreichischen Cho-Oyu-Expedition. *Ber. Deut. Wetterdienstes*, 54: 293–297.

REITER, E. R., 1960. Turbulenz im wolkenfreien Raum (Clear Air Turbulence). *Ber. Deut. Wetterdienstes*, 61: 42 pp.

REITER, E. R., 1961a. *Meteorologie der Strahlströme* (Jet-Streams). Springer, Wien, 473 pp.

REITER, E. R., 1961b. Project Jet Stream research flight No. 30, April 1957. *Quart. J. Roy. Meteorol. Soc.*, 87 (373): 332–345.

REITER, E. R., 1961c. The detailed structure of the wind field near the jet stream. *J. Meteorol.*, 18 (1): 9–30.

REITER, E. R., 1961d. Die nordamerikanische Strahlstromwetterlage vom 23. bis 27. Januar 1957 an Hand von Forschungsflügen des Project Jet Stream. *Beitr. Physik Atmosphäre*, 33 (3–4): 244–279.

REITER, E. R., 1962. Die vertikale Struktur des Strahlstromkernes aus Forschungsflügen des Project Jet Stream. *Ber. Deut. Wetterdienstes*, 80: 30 + 69 pp.

REITER, E. R., 1963a. *Jet-Stream Meteorology*. Univ. Chicago Press, Chicago, Ill., 515 pp.

REITER, E. R., 1963b. A case study of radioactive fallout. *J. Appl. Meteorol.*, 2 (6): 691–705.

REITER, E. R., 1963c. Note on the eddy kinetic energy distribution in relation to the jet stream. *J. Geophys. Res.*, 68 (6): 1785–1787.

REITER, E. R., 1963d. Exploratory study on the physical nature of certain mesostructural details in vertical wind profiles. *Colo. State Univ. Dept. Atmospheric Sci. Tech. Papers*, 47: 17 pp.

REITER, E. R., 1963e. A case study of severe clear air turbulence. *Arch. Meteorol. Geophys. Bioklimatol., Ser. A*, 13 (3–4): 379–389.

REITER, E. R., 1963f. Nature and observation of high-level turbulence, especially in clear air. *U.S. Navy Weather Res. Facility, Rept.*, NWRF-15-1262-071: 28 pp.

REITER, E. R., 1964a. Comments on paper by S. Penn and E. A. Martell, "An analysis of the radioactive fallout over North America in late September 1961". *J. Geophys. Res.*, 69 (4): 786–788.

REITER, E. R., 1964b. Jet streams and turbulence. *Australian Meteorol. Mag.*, 45: 13–31.

REITER, E. R., 1964c. CAT and SCAT. *Astronautics Aeron.*, 2 (5): 60–65.

REITER, E. R., 1964d. Clear air turbulence models and forecasting for Project TOPCAT, Second Phase, September 1–30, 1963. *Proj. TOPCAT Meteorol. Repts., Univ. Melbourne*, 3: 1–26.

REITER, E. R. and HEUBERGER, H., 1960. Jet-stream and retreat of the Indian summer monsoon and their effect upon the Austrian Cho-Oyu Expedition 1954. *Geografiska Ann.*, 42 (1): 17–35.

REITER, E. R. and MAHLMAN, J. D., 1964. Heavy radioactive fallout over the southern United States, November 1962. *Colo. State Univ., Dept. Atmospheric Sci., Tech. Papers*, 58: 21–49.

REITER, E. R. and NANIA, A., 1964. Jet-stream structure and clear-air turbulence (CAT). *J. Appl. Meteorol.*, 3 (3): 247–260.

REITER, E. R. and WHITE, P., 1964. Experiments in objective upperwind analysis and forecasting. *Colo. State Univ., Dept. Atmospheric Sci., Tech. Papers*, 50: 148 pp.

REITER, E. R., DURAN, B., GARST, G. S. and WHITE, P., 1962. Wind forecasting techniques for input into an Automatic Air Traffic Control (ATC) System. *Colo. State Univ., Dept. Atmospheric Sci., Tech. Papers*, 37: 36 pp.

REITER, E. R., LANG, H., MÖOK, R. and WENDLER, G., 1961. Analyse dreier Forschungsfluege des Project Jet Stream. *Arch. Meteorol., Geophys. Bioklimatol., Ser. A.*, 12: 183–224.

REX, D. F., 1950a. Blocking action in the middle troposphere and its effects upon regional climate, I. Aerological study of blocking action. *Tellus*, 2 (3): 196–211.

REX, D. F., 1950b. Blocking action in the middle troposphere and its effect upon regional climate, II. Climatology of blocking action. *Tellus*, 2 (4): 275–301.

REX, D. F., 1951. The effect of Atlantic blocking action upon European climate. *Tellus*, 3 (2): 100–111.

RICHARDSON, L. F., 1922. *Weather Prediction by Numerical Processes.* Cambridge Univ. Press, N.Y., 236 pp.

RIEHL, H., 1951. Aerology of tropical storms. In: *Compendium of Meteorology*. Am. Meteorol. Soc., Boston, pp.902–913.

RIEHL, H., 1954. *Tropical Meteorology*. McGraw-Hill, New York, N.Y., 392 pp.

RIEHL, 1961. Quantitative representation of the velocity distribution along the vertical. *Borg-Warner Controls, Contract BRD-139, Tasks 1–8, Final Rept., Appendices*, pp. 89–120.

RIEHL, H., 1962. Jet Streams of the atmosphere. *Colo. State Univ., Dept. Atmospheric Sci., Tech. Rept.*, 32: 117 pp.

RIEHL, H., 1963. Stationary aspects of the tropical general circulation. *Geofis. Intern.*, 3 (3): 53–68.

RIEHL, H. and FULTZ, D., 1957. Jet-stream and long waves in a steady rotating-dishpan experiment: Structure of the circulation. *Quart. J. Roy. Meteorol. Soc.*, 83 (356): 215–231.

RIEHL, H. and FULTZ, D., 1958. The general circulation in a steady rotating-dishpan experiment. *Quart. J. Roy. Meteorol. Soc.*, 84: 389–417.

RIEHL, H. and GRAY, W., 1962. On the latent heat release in a cyclone crossing the Rocky Mountains. *Colo. State Univ., Dept. Atmospheric Sci., Tech. Papers*, 35: 28 pp.

RIEHL, H. and MALKUS, J., 1961. Some aspects of Hurricane Daisy, 1958. *Tellus*, 13 (2): 181–213.

RIEHL, H., BERRY, F. A. and MAYNARD, H., 1955. Exploration of the jet-stream by aircraft during the 1952–1953 winter. *J. Meteorol.*, 12 (1): 26–35.

RODEWALD, M., 1936. Bemerkungen zu: Karl Wien, Die Wetterverhältnisse am Nanga Parbat während der Katastrophe auf der deutschen Himalaja-Expedition 1934. *Meteorol. Z.*, 53: 182–186.

ROSSBY, C. G., 1926. On the solution of problems of atmospheric motion by means of model experiments. *Monthly Weather Rev.*, 54 (6): 237–240.

ROSSBY, C. G., 1940. Planetary flow patterns in the atmosphere. *Quart. J. Roy. Meteorol. Soc.*, 66, Supplement: 68–87.

ROSSBY, C. G., 1945. Kinematic and hydrostatic properties of certain long waves in the westerlies. *Univ. Chicago, Dept. Meteorol., Misc. Rept.*, 5: 37 pp.

ROSSBY, C. G., 1947. On the distribution of angular velocity in gaseous envelopes under the influence of large-scale horizontal mixing processes. *Bull. Am. Meteorol. Soc.*, 28 (2): 53–68.

ROSSBY, C. G., 1948. On displacement and intensity changes of atmospheric vortices. *J. Marine Res.*, 7: 175–187.

RUDLOFF, W., 1950. Zur jährlichen Schwankung der Erddrehung. *Ann. Meteorol.*, 3 (11–12): 376–378.

SADLER, J. C., 1964. Tropical cyclones of the eastern North Pacific as revealed by TIROS observations. *J. Appl. Meteorol.*, 3 (4): 347–366.

SALTZMAN, B., 1961. Note on the role of mountains in the energy budget of the atmosphere. *Tellus*, 13 (2): 291–292.

SALTZMAN, B. and FLEISHER, A., 1960a. Spectrum of kinetic energy transfer due to large-scale horizontal Reynolds stresses. *Tellus*, 12 (1): 110–111.

SALTZMAN, B. and FLEISHER, A., 1960b. The exchange of kinetic energy between larger scales of atmospheric motion. *Tellus*, 12 (4): 374–377.

SALTZMAN, B. and FLEISHER, A., 1961. Further statistics on the modes of release of available potential energy. *J. Geophys. Res.*, 66 (7): 2271–2273.

SALTZMAN, B. and PEIXOTO, J. P., 1957. Harmonic analysis of the mean Northern Hemisphere wind field for the year 1950. *Quart. J. Roy. Meteorol. Soc.*, 83 (357): 360–364.

SALTZMAN, B. and TEWELES, S., 1964. Further statistics on the exchange of kinetic energy between harmonic components of the atmospheric flow. *Tellus*, 16 (4): 432–435.

SALTZMAN, B., GOTTUSO, R. M. and FLEISHER, A., 1961. The meridional eddy transport of kinetic energy at 500 mb. *Tellus*, 13 (2): 293–295.

SAUCIER, W. J., 1958. A summary of wind distribution in the jet streams of the southeast United States investigated by Project Jet Stream. *Texas A. M. Coll., Dept. Oceanog. Meteorol., Final Rept.*, Contract AF 19 (604) 1565: 6–57.

SAWYER, J. S., 1961. Quasi-periodic wind variations with height in the lower stratosphere. *Quart. J. Roy. Meteorol. Soc.*, 87 (371): 24–33.

SAWYER, S., 1962. Gravity waves in the atmosphere as a three-dimensional problem. *Quart. J. Roy. Meteorol. Soc.*, 88 (378): 412–425.

SCHEDLER, A., 1917. Über den Einfluss der Lufttemperatur in verschiedenen Höhen auf die Luftdruckschwankungen am Erdboden. *Beitr. Physik Freien Atmosphäre*, 7: 88–101.

SCHERHAG, R., 1948. *Neue Methoden der Wetteranalyse und Wetterprognose.* Springer, Berlin–Göttingen–Heidelberg, 424 S.

SCHINZE, G. und SIEGEL, R., 1943. Die luftmassenmässige Arbeitsweise. *Reichsamt Wetterdienst (Luftwaffe), Sonderband, Wiss. Abhandl.*, 99 pp.

SCHWERDTFEGER, W. and RADOK, U., 1959. Hodograph analysis as applied to the occurrence of clear-air turbulence. *J. Meteorol.*, 16: 588–592.

SCOGGINS, J. R. and VAUGHAN, W. W., 1963. Problems of atmospheric wind inputs for missile and space vehicle design. *AIAA AMS, Meeting, Fort Collins, Colo., 1963, Papers.*

SCORER, R. S., 1949. Theory of waves in the lee of mountains. *Quart. J. Roy. Meteorol. Soc.*, 75: 41–56.

SEREBRENY, S. M., WIEGMAN, E. J. and HADFIELD, R. G., 1962. Some characteristic features of the jet stream complex during selected synoptic conditions. *J. Appl. Meteorol.*, 1 (2): 137–153.

SHAPIRO, R., 1964. A mid-latitude biennial oscillation in the variance of the surface-pressure distribution. *Air Force Cambridge Res. Lab., AFCRL-64-723—Environ. Res. Papers*, 45: 328–331.

SHAPIRO, R. and WARD, F., 1962. A neglected cycle in sunspot number? *J. Atmospheric Sci.*, 19 (6): 506–508.

SHAW, P. J. R., 1962. A note on the prevalence of the katabatic wind of Antarctica. *Australian Meteorol. Mag.*, 36: 41–42.

SHOWALTER, A. K., 1943. *The Tornado: An Analysis of Antecedent Meteorological Conditions.* U.S. Weather Bur., Washington, D.C., 161 pp.

SIMPSON, R. H., 1952. Exploring eye of typhoon "Marge". *Bull. Am. Meteorol. Soc.*, 33 (7): 286–298.

SIMPSON, R. H., 1954. Hurricanes. *Sci. Am.*, 190 (6): 32–37.

SMAGORINSKY, J., 1953. The dynamical influence of large-scale heat sources and sinks on the quasi-stationary mean motions of the atmosphere. *Quart. J. Roy. Meteorol. Soc.*, 79: 342–366.

SMAGORINSKY, J., 1963. General circulation experiments with primitive equations. *Monthly Weather Rev.*, 9 (3): 99–164.

SPAR, J., 1960. A vertically integrated wet, diabatic model for the study of cyclogenesis. *Proc. Intern. Symp. Numerical Weather Prediction, Tokyo, 1960*, pp. 185–204.

STALEY, D. O., 1960. Evaluation of potential-vorticity changes near the tropopause and the related vertical motions, vertical advection of vorticity, and transfer of radioactive debris from stratosphere to troposphere. *J. Meteorol.*, 17 (6): 591–620.

STALEY, D. O., 1961. Comments on "Geostrophic and gradient departures in jet streams". *J. Meteorol.*, 18 (3): 420–421.

STEPANOVA, N. A., 1964. *Jet Streams over the U.S.S.R.* English transl.: *U.S. Army Missile Command, Redstone Arsenal Rept.*, RR-TR-64-2.

STRETEN, N. A., 1963. Some observations of Antarctic katabatic winds. *Australian Meteorol. Mag.*, 42: 1–23.

SUTCLIFFE, R. C., 1947. A contribution to the problem of development. *Quart. J. Roy. Meteorol. Soc.*, 73: 370–383.

SUTCLIFFE, R. C., 1951. Mean upper contour patterns of the Northern Hemisphere—the thermal synoptic view-point. *Quart. J. Roy. Meteorol. Soc.*, 77 (333): 435–440.

SUTCLIFFE, R. C. and BANNON, J. K., 1956. Seasonal changes in the upper air conditions in the Mediterranean–Middle East area. *Intern. Assoc. Meteorol. Atmospheric Phys., Rome, 1954, Sci. Proc.*, pp.322–334.

TAUBER, G. M., 1960. Characteristics of Antarctic katabatic winds. In: *Antarctic Meteorology.* Pergamon, Oxford, pp.52–64.

TROUP, A. J., 1961. Variations in upper tropospheric flow associated with the onset of the Australian summer monsoon. *Indian J. Meteorol. Geophys.*, 12 (2): 217–230.

TUCKER, G. B., 1960. The atmospheric budget of angular momentum. *Tellus*, 12 (2): 134–144.

VAN DE BOOGAARD, H. M. E., 1964. A preliminary investigation of the daily meridional transfer of atmospheric water vapour between the Equator and 40° N. *Tellus*, 16 (1): 43–54.

VAN LOON, H., 1956a. Blocking action in the Southern Hemisphere. 1. *Notos*, 5 (3): 171–175.

VAN LOON, H., 1956b. Description of a blocking situation in the central South Atlantic Ocean (April 29–May 11, 1956). *Notos*, 5 (2): 117–119.

VAN MIEGHEM, J., 1951. Hydrodynamic instability. In: *Compendium of Meteorology*. Am. Meteorol. Soc., Boston, pp.434–453.

VEIGAS, K. W. and OSTBY JR., F. P., 1963. Application of a moving-coordinate prediction model to east coast cyclones. *J. Appl. Meteorol.*, 2 (1): 24–38.

VENKITESHWARAN, S. P., 1950. Winds at 10 km and above over India and its neighbourhood. *India Meteorol. Dept., Mem.*, 28 (2).

VON FICKER, H., 1905. Innsbrucker Föhnstudien, I. Beiträge zur Dynamik des Föhns. *Denkschr. Kaiserl. Akad. Wiss., Wien, Math. Naturw. Kl.*, 78: 83–163.

VON FICKER, H., 1910. Innsbrucker Föhnstudien, IV. Weitere Beiträge zur Dynamik des Föhns. *Denkschr. Kaiserl. Akad. Wiss., Wien, Math. Naturw. Kl.*, 85: 113–173.

WAGNER, A., 1931. Zur Aerologie des indischen Monsuns. *Beitr. Geophysik*, 30: 196–238.

WEINSTEIN, A. I. and REITER, E. R., 1965. Mesoscale structure of 11–20 km winds with applications to missile operations. *Meteorol. Res. Inc. Rept.*, MRI 65 FR-213.

WEXLER, H., 1961. A boundary layer interpretation of the low-level jet. *Tellus*, 13 (3): 368–378.

WIEGMAN, E. J., HADFIELD, R. G. and SEREBRENY, S. M., 1964. Atlas of cloud vortex patterns observed in satellite photographs. *Stanford Res. Inst., Proj. 4526, Final Rept.*

WIIN-NIELSEN, A., BROWN, J. A. and DRAKE, M., 1963. On atmospheric energy conversions between the zonal flow and eddies. *Tellus*, 15 (3): 261–279.

WIIN-NIELSEN, A., BROWN, J. A. and DRAKE, M., 1964. Further studies of energy exchange between zonal flow and eddies. *Tellus*, 16 (2): 168–180.

WIPPERMANN, F., 1961. Zur Frage des Einflusses der Land- und Meerverteilung auf die Lage der quasistationären Tröge in einer atmosphärischen Zonalzirkulation. *Arch. Meteorol. Geophys. Bioklimatol., Ser.* A., 4: 112–121.

YAMAGUCHI, K., 1964. Cloud distribution revealed by TIROS III. *J. Meteorol. Soc. Japan. Ser.* 2, 42 (5): 285–297.

YANAI, M., 1961a. A detailed analysis of typhoon formation. *J. Meteorol. Soc. Japan, Ser. 2*, 39: 187–214.

YANAI, M., 1961b. Dynamical aspects of typhoon formation. *J. Meteorol. Soc. Japan, Ser. 2*, 39 (5): 282–309.

YANAI, M., 1963a. A comment on the creation of warm core in incipient typhoon. *Typhoon Res. Lab., Meteorol. Res. Inst., Tokyo, Tech. Rept.*, 1: 183–187.

YANAI, M., 1963b. A preliminary survey of large-scale disturbances over the tropical Pacific region. *Geofis. Intern.*, 3 (3): 73–84.

YANAI, M., 1964. Formation of tropical cyclones. *Rev. Geophys.*, 2 (2): 367–414.

YEH, T-CH., DAO, SH-Y. and LI, M-T., 1959. The abrupt change of circulation over the Northern Hemisphere during June and October. In: B. BOLIN (Editor), *The Atmosphere and sea in motion*. Oxford Univ. Press, London, pp.249–267.

YIN, M. T., 1949. A synoptic–aerologic study of the onset of the summer monsoon over India and Burma. *J. Meteorol.* 6: 393–400.